Compact High-Order Accurate Scheme for Laminar Incompressible Two-Phase Flows

Ahmed Sherif

MEMOIRE DE DOCTORAT DE

L'ECOLE CENTRALE DE NANTES
Et l'INSTITUTO SUPERIOR TECNICO LISBOA

ECOLE DOCTORALE N° 602
Sciences de l'Ingénierie et des Systèmes
Spécialité : *Mécanique des Milieux Fluides*

Par
Ahmed SHERIF

Compact High-Order Accurate Scheme for Laminar Incompressible Two-Phase Flows

Projet de recherche doctoral présenté et soutenu à l'Ecole Centrale de Nantes, le 31 janvier 2023
Unité de recherche : UMR6598, Laboratoire de recherche en Hydrodynamique, Énergétique et Environnement Atmosphérique (LHEEA)

Rapporteurs avant soutenance :

Sonia FERNANDEZ-MENDEZ	Professor, Universitat Politècnica de Catalunya, Espagne
Christophe CORRE	Professeur des universités, École Centrale de Lyon

Composition du Jury :

Président :	Eric SERRE	Directeur de recherche CNRS, Aix-Marseille Université
Examinateurs :	Sonia FERNANDEZ-MENDEZ	Professor, Universitat Politècnica de Catalunya, Espagne
	Christophe CORRE	Professeur des universités, École Centrale de Lyon
	Martin OBERLACK	Full professor, Technische Universität Darmstadt, Allemagne
	Carlos Manuel TIAGO TAVARES FERNANDES	Assistant professor, Instituto Superior Técnico Lisboa, Portugal
	Ganbo DENG	Ingénieur de recherche, École Centrale de Nantes

Directeur de recherches doctorales :	Michel VISONNEAU	Directeur de recherche CNRS, École Centrale de Nantes
Directeur de recherches doctorales :	Luis EÇA	Professor, Instituto Superior Técnico Lisboa, Portugal

Acknowledgments

First of all, I would like to thank my supervisors, Michel, Luís, and Ganbo, for their efforts and thoughtful comments throughout this work. Most importantly, I would like to thank them for being always understanding and open.

Further, I would like to thank the members of the PhD follow-up committee, Nicolas Moes and Martin Oberlack, for their thoughtful comments during our meetings.

I would also like to thank my friend and colleague Hashim Elzaabalawy for our fruitful discussions both technical and casual.

I'm also thankful to all my friends and colleagues in ECN for sharing the good and tough moments in the university and outside.

Finally, I cannot forget to thank my family and my fiancee for their unconditional support throughout the thesis.

I would like to show my gratitude to the funding organizations: This project has received funding from the European Union's Horizon 2020 research and innovation programme under the Marie Sklodowska Curie grant agreement No 764636 (ProTechTion programme). It is also funded by CNRS (Centre National de la Recherche Scientifique) in France.

Contents

Chapter 1

Introduction

1.1 Overview

The development of high-order accurate numerical schemes for Computational Fluid Dynamics (CFD) applications is getting a considerable attention in the research community [1, 2]. When it comes to research in high-order schemes, the family of DG-FEM is very popular[3, 4, 5, 6, 7, 8]. It has some interesting properties such as being locally conservative, stable for convection-dominated problems, and highly parallelized. In addition, DG methods are able to handle complex geometries and require simple treatment of boundary conditions while maintaining the high accuracy all over the computational domain. This makes DG methods very attractive for CFD applications.

One of the main CFD applications is the simulation of incompressible two-phase flows. This application involves a moving material interface between the two phases where local discontinuities in the flow field arise. One approach to resolve those discontinuities is to re-mesh the domain in each time step so that the mesh is fitted to the interface, then any of the standard spatial discretization techniques could be used, see for instance [9, 10, 11, 12, 13]. However such approach is not suitable for complex simulations because of its elevated computational cost due to re-meshing. Another more effective approach is to avoid the expensive procedure of re-meshing and use a fixed unfitted mesh through the whole computational/simulation domain, however, this requires a special technique to numerically resolve the local discontinuities in the flow field at the interface between the two fluids. An example of such techniques is X-FEM[14] which is based on enriching the standard FEM polynomial approximation in elements and faces where two fluids exist. The X-FEM method is used to solve two-phase flow problems, see for instance [15, 16, 17, 18, 19, 20]. Some work has been done to incorporate the concepts of X-FEM into a DG framework, as for instance the work presented in [21, 22, 23, 24] leading to the concept of eXtended DG (X-DG).

The main disadvantage of the standard DG method is the increased number of degrees of freedom due to the duplication of unknowns between elements. This in fact is not an issue when explicit time integration schemes are used in unsteady problems, where the DG method allows for element-by-element computations, which makes it possible to solve the problem in each element independently of the neighboring elements, i.e., parallelization is straightforward. However, for implicit time integration schemes or steady problems, this property is no longer available, and the increased number of coupled degrees of freedom makes the method computationally expensive.

The Hybridizable Discontinuous Galerkin (HDG) method applied for different problems in [25, 26, 27, 28, 29] evolved as a specific type of DG methods that solves the problem of DG being computationally expensive. The HDG method introduces additional unknowns

(solution traces) on the interfaces between elements (will be referred-to as mesh skeleton Γ), to enforce inter-element transmission conditions. This results in an increase in the total number of degrees of freedom. However, it allows to reformulate the problem so that the number of globally coupled degrees of freedom is drastically reduced. For this, the overhead is a more complicated assembling process for the global system of equations. However, this is not an issue because the computational cost and memory requirements are mainly dependent on the size of the global system. Another potential gain from the HDG method is the optimal convergence rates for both the primal variables and diffusive fluxes.

The standard HDG method for single-material Poisson problem is presented for instance by Sevilla and Huerta [29]. An extension of the standard HDG method to solve bi-material Poisson problem is presented by Gürkan et al.[30, 31, 32] where the eXtended HDG (X-HDG) method is introduced for the first time. The X-HDG method is known for the introduction of the solution trace as an extra unknown on the material interface, to enforce the transmission conditions across the material interface.

Considering single-phase incompressible flow problems, the standard HDG formulation, firstly introduced by Nguyen et al. in [28] and further presented for instance by Giacomini et al.[33] does not satisfy the divergence-free condition exactly. A novel divergence-free HDG formulation for single-phase is presented by Rhebergen and Wells [34] which yields point-wise exactly divergence-free velocity fields that is $\mathcal{H}(div)$-conforming for triangular and tetrahedral elements. This formulation was further developed and extended to quadrilateral and hexahedral elements in [35, 36]. The property of satisfying the divergence-free exactly is crucial for high Reynolds number and unsteady flow simulations [37]. The divergence-free HDG is different from the standard HDG in two aspects: The first aspect is the introduction of the pressure trace $\widehat{P}$ as an extra global unknown on the mesh skeleton to enforce the transmission condition of the continuity equation, i.e. enforce $[\![\boldsymbol{u} \cdot \boldsymbol{n}]\!]_\Gamma = 0$. This pressure trace has the same order of approximation as the velocity trace $\widehat{\boldsymbol{u}}$ in order to ensure that the velocity field is $\mathcal{H}(div)$-conforming. The second aspect is the use of divergence-free pressure-elements that interpolate the pressure inside each element using polynomials in the space of velocity divergence.

On the other hand, considering incompressible two-phase flow problems, the standard X-HDG method is firstly introduced by Gürkan et al.[38, 39]. This method is an extension of the standard HDG formulation. i.e. it does not satisfy the divergence-free condition exactly. The standard X-HDG introduces the velocity trace $\widetilde{\boldsymbol{u}}$ as an extra unknown on the material interface to enforce the transmission or jump conditions of the momentum equation across the material interface.

1.2 Present study

The work presented in this thesis is the extension of the divergence-free HDG method to solve two-phase incompressible flow problems. This method will be referred to as divergence-free X-HDG which is different from the standard X-HDG in two aspects: First aspect, it inherits the introduction of the pressure trace $\widehat{P}$ as an extra global unknown on the mesh skeleton as well as the use of the pressure-elements from the divergence-free HDG. Second, it introduces the pressure trace $\widetilde{P}$ as an extra unknown on the material interface, to enforce the transmission condition of the continuity equation across the material interface $\mathcal{I}$, i.e. enforce $[\![\boldsymbol{u} \cdot \boldsymbol{n}]\!]_\mathcal{I} = 0$, alongside with the velocity trace $\widetilde{\boldsymbol{u}}$. This method, to the best of the authors' knowledge, is introduced for the first time in the article [40] which is taken from the work reported in this thesis.

Another crucial part to complete the tool for solving the two-phase flow problem is the interface capturing technique. In this work, the Level-Set method [41, 42] is used. In each

time step, the interface is represented by a signed distance function that is positive on one side, negative on the other, and zero on the interface itself. This signed distance function is advected by the velocity field obtained from the Navier-Stokes solver. More specifically, the velocity at the interface. A basic implementation of the the Level-Set method is done using HDG discretization and without dealing with "re-initialization". Finally, the merge of the Navier-Stokes solver and the Level-Set method is done to have a complete solver for transient two-phase incompressible flows. This is not a trivial task, see for instance [43].

1.3 Outline

The thesis is divided into seven chapters. This Chapter 1 gives a general overview of the numerical treatment of two-phase flows with the FEM/DG/HDG methods. Furthermore, the scope of this work and the outline is presented. Chapter 2 introduces the definitions and notations to be used throughout the thesis manuscript. In addition, a brief overview regarding the concepts of X-FEM is introduced. In Chapter 3 the X-HDG method is presented for bi-material Poisson problem, which is the relatively easier problem to test and understand the use of X-FEM concepts within HDG discretization. Therein, the effect of bad cuts on the ill-conditioning of the linear system is shown. In addition, high-order convergence rates are shown as long as high-order integration quadrature is used for curved interfaces. Chapter 4 presents the novel divergence-free X-HDG method for two-phase Stokes flow problem. The main feature of the method being, point-wise divergence-free, is verified for problems with fixed interface location. For problems with moving interfaces, the Level-Set method is used as an interface-capturing method, which is presented in Chapter 5. In Chapter 6, the divergence-free X-HDG method is extended to the full two-phase incompressible Navier-Stokes flows where the treatment of transient and convective terms are discussed. In addition, the coupling of the flow field and the interface solvers is explained. Finally, Chapter 7 summarizes the thesis with conclusions and possible future developments.

Chapter 2

Preliminaries

2.1 Definitions and notations

2.1.1 The broken computational domain and the unfitted mesh

Let $\Omega \subset \mathbb{R}^d$ be a bounded domain by a boundary $\partial\Omega$. We also define $\overline{\Omega} := \Omega \cup \partial\Omega$. $\overline{\Omega}$ is divided into two disjoint subdomains

$$\overline{\Omega} = \overline{\Omega_1} \cup \overline{\Omega_2}, \qquad \Omega_1 \cap \Omega_2 = \emptyset$$

with an interface

$$\mathcal{I} = \overline{\Omega_1} \cap \overline{\Omega_2}.$$

The outward normal and the tangential unit vectors to the boundary $\partial\Omega$ are denoted by $\boldsymbol{n}$ and $\boldsymbol{t}$, respectively. Furthermore, the normal (heading from Ω_1 to Ω_2) and the tangential unit vectors to the interface $\mathcal{I}$ are denoted by $\widehat{\boldsymbol{n}}$ and $\widehat{\boldsymbol{t}}$, respectively. The partition of the boundary of the domain $\partial\Omega$ into a Dirichlet part Γ_D and a Neumann part Γ_N is considered. See Figure 2.1.

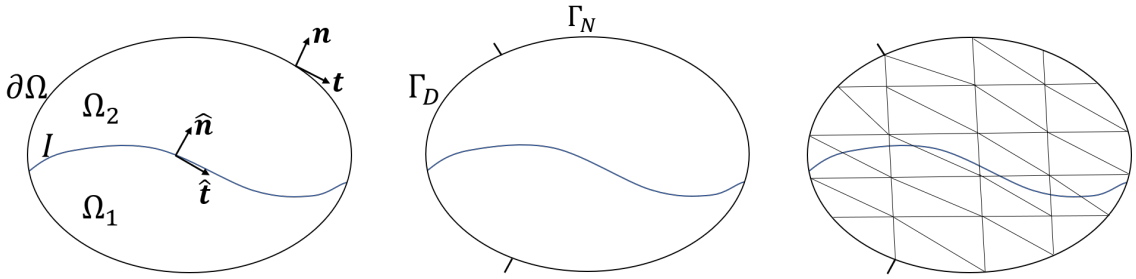

Figure 2.1: Schematic of a two-material continuum.

Further, the computational domain Ω is divided into $\mathtt{n_{el}}$ disjoint elements $K_i \in \mathbb{R}^d$ (where $i = 1 : \mathtt{n_{el}}$)

$$\overline{\Omega} = \bigcup_{i=1}^{\mathtt{n_{el}}} \overline{K_i}, \qquad K_i \cap K_j = \emptyset \qquad \text{for } i \neq j$$

with boundaries $\partial K_i \in \mathbb{R}^{d-1}$ where d is the spatial dimension. Note that this decomposition of the domain is meant to be unfitted to the interface $\mathcal{I}$. See Figure 2.1 (right).

Furthermore, The union of all $\mathtt{n_{fc}}$ faces Γ_f (where $f = 1 : \mathtt{n_{fc}}$) is denoted as

$$\Gamma := \bigcup_{i=1}^{\mathtt{n_{el}}} \partial K_i = \bigcup_{f=1}^{\mathtt{n_{fc}}} \Gamma_f$$

which are the black lines and curves shown in Figure 2.2 (left). Γ is also referred-to as *mesh skeleton*.

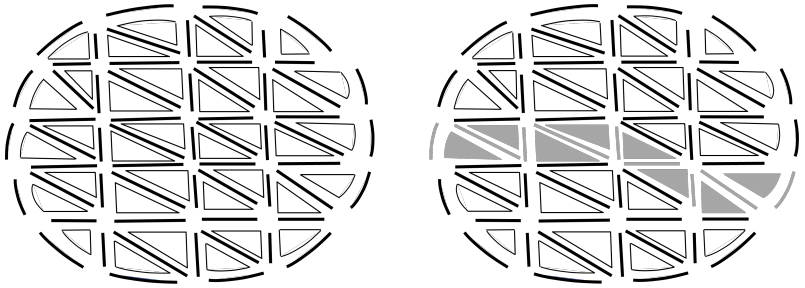

Figure 2.2: Schematic of the HDG mesh showing the mesh skeleton (left) with the cut elements and faces shown in grey (right).

Since the mesh is not fitted to the interface $\mathcal{I}$, this results in some elements and faces of the mesh to be cut by the interface. Those elements and faces are referred to as *cut elements* and *cut faces* which are shown in grey in Figure 2.2 (right). The uncut elements/faces are referred to as *standard* elements/faces.

The functions defined in cut elements/faces will be approximated by an enriched interpolation that allows for the representation of local discontinuities. More details are presented in the upcoming sections.

2.1.2 Approximation spaces

For ease of notations, a scalar space is denoted by the letter $\mathcal{S}$, a vector space is denoted by the letter $\mathcal{V}$ and a tensor space is denoted by the letter $\mathcal{T}$. Furthermore, those letters are given subscripts v or s. The subscript v refers to *volume* space where the functions defined in elements exist. The subscript s refers to *surface* space where the functions defined in the boundaries of elements exist. Finally, the superscript h is used to denote a *discrete* space. Note that the approximation spaces are defined for standard and cut elements/faces.

Non-discrete spaces
Scalar spaces for volume and surface:

$$\begin{aligned}
\mathcal{S}_v = \{\phi \in \mathcal{L}_2(\Omega) : \phi|_{K_i} &\in \mathcal{H}^1(K_i) && \text{if } K_i \cap \mathcal{I} = \emptyset,\\
\phi|_{K_i} &\in \mathcal{H}^1(K_i) \oplus H\mathcal{H}^1(K_i) && \text{if } K_i \cap \mathcal{I} \neq \emptyset\}\\
\mathcal{S}_s = \{\widehat{\phi} \in \mathcal{L}_2(\Gamma) : \widehat{\phi}|_{\Gamma_f} &\in \mathcal{H}^1(\Gamma_f) && \text{if } \Gamma_f \cap \mathcal{I} = \emptyset,\\
\widehat{\phi}|_{\Gamma_f} &\in \mathcal{H}^1(\Gamma_f) \oplus H\mathcal{H}^1(\Gamma_f) && \text{if } \Gamma_f \cap \mathcal{I} \neq \emptyset\}\\
\mathcal{S}_v^{div} = \{\phi \in \mathcal{L}_2(\Omega) : \phi|_{K_i} &\in \boldsymbol{\nabla}\cdot[\mathcal{H}^1(K_i)]^d && \text{if } K_i \cap \mathcal{I} = \emptyset,\\
\phi|_{K_i} &\in \boldsymbol{\nabla}\cdot[\mathcal{H}^1(K_i)]^d \oplus H\boldsymbol{\nabla}\cdot[\mathcal{H}^1(K_i)]^d && \text{if } K_i \cap \mathcal{I} \neq \emptyset\}
\end{aligned}$$

where the space $\mathcal{S}_v^{div}$ is a divergence-free space that is used to define divergence-free approximation functions for the pressure in incompressible Navier-Stokes formulation.
Vector spaces for volume and surface:

$$\begin{aligned}
\mathcal{V}_v = \{\boldsymbol{\psi} \in [\mathcal{L}_2(\Omega)]^d : \boldsymbol{\psi}|_{K_i} &\in [\mathcal{H}^1(K_i)]^d && \text{if } K_i \cap \mathcal{I} = \emptyset,\\
\boldsymbol{\psi}|_{K_i} &\in [\mathcal{H}^1(K_i)]^d \oplus H[\mathcal{H}^1(K_i)]^d && \text{if } K_i \cap \mathcal{I} \neq \emptyset\}\\
\mathcal{V}_s = \{\widehat{\boldsymbol{\psi}} \in [\mathcal{L}_2(\Gamma)]^d : \widehat{\boldsymbol{\psi}}|_{\Gamma_f} &\in [\mathcal{H}^1(\Gamma_f)]^d && \text{if } \Gamma_f \cap \mathcal{I} = \emptyset,\\
\widehat{\boldsymbol{\psi}}|_{\Gamma_f} &\in [\mathcal{H}^1(\Gamma_f)]^d \oplus H[\mathcal{H}^1(\Gamma_f)]^d && \text{if } \Gamma_f \cap \mathcal{I} \neq \emptyset\}
\end{aligned}$$

Tensor spaces for volume and surface:

$$\begin{aligned}
\mathcal{T}_v = \{\boldsymbol{\Psi} \in [\mathcal{L}_2(\Omega)]^{d\times d} : \boldsymbol{\Psi}|_{K_i} &\in [\mathcal{H}^1(K_i)]^{d\times d} && \text{if } K_i \cap \mathcal{I} = \emptyset,\\
\boldsymbol{\Psi}|_{K_i} &\in [\mathcal{H}^1(K_i)]^{d\times d} \oplus H[\mathcal{H}^1(K_i)]^{d\times d} && \text{if } K_i \cap \mathcal{I} \neq \emptyset\}\\
\mathcal{T}_s = \{\widehat{\boldsymbol{\Psi}} \in [\mathcal{L}_2(\Gamma)]^{d\times d} : \widehat{\boldsymbol{\Psi}}|_{\Gamma_f} &\in [\mathcal{H}^1(\Gamma_f)]^{d\times d} && \text{if } \Gamma_f \cap \mathcal{I} = \emptyset,\\
\widehat{\boldsymbol{\Psi}}|_{\Gamma_f} &\in [\mathcal{H}^1(\Gamma_f)]^{d\times d} \oplus H[\mathcal{H}^1(\Gamma_f)]^{d\times d} && \text{if } \Gamma_f \cap \mathcal{I} \neq \emptyset\}
\end{aligned}$$

Discrete spaces

Discrete scalar spaces for volume and surface:

$$\begin{aligned}
\mathcal{S}_v^h = \{\phi \in \mathcal{L}_2(\Omega) : \phi_h|_{K_i} &\in \mathcal{P}^m(K_i) && \text{if } K_i \cap \mathcal{I} = \emptyset,\\
\phi_h|_{K_i} &\in \mathcal{P}^m(K_i) \oplus H\mathcal{P}^m(K_i) && \text{if } K_i \cap \mathcal{I} \neq \emptyset\}\\
\mathcal{S}_s^h = \{\widehat{\phi} \in \mathcal{L}_2(\Gamma) : \widehat{\phi}_h|_{\Gamma_f} &\in \mathcal{P}^m(\Gamma_f) && \text{if } \Gamma_f \cap \mathcal{I} = \emptyset,\\
\widehat{\phi}_h|_{\Gamma_f} &\in \mathcal{P}^m(\Gamma_f) \oplus H\mathcal{P}^m(\Gamma_f) && \text{if } \Gamma_f \cap \mathcal{I} \neq \emptyset\}\\
\mathcal{S}_v^{div\,h} = \{\phi \in \mathcal{L}_2(\Omega) : \phi_h|_{K_i} &\in \boldsymbol{\nabla}\cdot[\mathcal{P}^m(K_i)]^d && \text{if } K_i \cap \mathcal{I} = \emptyset,\\
\phi_h|_{K_i} &\in \boldsymbol{\nabla}\cdot[\mathcal{P}^m(K_i)]^d \oplus H\boldsymbol{\nabla}\cdot[\mathcal{P}^m(K_i)]^d && \text{if } K_i \cap \mathcal{I} \neq \emptyset\}
\end{aligned}$$

Discrete vector spaces for volume and surface:

$$\begin{aligned}
\mathcal{V}_v^h = \{\boldsymbol{\psi} \in [\mathcal{L}_2(\Omega)]^d : \boldsymbol{\psi}_h|_{K_i} &\in [\mathcal{P}^m(K_i)]^d && \text{if } K_i \cap \mathcal{I} = \emptyset,\\
\boldsymbol{\psi}_h|_{K_i} &\in [\mathcal{P}^m(K_i)]^d \oplus H[\mathcal{P}^m(K_i)]^d && \text{if } K_i \cap \mathcal{I} \neq \emptyset\}\\
\mathcal{V}_s^h = \{\widehat{\boldsymbol{\psi}} \in [\mathcal{L}_2(\Gamma)]^d : \widehat{\boldsymbol{\psi}}_h|_{\Gamma_f} &\in [\mathcal{P}^m(\Gamma_f)]^d && \text{if } \Gamma_f \cap \mathcal{I} = \emptyset,\\
\widehat{\boldsymbol{\psi}}_h|_{\Gamma_f} &\in [\mathcal{P}^m(\Gamma_f)]^d \oplus H[\mathcal{P}^m(\Gamma_f)]^d && \text{if } \Gamma_f \cap \mathcal{I} \neq \emptyset\}
\end{aligned}$$

Discrete tensor spaces for volume and surface:

$$\begin{aligned}
\mathcal{T}_v^h = \{\boldsymbol{\Psi} \in [\mathcal{L}_2(\Omega)]^{d\times d} : \boldsymbol{\Psi}_h|_{K_i} &\in [\mathcal{P}^m(K_i)]^{d\times d} && \text{if } K_i \cap \mathcal{I} = \emptyset,\\
\boldsymbol{\Psi}_h|_{K_i} &\in [\mathcal{P}^m(K_i)]^{d\times d} \oplus H[\mathcal{P}^m(K_i)]^{d\times d} && \text{if } K_i \cap \mathcal{I} \neq \emptyset\}\\
\mathcal{T}_s^h = \{\widehat{\boldsymbol{\Psi}} \in [\mathcal{L}_2(\Gamma)]^{d\times d} : \widehat{\boldsymbol{\Psi}}_h|_{\Gamma_f} &\in [\mathcal{P}^m(\Gamma_f)]^{d\times d} && \text{if } \Gamma_f \cap \mathcal{I} = \emptyset,\\
\widehat{\boldsymbol{\Psi}}_h|_{\Gamma_f} &\in [\mathcal{P}^m(\Gamma_f)]^{d\times d} \oplus H[\mathcal{P}^m(\Gamma_f)]^{d\times d} && \text{if } \Gamma_f \cap \mathcal{I} \neq \emptyset\}
\end{aligned}$$

where $\mathcal{P}^m(K_i)$ and $\mathcal{P}^m(\Gamma_f)$ are the spaces of polynomial functions of degree at most $m \geq 1$ in element K_i (where $i = 1 : \mathtt{n_{el}}$) and face Γ_f (where $f = 1 : \mathtt{n_{fc}}$), respectively.
H is an enrichment function enriching the approximation in cut elements/faces to introduce discontinuities across the interface. H could be a *Heaviside* function defined, for instance, as

$$H = \begin{cases} 1 & \text{in } \Omega_1 \\ -1 & \text{in } \Omega_2 \end{cases} \tag{2.1.1}$$

More discussion about the enrichment function is presented in section 2.2.1.
The Lebesgue space $\mathcal{L}_2(\Omega)$ is the space of functions that are defined in Ω such that a function is square integrable, namely:

$$\mathcal{L}_2(\Omega) := \left\{ v : \Omega \to \mathbb{R}^d \;\middle|\; \int_\Omega v^2 < \infty \right\}$$

The Sobolev space $\mathcal{H}^1(\Omega)$ is the space of functions that are defined in Ω such that a function plus its first-order derivatives are square integrable, namely:

$$\mathcal{H}^1(\Omega) := \left\{ v : \Omega \to \mathbb{R}^d \;\middle|\; \int_\Omega v^2 < \infty,\ \int_\Omega |\nabla v|^2 < \infty \right\}$$

2.1.3 Functional settings

For any two scalar functions u and v in $\mathcal{L}_2(\Omega)$, we denote the volume integral as

$$(u, v)_\Omega = \int_\Omega uv \, \partial \boldsymbol{x}$$

and the surface integral as

$$\langle u, v \rangle_{\partial\Omega} = \int_{\partial\Omega} uv \, \partial s$$

For any two vector functions $\boldsymbol{u}$ and $\boldsymbol{v}$ in $[\mathcal{L}_2(\Omega)]^d$, we denote the volume integral as

$$(\boldsymbol{u}, \boldsymbol{v})_\Omega = \int_\Omega \boldsymbol{u} \cdot \boldsymbol{v} \, \partial \boldsymbol{x}$$

and the surface integral as

$$\langle \boldsymbol{u}, \boldsymbol{v} \rangle_{\partial\Omega} = \int_{\partial\Omega} \boldsymbol{u} \cdot \boldsymbol{v} \, \partial s$$

For any two tensor functions $\boldsymbol{U}$ and $\boldsymbol{V}$ in $[\mathcal{L}_2(\Omega)]^{d\times d}$, we denote the volume integral as

$$(\boldsymbol{U}, \boldsymbol{V})_\Omega = \int_\Omega \boldsymbol{U} : \boldsymbol{V} \, \partial \boldsymbol{x}$$

and the surface integral as

$$\langle \boldsymbol{U}, \boldsymbol{V} \rangle_{\partial\Omega} = \int_{\partial\Omega} \boldsymbol{U} : \boldsymbol{V} \, \partial s$$

2.1.4 Definitions of Jump and Average

The jump $[\![\odot \cdot \boldsymbol{n}]\!]$ operator across the interface $\mathcal{I}$ or a face Γ_f (where $f = 1 : \mathtt{n_{fc}}$) is defined as:

$$[\![\odot \cdot \boldsymbol{n}]\!] = \odot_{left} \cdot \boldsymbol{n}_{left} + \odot_{right} \cdot \boldsymbol{n}_{right}. \tag{2.1.2}$$

It is important to note that this definition always requires the outward normal vector $\boldsymbol{n}$ in the argument and always produces functions in the same space as the argument. For instance:

$$\begin{aligned} [\![u\boldsymbol{n}]\!] &= u^{left}\boldsymbol{n}^{left} + u^{right}\boldsymbol{n}^{right} \\ &= (u^{left} - u^{right})\boldsymbol{n}^{left}, \end{aligned}$$

and

$$\begin{aligned} [\![\mu\boldsymbol{\nabla} u \cdot \boldsymbol{n}]\!] &= \mu^{left}\boldsymbol{\nabla} u^{left} \cdot \boldsymbol{n}^{left} + \mu^{right}\boldsymbol{\nabla} u^{right} \cdot \boldsymbol{n}^{right} \\ &= (\mu^{left}\boldsymbol{\nabla} u^{left} - \mu^{right}\boldsymbol{\nabla} u^{right}) \cdot \boldsymbol{n}^{left}. \end{aligned}$$

The average $\{\odot\}$ operator is defined as

$$\{\odot\} = \frac{\odot_{left} + \odot_{right}}{2}. \tag{2.1.3}$$

and it doesn't require the outward normal vector $\boldsymbol{n}$ in the argument. For instance:

$$\{u\} = \frac{u^{left} + u^{right}}{2},$$

and

$$\{\mu\boldsymbol{\nabla} u\} = \frac{\mu^{left}\boldsymbol{\nabla} u^{left} + \mu^{right}\boldsymbol{\nabla} u^{right}}{2}.$$

2.2 Concepts of eXtended Finite Element Method (X-FEM)

2.2.1 Enrichment functions in cut elements

In the context of X-FEM [14, 44], in an element K_i cut by an interface $\mathcal{I}$, the standard FE polynomial approximation of a scalar function is enriched by adding extra terms to the interpolation as follows:

$$u|_{K_i}(\boldsymbol{\xi}) \approx u_h|_{K_i}(\boldsymbol{\xi}) = \underbrace{\sum_{j=1}^{\mathtt{n_{en}}} N_j(\boldsymbol{\xi}) U_j}_{\text{Standard FE}} + \underbrace{\sum_{j=1}^{\mathtt{n_{en}}} H(\boldsymbol{\xi}) N_j(\boldsymbol{\xi}) a_j}_{\text{Enrichment}} \quad \in \mathcal{S}_v^h, \quad \text{if } K_i \cap \mathcal{I} \neq \emptyset. \tag{2.2.1}$$

where $\mathtt{n_{en}}$ is the number of nodes per element, N_j is the polynomial shape function of order m associated to node j. U_j and a_j are the coefficients of the standard and enriched shape functions at node j. In a cut element, the approximation of the solution is enriched by an enrichment function H that allows for the representation of discontinuities within the element.

The type and nature of the enrichment function depend on the type of discontinuity to be modeled [45]. There are two types of discontinuities; *weak* and *strong*. The *weak* discontinuity is a continuous solution with discontinuous derivatives across an interface. On the other hand, the *strong* discontinuity is when the solution itself is discontinuous across the interface.

Heaviside enrichment for strong discontinuities

Problems with *strong* discontinuities are solved with X-FEM using a discontinuous *Heaviside enrichment* function, with easy implementation and providing optimal results for any order [14, 46], provided the geometry of the interface is accurately approximated.

Ridge enrichment for weak discontinuities

Weak discontinuity is usually reproduced by X-FEM using a *ridge enrichment* functions [47, 48, 49, 50, 51]. Based on the literature review and the comments in [45], *ridge enrichment* functions are optimal for linear finite elements and non-optimal for high-order.

Heaviside enrichment for weak discontinuities

The authors in [45] proposed using the discontinuous *Heaviside enrichment* function for problems with *weak* discontinuities, and the desired continuity of the solution is imposed in a weak form. For example, the use of *Heaviside enrichment* function for bi-material elliptic problem with *weak* discontinuity is presented by Gürkan et al. [30] using eXtended Hybridizable Discontinuous Galerkin method (X-HDG).

See Appendix A for more details on X-FEM enriched approximation in cut elements explained in 1D.

2.2.2 Material interface representation

The material interface is represented using a distance function $\phi^{DF}(\boldsymbol{x})$ that gives the shortest distance between a point and the interface. Assuming that the interface location is known, then each node i of the mesh is assigned a value Φ_i^{DF} that provides the information of how far this node is from the interface. The value of $\phi^{DF}(\boldsymbol{x})$ is zero on the interface, negative on one side (for instance in Ω_2), and positive on the other side (for instance in Ω_1).

Further, this distance function is interpolated within an element K_i using the standard FE shape functions as follows

$$\phi^{DF}|_{K_i}(\boldsymbol{x}) \approx \phi_h^{DF}|_{K_i}(\boldsymbol{x}) = \sum_{j=1}^{\mathtt{n_{en}}} N_j(\boldsymbol{x})\Phi_j^{DF} \tag{2.2.2}$$

meaning that the distance function is continuous across the interface. Furthermore, for problems with moving interfaces, the Level-Set method [52] is used to simulate the interface movement inside the computational domain.

2.2.3 Modified integration in cut elements and faces

One of the main ingredients in X-FEM is the modified integration quadrature in each cut element/face. For this purpose, it is a must to accurately represent the interface within each cut element/face. A material interface is generally curved. High-order accurate representation of the interface is crucial for optimal convergence, see [45, 49].

In this thesis, and for simplicity, only the simple case of an interface cutting through an element is discussed, where an interface cuts an element twice at two different faces, this is referred to as *basic* cut. Dealing with more complex cuts is discussed for instance by Gürkan et al. [30].

Simple subdivision approach

Linear representation of the interface As a starting point in the development, piecewise linear representation of a curved interface is adopted. Figure 2.3 summarizes the process for modifying the integration quadrature within a cut element and its faces as well, using the subdivision approach. The figure shows an interface cutting through an element twice at two different faces, yielding a triangular and a quadrilateral region. The quadrilateral region is subdivided into two triangles. Now, we have three triangles where standard Gauss quadrature rule are applied. The integration points in each of the three triangles are obtained using isoparametric transformation from the standard reference finite element.

Integration points on the material interface are also required, as they are used for computing integrals on the interface. Once the interface is approximated, the interface integration points are obtained using isoparametric transformation.

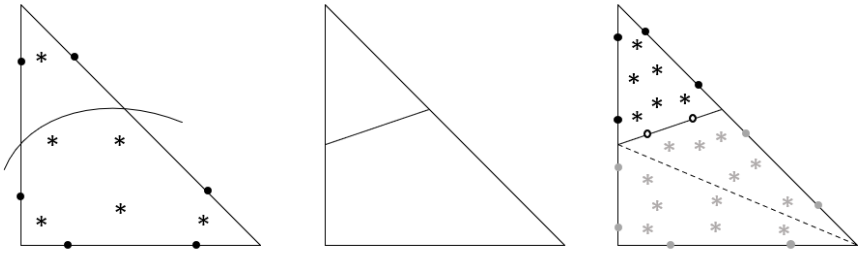

Figure 2.3: Element with standard integration points and a curved interface cutting through (left), linear representation of the interface (center), and element with modified quadrature (right). In the right plot, integration points in black and grey are in sub-domains Ω_1 and Ω_2, respectively. Asterisks represent integration points for volume integrals while dots represent points for surface integrals. Hollow dots represent integration points on the approximated material interface.

Higher order approximations of the interface are not as trivial as the linear approximation. However, it could be done using the concepts presented in Sevilla et al. [53].

ALGOIM code for QUADs and HEXs

The open-source C++ code ALGOIM developed by Robert Saye [54] is used to obtain high-order integration quadrature for implicitly defined domains in hyper-rectangles. For a cubic approximation of the interface, the modified quadrature are shown in Figure 2.4 for a mesh of 4 QUADs, and in Figure 2.5 for a mesh of 8 HEXs:

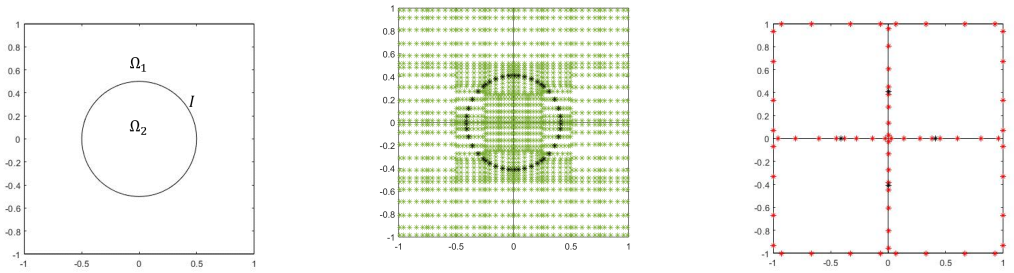

(a) 2D domain

(b) Elemental and interface quadrature

(c) Facial quadrature

Figure 2.4: Modified quadrature in cut Quad elements and 1D faces using the code ALGOIM.

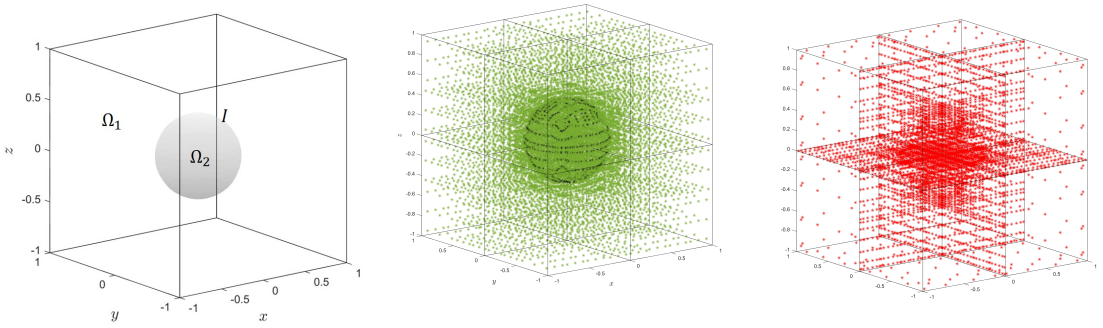

(a) 3D domain

(b) Elemental and interface quadrature

(c) Facial quadrature

Figure 2.5: Modified quadrature in cut Hex elements and Quad faces using the code ALGOIM.

Hierarchical-Moment-Fitting (HMF) approach for QUADs

Another approach to get modified integration quadrature, for cut elements, faces and the material interface, is the Hierarchical-Moment-Fitting (HMF) approach presented in [55]. This approach is used in BoSSS X-DG code [24]. However, it is not used in this thesis.

Chapter 3

X-HDG method for bi-material Poisson problem

3.1 Problem statement

A bi-material elliptic problem, whose solution presents a strong discontinuity at the interface, is stated as

$$\begin{cases} -\boldsymbol{\nabla}\cdot(\mu\boldsymbol{\nabla}u) = s & \text{in } \overline{\Omega_1}\cup\overline{\Omega_2}, \\ u = u_D & \text{on } \Gamma_D, \\ -\mu\boldsymbol{\nabla}u\cdot\boldsymbol{n} = g_N & \text{on } \Gamma_N, \\ u_1 - u_2 = \alpha & \text{on } \mathcal{I}, \\ [\![-\mu\boldsymbol{\nabla}u\cdot\boldsymbol{n}]\!] = g & \text{on } \mathcal{I}. \end{cases} \tag{3.1.1}$$

where u is the dependent variable to be determined from the solution of the problem, μ is a material property that is discontinuous across the interface $\mathcal{I}$ (that is, $\mu = \mu_i$ in Ω_i for $i = 1, 2$), s is a known source term, u_D is a prescribed value of the solution on the Dirichlet boundary Γ_D, g_N is a prescribed normal flux on the Neumann boundary Γ_N, α is the jump in u across the interface and g is an interface traction.

3.2 The mixed strong form

The strong form of Poisson's equation presented earlier by (3.1.1) could be written as a system of first order equations by introducing the vector variable $\boldsymbol{q} = -\mu\boldsymbol{\nabla}u$:

$$\begin{cases} \boldsymbol{\nabla}\cdot\boldsymbol{q} = s & \text{in } \overline{\Omega_1}\cup\overline{\Omega_2}, \\ \boldsymbol{q} + \mu\boldsymbol{\nabla}u = \boldsymbol{0} & \text{in } \overline{\Omega_1}\cup\overline{\Omega_2}, \\ u = u_D & \text{on } \Gamma_D, \\ \boldsymbol{q}\cdot\boldsymbol{n} = g_N & \text{on } \Gamma_N, \\ u_1 - u_2 = \alpha & \text{on } \mathcal{I}, \\ [\![\boldsymbol{q}\cdot\boldsymbol{n}]\!] = g & \text{on } \mathcal{I}. \end{cases} \tag{3.2.1}$$

This set of equations can be written for a finite element $K_i \in \overline{\Omega}$ as:

$$\begin{cases} \boldsymbol{\nabla}\cdot\boldsymbol{q} = s & \text{in } K_i \setminus \mathcal{I}, \\ \boldsymbol{q} + \mu\boldsymbol{\nabla}u = \boldsymbol{0} & \text{in } K_i \setminus \mathcal{I}, \\ u = u_D & \text{on } \partial K_i \cap \Gamma_D, \\ \boldsymbol{q}\cdot\boldsymbol{n} = g_N & \text{on } \partial K_i \cap \Gamma_N, \\ u_1 - u_2 = \alpha & \text{on } \mathcal{I}_i, \\ [\![\boldsymbol{q}\cdot\boldsymbol{n}]\!] = g & \text{on } \mathcal{I}_i. \end{cases} \tag{3.2.2}$$

where $\mathcal{I}_i := K_i \cap \mathcal{I}$ is the part of the interface in element K_i (if K_i is a cut element).

3.3 Extended hybridizable discontinuous Galerkin method

The standard HDG method for single-material Poisson problem is presented for instance in [29]. An extension of the standard HDG method to solve bi-material Poisson problem is presented in [30] where the eXtended HDG (X-HDG) method is explained. The X-HDG method is known for the introduction of the solution trace $\widetilde{u}$ as an extra unknown on the material interface $\mathcal{I}$ to enforce the interface traction, i.e. enforce $[\![\boldsymbol{q}\cdot\boldsymbol{n}]\!]_{\mathcal{I}} = g$.
The X-HDG method rewrites (3.2.2) as two equivalent problems. First the **local element-by-element problems** with Dirichlet boundary conditions, that is,

$$\left.\begin{aligned} \boldsymbol{\nabla}\cdot\boldsymbol{q} &= s && \text{in } K_i, \\ \boldsymbol{q} + \mu\boldsymbol{\nabla}u &= \boldsymbol{0} && \text{in } K_i, \\ u &= u_D && \text{on } \partial K_i \cap \Gamma_D, \\ u &= \widehat{u} && \text{on } \partial K_i \setminus \Gamma_D. \end{aligned}\right\} \text{ if } K_i \cap \mathcal{I} = \emptyset \tag{3.3.1a}$$

$$\left.\begin{aligned} \boldsymbol{\nabla}\cdot\boldsymbol{q} &= s && \text{in } K_i, \\ \boldsymbol{q} + \mu\boldsymbol{\nabla}u &= \boldsymbol{0} && \text{in } K_i, \\ u &= u_D && \text{on } \partial K_i \cap \Gamma_D, \\ u &= \widehat{u} && \text{on } \partial K_i \setminus \Gamma_D, \\ u_1 - u_2 &= \alpha && \text{on } \mathcal{I}_i, \\ [\![\boldsymbol{q}\cdot\boldsymbol{n}]\!] &= g && \text{on } \mathcal{I}_i. \end{aligned}\right\} \text{ if } K_i \cap \mathcal{I} \neq \emptyset \tag{3.3.1b}$$

for $i = 1, ..., \mathtt{n_{el}}$. A new variable $\widehat{u} \in \mathcal{S}_s(\Gamma \setminus \Gamma_D)$ is introduced which corresponds to the trace of u at the mesh faces $\Gamma \setminus \Gamma_D$. The trace $\widehat{u}$ is single valued variable on each face, with the same value when seen from both sides of an interior face. The local problems have been particularized for standard elements (3.3.1a) and for cut elements (3.3.1b). Given the trace $\widehat{u}$, the local problems (3.3.1) can be solved in each element to determine the solution $u \in \mathcal{S}_v(\Omega)$ and the flux $\boldsymbol{q} \in \mathcal{V}_v(\Omega)$. Thus, the problem now reduces to the determination of the trace $\widehat{u}$. This is done by solving a **global problem** that imposes transmission conditions (i.e. the continuity of the solution and the flux) across interior faces plus the Neumann boundary conditions, that is,

$$\begin{cases} [\![u\boldsymbol{n}]\!] = \boldsymbol{0} & \text{on } \Gamma \setminus \partial\Omega, \\ [\![\boldsymbol{q}\cdot\boldsymbol{n}]\!] = 0 & \text{on } \Gamma \setminus \partial\Omega, \\ \boldsymbol{q}\cdot\boldsymbol{n} = g_N & \text{on } \Gamma_N. \end{cases} \tag{3.3.2}$$

It is important to note that the continuity of the solution u across $\Gamma \setminus \partial\Omega$ is imposed by the Dirichlet boundary condition ($u = \widehat{u}$ on $\partial K_i \setminus \Gamma_D$) in the local problems (3.3.1) and the

fact that $\widehat{u}$ is single valued on Γ. Therefore, the first jump condition in equation (3.3.2) is always satisfied and so the global problem is reduced to

$$\begin{aligned} [\![\boldsymbol{q}\cdot\boldsymbol{n}]\!] &= 0 \qquad \text{on } \Gamma \setminus \partial\Omega, \\ \boldsymbol{q}\cdot\boldsymbol{n} &= g_N \qquad \text{on } \Gamma_N. \end{aligned} \tag{3.3.3}$$

3.4 Derivation of the weak forms

3.4.1 The weak form of the local problems

For a cut element

Consider a generic element K_i which is cut by the interface $\mathcal{I}$. The element is divided into two sub-volumes; $K_i \cap \Omega_1$ and $K_i \cap \Omega_2$ as shown in Figure 3.1.

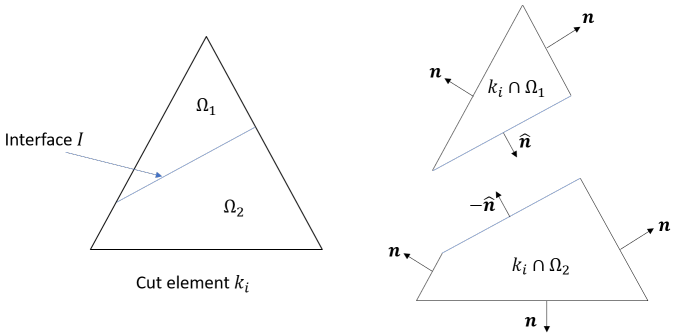

Figure 3.1: A schematic of a generic cut element.

Remark 1 One point that needs to be cleared here to avoid confusion with the notation; is that the approximation of a discontinuous scalar function defined in a cut element can be written in a general form as shown by equation (2.2.1)

$$u_h|_{K_i}(\boldsymbol{x}) = \underbrace{\sum_{j=1}^{\mathtt{n_{en}}} N_j(\boldsymbol{x})U_j}_{\text{Standard FE}} + \underbrace{\sum_{j=1}^{\mathtt{n_{en}}} H(\boldsymbol{x})N_j(\boldsymbol{x})a_j}_{\text{Enrichment}} \quad \in \mathcal{S}_v^h, \quad \text{if } K_i \cap \mathcal{I} \neq \emptyset$$

with the Heaviside function $H(\boldsymbol{x})$ defined as

$$H = \begin{cases} 1 & \text{in } K_i \cap \Omega_1 \\ -1 & \text{in } K_i \cap \Omega_2 \end{cases}$$

or alternatively as:

$$u = \begin{cases} u_1 \approx \displaystyle\sum_{j=1}^{\mathtt{n_{en}}} N_j(\boldsymbol{x})U_j + \sum_{j=1}^{\mathtt{n_{en}}} N_j(\boldsymbol{x})a_j & \text{in } K_i \cap \Omega_1 \\ u_2 \approx \displaystyle\sum_{j=1}^{\mathtt{n_{en}}} N_j(\boldsymbol{x})U_j - \sum_{j=1}^{\mathtt{n_{en}}} N_j(\boldsymbol{x})a_j & \text{in } K_i \cap \Omega_2 \end{cases}$$

End of Remark 1.

Note that in a cut element, the approximations of the functions $(u, \boldsymbol{q})$ are discontinuous. i.e. $u_h \in \mathcal{P}^m(K_i) \oplus H\mathcal{P}^m(K_i)$ and $\boldsymbol{q}_h \in [\mathcal{P}^m(K_i)]^d \oplus H[\mathcal{P}^m(K_i)]^d$.

Starting from here, for simplicity, all the approximated functions that should have a subscript (h) will be denoted without the subscript in an abuse of notations.

To obtain the weak form of the *first* equation in the local problems (3.3.1b), we perform the following steps:
Step 1: the governing equation is multiplied by a discontinuous scalar test function $\phi \in \mathcal{P}^m(K_i) \oplus H\mathcal{P}^m(K_i)$, and integrated over the two subdomains of the element K_i

$$(\phi_1, \boldsymbol{\nabla}\cdot\boldsymbol{q}_1)_{K_i\cap\Omega_1} + (\phi_2, \boldsymbol{\nabla}\cdot\boldsymbol{q}_2)_{K_i\cap\Omega_2} = (\phi, s)_{K_i} \tag{3.4.1}$$

Step 2: Green's theorem (integration by parts) is applied to incorporate surface integrals

$$\begin{aligned}
&-(\boldsymbol{\nabla}\phi_1, \boldsymbol{q}_1)_{K_i\cap\Omega_1} + \langle\phi_1, \boldsymbol{q}_1\cdot\boldsymbol{n}\rangle_{(\partial K_i\cap\Omega_1)\setminus\Gamma_D} + \langle\phi_1, \boldsymbol{q}_1\cdot\boldsymbol{n}\rangle_{(\partial K_i\cap\Omega_1)\cap\Gamma_D} + \langle\phi_1, \boldsymbol{q}_1\cdot\widehat{\boldsymbol{n}}\rangle_{\mathcal{I}_i}\\
&-(\boldsymbol{\nabla}\phi_2, \boldsymbol{q}_2)_{K_i\cap\Omega_2} + \langle\phi_2, \boldsymbol{q}_2\cdot\boldsymbol{n}\rangle_{(\partial K_i\cap\Omega_2)\setminus\Gamma_D} + \langle\phi_2, \boldsymbol{q}_2\cdot\boldsymbol{n}\rangle_{(\partial K_i\cap\Omega_2)\cap\Gamma_D} + \langle\phi_2, \boldsymbol{q}_2\cdot(-\widehat{\boldsymbol{n}})\rangle_{\mathcal{I}_i}\\
&= (\phi, s)_{K_i}
\end{aligned} \tag{3.4.2}$$

where we get surface integrals over the element boundary ∂K_i and the interface $\mathcal{I}_i$. Note that some terms can be combined to obtain

$$\begin{aligned}
-(\boldsymbol{\nabla}\phi, \boldsymbol{q})_{K_i} + \langle\phi, \boldsymbol{q}\cdot\boldsymbol{n}\rangle_{\partial K_i\setminus\Gamma_D} + \langle\phi, \boldsymbol{q}\cdot\boldsymbol{n}\rangle_{\partial K_i\cap\Gamma_D} + \langle\phi_1, \boldsymbol{q}_1\cdot\widehat{\boldsymbol{n}}\rangle_{\mathcal{I}_i} + \langle\phi_2, \boldsymbol{q}_2\cdot(-\widehat{\boldsymbol{n}})\rangle_{\mathcal{I}_i}\\
= (\phi, s)_{K_i}
\end{aligned} \tag{3.4.3}$$

Step 3: In the HDG method, the physical quantities $(u, \boldsymbol{q})$ are replaced by the numerical quantities $(\widehat{u}, \widehat{\boldsymbol{q}})$ on $\partial K_i \setminus \Gamma_D$, and the physical quantities $(u_1, u_2, \boldsymbol{q}_1, \boldsymbol{q}_2)$ are replaced by $(\widetilde{u}^i+\alpha, \widetilde{u}^i, \widetilde{\boldsymbol{q}}_1^i, \widetilde{\boldsymbol{q}}_2^i)$ on the interface $\mathcal{I}_i$. While on the intersection with the Dirichlet boundary, $(u, \boldsymbol{q})$ are replaced by $(u_D, \widehat{\boldsymbol{q}}^D)$

$$\begin{aligned}
-(\boldsymbol{\nabla}\phi, \boldsymbol{q})_{K_i} + \langle\phi, \widehat{\boldsymbol{q}}\cdot\boldsymbol{n}\rangle_{\partial K_i\setminus\Gamma_D} + \langle\phi, \widehat{\boldsymbol{q}}^D\cdot\boldsymbol{n}\rangle_{\partial K_i\cap\Gamma_D} + \langle\phi_1, \widetilde{\boldsymbol{q}}_1^i\cdot\widehat{\boldsymbol{n}}\rangle_{\mathcal{I}_i} + \langle\phi_2, \widetilde{\boldsymbol{q}}_2^i\cdot(-\widehat{\boldsymbol{n}})\rangle_{\mathcal{I}_i}\\
= (\phi, s)_{K_i}
\end{aligned} \tag{3.4.4}$$

where the numerical fluxes are defined as

$$\widehat{\boldsymbol{q}} := \boldsymbol{q} + \tau\mu(u-\widehat{u})\boldsymbol{n}, \tag{3.4.5a}$$

$$\widehat{\boldsymbol{q}}^D := \boldsymbol{q} + \tau\mu(u-u_D)\boldsymbol{n}, \tag{3.4.5b}$$

$$\widetilde{\boldsymbol{q}}_1^i := \boldsymbol{q}_1 + \tau^{\mathcal{I}}\mu_1(u_1-(\widetilde{u}^i+\alpha))\widehat{\boldsymbol{n}}, \tag{3.4.5c}$$

$$\widetilde{\boldsymbol{q}}_2^i := \boldsymbol{q}_2 + \tau^{\mathcal{I}}\mu_2(u_2-\widetilde{u}^i)(-\widehat{\boldsymbol{n}}). \tag{3.4.5d}$$

where $\widehat{u} \in \mathcal{S}_s^h(\Gamma_{ij})$ can be continuous (if $\Gamma_{ij}\cap\mathcal{I} = \emptyset$) or discontinuous (if $\Gamma_{ij}\cap\mathcal{I} \neq \emptyset$) function. Γ_{ij} is face j of element K_i. $\widetilde{u}^i \in \mathcal{P}^m(\mathcal{I}_i)$ is a continuous function defined on the interface $\mathcal{I}$. τ and $\tau^{\mathcal{I}}$ are positive stabilization parameters that have a significant effect on stability, accuracy and convergence. It was observed that τ has to be sufficiently large and $\tau^{\mathcal{I}}$ has to be inversely proportional to the average of μ to ensure optimal convergence, for instance $\tau^{\mathcal{I}} := 1/\{\mu\}$.
By introducing the definitions of the numerical fluxes into (3.4.4), we get:

$$\begin{aligned}
&-(\boldsymbol{\nabla}\phi, \boldsymbol{q})_{K_i} + \langle\phi, \boldsymbol{q}\cdot\boldsymbol{n}\rangle_{\partial K_i} + \langle\phi, \tau\mu(u-\widehat{u})\rangle_{\partial K_i\setminus\Gamma_D} + \langle\phi, \tau\mu(u-u_D)\rangle_{\partial K_i\cap\Gamma_D} + \langle\phi_1, \boldsymbol{q}_1\cdot\widehat{\boldsymbol{n}}\rangle_{\mathcal{I}_i}\\
&+ \langle\phi_2, \boldsymbol{q}_2\cdot(-\widehat{\boldsymbol{n}})\rangle_{\mathcal{I}_i} + \langle\phi_1, \tau^{\mathcal{I}}\mu_1(u_1-(\widetilde{u}^i+\alpha))\rangle_{\mathcal{I}_i} + \langle\phi_2, \tau^{\mathcal{I}}\mu_2(u_2-\widetilde{u}^i)\rangle_{\mathcal{I}_i} = (\phi, s)_{K_i}
\end{aligned} \tag{3.4.6}$$

Step 4: Doing integration by parts again for the first term on the left hand side, considering that $K_i = (K_i \cap \Omega_1) \cup (K_i \cap \Omega_2)$, yields

(3.4.7)
$$\begin{aligned}(\phi, \boldsymbol{\nabla}\cdot\boldsymbol{q})_{K_i} + \langle \phi, \tau\mu(u-\widehat{u})\rangle_{\partial K_i\setminus\Gamma_D} + \langle \phi, \tau\mu(u-u_D)\rangle_{\partial K_i\cap\Gamma_D} + \langle \phi_1, \tau^{\mathcal{I}}\mu_1(u_1-(\widetilde{u}^i+\alpha))\rangle_{\mathcal{I}_i} \\ + \langle \phi_2, \tau^{\mathcal{I}}\mu_2(u_2-\widetilde{u}^i)\rangle_{\mathcal{I}_i} = (\phi, s)_{K_i}\end{aligned}$$

and by taking the known terms to the right hand side we get (assuming $\widehat{u}$ is known)

(3.4.8)
$$\begin{aligned}(\phi, \boldsymbol{\nabla}\cdot\boldsymbol{q})_{K_i} + \langle \phi, \tau\mu u\rangle_{\partial K_i\setminus\Gamma_D} + \langle \phi, \tau\mu u\rangle_{\partial K_i\cap\Gamma_D} + \langle \phi_1, \tau^{\mathcal{I}}\mu_1(u_1-(\widetilde{u}^i+\alpha))\rangle_{\mathcal{I}_i} \\ + \langle \phi_2, \tau^{\mathcal{I}}\mu_2(u_2-\widetilde{u}^i)\rangle_{\mathcal{I}_i} = (\phi, s)_{K_i} + \langle \phi, \tau\mu\widehat{u}\rangle_{\partial K_i\setminus\Gamma_D} + \langle \phi, \tau\mu u_D\rangle_{\partial K_i\cap\Gamma_D}\end{aligned}$$

Combining and rearranging some terms we get

(3.4.9)
$$\begin{aligned}(\phi, \boldsymbol{\nabla}\cdot\boldsymbol{q})_{K_i} + \langle \phi, \tau\mu u\rangle_{\partial K_i} + \langle \phi_1, \tau^{\mathcal{I}}\mu_1 u_1\rangle_{\mathcal{I}_i} - \langle \phi_1, \tau^{\mathcal{I}}\mu_1(\widetilde{u}^i+\alpha)\rangle_{\mathcal{I}_i} \\ + \langle \phi_2, \tau^{\mathcal{I}}\mu_2 u_2\rangle_{\mathcal{I}_i} - \langle \phi_2, \tau^{\mathcal{I}}\mu_2\widetilde{u}^i\rangle_{\mathcal{I}_i} \\ = (\phi, s)_{K_i} + \langle \phi, \tau\mu\widehat{u}\rangle_{\partial K_i\setminus\Gamma_D} + \langle \phi, \tau\mu u_D\rangle_{\partial K_i\cap\Gamma_D}\end{aligned}$$

To obtain the weak form of the *second* equation in the local problems (3.3.1b):
Step 1: the governing equation is multiplied by a discontinuous vector test function $\boldsymbol{\psi} \in [\mathcal{P}^m(K_i)]^d \oplus H[\mathcal{P}^m(K_i)]^d$, and integrated over the two subdomains of the element K_i

$$(\boldsymbol{\psi}, \frac{1}{\mu}\boldsymbol{q})_{K_i} + (\boldsymbol{\psi}_1, \boldsymbol{\nabla}u_1)_{K_i\cap\Omega_1} + (\boldsymbol{\psi}_2, \boldsymbol{\nabla}u_2)_{K_i\cap\Omega_2} = 0 \tag{3.4.10}$$

Step 2: Green's theorem (integration by parts) is applied to incorporate surface integrals

(3.4.11)
$$\begin{aligned}(\boldsymbol{\psi}, \frac{1}{\mu}\boldsymbol{q})_{K_i} - (\boldsymbol{\nabla}\cdot\boldsymbol{\psi}_1, u_1)_{K_i\cap\Omega_1} + \langle \boldsymbol{\psi}_1, u_1\boldsymbol{n}\rangle_{(\partial K_i\cap\Omega_1)\setminus\Gamma_D} + \langle \boldsymbol{\psi}_1, u_1\boldsymbol{n}\rangle_{(\partial K_i\cap\Omega_1)\cap\Gamma_D} + \langle \boldsymbol{\psi}_1, u_1\widehat{\boldsymbol{n}}\rangle_{\mathcal{I}_i} \\ - (\boldsymbol{\nabla}\cdot\boldsymbol{\psi}_2, u_2)_{K_i\cap\Omega_2} + \langle \boldsymbol{\psi}_2, u_2\boldsymbol{n}\rangle_{(\partial K_i\cap\Omega_2)\setminus\Gamma_D} + \langle \boldsymbol{\psi}_2, u_2\boldsymbol{n}\rangle_{(\partial K_i\cap\Omega_2)\cap\Gamma_D} \\ + \langle \boldsymbol{\psi}_2, u_2(-\widehat{\boldsymbol{n}})\rangle_{\mathcal{I}_i} = 0\end{aligned}$$

where we get surface integrals over the element boundary ∂K_i and the interface $\mathcal{I}_i$. Note that some terms can be combined to obtain

(3.4.12)
$$\begin{aligned}(\boldsymbol{\psi}, \frac{1}{\mu}\boldsymbol{q})_{K_i} - (\boldsymbol{\nabla}\cdot\boldsymbol{\psi}, u)_{K_i} + \langle \boldsymbol{\psi}, u\boldsymbol{n}\rangle_{\partial K_i\setminus\Gamma_D} + \langle \boldsymbol{\psi}, u\boldsymbol{n}\rangle_{\partial K_i\cap\Gamma_D} + \langle \boldsymbol{\psi}_1, u_1\widehat{\boldsymbol{n}}\rangle_{\mathcal{I}_i} \\ + \langle \boldsymbol{\psi}_2, u_2(-\widehat{\boldsymbol{n}})\rangle_{\mathcal{I}_i} = 0\end{aligned}$$

Step 3: In the HDG method, the physical quantity u is replaced by the numerical quantity $\widehat{u}$ on $\partial K_i \setminus \Gamma_D$ and (u_1, u_2) are replaced by $(\widetilde{u}^i + \alpha, \widetilde{u}^i)$ on the interface $\mathcal{I}_i$. While on the intersection with the Dirichlet boundary, $u = u_D$,

(3.4.13)
$$\begin{aligned}(\boldsymbol{\psi}, \frac{1}{\mu}\boldsymbol{q})_{K_i} - (\boldsymbol{\nabla}\cdot\boldsymbol{\psi}, u)_{K_i} + \langle \boldsymbol{\psi}, \widehat{u}\boldsymbol{n}\rangle_{\partial K_i\setminus\Gamma_D} + \langle \boldsymbol{\psi}, u_D\boldsymbol{n}\rangle_{\partial K_i\cap\Gamma_D} + \langle \boldsymbol{\psi}_1, (\widetilde{u}^i+\alpha)\widehat{\boldsymbol{n}}\rangle_{\mathcal{I}_i} \\ + \langle \boldsymbol{\psi}_2, \widetilde{u}^i(-\widehat{\boldsymbol{n}})\rangle_{\mathcal{I}_i} = 0\end{aligned}$$

and by taking the known terms to the right hand side we get (assuming $\widehat{u}$ is known)

(3.4.14)
$$-(\boldsymbol{\psi}, \frac{1}{\mu}\boldsymbol{q})_{K_i} + (\boldsymbol{\nabla}\cdot\boldsymbol{\psi}, u)_{K_i} - \langle \boldsymbol{\psi}_1, (\widetilde{u}^i + \alpha)\widehat{\boldsymbol{n}}\rangle_{\mathcal{I}_i} - \langle \boldsymbol{\psi}_2, \widetilde{u}^i(-\widehat{\boldsymbol{n}})\rangle_{\mathcal{I}_i} = \langle \boldsymbol{\psi}, \widehat{u}\boldsymbol{n}\rangle_{\partial K_i \setminus \Gamma_D} + \langle \boldsymbol{\psi}, u_D \boldsymbol{n}\rangle_{\partial K_i \cap \Gamma_D}$$

note that the sign of the equation is changed in order to have a symmetric operator for the local problems (will be more obvious in the matrix forms shown later).

Regarding the *third* and *fourth* equations, $u = u_D$ on $\partial K_i \cap \Gamma_D$ and $u = \widehat{u}$ on $\partial K_i \setminus \Gamma_D$, in the local problems (3.3.1b), they have already been used in the step of going from equation (3.4.12) to equation (3.4.14) when u is replaced by $\widehat{u}$ and u_D in the third and fourth terms on the left hand side, respectively.

Regarding the *fifth* equation, $u_1 - u_2 = \alpha$ on $\mathcal{I}_i$, in the local problems (3.3.1b), it is weakly imposed in the step of going from equation (3.4.12) to equation (3.4.14) when (u_1, u_2) are replaced by $(\widetilde{u}^i + \alpha, \widetilde{u}^i)$ in the fifth and sixth terms on the left hand side considering the fact that $\widetilde{u}^i$ is single valued on $\mathcal{I}_i$.

To obtain the weak form of the *sixth* equation in the local problems (3.3.1b), we perform the following steps:
Step 1: the governing equation is multiplied by a continuous scalar test function $\widetilde{\phi} \in \mathcal{P}^m(\mathcal{I}_i)$, and integrated over the interface $\mathcal{I}_i$. In this step the expression of the jump is written in an extended form where the components from the left and the right appear

$$\langle \widetilde{\phi}, \boldsymbol{q}_1 \cdot \widehat{\boldsymbol{n}}\rangle_{\mathcal{I}_i} + \langle \widetilde{\phi}, \boldsymbol{q}_2 \cdot (-\widehat{\boldsymbol{n}})\rangle_{\mathcal{I}_i} = \langle \widetilde{\phi}, g\rangle_{\mathcal{I}_i} \tag{3.4.15}$$

Step 2: In the HDG method, the physical quantity $\boldsymbol{q}$ is replaced by the numerical quantity $\widetilde{\boldsymbol{q}}^i$ on the interface $\mathcal{I}_i$

$$\langle \widetilde{\phi}, \widetilde{\boldsymbol{q}}_1^i \cdot \widehat{\boldsymbol{n}}\rangle_{\mathcal{I}_i} + \langle \widetilde{\phi}, \widetilde{\boldsymbol{q}}_2^i \cdot (-\widehat{\boldsymbol{n}})\rangle_{\mathcal{I}_i} = \langle \widetilde{\phi}, g\rangle_{\mathcal{I}_i} \tag{3.4.16}$$

After introducing the numerical fluxes, that were defined earlier by equations (3.4.5c) and (3.4.5d), into equation (3.4.16), we get

(3.4.17)
$$\langle \widetilde{\phi}, \boldsymbol{q}_1 \cdot \widehat{\boldsymbol{n}}\rangle_{\mathcal{I}_i} + \langle \widetilde{\phi}, \boldsymbol{q}_2 \cdot (-\widehat{\boldsymbol{n}})\rangle_{\mathcal{I}_i} + \langle \widetilde{\phi}, \tau^{\mathcal{I}}\mu_1(u_1 - (\widetilde{u}^i + \alpha))\rangle_{\mathcal{I}_i} + \langle \widetilde{\phi}, \tau^{\mathcal{I}}\mu_2(u_2 - \widetilde{u}^i)\rangle_{\mathcal{I}_i} = \langle \widetilde{\phi}, g\rangle_{\mathcal{I}_i}$$

Rearranging some terms leads to

$$\begin{aligned}\langle \widetilde{\phi}, \boldsymbol{q}_1 \cdot \widehat{\boldsymbol{n}}\rangle_{\mathcal{I}_i} + \langle \widetilde{\phi}, \boldsymbol{q}_2 \cdot (-\widehat{\boldsymbol{n}})\rangle_{\mathcal{I}_i} + \langle \widetilde{\phi}, \tau^{\mathcal{I}}\mu_1 u_1\rangle_{\mathcal{I}_i} - \langle \widetilde{\phi}, \tau^{\mathcal{I}}\mu_1(\widetilde{u}^i + \alpha)\rangle_{\mathcal{I}_i} \\ + \langle \widetilde{\phi}, \tau^{\mathcal{I}}\mu_2 u_2\rangle_{\mathcal{I}_i} - \langle \widetilde{\phi}, \tau^{\mathcal{I}}\mu_2 \widetilde{u}^i\rangle_{\mathcal{I}_i} = \langle \widetilde{\phi}, g\rangle_{\mathcal{I}_i}\end{aligned} \tag{3.4.18}$$

The complete set of equations in a weak form for the local problem in a cut element
Recalling equations (3.4.9), (3.4.14), and (3.4.18), the weak form of the local problems in a cut element is: given $\widehat{u} \in \mathcal{S}_s^h(\Gamma_{ij} \setminus \Gamma_D)$ and $u_D \in \mathcal{S}_s(\Gamma_{ij} \cap \Gamma_D)$, where Γ_{ij} is the face j (which could be cut or uncut) of element K_i, find $u \in \mathcal{P}^m(K_i) \oplus H\mathcal{P}^m(K_i)$, $\boldsymbol{q} \in [\mathcal{P}^m(K_i)]^d \oplus H[\mathcal{P}^m(K_i)]^d$, and $\widetilde{u}^i \in \mathcal{P}^m(\mathcal{I}_i)$ such that

$$\begin{aligned}(\phi, \boldsymbol{\nabla}\cdot\boldsymbol{q})_{K_i} + \langle \phi, \tau\mu u\rangle_{\partial K_i} + \langle \phi_1, \tau^{\mathcal{I}}\mu_1 u_1\rangle_{\mathcal{I}_i} - \langle \phi_1, \tau^{\mathcal{I}}\mu_1(\widetilde{u}^i + \alpha)\rangle_{\mathcal{I}_i} \\ + \langle \phi_2, \tau^{\mathcal{I}}\mu_2 u_2\rangle_{\mathcal{I}_i} - \langle \phi_2, \tau^{\mathcal{I}}\mu_2 \widetilde{u}^i\rangle_{\mathcal{I}_i} \\ = (\phi, s)_{K_i} + \langle \phi, \tau\mu\widehat{u}\rangle_{\partial K_i \setminus \Gamma_D} + \langle \phi, \tau\mu u_D\rangle_{\partial K_i \cap \Gamma_D}\end{aligned} \tag{3.4.19a}$$

(3.4.19b)
$$-(\boldsymbol{\psi}, \frac{1}{\mu}\boldsymbol{q})_{K_i} + (\boldsymbol{\nabla}\cdot\boldsymbol{\psi}, u)_{K_i} - \langle \boldsymbol{\psi}_1, (\widetilde{u}^i + \alpha)\widehat{\boldsymbol{n}}\rangle_{\mathcal{I}_i} - \langle \boldsymbol{\psi}_2, \widetilde{u}^i(-\widehat{\boldsymbol{n}})\rangle_{\mathcal{I}_i} = \langle \boldsymbol{\psi}, \widehat{u}\boldsymbol{n}\rangle_{\partial K_i \setminus \Gamma_D} + \langle \boldsymbol{\psi}, u_D\boldsymbol{n}\rangle_{\partial K_i \cap \Gamma_D}$$

(3.4.19c)
$$\langle \widetilde{\phi}, \boldsymbol{q}_1\cdot\widehat{\boldsymbol{n}}\rangle_{\mathcal{I}_i} + \langle \widetilde{\phi}, \boldsymbol{q}_2\cdot(-\widehat{\boldsymbol{n}})\rangle_{\mathcal{I}_i} + \langle \widetilde{\phi}, \tau^{\mathcal{I}}\mu_1 u_1\rangle_{\mathcal{I}_i} - \langle \widetilde{\phi}, \tau^{\mathcal{I}}\mu_1(\widetilde{u}^i + \alpha)\rangle_{\mathcal{I}_i} + \langle \widetilde{\phi}, \tau^{\mathcal{I}}\mu_2 u_2\rangle_{\mathcal{I}_i} - \langle \widetilde{\phi}, \tau^{\mathcal{I}}\mu_2\widetilde{u}^i\rangle_{\mathcal{I}_i} = \langle \widetilde{\phi}, g\rangle_{\mathcal{I}_i}$$

for all the test functions ($\phi \in \mathcal{P}^m(K_i) \oplus H\mathcal{P}^m(K_i)$, $\boldsymbol{\psi} \in [\mathcal{P}^m(K_i)]^d \oplus H[\mathcal{P}^m(K_i)]^d$, and $\widetilde{\phi} \in \mathcal{P}^m(\mathcal{I}_i)$).

For a standard element

For a standard uncut element K_i, the weak forms of the local problems (3.3.1a) are exactly the same as those for a cut element after removing the interface terms. Note that the approximation spaces for all the functions will be continuous. i.e. $(\phi, u) \in \mathcal{P}^m(K_i)$, $(\boldsymbol{\psi}, \boldsymbol{q}) \in [\mathcal{P}^m(K_i)]^d$ and $\widehat{u} \in \mathcal{P}^m(\Gamma_{ij} \setminus \Gamma_D)$, where Γ_{ij} is the face j of element K_i. Therefore, the weak form of the local problems in a standard uncut element is: given $\widehat{u}$ and u_D, find $(u, \boldsymbol{q})$ such that

(3.4.20a)
$$(\phi, \boldsymbol{\nabla}\cdot\boldsymbol{q})_{K_i} + \langle \phi, \tau\mu u\rangle_{\partial K_i} = (\phi, s)_{K_i} + \langle \phi, \tau\mu\widehat{u}\rangle_{\partial K_i \setminus \Gamma_D} + \langle \phi, \tau\mu u_D\rangle_{\partial K_i \cap \Gamma_D}$$

(3.4.20b)
$$-(\boldsymbol{\psi}, \frac{1}{\mu}\boldsymbol{q})_{K_i} + (\boldsymbol{\nabla}\cdot\boldsymbol{\psi}, u)_{K_i} = \langle \boldsymbol{\psi}, \widehat{u}\boldsymbol{n}\rangle_{\partial K_i \setminus \Gamma_D} + \langle \boldsymbol{\psi}, u_D\boldsymbol{n}\rangle_{\partial K_i \cap \Gamma_D}$$

for all the test functions $(\phi, \boldsymbol{\psi})$.

3.4.2 The weak form of the global problem

We recall that the trace variable $\widehat{u} \in \mathcal{S}_s^h(\Gamma \setminus \Gamma_D)$ is required to solve the element-by-element local problems. This variable is obtained by solving the global problem (3.3.3).

To obtain the weak form of the *first* and *second* equations in the global problem (3.3.3):
Step 1: the first governing equation is multiplied by a scalar test function $\widehat{\phi} \in \mathcal{S}_s^h(\Gamma \setminus \Gamma_D)$, and integrated over the edges $\Gamma \setminus \partial\Omega$. In this step the expression of the jump is written in an extended form. The second governing equation (Neumann boundary condition) is also multiplied by the same test function $\widehat{\phi}$, and integrated over the Neumann boundary Γ_N

(3.4.21)
$$\langle \widehat{\phi}, \boldsymbol{q}^+\cdot\boldsymbol{n}^+\rangle_{\Gamma\setminus\partial\Omega} + \langle \widehat{\phi}, \boldsymbol{q}^-\cdot\boldsymbol{n}^-\rangle_{\Gamma\setminus\partial\Omega} = 0,$$

(3.4.22)
$$\langle \widehat{\phi}, \boldsymbol{q}\cdot\boldsymbol{n} - g_N\rangle_{\Gamma_N} = 0$$

Summing the two equations we get

(3.4.23)
$$\langle \widehat{\phi}, \boldsymbol{q}^+\cdot\boldsymbol{n}^+\rangle_{\Gamma\setminus\partial\Omega} + \langle \widehat{\phi}, \boldsymbol{q}^-\cdot\boldsymbol{n}^-\rangle_{\Gamma\setminus\partial\Omega} + \langle \widehat{\phi}, \boldsymbol{q}\cdot\boldsymbol{n} - g_N\rangle_{\Gamma_N} = 0$$

Step 2: In the HDG method, the physical quantity $\boldsymbol{q}$ is replaced by the numerical quantity $\widehat{\boldsymbol{q}}$ on the edges $\Gamma \setminus \Gamma_D$

(3.4.24)
$$\langle \widehat{\phi}, \widehat{\boldsymbol{q}}^+\cdot\boldsymbol{n}^+\rangle_{\Gamma\setminus\partial\Omega} + \langle \widehat{\phi}, \widehat{\boldsymbol{q}}^-\cdot\boldsymbol{n}^-\rangle_{\Gamma\setminus\partial\Omega} + \langle \widehat{\phi}, \widehat{\boldsymbol{q}}\cdot\boldsymbol{n} - g_N\rangle_{\Gamma_N} = 0$$

After introducing the numerical fluxes, defined by (3.4.5a), into equation (3.4.24), we get

(3.4.25)
$$\begin{aligned}\langle\widehat{\phi},\boldsymbol{q}^+\cdot\boldsymbol{n}^+\rangle_{\Gamma\setminus\partial\Omega}+\langle\widehat{\phi},\boldsymbol{q}^-\cdot\boldsymbol{n}^-\rangle_{\Gamma\setminus\partial\Omega}+\langle\widehat{\phi},\tau\mu(u^+-\widehat{u})\rangle_{\Gamma\setminus\partial\Omega}+\langle\widehat{\phi},\tau\mu(u^--\widehat{u})\rangle_{\Gamma\setminus\partial\Omega}\\+\langle\widehat{\phi},\boldsymbol{q}\cdot\boldsymbol{n}\rangle_{\Gamma_N}+\langle\widehat{\phi},\tau\mu(u-\widehat{u})\rangle_{\Gamma_N}=\langle\widehat{\phi},g_N\rangle_{\Gamma_N}\end{aligned}$$

Rearranging some terms we get

$$\begin{aligned}&\langle\widehat{\phi},\boldsymbol{q}^+\cdot\boldsymbol{n}^+\rangle_{\Gamma\setminus\partial\Omega}+\langle\widehat{\phi},\tau\mu u^+\rangle_{\Gamma\setminus\partial\Omega}-\langle\widehat{\phi},\tau\mu\widehat{u}\rangle_{\Gamma\setminus\partial\Omega}\\&+\langle\widehat{\phi},\boldsymbol{q}^-\cdot\boldsymbol{n}^-\rangle_{\Gamma\setminus\partial\Omega}+\langle\widehat{\phi},\tau\mu u^-\rangle_{\Gamma\setminus\partial\Omega}-\langle\widehat{\phi},\tau\mu\widehat{u}\rangle_{\Gamma\setminus\partial\Omega}\\&+\langle\widehat{\phi},\boldsymbol{q}\cdot\boldsymbol{n}\rangle_{\Gamma_N}+\langle\widehat{\phi},\tau\mu u\rangle_{\Gamma_N}-\langle\widehat{\phi},\tau\mu\widehat{u}\rangle_{\Gamma_N}=\langle\widehat{\phi},g_N\rangle_{\Gamma_N}\end{aligned}\tag{3.4.26}$$

For ease of implementation, it is written as a summation of surface integrals from all the elements in the computational domain. The weak form of the global problem is: Find $\widehat{u}\in\mathcal{S}_s^h(\Gamma\setminus\Gamma_D)$ such that

$$\sum_{i=1}^{\mathtt{n_{el}}}\Big\{\langle\widehat{\phi},\boldsymbol{q}\cdot\boldsymbol{n}\rangle_{\partial K_i\setminus\Gamma_D}+\langle\widehat{\phi},\tau\mu u\rangle_{\partial K_i\setminus\Gamma_D}-\langle\widehat{\phi},\tau\mu\widehat{u}\rangle_{\partial K_i\setminus\Gamma_D}\Big\}=\sum_{i=1}^{\mathtt{n_{el}}}\langle\widehat{\phi},g_N\rangle_{\partial K_i\cap\Gamma_N}\tag{3.4.27}$$

for all the test functions $\widehat{\phi}\in\mathcal{S}_s^h(\Gamma\setminus\Gamma_D)$.
Note that the variables u and $\boldsymbol{q}$ in the local problems, (3.4.19) for cut elements or (3.4.20) for standard elements, are functions of the trace variable $\widehat{u}$. In HDG, we substitute $(u,\boldsymbol{q})$ from the local problems into the global problem, therefore, we end up with just one variable which is $\widehat{u}$ in the global problem. This step is called hybridization.

3.5 Discretization of the weak forms

3.5.1 The discrete form of the local problems

For a cut element

Recalling the weak forms (3.4.19)

$$\begin{aligned}(\phi,\boldsymbol{\nabla}\cdot\boldsymbol{q})_{K_i}+\langle\phi,\tau\mu u\rangle_{\partial K_i}+\langle\phi_1,\tau^{\mathcal{I}}\mu_1u_1\rangle_{\mathcal{I}_i}-\langle\phi_1,\tau^{\mathcal{I}}\mu_1(\widetilde{u}^i+\alpha)\rangle_{\mathcal{I}_i}\\+\langle\phi_2,\tau^{\mathcal{I}}\mu_2u_2\rangle_{\mathcal{I}_i}-\langle\phi_2,\tau^{\mathcal{I}}\mu_2\widetilde{u}^i\rangle_{\mathcal{I}_i}\\=(\phi,s)_{K_i}+\langle\phi,\tau\mu\widehat{u}\rangle_{\partial K_i\setminus\Gamma_D}+\langle\phi,\tau\mu u_D\rangle_{\partial K_i\cap\Gamma_D}\end{aligned}\tag{3.5.1a}$$

(3.5.1b)
$$\begin{aligned}-(\boldsymbol{\psi},\frac{1}{\mu}\boldsymbol{q})_{K_i}+(\boldsymbol{\nabla}\cdot\boldsymbol{\psi},u)_{K_i}-\langle\boldsymbol{\psi}_1,(\widetilde{u}^i+\alpha)\widehat{\boldsymbol{n}}\rangle_{\mathcal{I}_i}-\langle\boldsymbol{\psi}_2,\widetilde{u}^i(-\widehat{\boldsymbol{n}})\rangle_{\mathcal{I}_i}\\=\langle\boldsymbol{\psi},\widehat{u}\boldsymbol{n}\rangle_{\partial K_i\setminus\Gamma_D}+\langle\boldsymbol{\psi},u_D\boldsymbol{n}\rangle_{\partial K_i\cap\Gamma_D}\end{aligned}$$

$$\begin{aligned}\langle\widetilde{\phi},\boldsymbol{q}_1\cdot\widehat{\boldsymbol{n}}\rangle_{\mathcal{I}_i}+\langle\widetilde{\phi},\boldsymbol{q}_2\cdot(-\widehat{\boldsymbol{n}})\rangle_{\mathcal{I}_i}+\langle\widetilde{\phi},\tau^{\mathcal{I}}\mu_1u_1\rangle_{\mathcal{I}_i}-\langle\widetilde{\phi},\tau^{\mathcal{I}}\mu_1(\widetilde{u}^i+\alpha)\rangle_{\mathcal{I}_i}\\+\langle\widetilde{\phi},\tau^{\mathcal{I}}\mu_2u_2\rangle_{\mathcal{I}_i}-\langle\widetilde{\phi},\tau^{\mathcal{I}}\mu_2\widetilde{u}^i\rangle_{\mathcal{I}_i}=\langle\widetilde{\phi},g\rangle_{\mathcal{I}_i}\end{aligned}\tag{3.5.1c}$$

Terms in equation (3.5.1a) are written as:

$$\begin{aligned}
\mathbf{A}_{uu}^{K_i}\,\mathbf{u}^i &= \langle \phi, \tau\mu u\rangle_{\partial K_i}\\
\mathbf{A}_{uu}^{\mathcal{I}_i}\,\mathbf{u}^i &= \langle \phi_1, \tau^{\mathcal{I}}\mu_1 u_1\rangle_{\mathcal{I}_i} + \langle \phi_2, \tau^{\mathcal{I}}\mu_2 u_2\rangle_{\mathcal{I}_i}\\
\mathbf{A}_{uq}^{K_i}\,\mathbf{q}^i &= (\phi, \boldsymbol{\nabla}\cdot\boldsymbol{q})_{K_i}\\
\mathbf{A}_{u\widehat{u}}^{K_i}\,\widehat{\mathbf{u}}^i &= \langle \phi, \tau\mu\widehat{u}\rangle_{\partial K_i\setminus\Gamma_D}\\
\mathbf{A}_{u\widetilde{u}^i}^{\mathcal{I}_i}\,\widetilde{\mathbf{u}}^i &= -\langle \phi_1, \tau^{\mathcal{I}}\mu_1\widetilde{u}^i\rangle_{\mathcal{I}_i} - \langle \phi_2, \tau^{\mathcal{I}}\mu_2\widetilde{u}^i\rangle_{\mathcal{I}_i}\\
\mathbf{f}_u^{K_i} &= (\phi, s)_{K_i} + \langle \phi, \tau\mu u_D\rangle_{\partial K_i\cap\Gamma_D} + \langle \phi_1, \tau^{\mathcal{I}}\mu_1\alpha\rangle_{\mathcal{I}_i}
\end{aligned}$$

Terms in equation (3.5.1b) are written as:

$$\begin{aligned}
\mathbf{A}_{qu}^{K_i}\,\mathbf{u}^i &= (\boldsymbol{\nabla}\cdot\boldsymbol{\psi}, u)_{K_i}\\
\mathbf{A}_{qq}^{K_i}\,\mathbf{q}^i &= -(\boldsymbol{\psi}, \frac{1}{\mu}\boldsymbol{q})_{K_i}\\
\mathbf{A}_{q\widetilde{u}^i}^{\mathcal{I}_i}\,\widetilde{\mathbf{u}}^i &= -\langle \boldsymbol{\psi}_1, \widetilde{u}^i\widehat{\boldsymbol{n}}\rangle_{\mathcal{I}_i} - \langle \boldsymbol{\psi}_2, \widetilde{u}^i(-\widehat{\boldsymbol{n}})\rangle_{\mathcal{I}_i}\\
\mathbf{A}_{q\widehat{u}}^{K_i}\,\widehat{\mathbf{u}}^i &= \langle \boldsymbol{\psi}, \widehat{u}\boldsymbol{n}\rangle_{\partial K_i\setminus\Gamma_D}\\
\mathbf{f}_q^{K_i} &= \langle \boldsymbol{\psi}, u_D\boldsymbol{n}\rangle_{\partial K_i\cap\Gamma_D} + \langle \boldsymbol{\psi}_1, \alpha\widehat{\boldsymbol{n}}\rangle_{\mathcal{I}_i}
\end{aligned}$$

Terms in equation (3.5.1c) are written as:

$$\begin{aligned}
\mathbf{A}_{\widetilde{u}^i u}^{\mathcal{I}_i}\,\mathbf{u}^i &= \langle \widetilde{\phi}, \tau^{\mathcal{I}}\mu_1 u_1\rangle_{\mathcal{I}_i} + \langle \widetilde{\phi}, \tau^{\mathcal{I}}\mu_2 u_2\rangle_{\mathcal{I}_i}\\
\mathbf{A}_{\widetilde{u}^i q}^{\mathcal{I}_i}\,\mathbf{q}^i &= \langle \widetilde{\phi}, \boldsymbol{q}_1\cdot\widehat{\boldsymbol{n}}\rangle_{\mathcal{I}_i} + \langle \widetilde{\phi}, \boldsymbol{q}_2\cdot(-\widehat{\boldsymbol{n}})\rangle_{\mathcal{I}_i}\\
\mathbf{A}_{\widetilde{u}^i\widetilde{u}^i}^{\mathcal{I}_i}\,\widetilde{\mathbf{u}}^i &= -\langle \widetilde{\phi}, \tau^{\mathcal{I}}\mu_1\widetilde{u}^i\rangle_{\mathcal{I}_i} - \langle \widetilde{\phi}, \tau^{\mathcal{I}}\mu_2\widetilde{u}^i\rangle_{\mathcal{I}_i}\\
\mathbf{f}_{\widetilde{u}^i}^{\mathcal{I}_i} &= \langle \widetilde{\phi}, g\rangle_{\mathcal{I}_i} + \langle \widetilde{\phi}, \tau^{\mathcal{I}}\mu_1\alpha\rangle_{\mathcal{I}_i}
\end{aligned}$$

Therefore, the discrete local problem in a cut element is written as:

$$[\mathbf{A}_{uu}^{K_i} + \mathbf{A}_{uu}^{\mathcal{I}_i}]\,\mathbf{u}^i + \mathbf{A}_{uq}^{K_i}\,\mathbf{q}^i + \mathbf{A}_{u\widetilde{u}^i}^{\mathcal{I}_i}\,\widetilde{\mathbf{u}}^i = \mathbf{A}_{u\widehat{u}}^{K_i}\,\widehat{\mathbf{u}}^i + \mathbf{f}_u^{K_i}, \tag{3.5.2a}$$

$$\mathbf{A}_{qu}^{K_i}\,\mathbf{u}^i + \mathbf{A}_{qq}^{K_i}\,\mathbf{q}^i + \mathbf{A}_{q\widetilde{u}^i}^{\mathcal{I}_i}\,\widetilde{\mathbf{u}}^i = \mathbf{A}_{q\widehat{u}}^{K_i}\,\widehat{\mathbf{u}}^i + \mathbf{f}_q^{K_i}, \tag{3.5.2b}$$

$$\mathbf{A}_{\widetilde{u}^i u}^{\mathcal{I}_i}\,\mathbf{u}^i + \mathbf{A}_{\widetilde{u}^i q}^{\mathcal{I}_i}\,\mathbf{q}^i + \mathbf{A}_{\widetilde{u}^i\widetilde{u}^i}^{\mathcal{I}_i}\,\widetilde{\mathbf{u}}^i = \mathbf{f}_{\widetilde{u}^i}^{\mathcal{I}_i}. \tag{3.5.2c}$$

From equation (3.5.2c), the vector $\widetilde{\mathbf{u}}^i$ could be written in terms of the local elemental values as

$$\begin{aligned}
\widetilde{\mathbf{u}}^i &= \mathbf{f}_{\widetilde{u}^i}^{\mathcal{I}_i} - [\mathbf{A}_{\widetilde{u}^i\widetilde{u}^i}^{\mathcal{I}_i}]^{-1}\,\mathbf{A}_{\widetilde{u}^i u}^{\mathcal{I}_i}\,\mathbf{u}^i - [\mathbf{A}_{\widetilde{u}^i\widetilde{u}^i}^{\mathcal{I}_i}]^{-1}\,\mathbf{A}_{\widetilde{u}^i q}^{\mathcal{I}_i}\,\mathbf{q}^i\\
&= \mathbf{f}_{\widetilde{u}^i}^{\mathcal{I}_i} + \mathbf{T}_u^i\,\mathbf{u}^i + \mathbf{T}_q^i\,\mathbf{q}^i.
\end{aligned} \tag{3.5.3}$$

where $\mathbf{T}_u^i = -[\mathbf{A}_{\widetilde{u}^i\widetilde{u}^i}^{\mathcal{I}_i}]^{-1}\,\mathbf{A}_{\widetilde{u}^i u}^{\mathcal{I}_i}$ and $\mathbf{T}_q^i = -[\mathbf{A}_{\widetilde{u}^i\widetilde{u}^i}^{\mathcal{I}_i}]^{-1}\,\mathbf{A}_{\widetilde{u}^i q}^{\mathcal{I}_i}$.
By substituting (3.5.3) into (3.5.2a) and (3.5.2b) we get

$$[\mathbf{A}_{uu}^{K_i} + \mathbf{A}_{uu}^{\mathcal{I}_i}]\,\mathbf{u}^i + \mathbf{A}_{uq}^{K_i}\,\mathbf{q}^i + \mathbf{A}_{u\widetilde{u}^i}^{\mathcal{I}_i}\,[\mathbf{f}_{\widetilde{u}^i}^{\mathcal{I}_i} + \mathbf{T}_u^i\,\mathbf{u}^i + \mathbf{T}_q^i\,\mathbf{q}^i] = \mathbf{A}_{u\widehat{u}}^{K_i}\,\widehat{\mathbf{u}}^i + \mathbf{f}_u^{K_i}, \tag{3.5.4a}$$

$$\mathbf{A}_{qu}^{K_i}\,\mathbf{u}^i + \mathbf{A}_{qq}^{K_i}\,\mathbf{q}^i + \mathbf{A}_{q\widetilde{u}^i}^{\mathcal{I}_i}\,[\mathbf{f}_{\widetilde{u}^i}^{\mathcal{I}_i} + \mathbf{T}_u^i\,\mathbf{u}^i + \mathbf{T}_q^i\,\mathbf{q}^i] = \mathbf{A}_{q\widehat{u}}^{K_i}\,\widehat{\mathbf{u}}^i + \mathbf{f}_q^{K_i}. \tag{3.5.4b}$$

rearranging some terms yields

$$[\mathbf{A}_{uu}^{K_i} + \mathbf{A}_{uu}^{\mathcal{I}_i} + \mathbf{A}_{u\widetilde{u}^i}^{\mathcal{I}_i}\,\mathbf{T}_u^i]\,\mathbf{u}^i + [\mathbf{A}_{uq}^{K_i} + \mathbf{A}_{u\widetilde{u}^i}^{\mathcal{I}_i}\,\mathbf{T}_q^i]\,\mathbf{q}^i = \mathbf{A}_{u\widehat{u}}^{K_i}\,\widehat{\mathbf{u}}^i + \mathbf{f}_u^{K_i} - \mathbf{A}_{u\widetilde{u}^i}^{\mathcal{I}_i}\,\mathbf{f}_{\widetilde{u}^i}^{\mathcal{I}_i}, \tag{3.5.5a}$$

$$[\mathbf{A}_{qu}^{K_i} + \mathbf{A}_{q\widetilde{u}^i}^{\mathcal{I}_i}\,\mathbf{T}_u^i]\,\mathbf{u}^i + [\mathbf{A}_{qq}^{K_i} + \mathbf{A}_{q\widetilde{u}^i}^{\mathcal{I}_i}\,\mathbf{T}_q^i]\,\mathbf{q}^i = \mathbf{A}_{q\widehat{u}}^{K_i}\,\widehat{\mathbf{u}}^i + \mathbf{f}_q^{K_i} - \mathbf{A}_{q\widetilde{u}^i}^{\mathcal{I}_i}\,\mathbf{f}_{\widetilde{u}^i}^{\mathcal{I}_i}. \tag{3.5.5b}$$

which is then written in matrix-vector form as

(3.5.6)
$$\begin{bmatrix} [\mathbf{A}_{uu}^{K_i} + \mathbf{A}_{uu}^{\mathcal{I}_i} + \mathbf{A}_{u\widetilde{u}^i}^{\mathcal{I}_i}\ \mathbf{T}_u^i] & [\mathbf{A}_{uq}^{K_i} + \mathbf{A}_{u\widetilde{u}^i}^{\mathcal{I}_i}\ \mathbf{T}_q^i] \\ [\mathbf{A}_{qu}^{K_i} + \mathbf{A}_{q\widetilde{u}^i}^{\mathcal{I}_i}\ \mathbf{T}_u^i] & [\mathbf{A}_{qq}^{K_i} + \mathbf{A}_{q\widetilde{u}^i}^{\mathcal{I}_i}\ \mathbf{T}_q^i] \end{bmatrix} \begin{Bmatrix} \mathbf{u}^i \\ \mathbf{q}^i \end{Bmatrix} = \begin{bmatrix} \mathbf{A}_{u\widehat{u}}^{K_i} \\ \mathbf{A}_{q\widehat{u}}^{K_i} \end{bmatrix} \widehat{\mathbf{u}}^i + \begin{Bmatrix} \mathbf{f}_u^{K_i} - \mathbf{A}_{u\widetilde{u}^i}^{\mathcal{I}_i}\ \mathbf{f}_{\widetilde{u}^i}^{\mathcal{I}_i} \\ \mathbf{f}_q^{K_i} - \mathbf{A}_{q\widetilde{u}^i}^{\mathcal{I}_i}\ \mathbf{f}_{\widetilde{u}^i}^{\mathcal{I}_i} \end{Bmatrix}$$

where the elemental variables are obtained by inverting the matrix to the left hand side (which is referred-to as $\mathbb{A}_i$)

(3.5.7)
$$\begin{Bmatrix} \mathbf{u}^i \\ \mathbf{q}^i \end{Bmatrix} = \mathbb{A}_i^{-1} \begin{bmatrix} \mathbf{A}_{u\widehat{u}}^{K_i} \\ \mathbf{A}_{q\widehat{u}}^{K_i} \end{bmatrix} \widehat{\mathbf{u}}^i + \mathbb{A}_i^{-1} \begin{Bmatrix} \mathbf{f}_u^{K_i} - \mathbf{A}_{u\widetilde{u}^i}^{\mathcal{I}_i}\ \mathbf{f}_{\widetilde{u}^i}^{\mathcal{I}_i} \\ \mathbf{f}_q^{K_i} - \mathbf{A}_{q\widetilde{u}^i}^{\mathcal{I}_i}\ \mathbf{f}_{\widetilde{u}^i}^{\mathcal{I}_i} \end{Bmatrix}$$

For a standard element

Recalling the weak forms (3.4.20):

(3.5.8a)
$$(\phi, \boldsymbol{\nabla}\cdot\boldsymbol{q})_{K_i} + \langle \phi, \tau\mu u\rangle_{\partial K_i} = (\phi, s)_{K_i} + \langle \phi, \tau\mu\widehat{u}\rangle_{\partial K_i\setminus\Gamma_D} + \langle \phi, \tau\mu u_D\rangle_{\partial K_i\cap\Gamma_D}$$

(3.5.8b)
$$-(\boldsymbol{\psi}, \frac{1}{\mu}\boldsymbol{q})_{K_i} + (\boldsymbol{\nabla}\cdot\boldsymbol{\psi}, u)_{K_i} = \langle \boldsymbol{\psi}, \widehat{u}\boldsymbol{n}\rangle_{\partial K_i\setminus\Gamma_D} + \langle \boldsymbol{\psi}, u_D\boldsymbol{n}\rangle_{\partial K_i\cap\Gamma_D}$$

Terms in equation (3.5.8a) are written as:

$$\begin{aligned} \mathbf{A}_{uu}^{K_i}\ \mathbf{u}^i &= \langle \phi, \tau\mu u\rangle_{\partial K_i} \\ \mathbf{A}_{uq}^{K_i}\ \mathbf{q}^i &= (\phi, \boldsymbol{\nabla}\cdot\boldsymbol{q})_{K_i} \\ \mathbf{A}_{u\widehat{u}}^{K_i}\ \widehat{\mathbf{u}}^i &= \langle \phi, \tau\mu\widehat{u}\rangle_{\partial K_i\setminus\Gamma_D} \\ \mathbf{f}_u^{K_i} &= (\phi, s)_{K_i} + \langle \phi, \tau\mu u_D\rangle_{\partial K_i\cap\Gamma_D} \end{aligned}$$

Terms in equation (3.5.8b) are written as:

$$\begin{aligned} \mathbf{A}_{qu}^{K_i}\ \mathbf{u}^i &= (\boldsymbol{\nabla}\cdot\boldsymbol{\psi}, u)_{K_i} \\ \mathbf{A}_{qq}^{K_i}\ \mathbf{q}^i &= -(\boldsymbol{\psi}, \frac{1}{\mu}\boldsymbol{q})_{K_i} \\ \mathbf{A}_{q\widehat{u}}^{K_i}\ \widehat{\mathbf{u}}^i &= \langle \boldsymbol{\psi}, \widehat{u}\boldsymbol{n}\rangle_{\partial K_i\setminus\Gamma_D} \\ \mathbf{f}_q^{K_i} &= \langle \boldsymbol{\psi}, u_D\boldsymbol{n}\rangle_{\partial K_i\cap\Gamma_D} \end{aligned}$$

Therefore, the discrete local problem in a standard element is written as:

(3.5.9a)
$$\mathbf{A}_{uu}^{K_i}\ \mathbf{u}^i + \mathbf{A}_{uq}^{K_i}\ \mathbf{q}^i = \mathbf{A}_{u\widehat{u}}^{K_i}\ \widehat{\mathbf{u}}^i + \mathbf{f}_u^{K_i},$$

(3.5.9b)
$$\mathbf{A}_{qu}^{K_i}\ \mathbf{u}^i + \mathbf{A}_{qq}^{K_i}\ \mathbf{q}^i = \mathbf{A}_{q\widehat{u}}^{K_i}\ \widehat{\mathbf{u}}^i + \mathbf{f}_q^{K_i}.$$

which is then written in matrix-vector form as

(3.5.10)
$$\begin{bmatrix} \mathbf{A}_{uu}^{K_i} & \mathbf{A}_{uq}^{K_i} \\ \mathbf{A}_{qu}^{K_i} & \mathbf{A}_{qq}^{K_i} \end{bmatrix} \begin{Bmatrix} \mathbf{u}^i \\ \mathbf{q}^i \end{Bmatrix} = \begin{bmatrix} \mathbf{A}_{u\widehat{u}}^{K_i} \\ \mathbf{A}_{q\widehat{u}}^{K_i} \end{bmatrix} \widehat{\mathbf{u}}^i + \begin{Bmatrix} \mathbf{f}_u^{K_i} \\ \mathbf{f}_q^{K_i} \end{Bmatrix}$$

where the elemental variables are obtained by inverting the matrix to the left hand side (which is referred-to as $\mathbb{A}_i$)

(3.5.11)
$$\begin{Bmatrix} \mathbf{u}^i \\ \mathbf{q}^i \end{Bmatrix} = \mathbb{A}_i^{-1} \begin{bmatrix} \mathbf{A}_{u\widehat{u}}^{K_i} \\ \mathbf{A}_{q\widehat{u}}^{K_i} \end{bmatrix} \widehat{\mathbf{u}}^i + \mathbb{A}_i^{-1} \begin{Bmatrix} \mathbf{f}_u^{K_i} \\ \mathbf{f}_q^{K_i} \end{Bmatrix}$$

3.5.2 The discrete form of the global problem

Recalling the weak form (3.4.27):

$$\sum_{i=1}^{\mathtt{n_{el}}}\left\{\langle\widehat{\phi},\boldsymbol{q}\cdot\boldsymbol{n}\rangle_{\partial K_i\setminus\Gamma_D}+\langle\widehat{\phi},\tau\mu u\rangle_{\partial K_i\setminus\Gamma_D}-\langle\widehat{\phi},\tau\mu\widehat{u}\rangle_{\partial K_i\setminus\Gamma_D}\right\}=\sum_{i=1}^{\mathtt{n_{el}}}\langle\widehat{\phi},g_N\rangle_{\partial K_i\cap\Gamma_N} \tag{3.5.12}$$

Terms in equation (3.5.12) are written as:

$$\begin{aligned}\mathbf{A}^{K_i}_{\widehat{u}u}\,\mathbf{u}^i&=\langle\widehat{\phi},\tau\mu u\rangle_{\partial K_i\setminus\Gamma_D}\\ \mathbf{A}^{K_i}_{\widehat{u}q}\,\mathbf{q}^i&=\langle\widehat{\phi},\boldsymbol{q}\cdot\boldsymbol{n}\rangle_{\partial K_i\setminus\Gamma_D}\\ \mathbf{A}^{K_i}_{\widehat{\widehat{u}}u}\,\widehat{\mathbf{u}}^i&=-\langle\widehat{\phi},\tau\mu\widehat{u}\rangle_{\partial K_i\setminus\Gamma_D}\\ \mathbf{f}^{K_i}_{\widehat{u}}&=\langle\widehat{\phi},g_N\rangle_{\partial K_i\cap\Gamma_N}\end{aligned}$$

Therefore, the discrete global problem is written as:

$$\sum_{i=1}^{\mathtt{n_{el}}}\left\{\mathbf{A}^{K_i}_{\widehat{u}u}\,\mathbf{u}^i+\mathbf{A}^{K_i}_{\widehat{u}q}\,\mathbf{q}^i+\mathbf{A}^{K_i}_{\widehat{\widehat{u}}u}\,\widehat{\mathbf{u}}^i\right\}=\sum_{i=1}^{\mathtt{n_{el}}}\mathbf{f}^{K_i}_{\widehat{u}}$$

which is then written in matrix-vector form as

$$\sum_{i=1}^{\mathtt{n_{el}}}\left\{\begin{bmatrix}\mathbf{A}^{K_i}_{\widehat{u}u} & \mathbf{A}^{K_i}_{\widehat{u}q}\end{bmatrix}\begin{Bmatrix}\mathbf{u}^i\\ \\ \mathbf{q}^i\end{Bmatrix}+\mathbf{A}^{K_i}_{\widehat{\widehat{u}}u}\,\widehat{\mathbf{u}}^i\right\}=\sum_{i=1}^{\mathtt{n_{el}}}\mathbf{f}^{K_i}_{\widehat{u}} \tag{3.5.13}$$

By inserting the solution of the local problem, (3.5.7) or (3.5.11), into (3.5.13) we get

$$\sum_{i=1}^{\mathtt{n_{el}}}\left\{\begin{bmatrix}\mathbf{A}^{K_i}_{\widehat{u}u} & \mathbf{A}^{K_i}_{\widehat{u}q}\end{bmatrix}\mathbb{A}_i^{-1}\begin{bmatrix}\mathbf{A}^{K_i}_{u\widehat{u}}\\ \\ \mathbf{A}^{K_i}_{q\widehat{u}}\end{bmatrix}\widehat{\mathbf{u}}^i+\begin{bmatrix}\mathbf{A}^{K_i}_{\widehat{u}u} & \mathbf{A}^{K_i}_{\widehat{u}q}\end{bmatrix}\mathbb{A}_i^{-1}\begin{Bmatrix}\mathbf{f}^{K_i}_{u}\\ \\ \mathbf{f}^{K_i}_{q}\end{Bmatrix}+\mathbf{A}^{K_i}_{\widehat{\widehat{u}}u}\,\widehat{\mathbf{u}}^i\right\}=\sum_{i=1}^{\mathtt{n_{el}}}\mathbf{f}^{K_i}_{\widehat{u}} \tag{3.5.14}$$

rearranging and moving the known terms to the right hand side yields

$$\sum_{i=1}^{\mathtt{n_{el}}}\left\{\left(\begin{bmatrix}\mathbf{A}^{K_i}_{\widehat{u}u} & \mathbf{A}^{K_i}_{\widehat{u}q}\end{bmatrix}\mathbb{A}_i^{-1}\begin{bmatrix}\mathbf{A}^{K_i}_{u\widehat{u}}\\ \\ \mathbf{A}^{K_i}_{q\widehat{u}}\end{bmatrix}+\mathbf{A}^{K_i}_{\widehat{\widehat{u}}u}\right)\widehat{\mathbf{u}}^i\right\}=\sum_{i=1}^{\mathtt{n_{el}}}\left\{\mathbf{f}^{K_i}_{\widehat{u}}-\begin{bmatrix}\mathbf{A}^{K_i}_{\widehat{u}u} & \mathbf{A}^{K_i}_{\widehat{u}q}\end{bmatrix}\mathbb{A}_i^{-1}\begin{Bmatrix}\mathbf{f}^{K_i}_{u}\\ \\ \mathbf{f}^{K_i}_{q}\end{Bmatrix}\right\} \tag{3.5.15}$$

which is written in simplified notation as

$$\mathbf{A}_{i=1}^{\mathtt{n_{el}}}\widehat{\mathbf{K}}^i\widehat{\mathbf{u}}^i=\mathbf{A}_{i=1}^{\mathtt{n_{el}}}\widehat{\mathbf{f}}^i \tag{3.5.16}$$

where $\mathbf{A}_{i=1}^{\mathtt{n_{el}}}$ denotes the assembly of all the finite element matrices/vectors into a global matrix/vector. Simplifying furthermore yields the global system of equations which is written as

$$\widehat{\mathbf{K}}\widehat{\mathbf{u}}=\widehat{\mathbf{f}} \tag{3.5.17}$$

3.6 Numerical examples

3.6.1 Example 1: straight interface with zero jump conditions

The bi-material Poisson problem introduced in section 3.1 is solved in this section using the eXtended Hybridizable Discontinuous Galerkin (X-HDG) method. A problem with known exact solution is presented in [30] that has zero jump conditions at the interface, i.e. $[\![u\boldsymbol{n}]\!]_{\mathcal{I}} = \mathbf{0}$ and $[\![\mu\boldsymbol{\nabla}u \cdot \boldsymbol{n}]\!]_{\mathcal{I}} = 0$. In this example a vertical interface $\mathcal{I}$ at $x = 0.2031$ is considered to divide the square domain $\Omega = [-1, 1]^2$ into two regions, Ω_1 and Ω_2, as shown in Figure 3.2 (left). The material properties and the analytical solution, shown in Figure 3.2 (right), are defined by:

$$\mu(\boldsymbol{x}) = \begin{cases} \mu_1 = 1 & \text{in } \Omega_1 \\ \mu_2 = 2.5 & \text{in } \Omega_2 \end{cases} \qquad u(\boldsymbol{x}) = \begin{cases} 5x^5 & \text{in } \Omega_1 \\ 2x^5 + 3(0.2031)^5 & \text{in } \Omega_2 \end{cases}$$

The corresponding source term is set to satisfy the analytical solution. Finally, Dirichlet conditions are set everywhere on the boundary except for the bottom boundary which is Neumann (flux from the analytical solution).

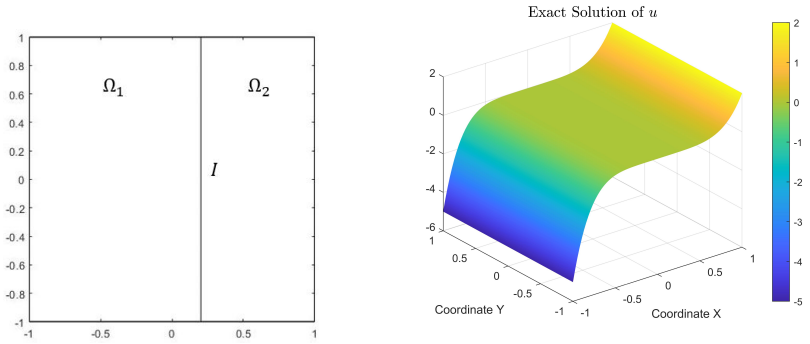

Figure 3.2: Example 1: Square domain with vertical interface (left), analytical solution (right).

The problem is solved on five meshes of triangles and the order of approximation is varied from $m = 1$ to $m = 4$. The stabilization parameters introduced in the HDG numerical fluxes by equation (3.4.5) are set as $\tau = 50$ and $\tau^{\mathcal{I}} = 1/\{\mu\}$. The mesh convergence plots for the solution u and the flux component q_1 are shown in Figure 3.3. Furthermore, the numerical solution of u and q_1 obtained on the coarsest mesh with triangles of order $m = 4$ is shown in Figure 3.4. Regarding the convergence of the solution u, it is noticed that optimal convergence of order ($m + 1$ in $\mathcal{L}_2$-norm, m in $\mathcal{H}^1$-norm) is achieved for all the degree approximations ($m = 1 : 4$) and is only deteriorated for degree $m = 4$. While for the convergence rate of the flux component q_1, it is slightly less than the optimal rate ($m + 1$ in $\mathcal{L}_2$-norm, m in $\mathcal{H}^1$-norm). Note that the optimal convergence is lost for $m = 4$ only at the finest mesh probably due to bad conditioning of the X-HDG global operator.

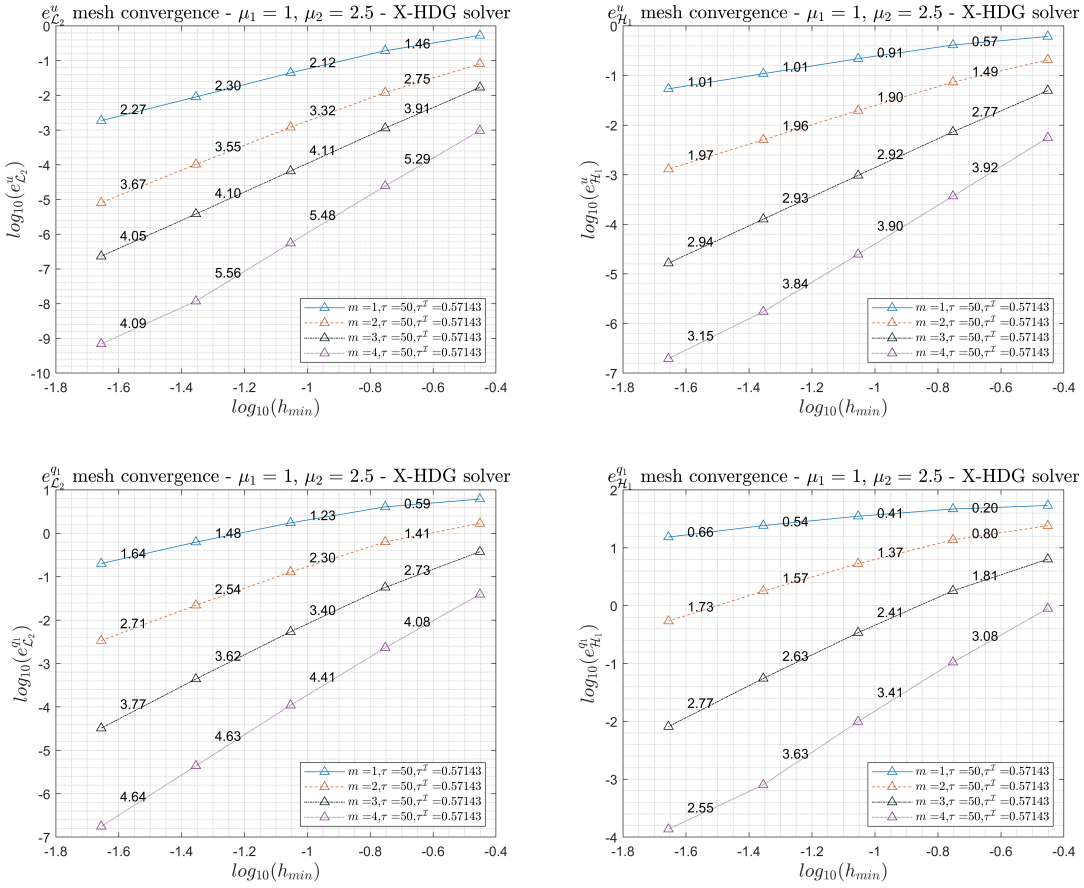

Figure 3.3: Example 1: Errors in u (top) and q_1 (bottom) vs. mesh size - $\mathcal{L}_2$-norm (left), $\mathcal{H}^1$-norm (right).

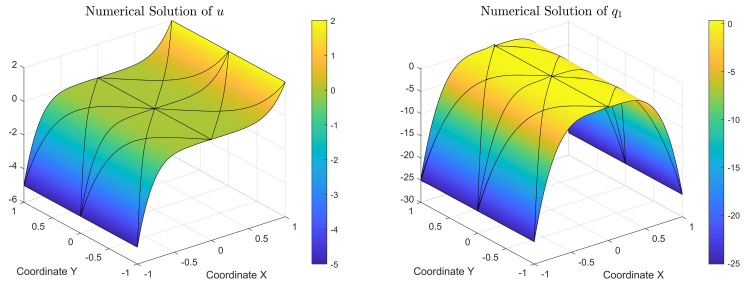

Figure 3.4: Example 1: The numerical solution of u and q_1 obtained on the coarsest mesh with triangles of order $m = 4$.

Checking the quality of cuts and conditioning:
To represent the quality of a cut, an elemental volume ratio is defined as $min(V_i/V)$; where V is the total volume of the element and V_i is the volume of the region in domain Ω_i within a cut element. A bad-cut is defined as a cut that gives a volume ratio less than 0.1 [30]. For each mesh, the percentage of cut elements with bad-cuts is recorded in Table 3.1 alongside with the minimum volume ratio among all cut elements in a given mesh. This percentage is calculated with respect to the total number of elements in the mesh, both

cut and uncut. Note that, the higher the value $min(V_i/V)$, the best. The best cut is when an element is halved, i.e. $min(V_i/V) = 0.5$.

Mesh TRIs	% of cut elements with volume ratio < 0.1	$min(V_i/V)$
mesh 1	00.00	0.35
mesh 2	18.75	0.03
mesh 3	09.37	0.07
mesh 4	00.00	0.28
mesh 5	00.00	0.25

Table 3.1: Example 1: Analysis of cuts in each mesh.

The condition numbers of the X-HDG global matrices for all the orders of approximation and each mesh refinement are recorded in Table 3.2. It is clearly seen that the operator becomes ill-conditioned with higher orders of approximation, which is probably the reason for the deteriorated convergence rate for degree $m = 4$ with the finest mesh as shown earlier in Figure 3.3.

Mesh TRIs	$m = 1$	$m = 2$	$m = 3$	$m = 4$
mesh 1	4.57E+03	5.74E+05	1.14E+08	7.09E+10
mesh 2	2.02E+03	1.94E+05	5.44E+07	4.70E+10
mesh 3	4.79E+03	4.62E+05	1.40E+08	3.30E+11
mesh 4	1.70E+04	2.54E+05	3.55E+07	2.36E+10
mesh 5	4.89E+04	2.64E+05	3.01E+07	9.65E+10

Table 3.2: Example 1: Condition number of the X-HDG global matrix.

3.6.2 Example 2: straight interface with jump conditions

This example tests the X-HDG method for a problem with a discontinuous solution across the interface. A problem that has a jump condition ($u_1 - u_2 = -1$) across a vertical interface $\mathcal{I}$ at $x = 0.4$ is solved. A square domain $\Omega = [-1, 1]^2$ is considered where $\Omega_1 := \{\boldsymbol{x} \in \Omega | x < 0.4\}$ and $\Omega_2 := \Omega \setminus \Omega_1$. The material properties are $\mu_1 = \mu_2 = 1$ and the analytical solution is:

$$u(\boldsymbol{x}) = \begin{cases} \sin(\pi x)\sin(\pi y) & \text{in } \Omega_1 \\ \sin(\pi x)\sin(\pi y) + 1 & \text{in } \Omega_2 \end{cases}$$

The corresponding source term is set to satisfy the analytical solution and Dirichlet conditions are set on the boundary.
This time, the problem is solved on five meshes of quadrilaterals and the order of approximation is varied from $m = 1$ to $m = 3$. In this example, the stabilization parameters are set as $\tau = 1$ and $\tau^{\mathcal{I}} = 0.001$. The interface stabilization parameter $\tau^{\mathcal{I}}$ is chosen carefully to ensure optimal convergence. The numerical solution of u obtained on the fourth mesh with quadrilaterals of order $m = 3$ is shown in Figure 3.5 alongside with the exact solution. It can be seen that the method can resolve strong discontinuities in the solution across the interface. Furthermore, the mesh convergence plots for the solution u and the flux component q_1 are shown in Figure 3.6. It is noticed that optimal convergence rates ($m + 1$ in $\mathcal{L}_2$-norm, m in $\mathcal{H}^1$-norm) are achieved for all degrees ($m = 1 : 3$) for both u and q_1.

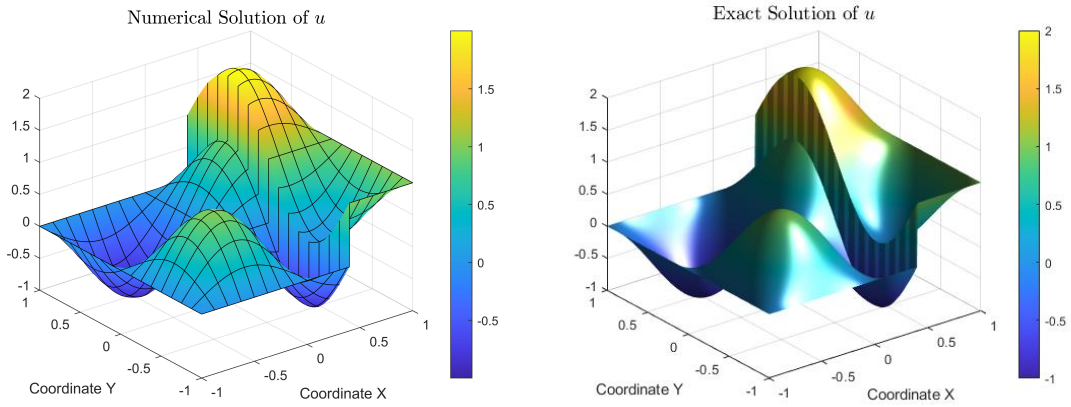

Figure 3.5: Example 2: The numerical solution of u obtained on the fourth mesh with quadrilaterals of order $m = 3$ (left) and the analytical solution (right).

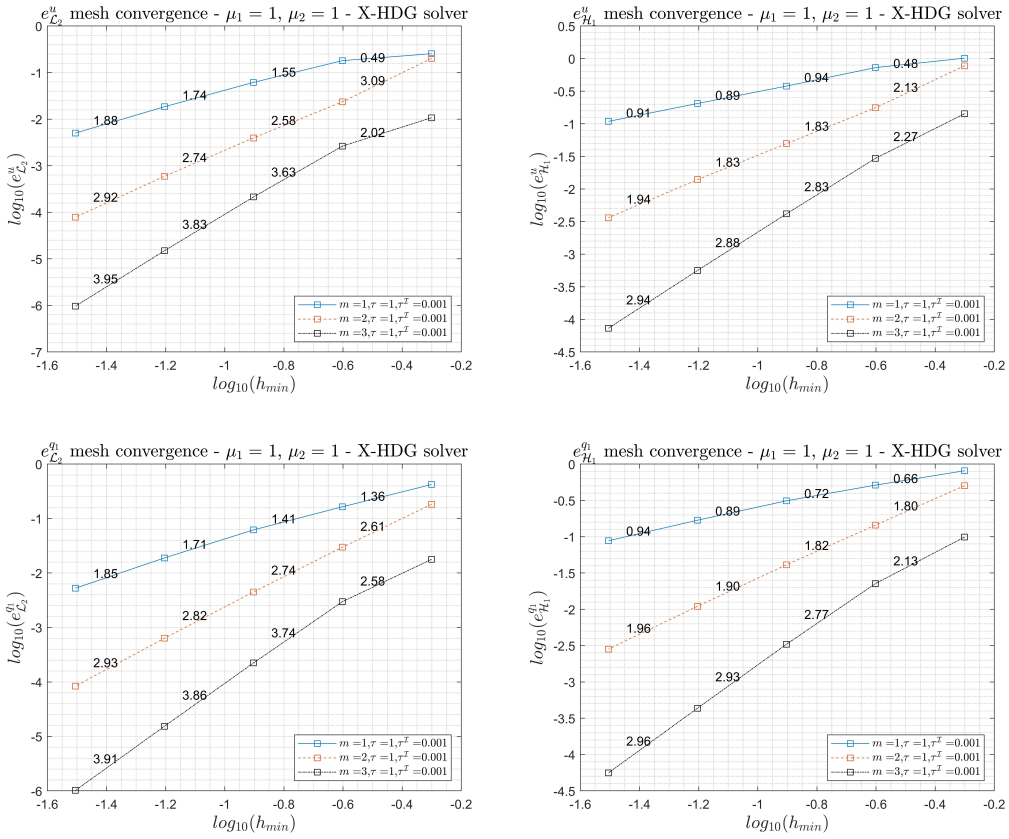

Figure 3.6: Example 2: Errors in u (top) and q_1 (bottom) vs. mesh size - $\mathcal{L}_2$-norm (left), $\mathcal{H}^1$-norm (right).

Checking the quality of cuts and conditioning:
For each mesh, the percentage of cut elements with bad-cuts is recorded in Table 3.3 alongside with the minimum volume ratio among all cut elements in a given mesh. Furthermore, the condition numbers of the X-HDG global matrices for all the orders of approximation and each mesh refinement are recorded in Table 3.4.

Mesh QUADs	% of cut elements with volume ratio < 0.1	$min(V_i/V)$
mesh 1	0.00	0.40
mesh 2	0.00	0.20
mesh 3	0.00	0.40
mesh 4	0.00	0.20
mesh 5	0.00	0.40

Table 3.3: Example 2: Analysis of cuts in each mesh.

Mesh QUADs	$m = 1$	$m = 2$	$m = 3$
mesh 1	1.35E+02	5.85E+03	4.96E+05
mesh 2	1.36E+03	4.43E+05	1.38E+08
mesh 3	6.58E+02	2.40E+04	1.34E+06
mesh 4	4.14E+03	1.23E+06	3.40E+08
mesh 5	4.21E+03	8.82E+04	4.32E+06

Table 3.4: Example 2: Condition number of the X-HDG global matrix.

3.6.3 Example 3: circular interface with zero jump conditions

Next, an example with a circular interface is considered to show the effect of the order of approximation of the interface on the results. Here, a linear approximation of the interface in each cut triangular element is considered regardless of the degree approximation of the solution. A circular interface $\mathcal{I}$ with radius $R = 0.41053$ divides a square domain $\Omega = [-1, 1]^2$ into two regions, Ω_1 and Ω_2, as shown in Figure 3.7 (left). The material properties and the analytical solution, shown in Figure 3.7 (right), are given as:

$$\mu(\boldsymbol{x}) = \begin{cases} \mu_1 = 100 & \text{in } \Omega_1 \\ \mu_2 = 1 & \text{in } \Omega_2 \end{cases} \qquad u(\boldsymbol{x}) = \begin{cases} \dfrac{1}{\mu_1}(x^2+y^2)^{5/2} & \text{in } \Omega_1 \\ \dfrac{1}{\mu_2}(x^2+y^2)^{5/2} + \left(\dfrac{1}{\mu_1} - \dfrac{1}{\mu_2}\right) R^5 & \text{in } \Omega_2 \end{cases}$$

The corresponding source term is $s = -25(x^2 + y^2)^{3/2}$. Finally, Dirichlet boundary conditions are set everywhere on the boundary except for the bottom boundary which is subject to the Neumann boundary conditions (flux from the analytical solution).

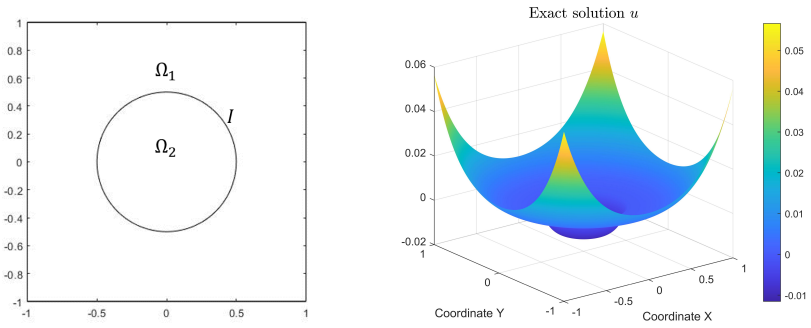

Figure 3.7: Example 3: Square domain with circular interface (left), analytical solution (right).

The problem is solved on five meshes of triangles and the order of approximation is varied from $m = 1$ to $m = 3$. The stabilization parameters introduced in the HDG numerical fluxes are set as $\tau = 50$ and $\tau^{\mathcal{I}} = 1/\{\mu\}$. The mesh convergence plots for the solution u and the flux component q_1 are shown in Figure 3.8. Furthermore, the numerical solution of u and q_1 obtained on the fourth mesh with triangles of order $m = 3$ is shown in Figure 3.9.

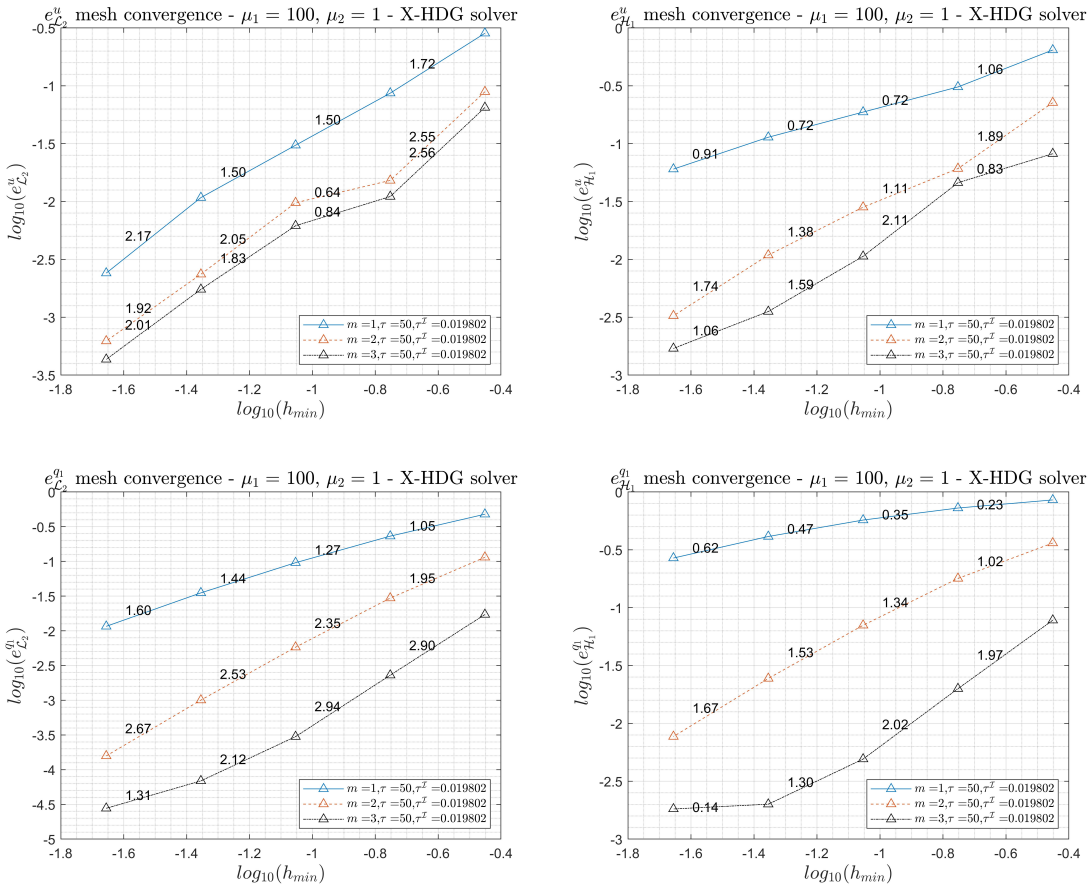

Figure 3.8: Example 3: Errors in u (top) and q_1 (bottom) vs. mesh size - $\mathcal{L}_2$-norm (left), $\mathcal{H}^1$-norm (right) - Meshes of triangles.

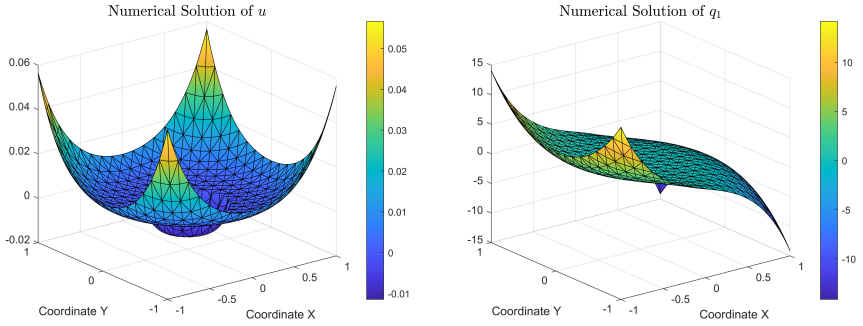

Figure 3.9: Example 3: The numerical solution of u and q_1 obtained on the fourth mesh with triangles of order $m = 3$.

It is noticed that optimal convergence of order ($m+1$ in $\mathcal{L}_2$-norm, m in $\mathcal{H}^1$-norm) is achieved for the solution u and slightly less for the flux component q_1, only for the linear ($m=1$) approximation, while the convergence is deteriorated for all the higher degrees ($m=2:3$). The reason is that linear approximation of the interface in each cut element is considered, which results in higher dominant local errors near the approximated interface thus leading to the loss of the optimal convergence rates for higher order approximations of the solution. In order to retain the optimal convergence rates for higher orders, it is a must that the interface is approximated with higher order as well, at least the same order as the elemental solution.

Checking the quality of cuts and conditioning for triangular meshes:
For each mesh, the percentage of cut elements with bad-cuts is recorded in Table 3.5 alongside with the minimum volume ratio among all cut elements in a given mesh.

Mesh TRIs	% of cut elements with volume ratio < 0.1	$min(V_i/V)$
mesh 1	00.00	0.24
mesh 2	20.00	0.06
mesh 3	12.50	0.09
mesh 4	06.25	0.02
mesh 5	03.12	0.09

Table 3.5: Example 3: Analysis of cuts in each mesh - Meshes of triangles.

The condition numbers of the X-HDG global matrices for all the orders of approximation and each mesh refinement are recorded in Table 3.6.

Mesh TRIs	$m=1$	$m=2$	$m=3$
mesh 1	3.02E+04	3.86E+05	1.17E+07
mesh 2	1.20E+05	5.40E+07	4.73E+10
mesh 3	6.77E+05	8.08E+08	4.69E+12
mesh 4	2.63E+05	1.07E+08	1.04E+12
mesh 5	2.30E+06	6.97E+09	1.84E+14

Table 3.6: Example 3: Condition number of the X-HDG global matrix - Meshes of triangles.

Note that the bad conditioning associated with $m=3$ and the last two meshes led to the respective degraded convergence of the flux component q_1 as seen in Figure 3.8.
Quadrilateral meshes:
The same problem is solved again but on quadrilateral meshes. Five meshes are used. For modifying the integration quadrature in cut elements, the high-order subdivision method developed by Robert Saye [54] is used.
The mesh convergence plots for the solution u and the flux component q_1 are shown in Figure 3.10. Again, optimal convergence of order ($m+1$ in $\mathcal{L}_2$-norm, m in $\mathcal{H}^1$-norm) is achieved for the solution u and slightly less for the flux component q_1, for all degrees ($m=1:3$).

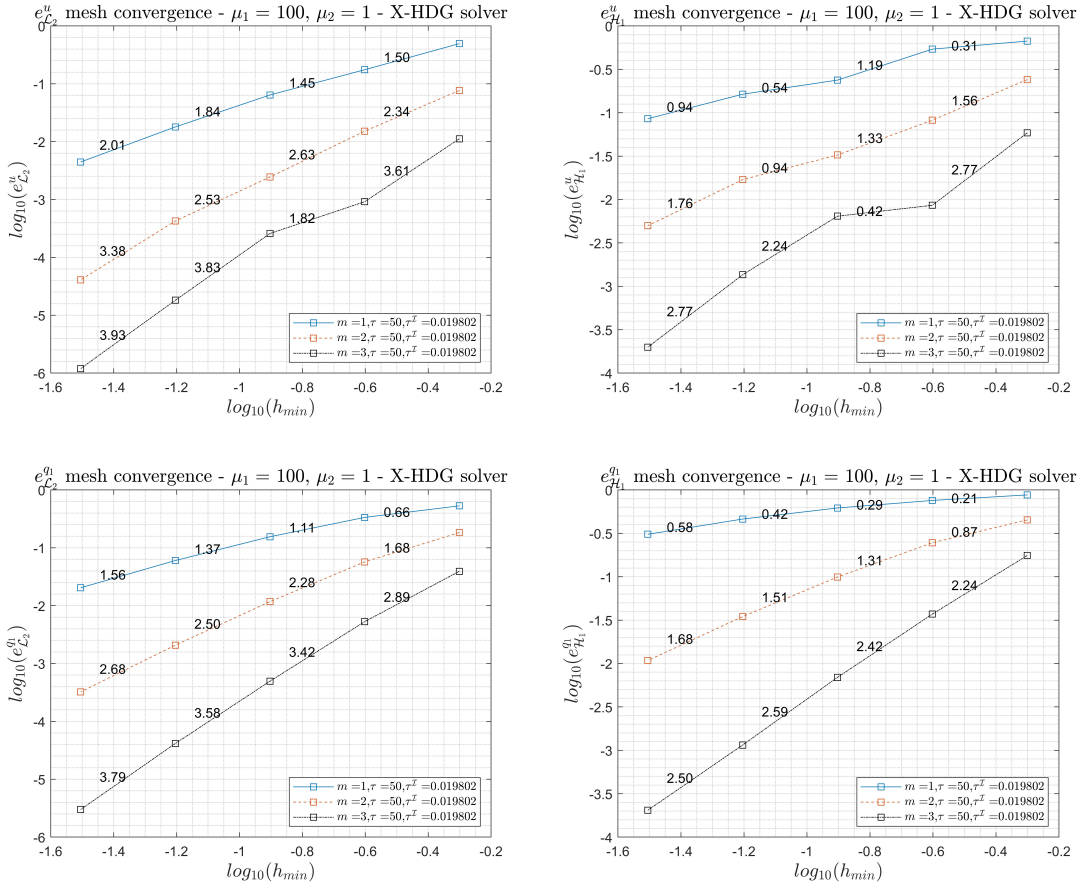

Figure 3.10: Example 3: Errors in u (top) and q_1 (bottom) vs. mesh size - $\mathcal{L}_2$-norm (left), $\mathcal{H}^1$-norm (right) - Meshes of quadrilaterals.

Checking the quality of cuts and conditioning for quadrilateral meshes:
The condition numbers of the X-HDG global matrices for all the orders of approximation and each mesh refinement are recorded in Table 3.7.

Mesh QUADs	$m = 1$	$m = 2$	$m = 3$
mesh 1	2.06E+04	2.28E+05	7.87E+06
mesh 2	2.93E+03	1.36E+05	4.83E+07
mesh 3	2.69E+04	1.02E+06	9.08E+07
mesh 4	1.93E+05	1.03E+08	3.09E+11
mesh 5	5.61E+04	9.26E+06	1.40E+10

Table 3.7: Example 3: Condition number of the X-HDG global matrix - Meshes of quadrilaterals.

3.7 Conclusions and final remarks

In this chapter, the X-HDG method is presented for bi-material Poisson problem. The main objective is to explain the concepts used to extend the standard HDG formulation to solve bi-material problems with possible discontinuities at the interface using unfitted meshes. It should be mentioned that this chapter does not contain any novelty. However, it was a fundamental step to understand the method and identify challenges for complex practical applications. Detailed derivation of the weak forms for the local problems in both cut and standard elements is presented. The unique idea behind the X-HDG method is the introduction of the trace of primal variable, of the same degree m, on the interface to enforce the transmission condition. Understanding those concepts for a simple problem like Poisson is essential for the development of the method to solve more complex problems such as incompressible Stokes and Navier-Stokes equations that will be presented in the next chapters.

The results obtained in the presented numerical examples showed high-order optimal convergence rates for problems with straight interface. For problems with curved interfaces, high-order optimal convergence rates were obtained as long as the interface is represented accurately, i.e. with the same degree m as the solution. This was only feasible for quadrilateral elements due to the presence of open-source codes that provide high-order integration quadrature in elements with curved cuts. As for triangles, only piece-wise linear approximation of the interface is considered. Developing higher-order integration quadrature for triangles with curved cuts is considered as future work.

Chapter 4

Divergence-free X-HDG method for two-phase Stokes flow problem

4.1 Problem statement

The incompressible two-phase Stokes flow problem is described by the following momentum and mass conservation equations:

$$\begin{cases} \boldsymbol{\nabla}\cdot(p\boldsymbol{I} - 2\mu\boldsymbol{\nabla}^s\boldsymbol{u}) = \rho\boldsymbol{f} & \text{in } \overline{\Omega_1}\cup\overline{\Omega_2}, \\ \boldsymbol{\nabla}\cdot\boldsymbol{u} = 0 & \text{in } \overline{\Omega_1}\cup\overline{\Omega_2}. \end{cases} \tag{4.1.1}$$

where p is the pressure field, $\boldsymbol{u}$ is the velocity field, $\boldsymbol{f}$ represents the volumetric body forces, ρ and μ are the density and the dynamic viscosity, respectively, that are discontinuous across the interface $\mathcal{I}$ (that is, $\rho = \rho_i$ and $\mu = \mu_i$ in Ω_i for $i = 1, 2$). Furthermore, $\boldsymbol{\nabla}^s\boldsymbol{u}$ is the symmetric part of the velocity gradient tensor given as $\boldsymbol{\nabla}^s\boldsymbol{u} = \frac{1}{2}(\boldsymbol{\nabla}\boldsymbol{u} + (\boldsymbol{\nabla}\boldsymbol{u})^T)$, and $\boldsymbol{I}$ is the identity tensor of size $d \times d$.

The previous set of equations can be written in a form that is normalized by the density, by dividing the momentum equation by ρ we get

$$\begin{cases} \boldsymbol{\nabla}\cdot(P\boldsymbol{I} - 2\nu\boldsymbol{\nabla}^s\boldsymbol{u}) = \boldsymbol{f} & \text{in } \overline{\Omega_1}\cup\overline{\Omega_2}, \\ \boldsymbol{\nabla}\cdot\boldsymbol{u} = 0 & \text{in } \overline{\Omega_1}\cup\overline{\Omega_2}. \end{cases} \tag{4.1.2}$$

where $P = p/\rho$ is the thermodynamic pressure (sometimes called kinematic pressure [56, Chapter 6]) and ν is the kinematic viscosity which is discontinuous across the interface $\mathcal{I}$ as well, that is $\nu = \nu_i$ in Ω_i for $i = 1, 2$.

Boundary conditions:

- Dirichlet:

$$\boldsymbol{u} = \boldsymbol{u}_D \qquad \text{on } \Gamma_D \tag{4.1.3}$$

- Neumann:

$$(P\boldsymbol{I} - 2\nu\boldsymbol{\nabla}^s\boldsymbol{u})\,\boldsymbol{n} = \boldsymbol{g}_N \qquad \text{on } \Gamma_N \tag{4.1.4}$$

where $\boldsymbol{u}_D$ is a prescribed value of the velocity on the Dirichlet boundary Γ_D, while $\boldsymbol{g}_N$ is a prescribed normal flux on the Neumann boundary Γ_N.

Interface conditions: The interface conditions between two viscous and immiscible fluids are [57]:

- Surface tension force balancing the jump in normal stress

$$[\![(P\boldsymbol{I} - 2\nu\boldsymbol{\nabla}^s\boldsymbol{u})\,\boldsymbol{n}]\!] = \boldsymbol{g}_s \quad \text{on} \quad \mathcal{I} \tag{4.1.5}$$

  where $\boldsymbol{g}_s$ is the surface tension force vector.

- Continuity of the velocity

$$[\![\boldsymbol{u}]\!] = 0 \quad \text{on} \quad \mathcal{I} \tag{4.1.6}$$

  where the jump $[\![\boldsymbol{u}]\!]$ is defined as $[\![\boldsymbol{u}]\!] := \boldsymbol{u}_{\Omega_1\cap\mathcal{I}} - \boldsymbol{u}_{\Omega_2\cap\mathcal{I}} := \boldsymbol{u}_1 - \boldsymbol{u}_2$

Note that the jump in density and viscosity (both dynamic and kinematic) across the interface, in addition to the surface tension force, lead to non-smooth field variables at the interface. First, the interface condition 4.1.6 states that the normal component of the velocity $u_n = \boldsymbol{u}\cdot\widehat{\boldsymbol{n}}$ and the tangential velocity component $u_s = \boldsymbol{u}\cdot\widehat{\boldsymbol{t}}$ must be continuous across the interface. However, it can be shown that the normal gradient $\frac{\partial}{\partial n}$ of the tangential velocity is discontinuous [58, 15]

$$[\![\frac{\partial u_s}{\partial n}]\!]_{\mathcal{I}} = -[\![\mu]\!]_{\mathcal{I}}\frac{\partial u_n}{\partial s} \tag{4.1.7}$$

where $\frac{\partial}{\partial s}$ is the tangential derivative. This means that the velocity has a kink across the interface if $\mu_1 \neq \mu_2$.

Furthermore, if we pre-multiply the surface tension condition by the normal vector to the interface $\widehat{\boldsymbol{n}}$ (pointing from Ω_1 to Ω_2) we can get an expression for the pressure jump at the interface as

$$\widehat{\boldsymbol{n}}\cdot(P_1\widehat{\boldsymbol{n}} - 2\nu_1\boldsymbol{\nabla}^s\boldsymbol{u}_1\cdot\widehat{\boldsymbol{n}} + P_2(-\widehat{\boldsymbol{n}}) - 2\nu_2\boldsymbol{\nabla}^s\boldsymbol{u}_2\cdot(-\widehat{\boldsymbol{n}})) = \widehat{\boldsymbol{n}}\cdot\boldsymbol{g}_s, \tag{4.1.8}$$

$$\leftrightarrow\ P_1 - 2\nu_1\widehat{\boldsymbol{n}}\cdot\boldsymbol{\nabla}^s\boldsymbol{u}_1\cdot\widehat{\boldsymbol{n}} - P_2 + 2\nu_2\widehat{\boldsymbol{n}}\boldsymbol{\nabla}^s\boldsymbol{u}_2\cdot\widehat{\boldsymbol{n}} = \widehat{\boldsymbol{n}}\cdot\boldsymbol{g}_s, \tag{4.1.9}$$

$$\leftrightarrow\ \widehat{\boldsymbol{n}}\cdot\boldsymbol{g}_s + 2\nu_1\widehat{\boldsymbol{n}}\cdot\boldsymbol{\nabla}^s\boldsymbol{u}_1\cdot\widehat{\boldsymbol{n}} - 2\nu_2\widehat{\boldsymbol{n}}\boldsymbol{\nabla}^s\boldsymbol{u}_2\cdot\widehat{\boldsymbol{n}} = P_1 - P_2. \tag{4.1.10}$$

Therefore the discontinuity in velocity gradient and the pressure at the interface has to be accounted for in the approximation.

4.2 The divergence-free X-HDG method

It is crucial to use an energy-stable numerical method for simulations featuring high Reynolds number or unsteady flows [37]. An energy-stable method satisfies two conditions: the point-wise divergence-free condition and the velocity field should be $\mathcal{H}(div)$-conforming, meaning that the jump in the normal velocity is zero across inter-element faces and the interface between the two fluids. An energy-stable HDG method for single-phase flow which yields point-wise exactly divergence-free velocity fields was developed by Rhebergen and Wells [34] for triangular and tetrahedral elements, and it was further developed and extended to quadrilateral and hexahedral elements by Elzaabalawy [35] and Elzaabalawy et al. [36].

The divergence-free HDG [34, 35, 36] is different from the standard HDG [28, 33] in two aspects; First, the pressure trace $\widehat{P}$ is introduced into the formulation as an extra global unknown on the mesh skeleton to enforce the transmission condition of the continuity

equation, i.e. enforce $[\![\boldsymbol{u}\cdot\boldsymbol{n}]\!]_\Gamma = 0$, this pressure trace has the same order of approximation as the velocity trace $\widehat{\boldsymbol{u}}$ in order to ensure that the velocity field is $\mathcal{H}(div)$-conforming. Second, the pressure inside each element is approximated using polynomials in the space of velocity divergence, i.e. $P(K_i) \in \mathcal{S}_v^{div}$. For triangular (2D) or tetrahedral (3D) elements, the divergence-free element corresponding to a velocity element of order m is an element of order $(m-1)$ [34]. However, this is not the case for quadrilateral (2D) or hexahedral (3D) elements, therefore, some specifically tailored elements are made to satisfy the divergence-free condition of the velocity field [35, 36]. This development was made for uniform rectangular/cubic elements without curved edges/faces.

When it comes to the two-phase incompressible flow problems, the standard eXtended HDG (standard X-HDG) method is firstly introduced by Gürkan et al. [38]. This method is an extension of the standard HDG formulation [28, 33]. i.e. it does not satisfy the divergence-free condition exactly. The standard X-HDG is known for the introduction of the velocity trace $\widetilde{\boldsymbol{u}}$ as an extra unknown on the material interface to enforce the transmission or jump conditions of the momentum equation across the material interface, i.e. enforce $[\![(P\boldsymbol{I} - 2\nu\boldsymbol{\nabla}^s\boldsymbol{u})\,\boldsymbol{n}]\!]_{\mathcal{I}} = \boldsymbol{g}_s$.

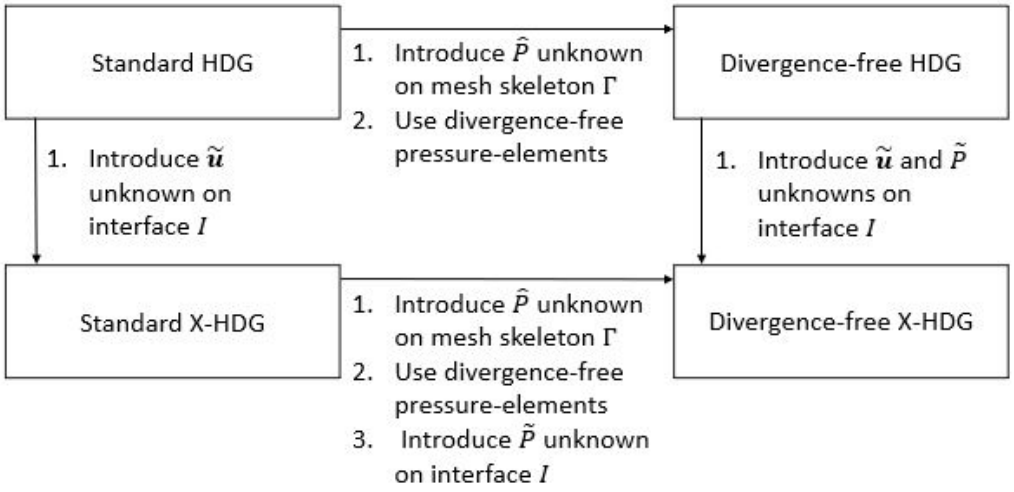

Figure 4.1: A summary of the formulations.

The novelty of this work which is presented in this section is the extension of the divergence-free HDG method to solve two-phase incompressible flow problems. The proposed method, referred to as divergence-free X-HDG, combines the concepts of the divergence-free HDG [34, 35] and the standard X-HDG [38] methods. First, it inherits the introduction of the pressure trace $\widehat{P}$ as an extra global unknown of the same order of the velocity trace $\widehat{\boldsymbol{u}}$ on the mesh skeleton. Second, divergence-free pressure-elements are used. Finally, the novel aspect of this method is that it introduces the pressure trace $\widetilde{P}$ as an extra unknown on the interface between the two fluids (to enforce $[\![\boldsymbol{u}\cdot\boldsymbol{n}]\!]_{\mathcal{I}} = 0$) alongside with the velocity trace $\widetilde{\boldsymbol{u}}$, where again both traces $\widetilde{P}$ and $\widetilde{\boldsymbol{u}}$ are of the same order of approximation. Note that the order of approximation for all the traces $\widehat{P}$, $\widehat{\boldsymbol{u}}$, $\widetilde{P}$ and $\widetilde{\boldsymbol{u}}$ is the same order of approximation of the velocity inside elements. See Figure 4.1 that sums up the developments made to reach the proposed method.

4.2.1 The mixed strong form

The strong form presented earlier by (4.1.2) can be written as a system of first order equations by introducing the tensor variable $\boldsymbol{L} = -2\boldsymbol{\nabla}^s\boldsymbol{u}$, for a generic finite element

$K_i \in \overline{\Omega}$ as:

$$
\begin{cases}
\boldsymbol{\nabla}\cdot(P\boldsymbol{I}+\nu\boldsymbol{L}) = \boldsymbol{f} & \text{in } K_i \setminus \mathcal{I}, \\
\boldsymbol{L} + 2\boldsymbol{\nabla}^s\boldsymbol{u} = \boldsymbol{0} & \text{in } K_i \setminus \mathcal{I}, \\
\boldsymbol{\nabla}\cdot\boldsymbol{u} = 0 & \text{in } K_i \setminus \mathcal{I}, \\
\boldsymbol{u} = \boldsymbol{u}_D & \text{on } \partial K_i \cap \Gamma_D, \\
(P\boldsymbol{I}+\nu\boldsymbol{L})\,\boldsymbol{n} = \boldsymbol{g}_N & \text{on } \partial K_i \cap \Gamma_N, \\
[\![(P\boldsymbol{I}+\nu\boldsymbol{L})\,\boldsymbol{n}]\!] = \boldsymbol{g}_s & \text{on } \mathcal{I}_i, \\
[\![\boldsymbol{u}\cdot\boldsymbol{n}]\!] = 0 & \text{on } \mathcal{I}_i.
\end{cases}
\tag{4.2.1}
$$

where $\mathcal{I}_i := K_i \cap \mathcal{I}$ is the part of the interface in element K_i (if K_i is a cut element).

4.2.2 X-HDG strong local and global problems

The *divergence-free X-HDG* method rewrites (4.2.1) as two equivalent problems. First the **local element-by-element problem** with Dirichlet boundary conditions, that is,

$$
\left.
\begin{aligned}
\boldsymbol{\nabla}\cdot(P\boldsymbol{I}+\nu\boldsymbol{L}) &= \boldsymbol{f} && \text{in } K_i \setminus \mathcal{I}, \\
\boldsymbol{L} + 2\boldsymbol{\nabla}^s\boldsymbol{u} &= \boldsymbol{0} && \text{in } K_i \setminus \mathcal{I}, \\
\boldsymbol{\nabla}\cdot\boldsymbol{u} &= 0 && \text{in } K_i \setminus \mathcal{I}, \\
\boldsymbol{u} &= \boldsymbol{u}_D && \text{on } \partial K_i \cap \Gamma_D, \\
\boldsymbol{u} &= \widehat{\boldsymbol{u}} && \text{on } \partial K_i \setminus \Gamma_D, \\
P &= P_N && \text{on } \partial K_i \cap \Gamma_N, \\
P &= \widehat{P} && \text{on } \partial K_i \setminus \Gamma_N, \\
[\![(P\boldsymbol{I}+\nu\boldsymbol{L})\,\boldsymbol{n}]\!] &= \boldsymbol{g}_s && \text{on } \mathcal{I}_i, \\
[\![\boldsymbol{u}\cdot\boldsymbol{n}]\!] &= 0 && \text{on } \mathcal{I}_i.
\end{aligned}
\right\} \text{ if } K_i \cap \mathcal{I} \neq \emptyset
\tag{4.2.2}
$$

for $i = 1, ..., \mathtt{n_{el}}$. A new variable $\widehat{\boldsymbol{u}} \in \mathcal{V}_s^h(\Gamma \setminus \Gamma_D)$ is introduced which corresponds to the trace of $\boldsymbol{u}$ at the mesh faces $\Gamma \setminus \Gamma_D$. The trace $\widehat{\boldsymbol{u}}$ is single valued variable on each face, with the same value when seen from both sides of an interior face. It is noted here that an extra equation has been introduced which corresponds to imposing the thermodynamic pressure on the boundary of the element to a newly introduced variable $\widehat{P} \in \mathcal{S}_s^h(\Gamma \setminus \Gamma_N)$ which corresponds to the trace of P at the mesh faces $\Gamma \setminus \Gamma_N$.

For standard X-HDG, we introduce the velocity trace $\widetilde{\boldsymbol{u}}$ as an extra unknown on the material interface to enforce the transmission or jump condition of the momentum equation across the material interface, i.e. enforce $[\![(P\boldsymbol{I}+\nu\boldsymbol{L})\,\boldsymbol{n}]\!]_{\mathcal{I}} = \boldsymbol{g}$. Furthermore, for divergence-free X-HDG, we also introduce the pressure trace $\widetilde{P}$ as an extra unknown on the material interface to enforce the transmission condition of the continuity equation across the material interface, i.e. enforce $[\![\boldsymbol{u}\cdot\boldsymbol{n}]\!]_{\mathcal{I}} = 0$. Note that $\widetilde{\boldsymbol{u}}$ and $\widetilde{P}$ are continuous functions defined on the interface. They act as Shuhr complements that are eliminated after solving for them. The reader is invited to read Appendix C for more details.

Given the traces $(\widehat{\boldsymbol{u}}, \widehat{P})$ and the boundary conditions $(\boldsymbol{u}_D, P_N)$, the local problems (4.2.2) can be solved in each element to determine the solution $\boldsymbol{u} \in \mathcal{V}_v^h(\Omega)$, $P \in \mathcal{S}_v^{div\,h}(\Omega)$ and the flux $\boldsymbol{L} \in \mathcal{T}_v^h(\Omega)$. Thus, the problem now reduces to the determination of the traces $(\widehat{\boldsymbol{u}}, \widehat{P})$. This is done by solving a **global problem** that imposes the transmission conditions (of the momentum and continuity equations) across element boundaries plus

the Neumann boundary conditions, that is,

$$\text{from momentum eqn.:} \begin{cases} [\![(P\boldsymbol{I}+\nu\boldsymbol{L})\,\boldsymbol{n}]\!] = \boldsymbol{0} & \text{on } \Gamma \setminus \partial\Omega, \\ (P\boldsymbol{I}+\nu\boldsymbol{L})\,\boldsymbol{n} = \boldsymbol{g}_N & \text{on } \Gamma_N, \end{cases}$$

(4.2.3)

$$\text{from continuity eqn.:} \begin{cases} [\![\boldsymbol{u}\cdot\boldsymbol{n}]\!] = 0 & \text{on } \Gamma \setminus \partial\Omega, \\ \boldsymbol{u}\cdot\boldsymbol{n} = \boldsymbol{u}_D\cdot\boldsymbol{n} & \text{on } \Gamma_D, \\ \boldsymbol{u}\cdot\boldsymbol{n} = \widehat{\boldsymbol{u}}\cdot\boldsymbol{n} & \text{on } \Gamma_N \end{cases}$$

4.2.3 X-HDG weak forms

Briefly, the weak forms are obtained by the following steps:

- First: multiply the governing equations by corresponding test functions and integrate over the two sub-domains (two phases).
- Second: apply integration by parts once to obtain surface integrals. Only in the first equation of 4.2.2, integration by parts is done twice for the viscous term.
- Third: replace the physical fluxes by some defined numerical fluxes, this is where stabilization parameters appear.

The detailed derivation of the weak forms is presented in details in Appendix D for the full transient Navier-Stokes equations. By neglecting both the transient and convective terms, Stokes flow equations are obtained.
Note that in a cut element, the approximations of the functions $(\boldsymbol{u}, \boldsymbol{L}, P)$ are discontinuous.
$\boldsymbol{u} \in [\mathcal{P}^m(K_i)]^d \oplus H[\mathcal{P}^m(K_i)]^d$,
$\boldsymbol{L} \in [\mathcal{P}^m(K_i)]^{d\times d} \oplus H[\mathcal{P}^m(K_i)]^{d\times d}$ and
$P \in \boldsymbol{\nabla}\cdot[\mathcal{P}^m(K_i)]^d \oplus H\boldsymbol{\nabla}\cdot[\mathcal{P}^m(K_i)]^d$.

In the divergence-free X-HDG method, the physical quantities $(\boldsymbol{u}, \boldsymbol{L}, P)$ are replaced by the numerical quantities $(\widehat{\boldsymbol{u}}, \widehat{\boldsymbol{L}}, \widehat{P})$ on $\partial K_i \setminus \Gamma_D$. Further, on the interface $\mathcal{I}_i$, the physical quantities $(\boldsymbol{u}, \boldsymbol{L}_1, \boldsymbol{L}_2, P_1, P_2)$ are replaced by the numerical quantities $(\widetilde{\boldsymbol{u}}^i, \widetilde{\boldsymbol{L}}_1^i + \boldsymbol{\delta}_{\boldsymbol{L}}, \widetilde{\boldsymbol{L}}_2^i, \widetilde{P}^i + \delta_P, \widetilde{P}^i)$. Furthermore, on the intersection with the Dirichlet boundary $\partial K_i \cap \Gamma_D$, the physical quantities $(\boldsymbol{u}, \boldsymbol{L}, P)$ are replaced by $(\boldsymbol{u}_D, \widehat{\boldsymbol{L}}_D, \widehat{P})$. Finally, that pressure trace $\widehat{P}$ is replaced by P_N on the Neumann boundary $\partial K_i \setminus \Gamma_N$.
Note that the discontinuities in the velocity gradient and the pressure across the interface are taken into consideration by introducing the two variables δ_P and $\boldsymbol{\delta}_{\boldsymbol{L}}$. Those two variables are replaced in the weak forms by the surface tension force vector where $\delta_P\widehat{\boldsymbol{n}} + \nu_1\boldsymbol{\delta}_{\boldsymbol{L}}\widehat{\boldsymbol{n}} = \boldsymbol{g}_s$.

Furthermore, the numerical fluxes used in the weak forms are defined as:

$$\widehat{\boldsymbol{L}} := \boldsymbol{L} + \tau(\boldsymbol{u}-\widehat{\boldsymbol{u}})\otimes\boldsymbol{n} + \tau\boldsymbol{n}\otimes(\boldsymbol{u}-\widehat{\boldsymbol{u}}) \qquad \text{on } \Gamma\setminus\Gamma_D, \tag{4.2.4a}$$

$$\widehat{\boldsymbol{L}}_D := \boldsymbol{L} + \tau(\boldsymbol{u}-\boldsymbol{u}_D)\otimes\boldsymbol{n} + \tau\boldsymbol{n}\otimes(\boldsymbol{u}-\boldsymbol{u}_D) \qquad \text{on } \Gamma_D, \tag{4.2.4b}$$

$$\widetilde{\boldsymbol{L}}_1^i := \boldsymbol{L}_1 + \tau^{\mathcal{I}}(\boldsymbol{u}_1-\widetilde{\boldsymbol{u}}^i)\otimes\widehat{\boldsymbol{n}} + \tau^{\mathcal{I}}\widehat{\boldsymbol{n}}\otimes(\boldsymbol{u}_1-\widetilde{\boldsymbol{u}}^i) \qquad \text{on } \mathcal{I}|_{\Omega_1}, \tag{4.2.4c}$$

$$\widetilde{\boldsymbol{L}}_2^i := \boldsymbol{L}_2 - \tau^{\mathcal{I}}(\boldsymbol{u}_2-\widetilde{\boldsymbol{u}}^i)\otimes\widehat{\boldsymbol{n}} - \tau^{\mathcal{I}}\widehat{\boldsymbol{n}}\otimes(\boldsymbol{u}_2-\widetilde{\boldsymbol{u}}^i) \qquad \text{on } \mathcal{I}|_{\Omega_2}, \tag{4.2.4d}$$

where $\widehat{\boldsymbol{u}} \in \mathcal{V}_s^h(\Gamma_{ij})$ and $\widehat{P} \in \mathcal{S}_s^h(\Gamma_{ij})$ could be continuous (if $\Gamma_{ij}\cap\mathcal{I} = \emptyset$) or discontinuous (if $\Gamma_{ij}\cap\mathcal{I} \neq \emptyset$) functions. Γ_{ij} is face j of element K_i. $\widetilde{\boldsymbol{u}}^i \in [\mathcal{P}^m(\mathcal{I}_i)]^d$ is a continuous vector function defined on the interface $\mathcal{I}$. $\widetilde{P}^i \in \mathcal{P}^m(\mathcal{I}_i)$ is a continuous scalar function defined on the interface $\mathcal{I}$. τ and $\tau^{\mathcal{I}}$ are stabilization parameters for the viscous flux on the

element faces ∂K_i and the material interface $\mathcal{I}_i$, respectively. The choice of the stabilization parameter τ is discussed extensively in [35, 59] for the uncut elements. Based on several numerical trials, the interface stabilization parameter has to be inversely proportional to the average of ν to ensure optimal convergence, for instance $\tau^{\mathcal{I}} := 1/\{\nu\}$.

Weak local problems in cut elements

The weak form of the local problems in cut elements is: given $\widehat{\boldsymbol{u}} \in \mathcal{V}_s^h(\Gamma_{ij} \setminus \Gamma_D)$, $\boldsymbol{u}_D \in \mathcal{V}_s(\Gamma_{ij} \cap \Gamma_D)$, $\widehat{P} \in \mathcal{S}_s^h(\Gamma_{ij} \setminus \Gamma_N)$ and $P_N \in \mathcal{S}_s^h(\Gamma_{ij} \cap \Gamma_N)$, where Γ_{ij} is the face j (which could be cut or uncut) of element K_i, find $\boldsymbol{u} \in [\mathcal{P}^m(K_i)]^d \oplus H[\mathcal{P}^m(K_i)]^d$, $\boldsymbol{L} \in [\mathcal{P}^m(K_i)]^{d\times d} \oplus H[\mathcal{P}^m(K_i)]^{d\times d}$, $P \in \boldsymbol{\nabla}\cdot[\mathcal{P}^m(K_i)]^d \oplus H\boldsymbol{\nabla}\cdot[\mathcal{P}^m(K_i)]^d$, $\widetilde{\boldsymbol{u}}^i \in [\mathcal{P}^m(\mathcal{I}_i)]^d$, and $\widetilde{P}^i \in \mathcal{P}^m(\mathcal{I}_i)$ such that

(4.2.5a)
$$
\begin{aligned}
&\left(\boldsymbol{\psi}, \boldsymbol{\nabla}\cdot(\nu\boldsymbol{L})\right)_{K_i} - \left(\boldsymbol{\nabla}\boldsymbol{\psi}, P\boldsymbol{I}\right)_{K_i} + \langle \boldsymbol{\psi}, \nu\tau\boldsymbol{u}\rangle_{\partial K_i} + \langle \boldsymbol{\psi}, \nu\tau(\boldsymbol{u}\cdot\boldsymbol{n})\boldsymbol{n}\rangle_{\partial K_i} + \langle \boldsymbol{\psi}_1 - \boldsymbol{\psi}_2, \widetilde{P}^i\widehat{\boldsymbol{n}}\rangle_{\mathcal{I}_i} \\
&+ \langle \boldsymbol{\psi}_1, \nu_1\tau^{\mathcal{I}}\boldsymbol{u}_1\rangle_{\mathcal{I}_i} - \langle \boldsymbol{\psi}_1, \nu_1\tau^{\mathcal{I}}\widetilde{\boldsymbol{u}}^i\rangle_{\mathcal{I}_i} + \langle \boldsymbol{\psi}_1, \nu_1\tau^{\mathcal{I}}(\boldsymbol{u}_1\cdot\widehat{\boldsymbol{n}})\widehat{\boldsymbol{n}}\rangle_{\mathcal{I}_i} - \langle \boldsymbol{\psi}_1, \nu_1\tau^{\mathcal{I}}(\widetilde{\boldsymbol{u}}^i\cdot\widehat{\boldsymbol{n}})\widehat{\boldsymbol{n}}\rangle_{\mathcal{I}_i} \\
&+ \langle \boldsymbol{\psi}_2, \nu_2\tau^{\mathcal{I}}\boldsymbol{u}_2\rangle_{\mathcal{I}_i} - \langle \boldsymbol{\psi}_2, \nu_2\tau^{\mathcal{I}}\widetilde{\boldsymbol{u}}^i\rangle_{\mathcal{I}_i} + \langle \boldsymbol{\psi}_2, \nu_2\tau^{\mathcal{I}}(\boldsymbol{u}_2\cdot\widehat{\boldsymbol{n}})\widehat{\boldsymbol{n}}\rangle_{\mathcal{I}_i} - \langle \boldsymbol{\psi}_2, \nu_2\tau^{\mathcal{I}}(\widetilde{\boldsymbol{u}}^i\cdot\widehat{\boldsymbol{n}})\widehat{\boldsymbol{n}}\rangle_{\mathcal{I}_i} \\
&= \left(\boldsymbol{\psi}, \boldsymbol{f}\right)_{K_i} - \langle \boldsymbol{\psi}, \widehat{P}\boldsymbol{n}\rangle_{\partial K_i\setminus\Gamma_N} - \langle \boldsymbol{\psi}, P_N\boldsymbol{n}\rangle_{\partial K_i\cap\Gamma_N} - \langle \boldsymbol{\psi}_1, \boldsymbol{g}_s\rangle_{\mathcal{I}_i} \\
&+ \langle \boldsymbol{\psi}, \nu\tau\widehat{\boldsymbol{u}}\rangle_{\partial K_i\setminus\Gamma_D} + \langle \boldsymbol{\psi}, \nu\tau(\widehat{\boldsymbol{u}}\cdot\boldsymbol{n})\boldsymbol{n}\rangle_{\partial K_i\setminus\Gamma_D} + \langle \boldsymbol{\psi}, \nu\tau\boldsymbol{u}_D\rangle_{\partial K_i\cap\Gamma_D} + \langle \boldsymbol{\psi}, \nu\tau(\boldsymbol{u}_D\cdot\boldsymbol{n})\boldsymbol{n}\rangle_{\partial K_i\cap\Gamma_D}
\end{aligned}
$$

(4.2.5b)
$$
\begin{aligned}
&- \left(\boldsymbol{\Psi}, \boldsymbol{L}\right)_{K_i} + \left(\boldsymbol{\nabla}^s\cdot\boldsymbol{\Psi}, \boldsymbol{u}\right)_{K_i} - \langle \boldsymbol{\Psi}_1, \widetilde{\boldsymbol{u}}^i\otimes\widehat{\boldsymbol{n}}\rangle_{\mathcal{I}_i} - \langle \boldsymbol{\Psi}_1, \widehat{\boldsymbol{n}}\otimes\widetilde{\boldsymbol{u}}^i\rangle_{\mathcal{I}_i} + \langle \boldsymbol{\Psi}_2, \widetilde{\boldsymbol{u}}^i\otimes\widehat{\boldsymbol{n}}\rangle_{\mathcal{I}_i} + \langle \boldsymbol{\Psi}_2, \widehat{\boldsymbol{n}}\otimes\widetilde{\boldsymbol{u}}^i\rangle_{\mathcal{I}_i} \\
&= \langle \boldsymbol{\Psi}, \widehat{\boldsymbol{u}}\otimes\boldsymbol{n}\rangle_{\partial K_i\setminus\Gamma_D} + \langle \boldsymbol{\Psi}, \boldsymbol{n}\otimes\widehat{\boldsymbol{u}}\rangle_{\partial K_i\setminus\Gamma_D} + \langle \boldsymbol{\Psi}, \boldsymbol{u}_D\otimes\boldsymbol{n}\rangle_{\partial K_i\cap\Gamma_D} + \langle \boldsymbol{\Psi}, \boldsymbol{n}\otimes\boldsymbol{u}_D\rangle_{\partial K_i\cap\Gamma_D}
\end{aligned}
$$

(4.2.5c)
$$
-\left(\phi, \boldsymbol{\nabla}\cdot\boldsymbol{u}\right)_{K_i} = 0
$$

(4.2.5d)
$$
\begin{aligned}
&\langle \widetilde{\boldsymbol{\psi}}, \nu_1\boldsymbol{L}_1\widehat{\boldsymbol{n}}\rangle_{\mathcal{I}_i} - \langle \widetilde{\boldsymbol{\psi}}, \nu_2\boldsymbol{L}_2\widehat{\boldsymbol{n}}\rangle_{\mathcal{I}_i} \\
&+\langle \widetilde{\boldsymbol{\psi}}, \nu_1\tau^{\mathcal{I}}\boldsymbol{u}_1\rangle_{\mathcal{I}_i} - \langle \widetilde{\boldsymbol{\psi}}, \nu_1\tau^{\mathcal{I}}\widetilde{\boldsymbol{u}}^i\rangle_{\mathcal{I}_i} + \langle \widetilde{\boldsymbol{\psi}}, \nu_1\tau^{\mathcal{I}}(\boldsymbol{u}_1\cdot\widehat{\boldsymbol{n}})\widehat{\boldsymbol{n}}\rangle_{\mathcal{I}_i} - \langle \widetilde{\boldsymbol{\psi}}, \nu_1\tau^{\mathcal{I}}(\widetilde{\boldsymbol{u}}^i\cdot\widehat{\boldsymbol{n}})\widehat{\boldsymbol{n}}\rangle_{\mathcal{I}_i} \\
&+\langle \widetilde{\boldsymbol{\psi}}, \nu_2\tau^{\mathcal{I}}\boldsymbol{u}_2\rangle_{\mathcal{I}_i} - \langle \widetilde{\boldsymbol{\psi}}, \nu_2\tau^{\mathcal{I}}\widetilde{\boldsymbol{u}}^i\rangle_{\mathcal{I}_i} + \langle \widetilde{\boldsymbol{\psi}}, \nu_2\tau^{\mathcal{I}}(\boldsymbol{u}_2\cdot\widehat{\boldsymbol{n}})\widehat{\boldsymbol{n}}\rangle_{\mathcal{I}_i} - \langle \widetilde{\boldsymbol{\psi}}, \nu_2\tau^{\mathcal{I}}(\widetilde{\boldsymbol{u}}^i\cdot\widehat{\boldsymbol{n}})\widehat{\boldsymbol{n}}\rangle_{\mathcal{I}_i} = 0
\end{aligned}
$$

(4.2.5e)
$$
\langle \widetilde{\phi}, \boldsymbol{u}_1\cdot\widehat{\boldsymbol{n}}\rangle_{\mathcal{I}_i} - \langle \widetilde{\phi}, \boldsymbol{u}_2\cdot\widehat{\boldsymbol{n}}\rangle_{\mathcal{I}_i} = 0
$$

for all the test functions $\boldsymbol{\psi} \in [\mathcal{P}^m(K_i)]^d \oplus H[\mathcal{P}^m(K_i)]^d$, $\boldsymbol{\Psi} \in [\mathcal{P}^m(K_i)]^{d\times d} \oplus H[\mathcal{P}^m(K_i)]^{d\times d}$, $\phi \in \boldsymbol{\nabla}\cdot[\mathcal{P}^m(K_i)]^d \oplus H\boldsymbol{\nabla}\cdot[\mathcal{P}^m(K_i)]^d$, $\widetilde{\boldsymbol{\psi}} \in [\mathcal{P}^m(\mathcal{I}_i)]^d$, and $\widetilde{\phi} \in \mathcal{P}^m(\mathcal{I}_i)$.

Weak local problems in standard elements

For a standard uncut element K_i, the weak forms of the local problems are exactly the same as those for a cut element after removing the interface terms. Note that the approximation spaces for all the functions are continuous. i.e. $(\boldsymbol{\psi}, \boldsymbol{u}) \in [\mathcal{P}^m(K_i)]^d$, $(\boldsymbol{\Psi}, \boldsymbol{L}) \in [\mathcal{P}^m(K_i)]^{d\times d}$, $(\phi, P) \in \boldsymbol{\nabla}\cdot[\mathcal{P}^m(K_i)]^d$, $\widehat{\boldsymbol{u}} \in [\mathcal{P}^m(\Gamma_{ij} \setminus \Gamma_D)]^d$ and $\widehat{P} \in \mathcal{P}^m(\Gamma_{ij})$, where Γ_{ij} is the face j of element K_i.
Therefore, the weak form of the local problems in a standard uncut element is: given $(\widehat{\boldsymbol{u}}, \boldsymbol{u}_D, \widehat{P}, P_N)$, find $(\boldsymbol{u}, \boldsymbol{L}, P)$ such that

(4.2.6a)
$$
\begin{aligned}
&\left(\boldsymbol{\psi}, \boldsymbol{\nabla}\cdot(\nu\boldsymbol{L})\right)_{K_i} - \left(\boldsymbol{\nabla}\boldsymbol{\psi}, P\boldsymbol{I}\right)_{K_i} + \langle \boldsymbol{\psi}, \nu\tau\boldsymbol{u}\rangle_{\partial K_i} + \langle \boldsymbol{\psi}, \nu\tau(\boldsymbol{u}\cdot\boldsymbol{n})\boldsymbol{n}\rangle_{\partial K_i} \\
&= \left(\boldsymbol{\psi}, \boldsymbol{f}\right)_{K_i} - \langle \boldsymbol{\psi}, \widehat{P}\boldsymbol{n}\rangle_{\partial K_i\setminus\Gamma_N} - \langle \boldsymbol{\psi}, P_N\boldsymbol{n}\rangle_{\partial K_i\cap\Gamma_N} \\
&+ \langle \boldsymbol{\psi}, \nu\tau\widehat{\boldsymbol{u}}\rangle_{\partial K_i\setminus\Gamma_D} + \langle \boldsymbol{\psi}, \nu\tau(\widehat{\boldsymbol{u}}\cdot\boldsymbol{n})\boldsymbol{n}\rangle_{\partial K_i\setminus\Gamma_D} + \langle \boldsymbol{\psi}, \nu\tau\boldsymbol{u}_D\rangle_{\partial K_i\cap\Gamma_D} + \langle \boldsymbol{\psi}, \nu\tau(\boldsymbol{u}_D\cdot\boldsymbol{n})\boldsymbol{n}\rangle_{\partial K_i\cap\Gamma_D}
\end{aligned}
$$

$$
\begin{aligned}
-(\boldsymbol{\Psi},\boldsymbol{L})_{K_i}+(\boldsymbol{\nabla}^s\cdot\boldsymbol{\Psi},\boldsymbol{u})_{K_i} =&\langle\boldsymbol{\Psi},\widehat{\boldsymbol{u}}\otimes\boldsymbol{n}\rangle_{\partial K_i\setminus\Gamma_D}+\langle\boldsymbol{\Psi},\boldsymbol{n}\otimes\widehat{\boldsymbol{u}}\rangle_{\partial K_i\setminus\Gamma_D}\\
&+\langle\boldsymbol{\Psi},\boldsymbol{u}_D\otimes\boldsymbol{n}\rangle_{\partial K_i\cap\Gamma_D}+\langle\boldsymbol{\Psi},\boldsymbol{n}\otimes\boldsymbol{u}_D\rangle_{\partial K_i\cap\Gamma_D}
\end{aligned}
\tag{4.2.6b}
$$

$$
-(\phi,\boldsymbol{\nabla}\cdot\boldsymbol{u})_{K_i}=0 \tag{4.2.6c}
$$

for all the test functions $(\boldsymbol{\psi},\boldsymbol{\Psi},\phi)$.

Weak global problem

The weak form of the divergence-free X-HDG global problem for Stokes flow is: Find $\widehat{\boldsymbol{u}}\in\mathcal{V}_s^h(\Gamma\setminus\Gamma_D)$ and $\widehat{P}\in\mathcal{S}_s^h(\Gamma\setminus\Gamma_N)$ such that

$$
\begin{aligned}
\sum_{i=1}^{\mathtt{nel}}\Big\{&\langle\widehat{\boldsymbol{\psi}},\widehat{P}\boldsymbol{n}\rangle_{\partial K_i\setminus\partial\Omega}+\langle\widehat{\boldsymbol{\psi}},\nu\boldsymbol{L}\boldsymbol{n}\rangle_{\partial K_i\setminus\Gamma_D}+\langle\widehat{\boldsymbol{\psi}},\nu\tau\boldsymbol{u}\rangle_{\partial K_i\setminus\Gamma_D}-\langle\widehat{\boldsymbol{\psi}},\nu\tau\widehat{\boldsymbol{u}}\rangle_{\partial K_i\setminus\Gamma_D}+\langle\widehat{\boldsymbol{\psi}},\nu\tau(\boldsymbol{u}\cdot\boldsymbol{n})\boldsymbol{n}\rangle_{\partial K_i\setminus\Gamma_D}\\
&-\langle\widehat{\boldsymbol{\psi}},\nu\tau(\widehat{\boldsymbol{u}}\cdot\boldsymbol{n})\boldsymbol{n}\rangle_{\partial K_i\setminus\Gamma_D}\Big\}=\sum_{i=1}^{\mathtt{nel}}\Big\{\langle\widehat{\boldsymbol{\psi}},\boldsymbol{g}_N\rangle_{\partial K_i\cap\Gamma_N}-\langle\widehat{\boldsymbol{\psi}},P_N\boldsymbol{n}\rangle_{\partial K_i\cap\Gamma_N}\Big\}
\end{aligned}
\tag{4.2.7a}
$$

$$
\sum_{i=1}^{\mathtt{nel}}\Big\{\langle\widehat{\phi},\boldsymbol{u}\cdot\boldsymbol{n}\rangle_{\partial K_i}-\langle\widehat{\phi},\widehat{\boldsymbol{u}}\cdot\boldsymbol{n}\rangle_{\partial K_i\cap\Gamma_N}\Big\}=\sum_{i=1}^{\mathtt{nel}}\langle\widehat{\phi},\boldsymbol{u}_D\cdot\boldsymbol{n}\rangle_{\partial K_i\cap\Gamma_D} \tag{4.2.7b}
$$

4.2.4 X-HDG discrete form

The local problem 4.2.5 in a cut element K_i is written in a matrix-vector form as:

$$
\begin{bmatrix}
\left[\mathbf{A}_{uu}^{K_i}+\mathbf{A}_{uu}^{\mathcal{I}_i}\right] & \mathbf{A}_{uL}^{K_i} & \mathbf{A}_{up}^{K_i} & \mathbf{A}_{u\widetilde{u}^i}^{\mathcal{I}_i} & \mathbf{A}_{u\widetilde{p}^i}^{\mathcal{I}_i}\\
\mathbf{A}_{Lu}^{K_i} & \mathbf{A}_{LL}^{K_i} & \mathbf{0} & \mathbf{A}_{L\widetilde{u}^i}^{\mathcal{I}_i} & \mathbf{0}\\
\mathbf{A}_{pu}^{K_i} & \mathbf{0} & \mathbf{0} & \mathbf{0} & \mathbf{0}\\
\mathbf{A}_{\widetilde{u}^iu}^{\mathcal{I}_i} & \mathbf{A}_{\widetilde{u}^iL}^{\mathcal{I}_i} & \mathbf{0} & \mathbf{A}_{\widetilde{u}^i\widetilde{u}^i}^{\mathcal{I}_i} & \mathbf{0}\\
\mathbf{A}_{\widetilde{p}^iu}^{\mathcal{I}_i} & \mathbf{0} & \mathbf{0} & \mathbf{0} & \mathbf{0}
\end{bmatrix}
\begin{Bmatrix}\mathbf{u}^i\\ \mathbf{L}^i\\ \mathbf{p}^i\\ \widetilde{\mathbf{u}}^i\\ \widetilde{\mathbf{p}}^i\end{Bmatrix}=
\begin{bmatrix}\mathbf{A}_{u\widehat{u}}^{K_i}\\ \mathbf{A}_{L\widehat{u}}^{K_i}\\ \mathbf{0}\\ \mathbf{0}\\ \mathbf{0}\end{bmatrix}\widehat{\mathbf{u}}^i+
\begin{bmatrix}\mathbf{A}_{u\widehat{p}}^{K_i}\\ \mathbf{0}\\ \mathbf{0}\\ \mathbf{0}\\ \mathbf{0}\end{bmatrix}\widehat{\mathbf{p}}^i+
\begin{Bmatrix}\mathbf{f}_u^{K_i}\\ \mathbf{f}_L^{K_i}\\ \mathbf{0}\\ \mathbf{0}\\ \mathbf{0}\end{Bmatrix}
\tag{4.2.8}
$$

while in a standard uncut element K_i, the matrix-vector form of the local problem 4.2.6 is written as

$$
\begin{bmatrix}
\mathbf{A}_{uu}^{K_i} & \mathbf{A}_{uL}^{K_i} & \mathbf{A}_{up}^{K_i}\\
\mathbf{A}_{Lu}^{K_i} & \mathbf{A}_{LL}^{K_i} & \mathbf{0}\\
\mathbf{A}_{pu}^{K_i} & \mathbf{0} & \mathbf{0}
\end{bmatrix}
\begin{Bmatrix}\mathbf{u}^i\\ \mathbf{L}^i\\ \mathbf{p}^i\end{Bmatrix}=
\begin{bmatrix}\mathbf{A}_{u\widehat{u}}^{K_i}\\ \mathbf{A}_{L\widehat{u}}^{K_i}\\ \mathbf{0}\end{bmatrix}\widehat{\mathbf{u}}^i+
\begin{bmatrix}\mathbf{A}_{u\widehat{p}}^{K_i}\\ \mathbf{0}\\ \mathbf{0}\end{bmatrix}\widehat{\mathbf{p}}^i+
\begin{Bmatrix}\mathbf{f}_u^{K_i}\\ \mathbf{f}_L^{K_i}\\ \mathbf{0}\end{Bmatrix}
\tag{4.2.9}
$$

After the hybridization step (inserting the algebraic expressions of $\boldsymbol{u}$ and $\boldsymbol{L}$) from the local problem into the global problem 4.2.7, the full global problem is written in a

matrix-vector form as:

$$\mathop{\mathbf{A}}_{i=1}^{\mathtt{n_{el}}} \begin{bmatrix} \left[\mathbf{A}_{\widehat{uu}}^{K_i}\,\mathbf{Z}_{u\widehat{u}}^{K_i} + \mathbf{A}_{\widehat{uL}}^{K_i}\,\mathbf{Z}_{L\widehat{u}}^{K_i} + \mathbf{A}_{\widehat{\widehat{uu}}}^{K_i}\right] & \left[\mathbf{A}_{\widehat{uu}}^{K_i}\,\mathbf{Z}_{u\widehat{p}}^{K_i} + \mathbf{A}_{\widehat{uL}}^{K_i}\,\mathbf{Z}_{L\widehat{p}}^{K_i} + \mathbf{A}_{\widehat{\widehat{up}}}^{K_i}\right] \\ \left[\mathbf{A}_{\widehat{pu}}^{K_i}\,\mathbf{Z}_{u\widehat{u}}^{K_i} + \mathbf{A}_{\widehat{\widehat{pu}}}^{K_i}\right] & \left[\mathbf{A}_{\widehat{pu}}^{K_i}\,\mathbf{Z}_{u\widehat{p}}^{K_i}\right] \end{bmatrix} \begin{Bmatrix} \widehat{\mathbf{u}}^i \\ \widehat{\mathbf{p}}^i \end{Bmatrix} = \mathop{\mathbf{A}}_{i=1}^{\mathtt{n_{el}}} \begin{Bmatrix} \mathbf{f}_{\widehat{u}}^{K_i} - \mathbf{A}_{\widehat{uu}}^{K_i}\,\mathbf{z}_u^{K_i} - \mathbf{A}_{\widehat{uL}}^{K_i}\,\mathbf{z}_L^{K_i} \\ \mathbf{f}_{\widehat{p}}^{K_i} - \mathbf{A}_{\widehat{pu}}^{K_i}\,\mathbf{z}_u^{K_i} \end{Bmatrix} \tag{4.2.10}$$

The solution procedure is as follows: the discrete trace variables $\widehat{\mathbf{u}}$ and $\widehat{\mathbf{p}}$ are obtained by solving the following discrete global problem

$$\widehat{\mathbf{K}} \begin{Bmatrix} \widehat{\mathbf{u}} \\ \widehat{\mathbf{p}} \end{Bmatrix} = \widehat{\mathbf{f}} \tag{4.2.11}$$

then the local problems are solved element-by-element, for $i = 1, ..., \mathtt{n_{el}}$:

$$\begin{Bmatrix} \mathbf{u}^i \\ \mathbf{L}^i \\ \mathbf{p}^i \end{Bmatrix} = \mathbf{Z}_{\widehat{u}}^{K_i}\,\widehat{\mathbf{u}}^i + \mathbf{Z}_{\widehat{p}}^{K_i}\,\widehat{\mathbf{p}}^i + \mathbf{z}^{K_i} \tag{4.2.12}$$

See Appendix C for more details on spatial discretization and implementation details, where all the presented matrices and vectors are defined.

4.2.5 Divergence-free 2D elements

One of the main features of the presented X-HDG method is that it satisfies the divergence-free condition point-wise. For this, the pressure inside an element should be approximated with basis that belong to the space of divergence of the basis that is used to approximate the velocity.

Recall the discrete polynomial space of order m used to approximate the velocity inside an element K_i

$$\begin{aligned} \mathcal{V}_v^h = \{\boldsymbol{\psi} \in [\mathcal{L}_2(\Omega)]^d : \boldsymbol{\psi}_h|_{K_i} &\in [\mathcal{P}^m(K_i)]^d && \text{if } K_i \cap \mathcal{I} = \emptyset, \\ \boldsymbol{\psi}_h|_{K_i} &\in [\mathcal{P}^m(K_i)]^d \oplus H[\mathcal{P}^m(K_i)]^d && \text{if } K_i \cap \mathcal{I} \neq \emptyset\} \end{aligned}$$

and also the discrete polynomial space used to approximate the pressure

$$\begin{aligned} \mathcal{S}_v^{div\,h} = \{\phi \in \mathcal{L}_2(\Omega) : \phi_h|_{K_i} &\in \boldsymbol{\nabla}\cdot[\mathcal{P}^m(K_i)]^d && \text{if } K_i \cap \mathcal{I} = \emptyset, \\ \phi_h|_{K_i} &\in \boldsymbol{\nabla}\cdot[\mathcal{P}^m(K_i)]^d \oplus H\boldsymbol{\nabla}\cdot[\mathcal{P}^m(K_i)]^d && \text{if } K_i \cap \mathcal{I} \neq \emptyset\} \end{aligned}$$

As mentioned in [35], for triangular and tetrahedral elements, the pressure element would be a standard finite triangular element of order $(m-1)$. However, for quadrilaterals and hexahedrals, the pressure element is an element with reduced basis functions where the highest order term $x^m y^m$ (in 2D) or $x^m y^m z^m$ (in 3D) is removed. As a result, this pressure element with degree m_{reduced} would have one node less when compared to full element of degree m. The reader is invited to check the original work of Elzaabalawy [35] where the full details of reduced quadrilaterals and hexahedrals is introduced. A summary is also presented in Appendix B.

It is necessary to note that quadrilateral or hexahedral pressure elements of order $(m-1)$ do not satisfy the point-wise divergence-free condition. On the other hand, pressure elements with order m, regardless the element shape, violate the LBB condition [56, 60].

Considering a standard triangular uncut reference element K_i in Figure 4.2, the black circles are the solution nodes in the element and on the skeleton Γ. The black asterisks are the elemental integration Gauss points. The red asterisks are the facial integration Gauss points for the faces of the element and the skeleton. If the element is cut as shown in Figure 4.3, the integration points are modified inside the element and on the cut elemental and skeleton faces. If the material interface is approximated linearly within the cut elements, then the material interface's nodes and integration points would be represented in blue circles and asterisks, respectively. Note that the divergence-free pressure triangular element is an element of order $(m-1)$.

For quadrilaterals, the divergence-free pressure elements of degree m_{reduced}, with modified basis and an eliminated node, are shown in Figures 4.4 and 4.5 for standard and cut elements, respectively.

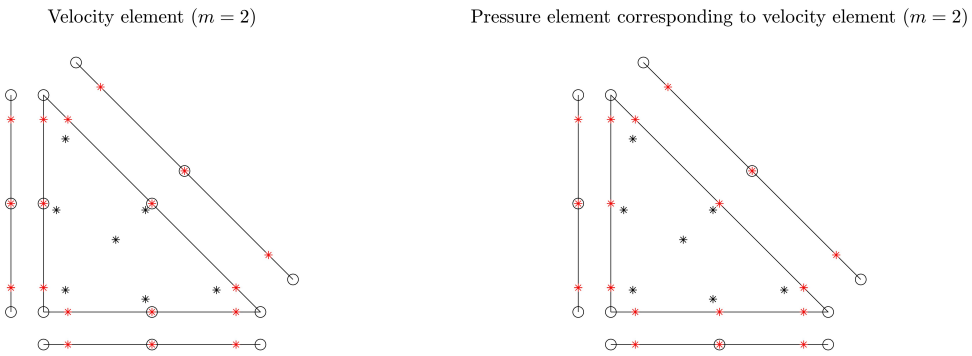

Figure 4.2: Standard uncut velocity triangular element of degree $m = 2$ (left) and its corresponding divergence-free pressure element (right) - pair of $(m, m-1)$ triangles.

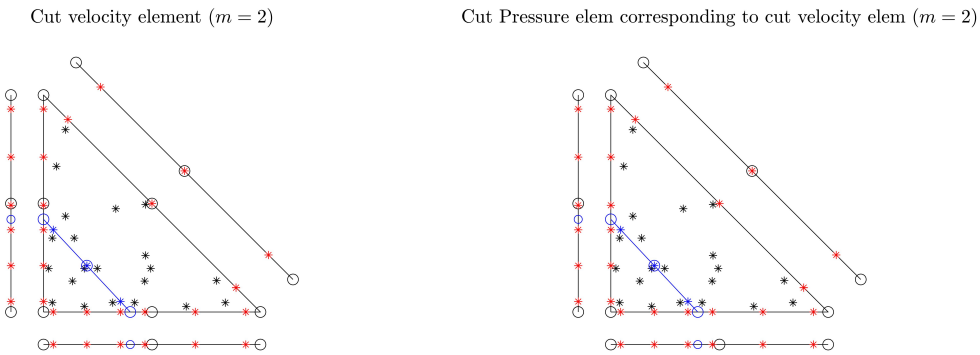

Figure 4.3: Cut velocity triangular element of degree $m = 2$ (left) and its corresponding divergence-free pressure element (right) - pair of $(m, m-1)$ cut triangles.

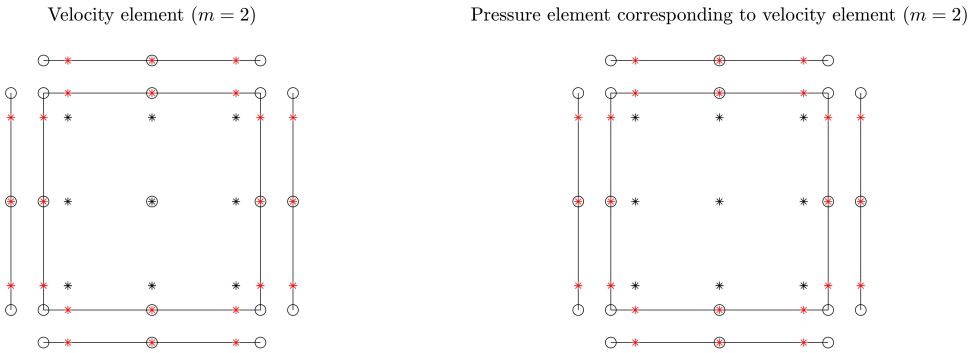

Figure 4.4: Standard uncut velocity quadrilateral element of degree $m = 2$ (left) and its corresponding divergence-free pressure element (right). Note the eliminated node from the center of the pressure element - pair of (m, m_{reduced}) quadrilaterals.

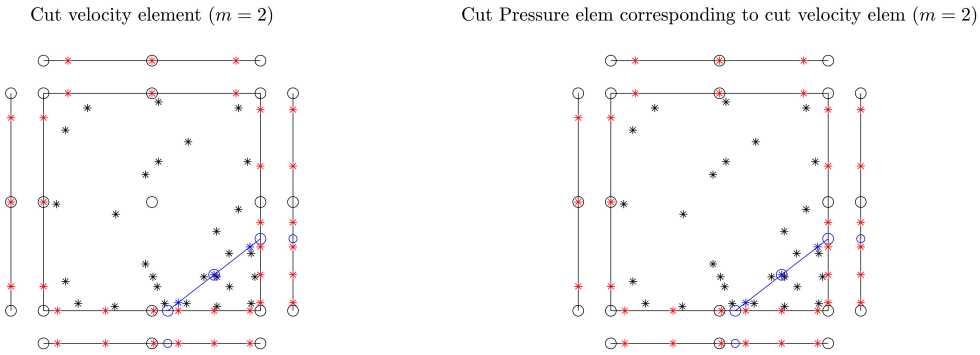

Figure 4.5: Cut velocity quadrilateral element of degree $m = 2$ (left) and its corresponding divergence-free pressure element (right). Note the eliminated node from the center of the pressure element - pair of (m, m_{reduced}) cut quadrilaterals.

4.3 Numerical examples

The two-phase Stokes problem introduced in section 4.1 is solved in this section using the novel divergence-free X-HDG formulation introduced in this chapter. Three numerical examples with known analytical solutions are shown. The first example involves continuous velocity and pressure across a straight material interface. The second example is the same as the first but with a discontinuity in the pressure. Finally, the third example involves a curved material interface. Five unfitted meshes of triangles with $4n^2$ elements and five unfitted meshes of quadrilaterals with n^2 elements are employed, where $n = 2, 4, 8, 16, 32$. In all the three examples, the corresponding source term, Dirichlet and Neumann conditions as well as the interface jumps are set to satisfy the analytical solution.

4.3.1 Example 1: straight interface without pressure jump

A problem with known exact solution is presented in [38] that has zero jump conditions at the interface. In this example a horizontal interface $\mathcal{I}$ at $y = 0$ is considered to divide the square domain $\Omega = [-1, 1] * [-0.4, 1.6]$ into two regions, $\Omega_1 := \{\boldsymbol{x} \in \Omega | y < 0\}$ and $\Omega_2 := \Omega \setminus \Omega_1$ as shown in Figure 4.6. The kinematic viscosity and the analytical velocity

and pressure are given by:

$$\nu(\boldsymbol{x}) = \begin{cases} \nu_1 = 1 & \text{in } \Omega_1 \\ \nu_2 = 2 & \text{in } \Omega_2 \end{cases}$$

$$\boldsymbol{u}(\boldsymbol{x}) = \begin{cases} [(x^5 y)/\nu_1,\ (-2.5x^4 y^2)/\nu_1]^T & \text{in } \Omega_1 \\ [(x^5 y)/\nu_2,\ (-2.5x^4 y^2)/\nu_2]^T & \text{in } \Omega_2 \end{cases}$$

$$P(\boldsymbol{x}) = x + y \quad \text{in } \Omega$$

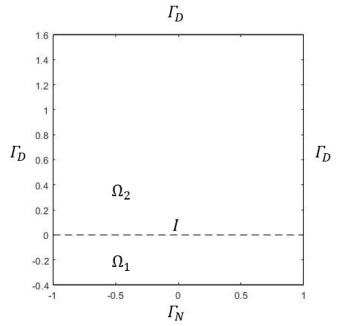

Figure 4.6: Domain for Examples 1 and 2.

Dirichlet boundary conditions are set everywhere on the boundary except for the bottom boundary which is subject to Neumann boundary conditions derived from the analytical solution. The order of approximation of the velocity is varied from $m = 2$ to 3. The stabilization parameters introduced in the X-HDG numerical fluxes by equation (4.2.4) are set as $\tau = 1$ and $\tau^{\mathcal{I}} = 1/\{\nu\}$.

First, the results obtained with meshes of triangles are shown and analyzed. As mentioned earlier for triangular elements, in order to satisfy the divergence-free condition, velocity elements of order m and pressure elements of order $(m-1)$ are used. This velocity-pressure pair of elements will be referred to as "Meshes of $(m, m-1)$ triangles".

An important feature of the presented HDG formulation is that it satisfies the divergence-free condition. For this, the maximum point-wise divergence of the velocity $\boldsymbol{\nabla}\cdot\boldsymbol{u}$ is presented in Table 4.1. It is noticed that the divergence-free condition is satisfied to the order $\mathcal{O}(10^{-11})$ and $\mathcal{O}(10^{-8})$ for $m = 2$ and $m = 3$, respectively. Moreover, a plot of the velocity divergence on mesh 3 with degree approximation $m = 3$ is shown in Figure 4.7, it can be seen that the velocity divergence is relatively higher in a small percentage of the elements, specifically in cut elements, whose X-HDG local operators have relatively degraded conditioning, when compared to the rest of the standard uncut elements where the divergence-free condition could be satisfied to the order $\mathcal{O}(10^{-16})$ to $\mathcal{O}(10^{-13})$ on almost 95% of the elements. It is necessary to mention that the relatively high values of $\boldsymbol{\nabla}\cdot\boldsymbol{u}$ are numerical residuals of the linear system solver, which could be further enhanced but it is not the focus of this thesis. Furthermore, the velocity field is $\mathcal{H}(div)$ which means that the jumps in the normal velocities across inter-elements faces and the material interface are zero, this can be seen clearly from Tables 4.2 and 4.3 where the $\mathcal{L}_\infty$-norm of the jump $[\![\boldsymbol{u}\cdot\boldsymbol{n}]\!]$ across inter-element faces and the material interface is presented. The numerical values of the recorded jumps are of the order $\mathcal{O}(10^{-16})$ to $\mathcal{O}(10^{-13})$. Satisfying both divergence-free condition and zero jumps in normal velocities are two essential requirements for the method to be energy-stable.

Mesh TRIs	$\tau = 1, \tau^{\mathcal{I}} = 1/\{\nu\}$	
	$m = 2$	$m = 3$
mesh 1	5.24E-11	3.03E-08
mesh 2	2.63E-13	2.07E-10
mesh 3	6.31E-12	8.72E-10
mesh 4	1.26E-12	4.27E-10
mesh 5	3.62E-11	7.83E-09

Table 4.1: Ex 1: Max. divergence of velocity $||\boldsymbol{\nabla}\cdot\boldsymbol{u}||_\infty$ - Meshes of $(m, m-1)$ triangles.

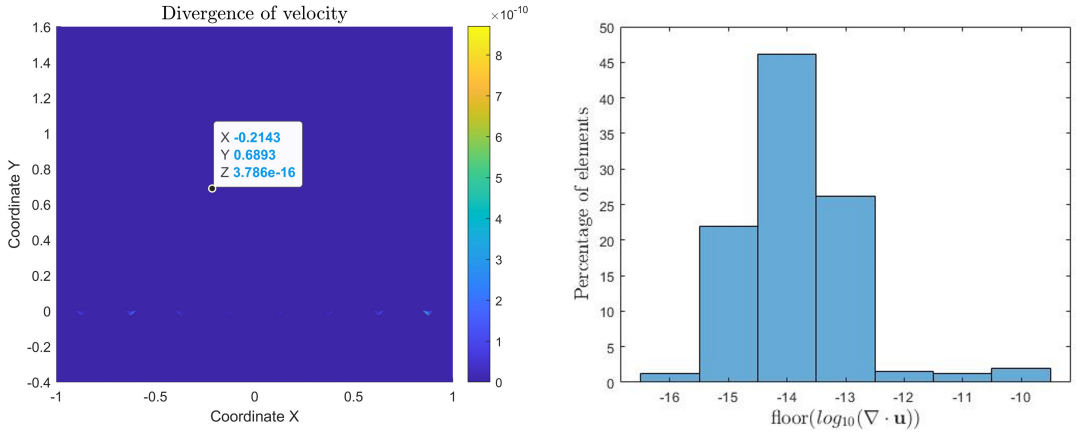

Figure 4.7: Ex 1: $\boldsymbol{\nabla} \cdot \boldsymbol{u}$ plotted for $m = 3$/mesh 3 of $(m, m-1)$ triangles (left), and a histogram showing the percentage of elements with their respective order of velocity-divergence (right).

Mesh TRIs	$\tau = 1, \tau^{\mathcal{I}} = 1/\{\nu\}$	
	$m = 2$	$m = 3$
mesh 1	2.01E-14	1.67E-13
mesh 2	1.78E-15	7.27E-14
mesh 3	1.99E-15	3.74E-14
mesh 4	3.55E-15	1.24E-13
mesh 5	9.99E-15	1.38E-13

Table 4.2: Ex 1: Max. inter-elements jump: $||[\![\boldsymbol{u} \cdot \boldsymbol{n}]\!]_{\Gamma \setminus \partial\Omega}||_\infty$ - Meshes of $(m, m-1)$ triangles.

Mesh TRIs	$\tau = 1, \tau^{\mathcal{I}} = 1/\{\nu\}$	
	$m = 2$	$m = 3$
mesh 1	7.03E-15	3.87E-13
mesh 2	9.18E-16	3.34E-14
mesh 3	7.76E-16	4.71E-14
mesh 4	7.45E-16	3.66E-14
mesh 5	7.92E-16	1.34E-14

Table 4.3: Ex 1: Max. free-surface jump: $||[\![\boldsymbol{u} \cdot \boldsymbol{n}]\!]_{\mathcal{I}}||_\infty$ - Meshes of $(m, m-1)$ triangles.

An important test to assess the performance of the proposed formulation is to check the mesh convergence rates, see Figure 4.8 where convergence rates are indicated. Regarding the convergence of the x-velocity u and the flux component L_1, it is observed that optimal convergence of order ($m+1$ in $\mathcal{L}_2$-norm, m in $\mathcal{H}^1$-norm) is achieved. Regarding the pressure P that was approximated with degree $(m-1)$, the expected/optimal convergence rates should be (m in $\mathcal{L}_2$-norm, $m-1$ in $\mathcal{H}^1$-norm), however, super-convergence of order ($m+1$ in $\mathcal{L}_2$-norm, m in $\mathcal{H}^1$-norm) is observed.

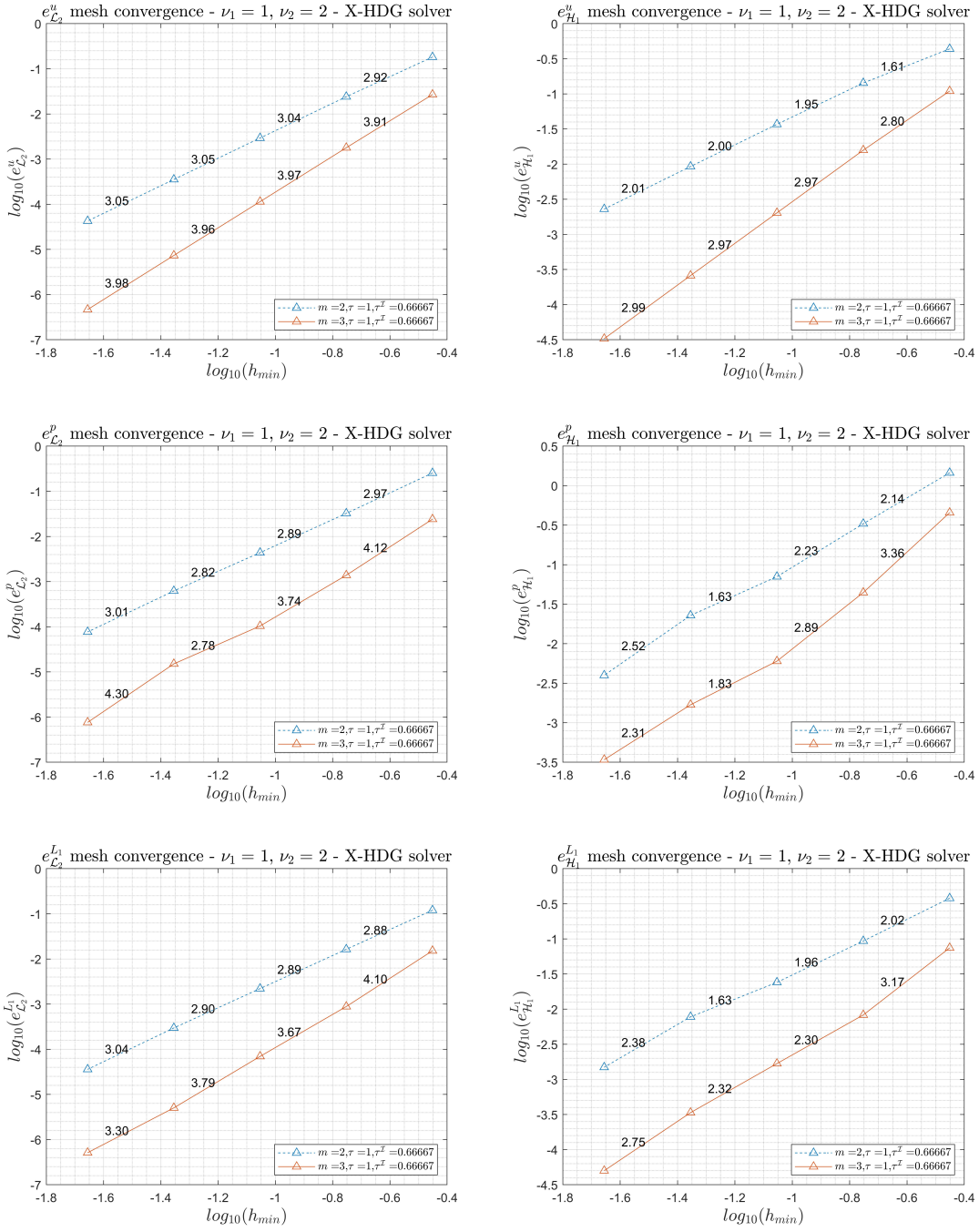

Figure 4.8: Ex 1: Errors in x-velocity u (top), pressure P (middle), and flux component L_1 (bottom) vs. mesh size - $\mathcal{L}_2$-norm (left), $\mathcal{H}^1$-norm (right) - Meshes of $(m, m-1)$ triangles.

Next, the results obtained with meshes of quadrilaterals are shown and analyzed. As mentioned earlier for quadrilateral elements, in order to satisfy the divergence-free condition, velocity elements of degree m and reduced pressure elements of degree m_{reduced} are used. This velocity-pressure pair of elements will be referred to as "Meshes of (m, m_{reduced}) quadrilaterals". For the case of quadrilaterals, the boundary conditions are Neumann everywhere except for the right boundary which is Dirichlet.

Again, the maximum point-wise divergence of the velocity $\boldsymbol{\nabla} \cdot \boldsymbol{u}$ is presented in Table 4.4 for all degrees and mesh refinements. It is noticed that the divergence-free condition is satisfied to the order $\mathcal{O}(10^{-11})$ and $\mathcal{O}(10^{-9})$ for $m = 2$ and $m = 3$, respectively. Moreover, a plot of the velocity divergence on mesh 3 with degree approximation $m = 3$ is shown in Figure 4.9, where it is noticed that the velocity divergence is relatively higher in cut elements with relatively degraded conditioning of the X-HDG local operators. Further, the divergence-free condition could be satisfied to the order $\mathcal{O}(10^{-15})$ to $\mathcal{O}(10^{-13})$ on almost 90% of the elements.

Mesh QUADs	$\tau = 1, \tau^{\mathcal{I}} = 1/\{\nu\}$	
	$m = 2$	$m = 3$
mesh 1	1.02E-13	6.34E-12
mesh 2	4.53E-12	3.79E-09
mesh 3	3.31E-13	1.15E-11
mesh 4	2.09E-11	9.99E-09
mesh 5	3.26E-12	1.20E-10

Table 4.4: Ex 1: Max. divergence of velocity $||\boldsymbol{\nabla} \cdot \boldsymbol{u}||_{\infty}$ - Meshes of (m, m_{reduced}) quadrilaterals.

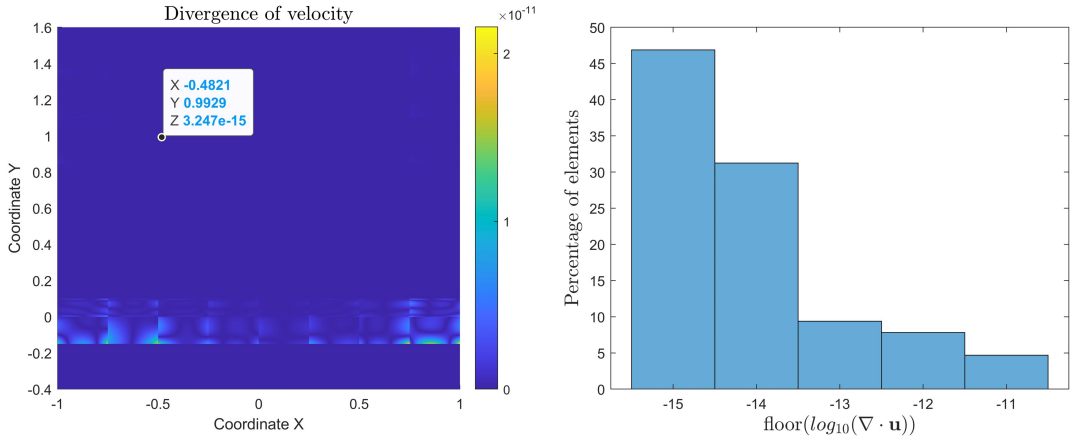

Figure 4.9: Ex 1: $\boldsymbol{\nabla} \cdot \boldsymbol{u}$ plotted for $m = 3$/mesh 3 of (m, m_{reduced}) quadrilaterals (left), and a histogram showing the percentage of elements with their respective order of velocity-divergence (right).

Furthermore, the velocity field is $\mathcal{H}(div)$ which means that the jumps in the normal velocities across inter-elements faces and the free-surface are zero, this can be seen clearly from Tables 4.5 and 4.6 where the $\mathcal{L}_{\infty}$-norm of the jump $[\![\boldsymbol{u} \cdot \boldsymbol{n}]\!]$ across inter-element faces and the free-surface is presented. The numerical values of the recorded jumps are of the order $\mathcal{O}(10^{-16})$ to $\mathcal{O}(10^{-12})$.

Mesh QUADs	$\tau = 1, \tau^{\mathcal{I}} = 1/\{\nu\}$	
	$m = 2$	$m = 3$
mesh 1	2.25E-15	3.22E-14
mesh 2	3.33E-16	9.99E-16
mesh 3	1.33E-15	2.66E-15
mesh 4	1.33E-15	1.47E-14
mesh 5	9.10E-15	4.34E-14

Table 4.5: Ex 1: Max. inter-elements jump: $||[\![\boldsymbol{u} \cdot \boldsymbol{n}]\!]_{\Gamma \setminus \partial\Omega}||_\infty$ - Meshes of (m, m_{reduced}) quadrilaterals.

Mesh QUADs	$\tau = 1, \tau^{\mathcal{I}} = 1/\{\nu\}$	
	$m = 2$	$m = 3$
mesh 1	3.81E-15	7.66E-14
mesh 2	1.89E-14	2.60E-12
mesh 3	2.08E-15	1.34E-14
mesh 4	6.05E-15	1.85E-13
mesh 5	1.27E-15	6.21E-15

Table 4.6: Ex 1: Max. free-surface jump: $||[\![\boldsymbol{u} \cdot \boldsymbol{n}]\!]_{\mathcal{I}}||_\infty$ - Meshes of (m, m_{reduced}) quadrilaterals.

Regarding convergence rates on meshes of (m, m_{reduced}) quadrilaterals, see Figure 4.10. It is observed that optimal convergence of order ($m + 1$ in $\mathcal{L}_2$-norm, m in $\mathcal{H}^1$-norm) is achieved for the x-velocity u that was approximated with order m. It should be noted that in the original work of Elzaabalawy [35] where divergence-free (m, m_{reduced}) quadrilaterals is firstly introduced, sub-optimal convergence rate for the velocity (m in $\mathcal{L}_2$-norm) is reported.

As for the pressure P, sub-optimal convergence of order ($m - 1$ in $\mathcal{L}_2$-norm, $m - 2$ in $\mathcal{H}^1$-norm) is achieved as reported in the work of Elzaabalawy [35]. Furthermore, for the flux component L_1, sub-optimal convergence of order (m in $\mathcal{L}_2$-norm, $m - 1$ in $\mathcal{H}^1$-norm) is achieved.

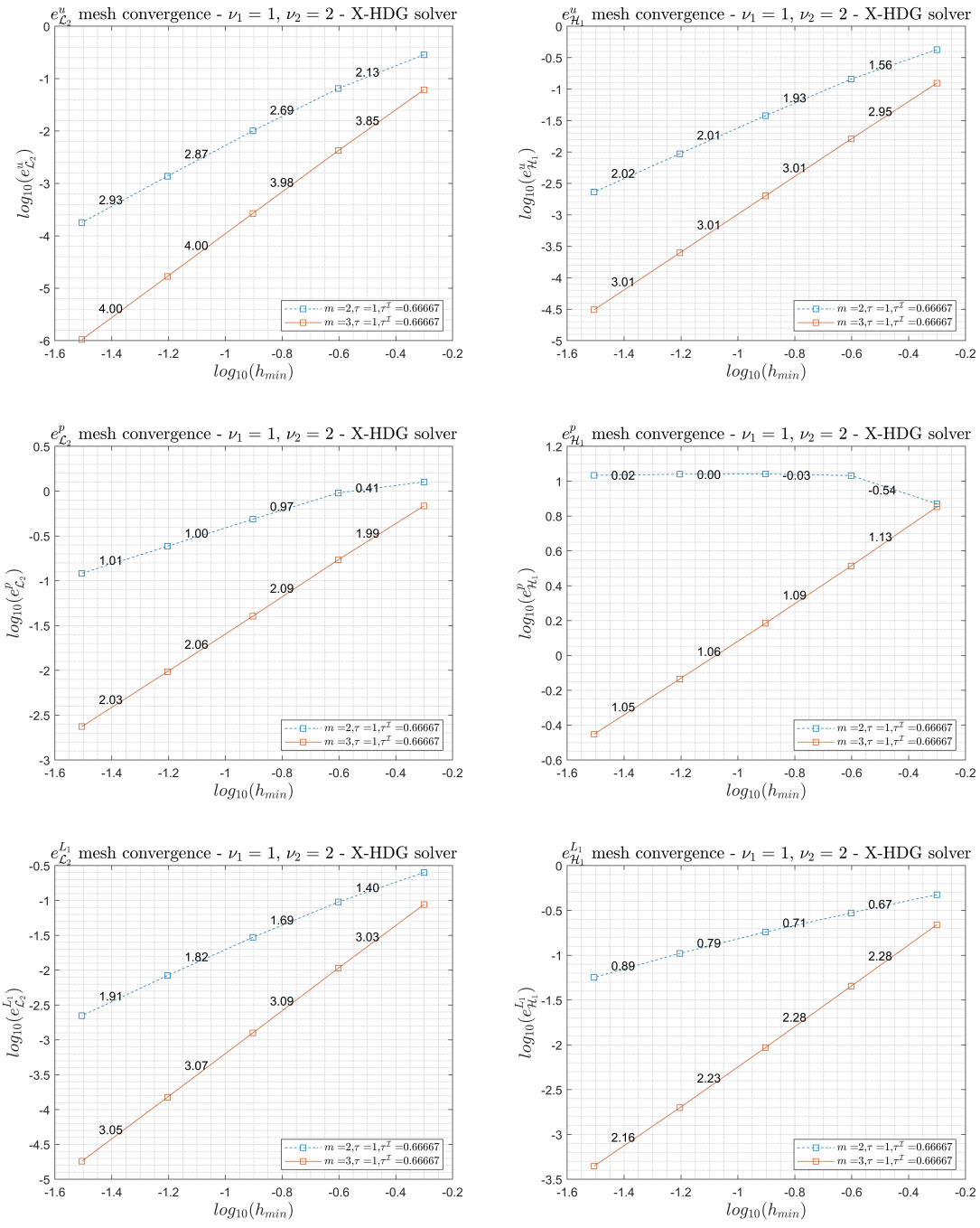

Figure 4.10: Ex 1: Errors in x-velocity u (top), pressure P (middle), and flux component L_1 (bottom) vs. mesh size - $\mathcal{L}_2$-norm (left), $\mathcal{H}^1$-norm (right) - Meshes of (m, m_{reduced}) quadrilaterals.

4.3.2 Example 2: straight interface with pressure jump

The previous problem is modified to have a discontinuous pressure field where the analytical pressure is given by:

$$P(\boldsymbol{x}) = \begin{cases} x + y & \text{in } \Omega_1 \\ x + y + 1 & \text{in } \Omega_2 \end{cases}$$

Again, the numerical results obtained using meshes of $(m, m-1)$ triangles are shown first. The numerical pressure and velocities obtained using the third mesh and velocity order $m = 3$ are shown in Figure 4.11, where the resolved sharp discontinuous pressure can be seen. The maximum point-wise $\boldsymbol{\nabla} \cdot \boldsymbol{u}$ is presented in Table 4.7. Moreover, a plot of the velocity divergence on mesh 3 with degree approximation $m = 3$ is shown in Figure 4.12, where it is shown that the divergence-free condition is satisfied. Furthermore, the $\mathcal{L}_\infty$-norm of the jump $[\![\boldsymbol{u} \cdot \boldsymbol{n}]\!]$ across inter-element faces and the free-surface is presented in Tables 4.8 and 4.9, respectively. Finally, the mesh convergence plots are shown in Figure 4.13.

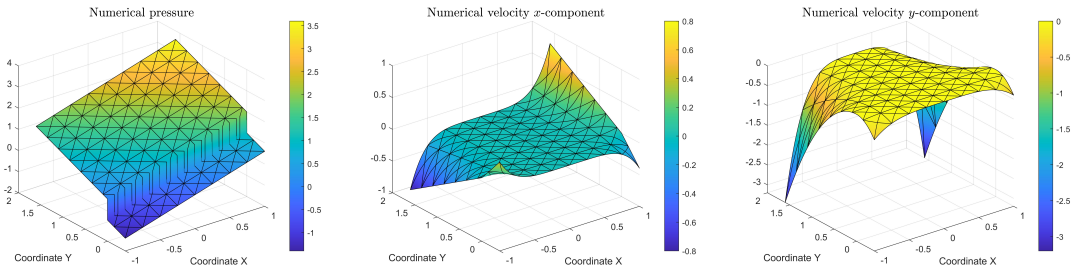

Figure 4.11: Ex 2: Numerical solution obtained using $m = 3$/mesh 3 of $(m, m-1)$ triangles: Pressure P (left), x-velocity u (middle), and y-velocity v (right).

Mesh TRIs	$\tau = 1, \tau^{\mathcal{I}} = 1/\{\nu\}$	
	$m = 2$	$m = 3$
mesh 1	4.97E-11	3.06E-08
mesh 2	2.75E-13	2.07E-10
mesh 3	1.07E-11	1.19E-09
mesh 4	1.65E-12	4.99E-09
mesh 5	4.42E-11	1.24E-08

Table 4.7: Ex 2: Max. divergence of velocity $||\boldsymbol{\nabla} \cdot \boldsymbol{u}||_\infty$ - Meshes of $(m, m-1)$ triangles.

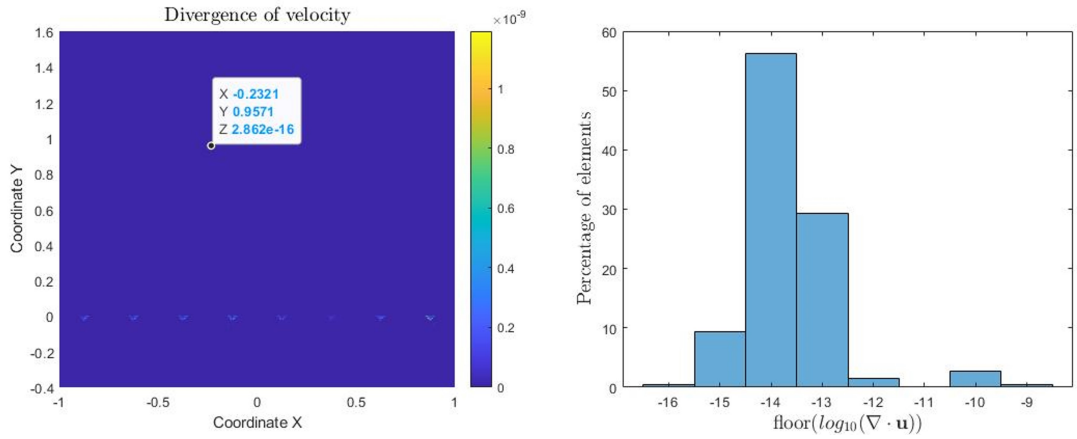

Figure 4.12: Ex 2: $\boldsymbol{\nabla} \cdot \boldsymbol{u}$ plotted for $m = 3$/mesh 3 of $(m, m-1)$ triangles (left), and a histogram showing the percentage of elements with their respective order of velocity-divergence (right).

Mesh TRIs	$\tau = 1, \tau^{\mathcal{I}} = 1/\{\nu\}$	
	$m = 2$	$m = 3$
mesh 1	2.37E-14	2.71E-13
mesh 2	7.14E-16	5.64E-14
mesh 3	2.22E-15	6.06E-14
mesh 4	4.44E-15	1.83E-13
mesh 5	9.31E-15	2.45E-13

Table 4.8: Ex 2: Max. inter-elements jump: $||[\![\boldsymbol{u} \cdot \boldsymbol{n}]\!]_{\Gamma \setminus \partial\Omega}||_\infty$ - Meshes of $(m, m-1)$ triangles.

Mesh TRIs	$\tau = 1, \tau^{\mathcal{I}} = 1/\{\nu\}$	
	$m = 2$	$m = 3$
mesh 1	9.14E-15	4.19E-13
mesh 2	8.59E-16	3.91E-14
mesh 3	8.67E-16	5.47E-14
mesh 4	1.11E-15	4.29E-14
mesh 5	1.36E-15	1.83E-14

Table 4.9: Ex 2: Max. free-surface jump: $||[\![\boldsymbol{u} \cdot \boldsymbol{n}]\!]_{\mathcal{I}}||_\infty$ - Meshes of $(m, m-1)$ triangles.

The discontinuity in pressure did not pose any issue regarding the convergence where optimal convergence rates ($m+1$ in $\mathcal{L}_2$-norm, m in $\mathcal{H}^1$-norm) are achieved for both x-velocity u and flux component L_1, and super-convergence ($m+1$ in $\mathcal{L}_2$-norm, m in $\mathcal{H}^1$-norm) is observed for the pressure P. It is also noticed that the divergence-free condition is satisfied to the order $\mathcal{O}(10^{-11})$ and $\mathcal{O}(10^{-8})$ for $m = 2$ and $m = 3$, respectively. Those relatively higher values appear again in small percentage of elements whose X-HDG local operators have relatively degraded conditioning. However, the divergence-free condition is satisfied to the order $\mathcal{O}(10^{-16})$ to $\mathcal{O}(10^{-13})$ on almost 97% of the elements. Moreover, the jumps in the normal velocities across inter-elements faces and the free-surface are of the order $\mathcal{O}(10^{-16})$ to $\mathcal{O}(10^{-13})$ similarly to the previous example.

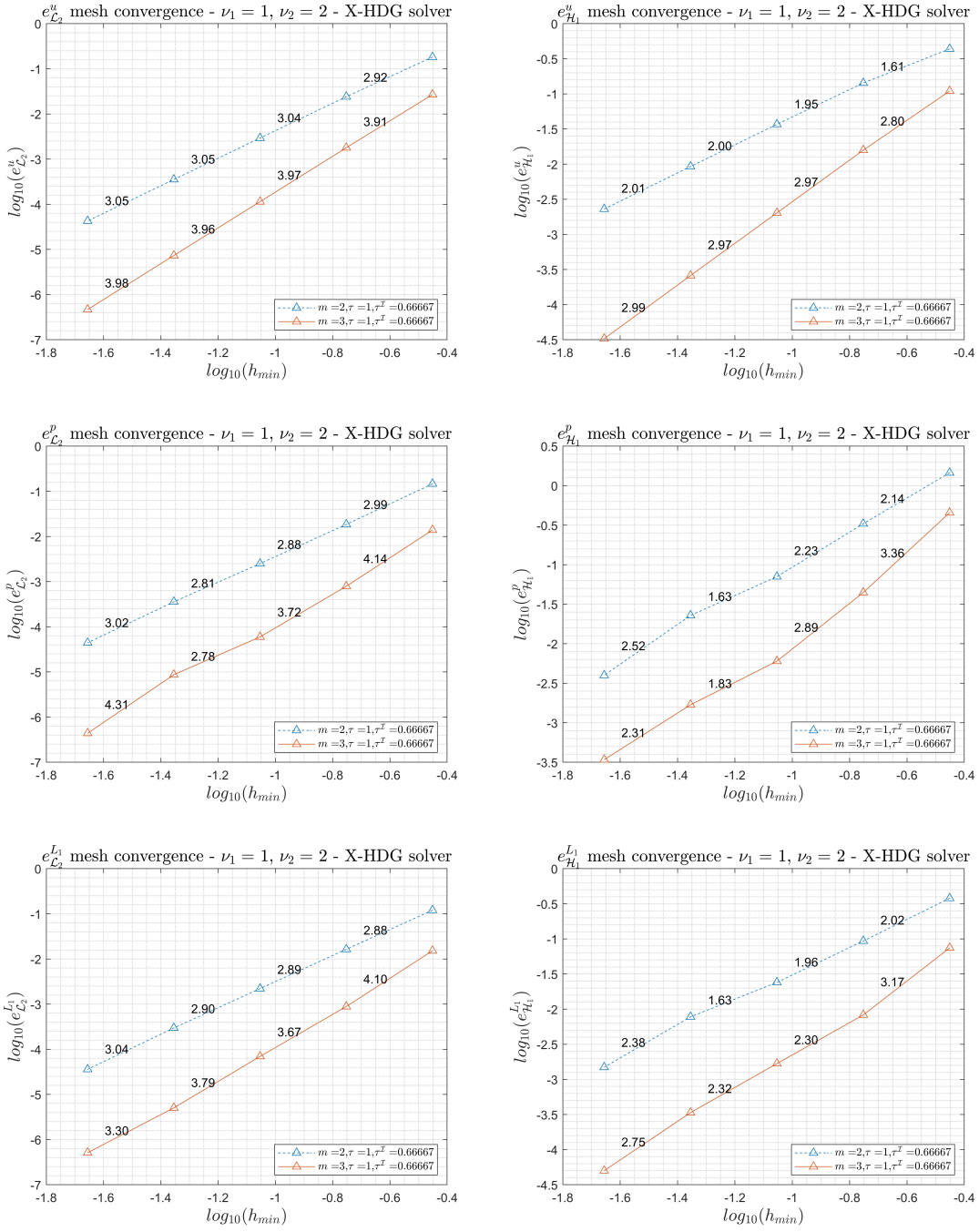

Figure 4.13: Ex 2: Errors in x-velocity u (top), pressure P (middle), and flux component L_1 (bottom) vs. mesh size - $\mathcal{L}_2$-norm (left), $\mathcal{H}^1$-norm (right) - Meshes of $(m, m-1)$ triangles.

Next, the results obtained with meshes of (m, m_{reduced}) quadrilaterals are shown and analyzed. The numerical pressure and velocities obtained using the third mesh and velocity order $m = 3$ are shown in Figure 4.14, where the resolved sharp discontinuous pressure can be seen. It is also observed that the numerical error in pressure is more visible when compared to the numerical pressure obtained with $(m, m-1)$ triangles.

The maximum point-wise $\boldsymbol{\nabla} \cdot \boldsymbol{u}$ is presented in Table 4.10. It is observed that the divergence-free condition is satisfied to the order $\mathcal{O}(10^{-11})$ and $\mathcal{O}(10^{-8})$ for $m = 2$ and $m = 3$, respectively. Moreover, a plot of the velocity divergence on mesh 3 with degree approximation $m = 3$ is shown in Figure 4.15, where it is shown that the divergence-free condition is satisfied to the order $\mathcal{O}(10^{-15})$ to $\mathcal{O}(10^{-13})$ on almost 88% of the elements. Again, only a small percentage of elements suffer from the degraded conditioning of the X-HDG local operator resulting in a relatively higher values for the divergence of velocity in those elements.

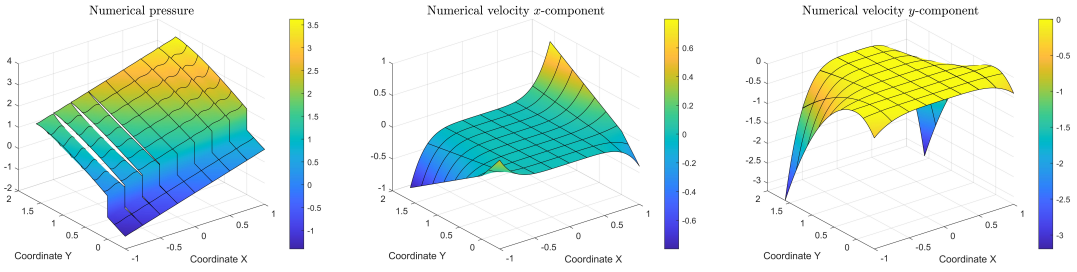

Figure 4.14: Ex 2: Numerical solution obtained using $m = 3$/mesh 3 of (m, m_{reduced}) quadrilaterals: Pressure P (left), x-velocity u (middle), and y-velocity v (right).

Mesh QUADs	$\tau = 1, \tau^{\mathcal{I}} = 1/\{\nu\}$	
	$m = 2$	$m = 3$
mesh 1	1.60E-13	8.22E-12
mesh 2	4.20E-12	3.83E-09
mesh 3	4.11E-13	1.12E-11
mesh 4	3.08E-11	1.93E-08
mesh 5	3.27E-12	2.84E-10

Table 4.10: Ex 2: Max. divergence of velocity $||\boldsymbol{\nabla} \cdot \boldsymbol{u}||_\infty$ - Meshes of (m, m_{reduced}) quadrilaterals.

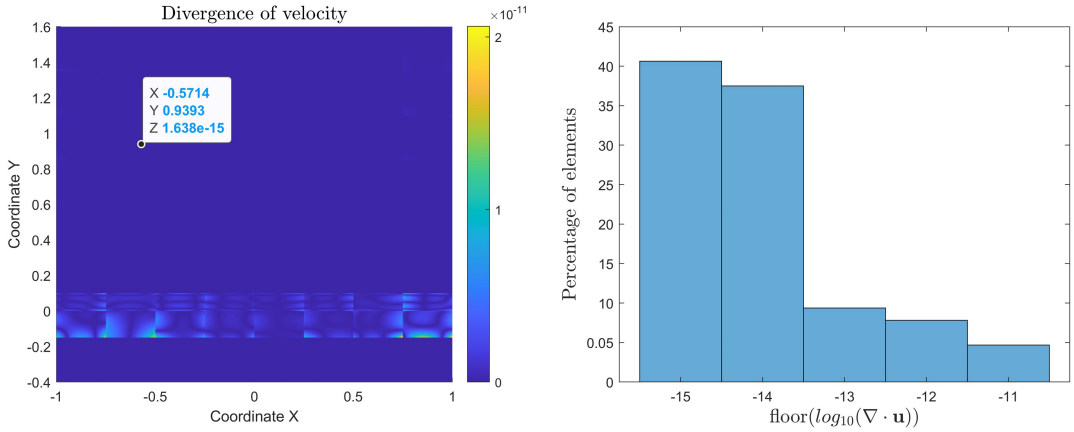

Figure 4.15: Ex 2: $\boldsymbol{\nabla} \cdot \boldsymbol{u}$ plotted for $m = 3$/mesh 3 of (m, m_{reduced}) quadrilaterals (left), and a histogram showing the percentage of elements with their respective order of velocity-divergence (right).

Furthermore, the $\mathcal{L}_\infty$-norm of the jump $[\![\boldsymbol{u} \cdot \boldsymbol{n}]\!]$ across inter-element faces and the material interface is presented in Tables 4.11 and 4.12, respectively, where again, the jumps in the normal velocities across inter-elements faces and the free-surface are of the order $\mathcal{O}(10^{-16})$ to $\mathcal{O}(10^{-12})$.

Mesh QUADs	$\tau = 1, \tau^{\mathcal{I}} = 1/\{\nu\}$	
	$m = 2$	$m = 3$
mesh 1	1.61E-15	3.98E-14
mesh 2	5.55E-16	7.77E-16
mesh 3	8.88E-16	3.10E-15
mesh 4	1.11E-15	1.43E-14
mesh 5	8.99E-15	4.30E-14

Table 4.11: Ex 2: Max. inter-elements jump: $||[\![\boldsymbol{u} \cdot \boldsymbol{n}]\!]_{\Gamma \setminus \partial\Omega}||_\infty$ - Meshes of (m, m_{reduced}) quadrilaterals.

Mesh QUADs	$\tau = 1, \tau^{\mathcal{I}} = 1/\{\nu\}$	
	$m = 2$	$m = 3$
mesh 1	4.55E-15	7.86E-14
mesh 2	1.90E-14	2.60E-12
mesh 3	1.88E-15	1.37E-14
mesh 4	7.67E-15	3.92E-13
mesh 5	2.53E-15	1.01E-14

Table 4.12: Ex 2: Max. free-surface jump: $||[\![\boldsymbol{u} \cdot \boldsymbol{n}]\!]_{\mathcal{I}}||_\infty$ - Meshes of (m, m_{reduced}) quadrilaterals.

Finally, the mesh convergence plots are shown in Figure 4.16. Similar to the previous example without pressure jump, it is observed that optimal convergence of order $(m+1$ in $\mathcal{L}_2$-norm, m in $\mathcal{H}^1$-norm) is achieved for the x-velocity u. Sub-optimal convergence of order $(m-1$ in $\mathcal{L}_2$-norm, $m-2$ in $\mathcal{H}^1$-norm) is achieved for the pressure P. Finally, for the flux component L_1, sub-optimal convergence of order (m in $\mathcal{L}_2$-norm, $m-1$ in $\mathcal{H}^1$-norm) is achieved.

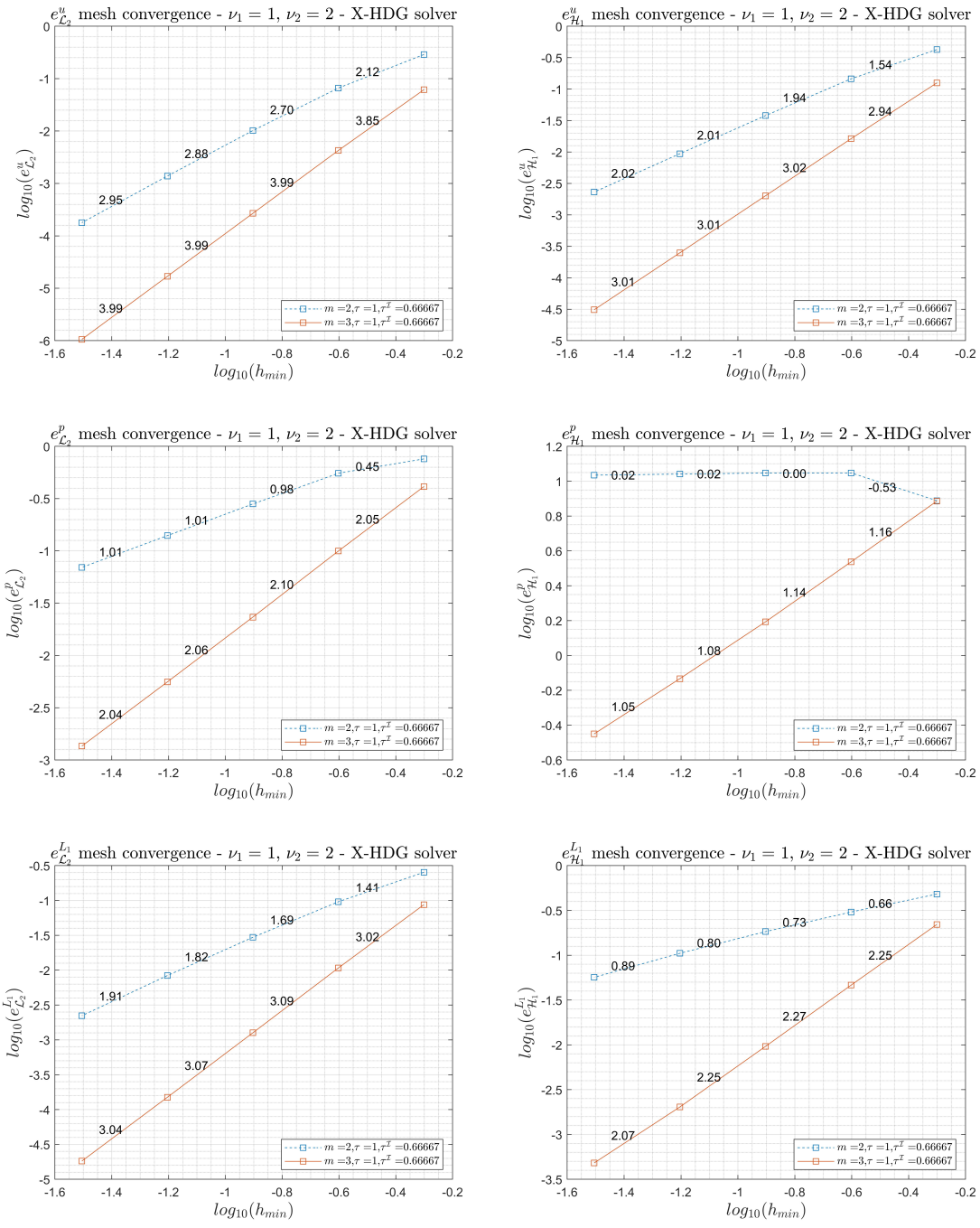

Figure 4.16: Ex 2: Errors in x-velocity u (top), pressure P (middle), and flux component L_1 (bottom) vs. mesh size - $\mathcal{L}_2$-norm (left), $\mathcal{H}^1$-norm (right) - Meshes of (m, m_{reduced}) quadrilaterals.

4.3.3 Example 3: steady problem with circular material interface

This example with a circular interface is considered to show the effect of the order of approximation of the interface on the results. For meshes with triangular elements, a linear approximation of the interface in each cut element is considered regardless of the degree approximation of the solution. However, for meshes with quadrilateral elements, the interface is approximated with the same order of approximation as the velocity m or even higher $2m+1$.

A more realistic problem with known exact solution similar to that presented in [18] is considered. A bubble with radius $R = 0.41053$ forms a circular interface $\mathcal{I}$ that divides a square domain $\Omega = [-1,1]^2$ into two regions, $\Omega_1 := \{\boldsymbol{x} \in \Omega | \|\boldsymbol{x}\| > R\}$ and $\Omega_2 := \Omega \setminus \Omega_1$ as shown in Figure 4.17.

the non-dimensional kinematic viscosities are:

$$\nu(\boldsymbol{x}) = \begin{cases} \nu_1 = 0.1 & \text{in } \Omega_1 \\ \nu_2 = 1.5 & \text{in } \Omega_2 \end{cases}$$

The analytical velocity is given in terms of the radius $r = \sqrt{x^2+y^2}$ as:

$$\boldsymbol{u}(\boldsymbol{x}) = \begin{cases} [-y\alpha(r)e^{-r^2},\ x\alpha(r)e^{-r^2}]^T & \text{in } \Omega_1 \\ [-y\alpha(r)e^{-r^2},\ x\alpha(r)e^{-r^2}]^T & \text{in } \Omega_2 \end{cases}$$

where $\alpha(r)$ is defined as:

$$\alpha(r) = \begin{cases} \dfrac{1}{\nu_1} + \left(\dfrac{1}{\nu_2} - \dfrac{1}{\nu_1}\right) e^{r^2-R^2} & \text{in } \Omega_1 \\ \dfrac{1}{\nu_2} & \text{in } \Omega_2 \end{cases}$$

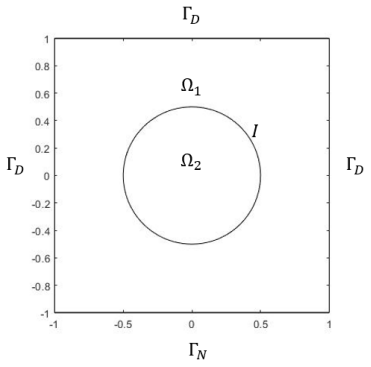

Figure 4.17: Domain for Example 3.

and the analytical pressure is given as:

$$P(\boldsymbol{x}) = \begin{cases} x^3 & \text{in } \Omega_1 \\ x^3 + \tau_s\kappa(\boldsymbol{x}) = x^3 + 2\tau_s/R & \text{in } \Omega_2 \end{cases}$$

where τ_s is the surface tension coefficient and $\kappa(\boldsymbol{x}) = 2/R$ is the local curvature of the interface. Note the pressure jump $P_1 - P_2 = 2\tau_s/R$. Finally, Dirichlet boundary conditions are set everywhere on the boundary except for the bottom boundary which is subject to Neumann boundary conditions derived from the analytical solution.

First, the results obtained with meshes of $(m, m-1)$ triangles are shown and analyzed. The order of approximation of the velocity is varied from $m = 1$ to $m = 2$. The stabilization parameters introduced in the X-HDG numerical fluxes are set as $\tau = 1$ and $\tau^{\mathcal{I}} = 0.001$. Lastly, as mentioned earlier for triangular elements, in order to satisfy the divergence-free condition, pressure elements of degree $(m-1)$ are used.

The numerical pressure obtained with the fourth mesh and velocity order $m = 2$ is shown in Figure 4.18 where the resolved sharp discontinuous pressure can be seen. The maximum point-wise divergence of the velocity $\boldsymbol{\nabla} \cdot \boldsymbol{u}$ is presented in Table 4.13 to be checked. It is noticed that the divergence-free condition is satisfied to the order $\mathcal{O}(10^{-13})$ and $\mathcal{O}(10^{-10})$ for $m = 1$ and $m = 2$, respectively. Moreover, a plot of the velocity divergence on mesh 3 with degree approximation $m = 2$ is shown in Figure 4.19 where again it can be seen that the velocity divergence are of the order $\mathcal{O}(10^{-15})$ to $\mathcal{O}(10^{-13})$ on almost 95% of the elements. Moreover, the jumps in the normal velocities $[\![\boldsymbol{u} \cdot \boldsymbol{n}]\!]$ across

inter-elements faces and the free-surface are of the order $\mathcal{O}(10^{-15})$ to $\mathcal{O}(10^{-13})$ as shown in Tables 4.14 and 4.15.

The mesh convergence plots are shown in Figure 4.20 excluding the coarsest mesh. For the case of $m = 1$, the same observations from the previous two examples are again noted here, where optimal convergence rates ($m + 1$ in $\mathcal{L}_2$-norm, m in $\mathcal{H}^1$-norm) are achieved for both x-velocity u and flux component L_1, and super-convergence ($m + 1$ in $\mathcal{L}_2$-norm) is observed for the pressure P. However, this is not the case for $m = 2$ where the convergence rates in $\mathcal{L}_2$-norm remain the same as for $m = 1$. This is expected because of the linear approximation of the interface that leads to dominant local errors at the interface, see for instance the error in the pressure field obtained with the fourth mesh and velocity order $m = 2$ in Figure 4.18. So in order to restore the optimal convergence rates, the interface has to be accurately represented [38].

Nonetheless, the error level for $m = 2$ is one order of magnitude smaller than for $m = 1$ as seen from Figure 4.20, which is a valuable improvement from an engineering point of view.

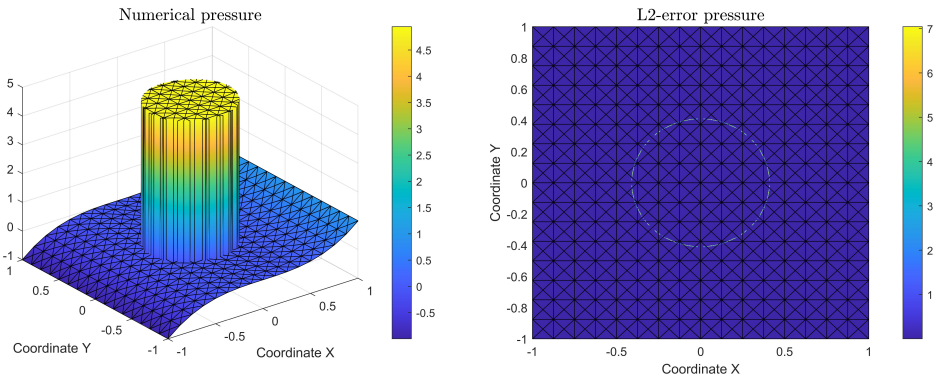

Figure 4.18: Ex 3: Numerical pressure obtained on mesh 4 of $(m, m-1)$ triangles and velocity order $m = 2$ (left), and the corresponding point-wise $\mathcal{L}_2$-norm error (right).

Mesh TRIs	$\tau = 1, \tau^{\mathcal{I}} = 0.001$	
	$m = 1$	$m = 2$
mesh 1	7.22E-15	1.04E-13
mesh 2	7.66E-14	2.27E-11
mesh 3	1.09E-13	9.44E-12
mesh 4	1.09E-13	3.47E-11
mesh 5	2.37E-12	2.54E-10

Table 4.13: Ex 3: Max. divergence of velocity $||\boldsymbol{\nabla} \cdot \boldsymbol{u}||_\infty$ - Meshes of $(m, m-1)$ triangles.

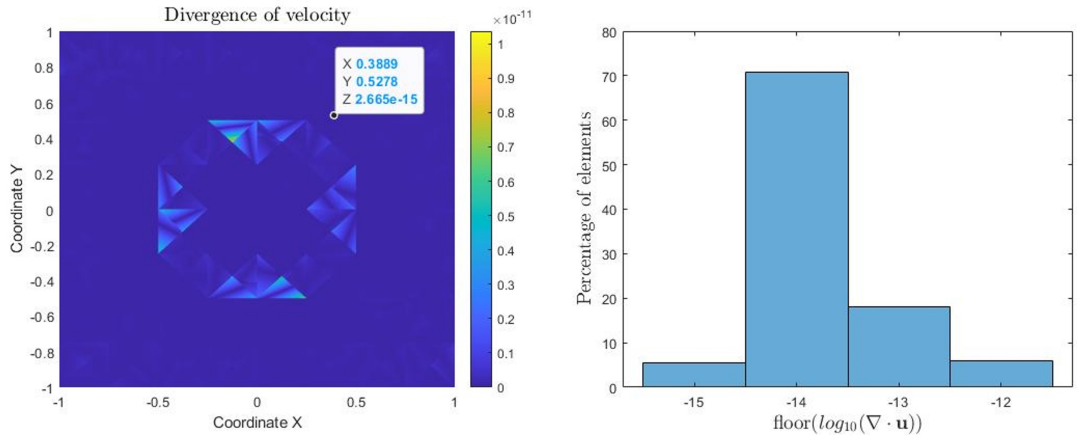

Figure 4.19: Ex 3: $\boldsymbol{\nabla} \cdot \boldsymbol{u}$ plotted for $m = 2$/mesh 3 of $(m, m-1)$ triangles (left), and a histogram showing the percentage of elements with their respective order of velocity-divergence (right).

Mesh TRIs	$\tau = 1, \tau^{\mathcal{I}} = 0.001$	
	$m = 1$	$m = 2$
mesh 1	3.11E-15	7.16E-15
mesh 2	9.34E-15	1.11E-13
mesh 3	2.55E-14	5.19E-14
mesh 4	1.43E-14	2.93E-14
mesh 5	3.62E-14	1.11E-13

Table 4.14: Ex 3: Max. inter-elements jump: $||[\![\boldsymbol{u} \cdot \boldsymbol{n}]\!]_{\Gamma \setminus \partial\Omega}||_\infty$ - Meshes of $(m, m-1)$ triangles.

Mesh TRIs	$\tau = 1, \tau^{\mathcal{I}} = 0.001$	
	$m = 1$	$m = 2$
mesh 1	4.97E-15	4.07E-15
mesh 2	2.86E-14	2.51E-14
mesh 3	1.30E-14	1.53E-14
mesh 4	6.94E-15	6.54E-14
mesh 5	1.68E-14	9.97E-14

Table 4.15: Ex 3: Max. free-surface jump: $||[\![\boldsymbol{u} \cdot \boldsymbol{n}]\!]_{\mathcal{I}}||_\infty$ - Meshes of $(m, m-1)$ triangles.

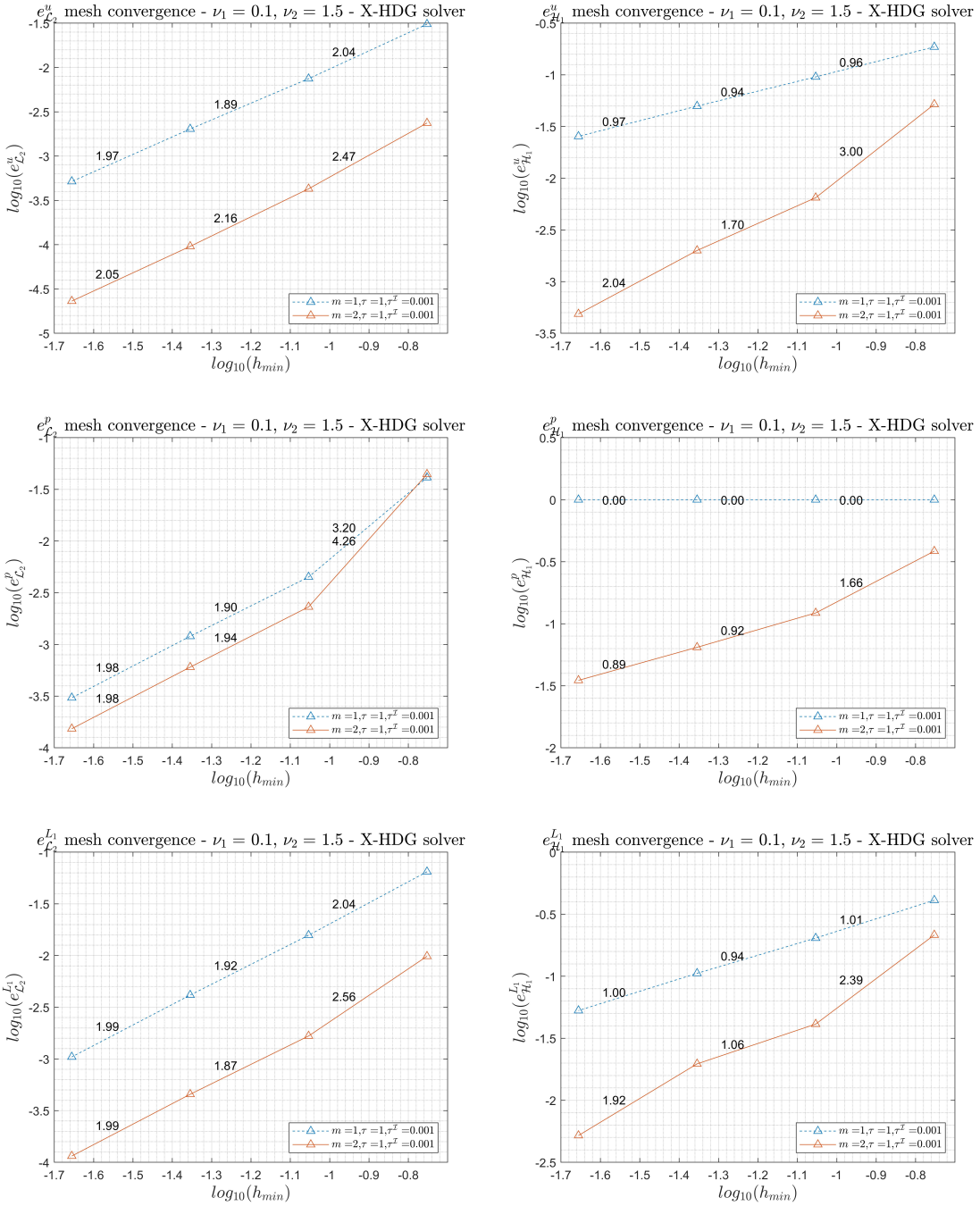

Figure 4.20: Ex 3: Errors in x-velocity u (top), pressure P (middle), and flux component L_1 (bottom) vs. mesh size - $\mathcal{L}_2$-norm (left), $\mathcal{H}^1$-norm (right) - Meshes of $(m, m-1)$ triangles.

Next, the results obtained with meshes of (m, m_{reduced}) quadrilaterals are shown and analyzed. The interface is approximated with order $m^{\mathcal{I}} = 5$ in each cut element. For the case of quadrilaterals, the boundary conditions are Neumann everywhere except for the right boundary which is Dirichlet. Furthermore, the degree of approximation for the velocity is varied from $m = 2$ to $m = 3$.

The maximum point-wise divergence of the velocity $\boldsymbol{\nabla} \cdot \boldsymbol{u}$ is presented in Table 4.16. It is noticed that higher values of the point-wise divergence of the velocity are obtained. However, considering for instance the case of $m = 3$ and mesh 3, the point-wise divergence of velocity is of order $\mathcal{O}(10^{-14})$ to $\mathcal{O}(10^{-12})$ on almost 80% of the elements as shown in Figure 4.21.

Mesh	$\tau = 1, \tau^{\mathcal{I}} = 0.001$		
QUADs	$m = 1$	$m = 2$	$m = 3$
mesh 1	-	9.23E-06	3.94E-03
mesh 2	-	6.98E-10	3.13E-04
mesh 3	-	3.11E-04	1.44E-03
mesh 4	-	3.01E-04	2.19E-02
mesh 5	-	1.75E-04	4.34E-02

Table 4.16: Ex 3: Max. divergence of velocity $||\boldsymbol{\nabla} \cdot \boldsymbol{u}||_\infty$ - Meshes of (m, m_{reduced}) quadrilaterals.

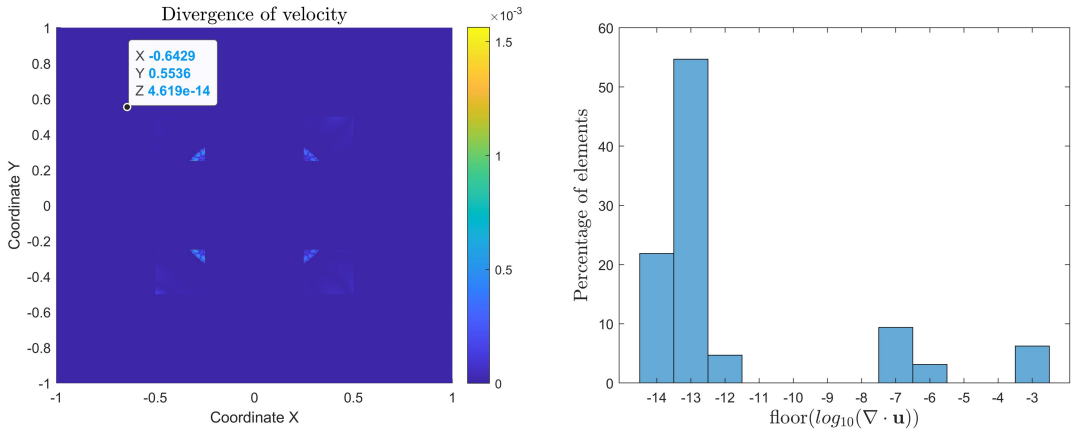

Figure 4.21: Ex 3: $\boldsymbol{\nabla} \cdot \boldsymbol{u}$ plotted for $m = 3$/mesh 3 of (m, m_{reduced}) quadrilaterals (left), and a histogram showing the percentage of elements with their respective order of velocity-divergence (right).

Moreover, the jumps in the normal velocities $[\![\boldsymbol{u} \cdot \boldsymbol{n}]\!]$ across inter-elements faces are of the order $\mathcal{O}(10^{-15})$ to $\mathcal{O}(10^{-10})$ as shown in Table 4.17 and are exactly zero across the free-surface as seen in Table 4.18.

Mesh	$\tau = 1, \tau^{\mathcal{I}} = 0.001$		
QUADs	$m = 1$	$m = 2$	$m = 3$
mesh 1	-	2.72E-10	3.59E-10
mesh 2	-	1.43E-13	8.44E-11
mesh 3	-	4.44E-15	2.71E-13
mesh 4	-	4.44E-15	8.71E-11
mesh 5	-	2.57E-14	7.21E-11

Table 4.17: Ex 3: Max. inter-elements jump: $||[\![\boldsymbol{u} \cdot \boldsymbol{n}]\!]_{\Gamma \setminus \partial\Omega}||_\infty$ - Meshes of (m, m_{reduced}) quadrilaterals.

Mesh	$\tau = 1, \tau^{\mathcal{I}} = 0.001$		
QUADs	$m = 1$	$m = 2$	$m = 3$
mesh 1	-	0	0
mesh 2	-	0	0
mesh 3	-	0	0
mesh 4	-	0	0
mesh 5	-	0	0

Table 4.18: Ex 3: Max. free-surface jump: $|||[\![\boldsymbol{u} \cdot \boldsymbol{n}]\!]_{\mathcal{I}}||_{\infty}$ - Meshes of (m, m_{reduced}) quadrilaterals.

The numerical pressures obtained with both $m = 2$ and $m = 3$ on meshes 3 to 5 are shown in Figure 4.22, where the numerical errors are clearly visible! the reason is most probably the ill-conditioning of the assembled X-HDG global operator (see Table 4.19). This issue is more visible in the case of $m = 2$ as seen in Figure 4.22 even though the X-HDG global matrices are better conditioned for $m = 2$ when compared to $m = 3$. The reason behind this is actually not clear thus further investigation is needed.

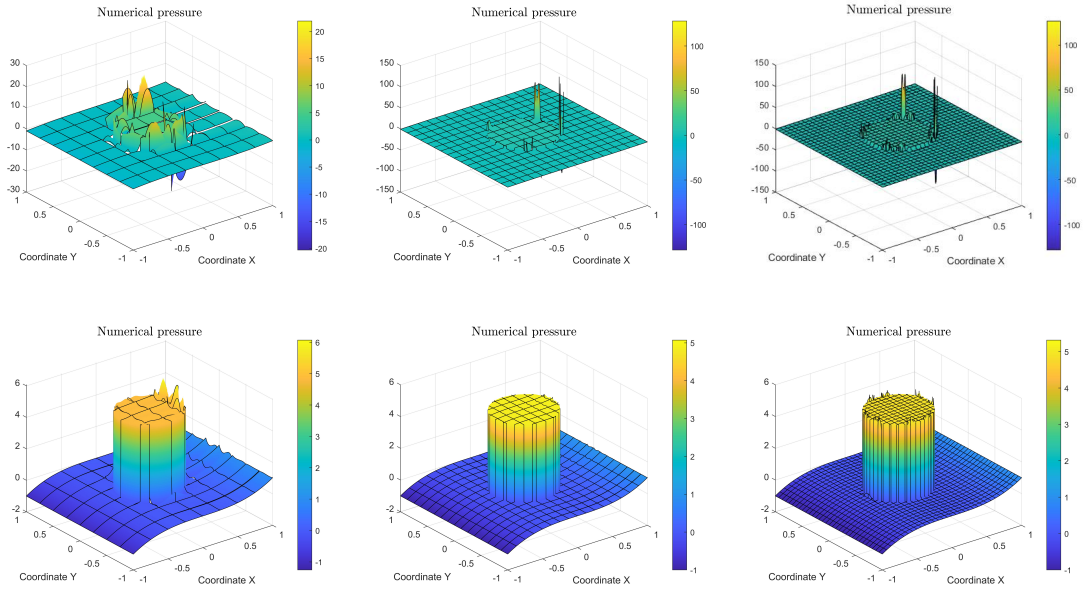

Figure 4.22: Ex 3: Numerical pressure obtained on meshes 3:5 with velocity order $m = 2$ (top) and $m = 3$ (bottom) - Meshes of (m, m_{reduced}) quadrilaterals.

Mesh	$\tau = 1, \tau^{\mathcal{I}} = 0.001$		
QUADs	$m = 1$	$m = 2$	$m = 3$
mesh 1	-	1.21E+19	9.47E+19
mesh 2	-	2.59E+20	1.64E+19
mesh 3	-	2.18E+10	4.80E+12
mesh 4	-	3.86E+11	4.50E+14
mesh 5	-	1.60E+11	5.33E+13

Table 4.19: Ex 3: Condition number of the X-HDG global operator - Meshes of (m, m_{reduced}) quadrilaterals.

Furthermore, the mesh convergence plots are shown in Figure 4.23. It is observed that sub-optimal rates are obtained for both x-velocity u and flux component L_1. As for the pressure, it is difficult to draw out a conclusion regarding the convergence.

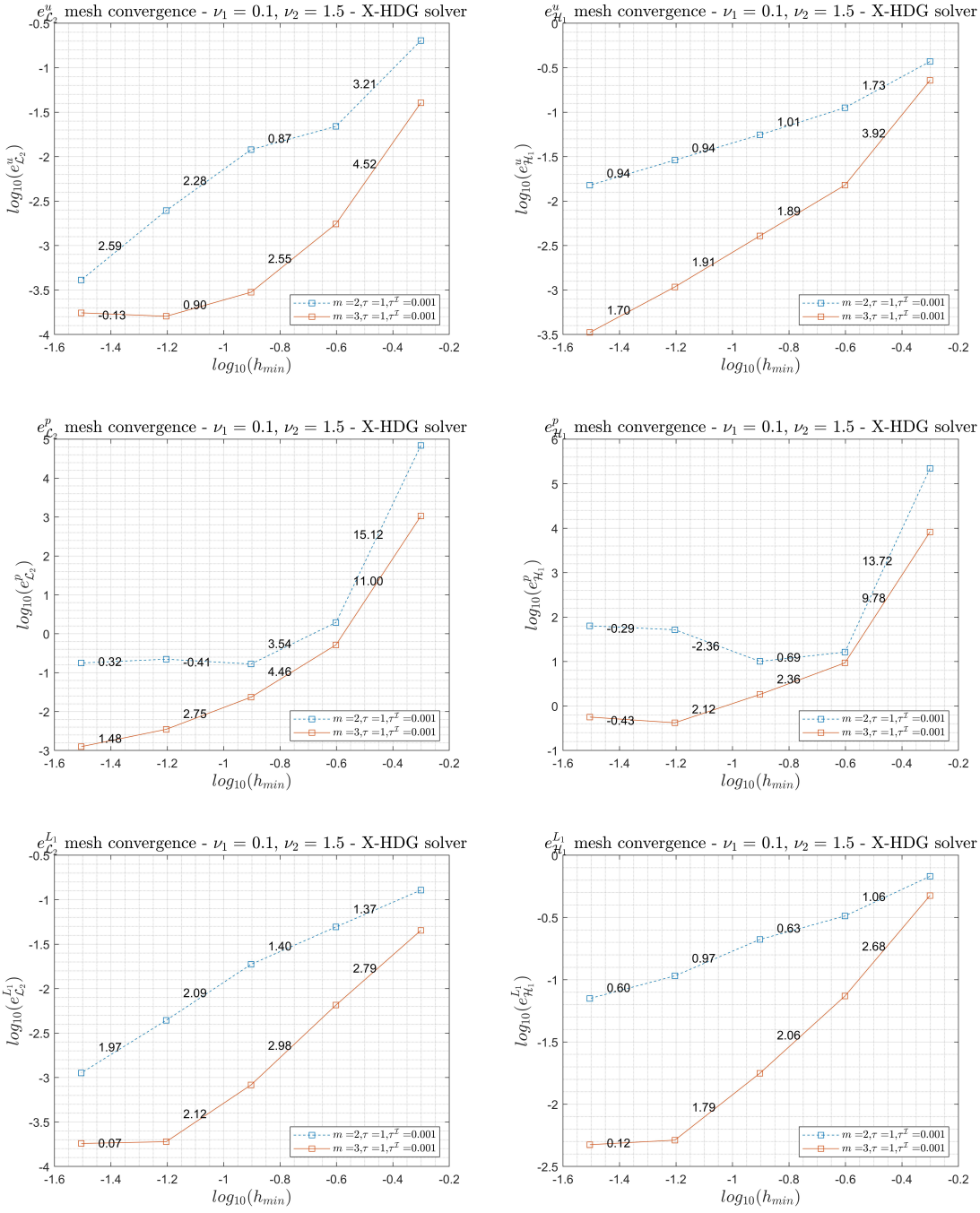

Figure 4.23: Ex 3: Errors in x-velocity u (top), pressure P (middle), and flux component L_1 (bottom) vs. mesh size - $\mathcal{L}_2$-norm (left), $\mathcal{H}^1$-norm (right) - Meshes of (m, m_{reduced}) quadrilaterals.

Finally, the results obtained with meshes of $(m, m-1)$ quadrilaterals are shown and analyzed. This velocity-pressure pair does not provide pointwise divergence-free velocity field. Here, the degree of approximation for the velocity is varied from $m = 1$ to $m = 3$. Furthermore, the interface is approximated with order $m^{\mathcal{I}} = m$ in each cut element. The reason behind testing $(m, m-1)$ quadrilaterals is to check if the numerical errors in the pressure would still be clearly seen as in the case of (m, m_{reduced}) quadrilaterals.

First of all, the maximum point-wise divergence of the velocity $\boldsymbol{\nabla} \cdot \boldsymbol{u}$ is presented in Table 4.20, and as expected, the divergence-free condition is not satisfied where values of order $\mathcal{O}(10^0)$ to $\mathcal{O}(10^{-2})$ are obtained. Moreover, a plot of the velocity divergence on mesh 3 with degree approximation $m = 3$ is shown in Figure 4.24 where again it can be seen that the velocity divergence are of the order $\mathcal{O}(10^{-4})$ to $\mathcal{O}(10^{-2})$ on 100% of the elements.

Mesh QUADs	$\tau = 1, \tau^{\mathcal{I}} = 0.001$		
	$m = 1$	$m = 2$	$m = 3$
mesh 1	1.68E-00	4.04E-00	2.15E-00
mesh 2	3.06E-00	9.76E-01	1.51E-01
mesh 3	2.15E-00	4.31E-01	2.10E-02
mesh 4	1.64E-00	2.13E-01	1.35E-02
mesh 5	1.14E-00	3.26E-01	1.99E-02

Table 4.20: Ex 3: Max. divergence of velocity $||\boldsymbol{\nabla} \cdot \boldsymbol{u}||_\infty$ - Meshes of $(m, m-1)$ quadrilaterals.

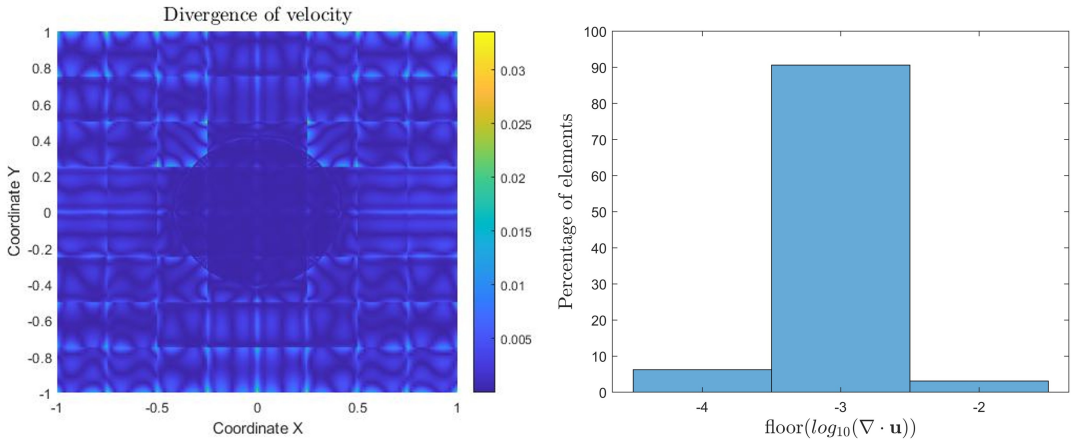

Figure 4.24: Ex 3: $\boldsymbol{\nabla} \cdot \boldsymbol{u}$ plotted for $m = 3$/mesh 3 of $(m, m-1)$ quadrilaterals (left), and a histogram showing the percentage of elements with their respective order of velocity-divergence (right).

The numerical pressures obtained with both $m = 2$ and $m = 3$ on meshes 3 to 5 are shown in Figure 4.25, where the discontinuity is sharply represented compared to the case of (m, m_{reduced}) quadrilaterals. Note the condition numbers of the assembled X-HDG global operators of all tested degrees and meshes in Table 4.21. It is observed that the X-HDG global operators of $(m, m-1)$ quadrilaterals are better conditioned when compared to (m, m_{reduced}) quadrilaterals.

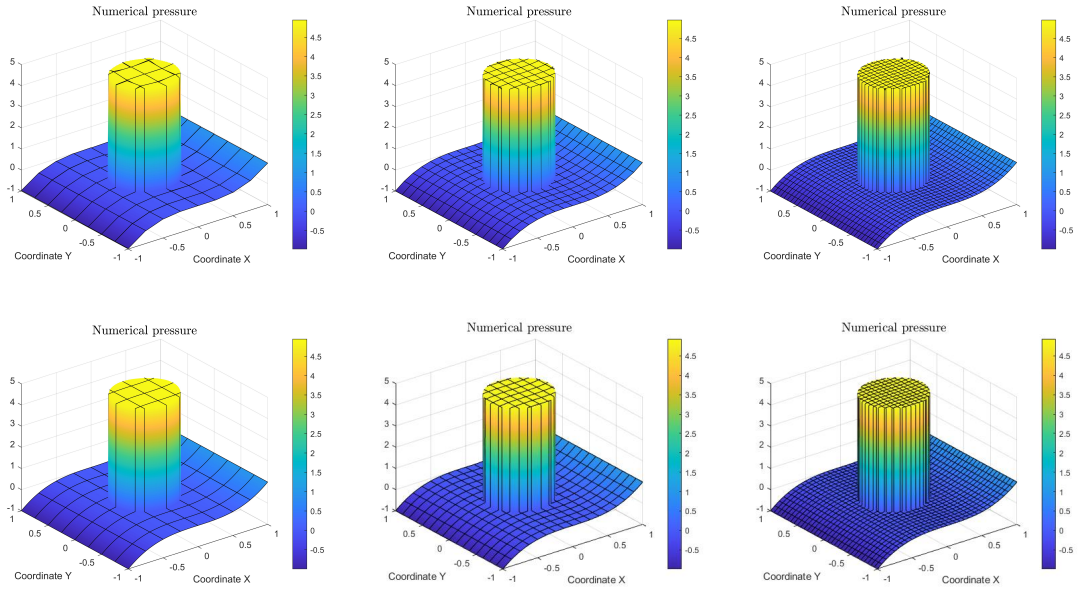

Figure 4.25: Ex 3: Numerical pressure obtained on meshes 3:5 with velocity order $m = 2$ (top) and $m = 3$ (bottom) - Meshes of $(m, m-1)$ quadrilaterals.

Mesh QUADs	$\tau = 1, \tau^{\mathcal{I}} = 0.001$		
	$m = 1$	$m = 2$	$m = 3$
mesh 1	2.56E+04	1.71E+06	7.32E+07
mesh 2	2.44E+07	8.23E+10	2.12E+14
mesh 3	1.29E+05	2.25E+08	1.85E+10
mesh 4	3.92E+06	1.14E+11	4.08E+14
mesh 5	2.54E+06	6.92E+10	4.62E+12

Table 4.21: Ex 3: Condition number of the X-HDG global operator - Meshes of $(m, m-1)$ quadrilaterals.

Finally, the mesh convergence plots are shown in Figure 4.26. For the x-velocity u, optimal convergence rate ($m+1$ in $\mathcal{L}_2$-norm) is achieved except for the last mesh refinement with $m = 2$ and the last two refinements with $m = 3$. As for the pressure P, optimal convergence rates (m in $\mathcal{L}_2$-norm, $m-1$ in $\mathcal{H}^1$-norm) are observed except for the last mesh refinement with $m = 3$. Lastly, for the flux component L_1, optimal convergence ($m+1$ in $\mathcal{L}_2$-norm, m in $\mathcal{H}^1$-norm) is only achieved for $m = 1$, while sub-optimal rates (m in $\mathcal{L}_2$-norm, $m-1$ in $\mathcal{H}^1$-norm) for $m = 2$ and $m = 3$ are obtained except for the last two mesh refinements with $m = 3$.

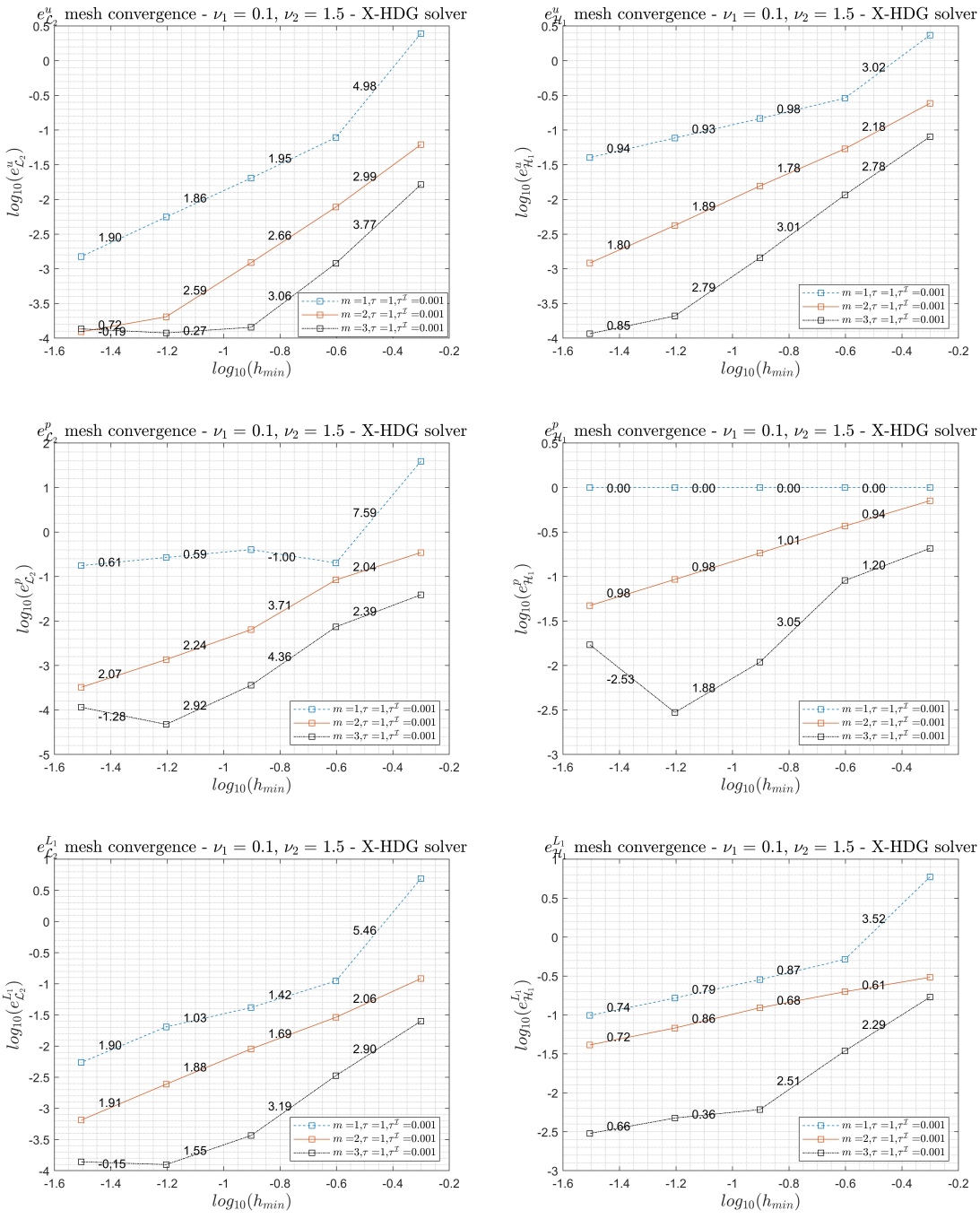

Figure 4.26: Ex 3: Errors in x-velocity u (top), pressure P (middle), and flux component L_1 (bottom) vs. mesh size - $\mathcal{L}_2$-norm (left), $\mathcal{H}^1$-norm (right) - Meshes of $(m, m-1)$ quadrilaterals.

4.4 Conclusions and final remarks

An energy-stable formulation for two-phase incompressible Stokes equation that is mass and momentum conserving is proposed. This method is an extension of the formulation presented in the work of Elzaabalawy [35] for single-phase incompressible Navier-Stokes equations. It is also considered as an extension of the X-HDG method for two-phase Stokes equation proposed by Gürkan et al. [38]. The method computes exactly point-wise divergence-free, and $\mathcal{H}(div)$-conforming velocity fields. The key point of the proposed method is the usage of pressure elements that uses polynomials in the space of divergence of polynomial basis that are used to approximate the velocity. In addition, traces of velocity and pressure, of the same order m as the velocity, are introduced on the inter-element faces and the interface to enforce the transmission conditions of the conservation equations. What is truly unique in the proposed method is the introduction of the pressure trace variable of degree m on the interface to enforce the continuity of normal velocity, thus enforcing mass conservation across the interface.

The method is tested on meshes of $(m, m-1)$ triangles with piece-wise linear approximation of the interface as well as on meshes of (m, m_{reduced}) quadrilaterals with piece-wise high-order approximation of the interface. The results showed the capability of the method to accurately resolve local discontinuities without the need for re-meshing to fit the interface, however better results were obtained with meshes of triangles.

As for triangles, higher-order convergence rates were obtained for problems with straight interface that guarantee an exact representation of the interface. On the other hand, for problems with curved interfaces, the observed convergence for degree $m = 1$ is the same as in problems with straight interfaces. However, this is not the case for higher m where the convergence rates remain the same as for $m = 1$ but with lower error magnitudes. This is expected because of the linear approximation of the interface, within each cut element, that leads to dominant local errors at the interface. So in order to restore higher-order convergence rates, the interface has to be accurately represented. Developing higher-order integration quadrature for triangles with curved cuts is considered as future work.

As for quadrilaterals, good results were obtained for problems with straight interface. However, further investigation is needed to determine the issue behind obtaining numerical pressure with relatively noticeable error in problems with curved interfaces.

As a conclusion, it would be favorable to use the proposed method on meshes of $(m, m-1)$ triangles with piece-wise linear approximation of curved interfaces. The reason is the robustness of this pair of velocity-pressure elements. In addition, the achieved accuracy with this pair of elements is acceptable from an engineering point of view.

Chapter 5

The Level-Set method for moving interfaces

The level-set method is an interface capturing method, where a signed-distance function ϕ is used to describe the location of the interface. The function ϕ is positive on one side of the interface and negative on the other side. Furthermore, the iso-contour $\phi = 0$ is the interface itself.

At any point $\boldsymbol{x}$ in a domain Ω, the minimum distance to an interface $\mathcal{I}$ is computed as

$$\begin{aligned} d(\boldsymbol{x}) &= \min(|\boldsymbol{x} - \boldsymbol{x}_I|) \qquad \forall\, \boldsymbol{x}_I \in \mathcal{I}, \\ &= |\boldsymbol{x} - \boldsymbol{x}_c| \end{aligned} \tag{5.0.1}$$

where $\boldsymbol{x}_c$ is the closest point on the interface to point $\boldsymbol{x}$, and $|\odot|$ is the Euclidean norm, i.e $|\boldsymbol{x} - \boldsymbol{x}_c| = \sqrt{(x_1 - x_{c1})^2 + (x_2 - x_{c2})^2 + (x_3 - x_{c3})^2}$.

The level-set function is a signed distance function defined as

$$|\phi(\boldsymbol{x})| = d(\boldsymbol{x}) \qquad \forall\, \boldsymbol{x} \in \Omega \tag{5.0.2}$$

meaning that

$$\phi(\boldsymbol{x}) = \begin{cases} +d(\boldsymbol{x}) & \forall \boldsymbol{x} \in \Omega^+, \\ 0 & \forall \boldsymbol{x} \in \mathcal{I}, \\ -d(\boldsymbol{x}) & \forall \boldsymbol{x} \in \Omega^-. \end{cases} \tag{5.0.3}$$

Note that the signed distance function should always satisfy the following property

$$|\boldsymbol{\nabla}\phi| = 1 \tag{5.0.4}$$

Furthermore, the unit normal vector $\boldsymbol{n}$ on the interface (pointing in the direction of increasing ϕ, i.e. from Ω^- to Ω^+) is computed as

$$\boldsymbol{n} = \frac{\boldsymbol{\nabla}\phi}{|\boldsymbol{\nabla}\phi|} = \boldsymbol{\nabla}\phi \tag{5.0.5}$$

and the mean curvature of the interface is computed as

$$\kappa = \boldsymbol{\nabla}\cdot\boldsymbol{n} = \boldsymbol{\nabla}\cdot(\frac{\boldsymbol{\nabla}\phi}{|\boldsymbol{\nabla}\phi|}) = \boldsymbol{\nabla}\cdot\boldsymbol{\nabla}\phi \tag{5.0.6}$$

See [41] for more details.

In general, we are interested in solving for the level-set only in the vicinity of the interface. However, we solve for it in the whole computational domain for ease of computations. Here, one assumption is taken into consideration: the signed-distance property $|\boldsymbol{\nabla}\phi| = 1$ is always satisfied so no re-initialization (re-distancing) is needed.

5.1 The Model equation

The evolution of the level-set is described using the transient linear advection equation of $\phi = \phi(\boldsymbol{x}, t)$ by the velocity field $\boldsymbol{u}$.

$$\frac{\partial \phi}{\partial t} + \boldsymbol{\nabla} \cdot (\boldsymbol{u}\phi) = 0 \qquad \in \Omega \times (0, T), \tag{5.1.1}$$

that is further expanded to

$$\frac{\partial \phi}{\partial t} + \boldsymbol{u} \cdot \boldsymbol{\nabla}\phi + \phi \boldsymbol{\nabla} \cdot \boldsymbol{u} = 0 \qquad \in \Omega \times (0, T), \tag{5.1.2}$$

if $\boldsymbol{u}$ is a divergence-free advection velocity obtained from the Navier-Stokes solver, then the third term on the left hand side of 5.1.2 would be removed. However, the interface is not advected by the velocity obtained from Navier-Stokes solver, it is rather advected by an extension velocity $\boldsymbol{u}_{\text{ext}}(\boldsymbol{x}, t) := \boldsymbol{u}(\boldsymbol{x}_c, t)$ which is the velocity at the interface that is extended throughout the whole domain. This means that for any point $\boldsymbol{x} \in \Omega$, the velocity is equal to the that of the closest point on the interface [61, 62]. Therefore, the level-set equation becomes

$$\frac{\partial \phi}{\partial t} + \boldsymbol{u}_{\text{ext}} \cdot \boldsymbol{\nabla}\phi + \phi \boldsymbol{\nabla} \cdot \boldsymbol{u}_{\text{ext}} = 0 \qquad \in \Omega \times (0, T), \tag{5.1.3}$$

or it could be written again in the conservative form as

$$\frac{\partial \phi}{\partial t} + \boldsymbol{\nabla} \cdot (\boldsymbol{u}_{\text{ext}}\phi) = 0 \qquad \in \Omega \times (0, T). \tag{5.1.4}$$

Initial conditions
The initial position of the interface is known and is given as

$$\phi(\boldsymbol{x}, t_0) = d_0(\boldsymbol{x})$$

where $d_0(\boldsymbol{x})$ is the initial signed-distance to the interface.

Since we are interested in the solution of the level-set only in the vicinity of the interface, we will redefine the initial conditions so that the signed-distance is only valid in a pre-specified area (or volume in 3D) close to the interface, for instance

$$\phi_0(\boldsymbol{x}) = \begin{cases} \epsilon & \text{for } d_0(\boldsymbol{x}) > \epsilon, \\ d_0 & \text{for } -\epsilon \leq d_0(\boldsymbol{x}) \leq \epsilon, \\ -\epsilon & \text{for } d_0(\boldsymbol{x}) < -\epsilon. \end{cases} \tag{5.1.5}$$

where ϵ is a small normal distance from the interface that depends on the mesh size so that at least two or three layers of adjacent elements are included in the area of interest, see Figure 5.1. This approach is beneficial for imposing the boundary conditions as shown next. A similar approach is presented in Marchandise et al. [63].

Boundary conditions
The domain boundary is defined as $\partial\Omega = \Gamma_{in} \cup \Gamma_{out}$, where Γ_{in} is the inflow boundary and Γ_{out} is the outflow boundary, which are defined based on the direction of normal velocity at the boundary. Let $u_n = \boldsymbol{u}_{\text{ext}} \cdot \boldsymbol{n}$ be the normal component of the velocity vector where $\boldsymbol{n}$ is the outward unit normal vector to the boundary $\partial\Omega$, then Γ_{in} and Γ_{out} are defined as follows

$$\Gamma_{in} = \{\boldsymbol{x} \in \partial\Omega \mid u_n < 0\}, \; \Gamma_{out} = \{\boldsymbol{x} \in \partial\Omega \mid u_n > 0\}. \tag{5.1.6}$$

Note that boundary conditions are imposed only on the inflow part of the boundary Γ_{in} which is always the case for hyperbolic problems. The reason behind this is explained using the method of characteristics (MOC), where at the outflow boundary, all the characteristics are going out of the domain, thus, we can not impose any boundary condition at the outflow.

It is also not physical to know the distance between the interface and the domain boundary apriori, therefore we use the same data from the initial conditions defined in 5.1.5 and apply it as Dirichlet boundary conditions at the inlet. This approach is possible since we are only interested in the solution of the level-set in the vicinity of the interface.

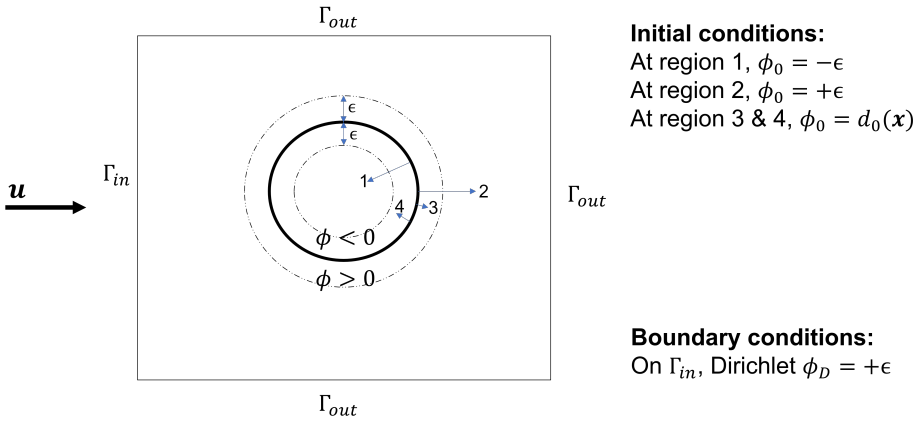

Figure 5.1: A schematic of the level-set problem setup for initial and boundary conditions.

In problems where the material interface cuts the domain boundary ($\partial\Omega$). We can't use the previous approach where we use data from the initial conditions as Dirichlet conditions at the inlet. Instead, we use the velocity field (from the previous) at the inlet boundary to get the value of the Level-Set function at that inlet and apply it as Dirichlet BCs. Otherwise, the Level-Set is fixed at inlet which is reasonable if the inlet is a far-field inlet.

5.2 The strong forms

The HDG formulation rewrites 5.1.4 as two equivalent problems. First, the local element-by-element problem introducing the trace variable $\widehat{\phi}$ which acts as Dirichlet boundary condition for the element, namely

$$\begin{cases} \dfrac{\partial \phi_i}{\partial t} + \boldsymbol{\nabla}\cdot\boldsymbol{f}(\phi_i) = 0 & in\ \Omega_i \times (0,T), \\ \phi_i = \phi_D & on\ \partial\Omega_i \cap \Gamma_{in} \times (0,T), \\ \phi_i = \widehat{\phi} & on\ \partial\Omega_i \setminus \partial\Omega \times (0,T), \\ \phi_i = \phi_0 & in\ \Omega_i \times \{0\}, \end{cases} \tag{5.2.1}$$

for $i = 1, ..., \mathtt{n_{el}}$. Here, the equation in the conservative form is considered where $\boldsymbol{f}(\phi) = \boldsymbol{u}_{\text{ext}}\phi$.

Second, a global problem is defined to determine $\widehat{\phi}$, this problem corresponds to the imposition of the continuity of the normal fluxes along the internal interface $\Gamma \setminus \partial\Omega$

$$[\![\boldsymbol{n}\cdot\boldsymbol{f}(\phi)]\!] = 0 \qquad on\ \Gamma \setminus \partial\Omega. \tag{5.2.2}$$

5.3 The weak forms

The weak formulation for each element equivalent to 5.2.1 is as follows: for $i = 1, ..., \mathtt{n_{el}}$, given ϕ_D on $\partial\Omega_i \cap \Gamma_{in}$ and $\widehat{\phi}$ on $\partial\Omega_i \setminus \partial\Omega$, find ϕ_i that satisfies

$$(\frac{\partial \phi_i}{\partial t}, v)_{K_i} - (\boldsymbol{f}(\phi_i), \boldsymbol{\nabla} v)_{K_i} + \langle \widehat{\boldsymbol{f}} \cdot \boldsymbol{n}, v \rangle_{\partial K_i} = 0 \tag{5.3.1}$$

for all test functions v, where the numerical traces of the fluxes $\widehat{\boldsymbol{f}}$ must be defined.

The numerical traces of the fluxes are defined face-by-face (i.e. for $j = 1, ..., \mathtt{n}^i_{\mathtt{fc}}$) on each element (i.e. for $i = 1, ..., \mathtt{n_{el}}$):

$$\widehat{\boldsymbol{f}}_j \cdot \boldsymbol{n}_j := \begin{cases} \boldsymbol{f}_j(\phi_i) \cdot \boldsymbol{n}_j + \tau_j(\phi_i - \phi_D) & on\ \partial\Omega_i \cap \Gamma_{in}, \\ \boldsymbol{f}_j(\phi_i) \cdot \boldsymbol{n}_j + \tau_j(\phi_i - \phi_{outflow}) & on\ \partial\Omega_i \cap \Gamma_{out}, \\ \boldsymbol{f}_j(\phi_i) \cdot \boldsymbol{n}_j + \tau_j(\phi_i - \widehat{\phi}_j) & on\ \Gamma \setminus \partial\Omega. \end{cases} \tag{5.3.2}$$

where $\mathtt{n_{fc}}$ is the number of element faces/edges and τ_j being a stabilization parameter whose selection affects the stability, accuracy, and convergence properties of the resulting HDG method. Note that $\phi_{outflow}$ represents the value of ϕ on a face that belongs to the outflow boundary Γ_{out}. Usually, in hyperbolic problems $\phi_{outflow}$ is interpolated using the value of ϕ from inside the domain. The reason is explained using the method of characteristics (MOC), where at the outflow boundary, all the characteristics are going out of the domain.

The stabilization parameter τ_j could be defined as follows

$$\begin{aligned} \tau_j &:= \max_{\boldsymbol{x} \in \Gamma} |\boldsymbol{u}_{\text{ext}} \cdot \boldsymbol{n}_j|, \\ \tau_j &:= |\boldsymbol{u}_{\text{ext}} \cdot \boldsymbol{n}_j|. \end{aligned} \tag{5.3.3}$$

which corresponds to the global Lax-Friedrichs and the local Lax-Friedrichs solvers, respectively [64].

The weak formulation of the global problem equivalent to 5.2.2 is simply: find $\widehat{\phi}$ for all test functions μ such that

$$\sum_{i=1}^{\mathtt{n_{el}}} \langle \widehat{\boldsymbol{f}} \cdot \boldsymbol{n}, \mu \rangle_{\partial\Omega_i \setminus \partial\Omega} = 0 \tag{5.3.4}$$

Substituting the definition for the numerical traces of fluxes given by 5.3.2 into both the local 5.3.1 and global 5.3.4 problems, we get the following equation for the local problems

$$\begin{aligned} (\frac{\partial \phi_i}{\partial t}, v)_{K_i} - (\boldsymbol{f}(\phi_i), \boldsymbol{\nabla} v)_{K_i} + \langle \boldsymbol{f}(\phi_i) \cdot \boldsymbol{n}, v \rangle_{\partial K_i} + \langle \tau \phi_i, v \rangle_{\partial K_i} \\ - \langle \tau \phi_D, v \rangle_{\partial\Omega_i \cap \Gamma_{in}} - \langle \tau \phi_{outflow}, v \rangle_{\partial\Omega_i \cap \Gamma_{out}} - \langle \tau \widehat{\phi}, v \rangle_{\partial\Omega_i \setminus \partial\Omega} = 0 \end{aligned} \tag{5.3.5}$$

and the following equation for the global problem

$$\sum_{i=1}^{\mathtt{n_{el}}} \left[\langle \boldsymbol{f}(\phi_i) \cdot \boldsymbol{n}, \mu \rangle_{\partial\Omega_i \setminus \partial\Omega} + \langle \tau \phi_i, \mu \rangle_{\partial\Omega_i \setminus \partial\Omega} - \langle \tau \widehat{\phi}_i, \mu \rangle_{\partial\Omega_i \setminus \partial\Omega} \right] = 0 \tag{5.3.6}$$

5.4 The semi-discrete forms

The semi-discrete forms of the local and global problems are written as: find $(u_i^h, \widehat{u}^h) \in \mathcal{S}_v^h(\Omega_i) \times \mathcal{S}_v^h(\Gamma)$ that satisfies

$$(\frac{\partial \phi_i^h}{\partial t}, v^h)_{K_i} - (\boldsymbol{f}(\phi_i^h), \boldsymbol{\nabla} v^h)_{K_i} + \langle \boldsymbol{f}(\phi_i^h)\cdot \boldsymbol{n}, v^h\rangle_{\partial K_i} + \langle \tau \phi_i^h, v^h\rangle_{\partial K_i} \\ -\langle \tau \phi_D, v^h\rangle_{\partial\Omega_i\cap\Gamma_{in}} - \langle \tau \phi_{outflow}, v^h\rangle_{\partial\Omega_i\cap\Gamma_{out}} - \langle \tau \widehat{\phi}^h, v^h\rangle_{\partial\Omega_i\setminus\partial\Omega} = (f, v^h)_{K_i} \tag{5.4.1}$$

$$\sum_{i=1}^{\mathtt{n_{el}}}\left[\langle \boldsymbol{f}(\phi_i^h)\cdot\boldsymbol{n}, \mu^h\rangle_{\partial\Omega_i\setminus\partial\Omega} + \langle \tau\phi_i^h, \mu^h\rangle_{\partial\Omega_i\setminus\partial\Omega} - \langle \tau\widehat{\phi}^h, \mu^h\rangle_{\partial\Omega_i\setminus\partial\Omega}\right] = 0 \tag{5.4.2}$$

for all test functions $(v^h, \mu^h) \in \mathcal{S}_v^h(\Omega_i) \times \mathcal{S}_v^h(\Gamma)$ and all $t \in (0, T)$.

Next, this semi-discrete HDG formulation is discretized in space then in time using implicit or explicit time-stepping methods.

5.5 Spatial discretization

Polynomial interpolation of functions using nodal values is defined as follows

$$\phi^h(\boldsymbol{\xi}^e) = \sum_{j=1}^{\mathtt{n_{en}}} N_j(\boldsymbol{\xi}^e)\Phi_j \qquad \in \mathcal{S}_v^h, \tag{5.5.1}$$

$$\widehat{\phi}^h(\boldsymbol{\xi}^f) = \sum_{j=1}^{\mathtt{n_{fn}}} \widehat{N}_j(\boldsymbol{\xi}^f)\widehat{\Phi}_j \qquad \in \mathcal{S}_s^h. \tag{5.5.2}$$

on a reference element with local coordinates $\boldsymbol{\xi}^e = [\xi_1^e, ..., \xi_{\mathtt{n_{sd}}}^e]$ and a reference face/edge with local coordinates $\boldsymbol{\xi}^f = [\xi_1^f, ..., \xi_{\mathtt{n_{sd}}-1}^f]$, respectively. Here, Φ_j and $\widehat{\Phi}_j$ are nodal values, N_j are polynomial shape functions of order m in each element, $\mathtt{n_{en}}$ is the number of nodes per element, $\widehat{N}_j$ are polynomial shape functions of order m in each face/edge, and $\mathtt{n_{fn}}$ is the corresponding number of nodes per face/edge. Note that also the test functions (v^h, μ^h) are interpolated in a similar way.

It is useful to write the polynomial interpolations of the functions as follows

$$\begin{aligned}
\phi_i^h &= \boldsymbol{N}^T(\boldsymbol{\xi}^e)\boldsymbol{\phi}_i,\\
\widehat{\phi}_{i,j}^h &= \widehat{\boldsymbol{N}}^T(\boldsymbol{\xi}^f)\widehat{\boldsymbol{\phi}}_{i,j},\\
v^h &= \boldsymbol{v}\boldsymbol{N}(\boldsymbol{\xi}^e) = \boldsymbol{N}^T(\boldsymbol{\xi}^e)\boldsymbol{v}^T,\\
\mu^h &= \boldsymbol{\mu}\widehat{\boldsymbol{N}}(\boldsymbol{\xi}^f).
\end{aligned}$$

where $\boldsymbol{N}(\boldsymbol{\xi}^e) = [N_1\ N_2\ ...\ N_{\mathtt{n_{en}}}]^T$, $\widehat{\boldsymbol{N}}(\boldsymbol{\xi}^f) = [\widehat{N}_1\ \widehat{N}_2\ ...\ \widehat{N}_{\mathtt{n_{fn}}}]^T$, $\boldsymbol{\phi}_i$ is a column vector of the nodal values of ϕ^h in element i, $\widehat{\boldsymbol{\phi}}_{i,j}$ is a column vector of the nodal values of $\widehat{\phi}^h$ on face/edge j adjacent to element i, $\boldsymbol{v} = [v_1\ v_2\ ...\ v_{\mathtt{n_{en}}}]$ and $\boldsymbol{\mu} = [\mu_1\ \mu_2\ ...\ \mu_{\mathtt{n_{fn}}}]$ where they represent the nodal values of the test functions.

The terms in the semi-discrete form of the problem are written in expanded form:

$$(\frac{\partial \phi_i^h}{\partial t}, v^h)_{K_i} = \boldsymbol{v}\int_{\Omega_{ref}} \boldsymbol{N}\boldsymbol{N}^T|\boldsymbol{J}^e|\ d\Omega_{ref}\ \frac{\partial \boldsymbol{\phi}_i}{\partial t} = \boldsymbol{v}\boldsymbol{A}_i\frac{\partial \boldsymbol{\phi}_i}{\partial t} \tag{5.5.3}$$

$$(\boldsymbol{f}(\phi_i^h), \boldsymbol{\nabla} v^h)_{K_i} = (\boldsymbol{u}\phi_i^h, \boldsymbol{\nabla} v^h)_{K_i} = \boldsymbol{v}\int_{\Omega_{ref}} \boldsymbol{\nabla}\boldsymbol{N}\boldsymbol{u}\boldsymbol{N}^T|\boldsymbol{J}^e|\ d\Omega_{ref}\ \boldsymbol{\phi}_i = \boldsymbol{v}\boldsymbol{B}_i\boldsymbol{\phi}_i \tag{5.5.4}$$

$$\langle \boldsymbol{f}(\phi_i^h)\cdot\boldsymbol{n}, v^h\rangle_{\partial K_i} = \langle \boldsymbol{u}\phi_i^h\cdot\boldsymbol{n}, v^h\rangle_{\partial K_i} = \boldsymbol{v}\int_{\partial\Omega_{ref}} \boldsymbol{N}\boldsymbol{N}^T(\boldsymbol{u}\cdot\boldsymbol{n})|\boldsymbol{J}^f|\ d\Gamma_{ref}\ \boldsymbol{\phi}_i = \boldsymbol{v}\boldsymbol{C}_i\boldsymbol{\phi}_i \tag{5.5.5}$$

$$\langle \tau\phi_i^h, v^h \rangle_{\partial K_i} = \boldsymbol{v} \int_{\partial\Omega_{ref}} \tau \boldsymbol{N}\boldsymbol{N}^T |\boldsymbol{J}^f| \; d\Gamma_{ref} \; \boldsymbol{\phi}_i = \boldsymbol{v}\boldsymbol{D}_i\boldsymbol{\phi}_i \tag{5.5.6}$$

$$\langle \tau\phi_D, v^h \rangle_{\partial\Omega_i \cap \Gamma_{in}} = \boldsymbol{v} \int_{\partial\Omega_{ref} \cap \Gamma_{in}} \boldsymbol{N}\tau\phi_D |\boldsymbol{J}^f| \; d\Gamma_{ref} = \boldsymbol{v}\boldsymbol{E}_i \tag{5.5.7}$$

$$\langle \tau\phi_{outflow}, v^h \rangle_{\partial\Omega_i \cap \Gamma_{out}} = \boldsymbol{v} \int_{\partial\Omega_{ref} \cap \Gamma_{out}} \boldsymbol{N}\tau\phi_{outflow} |\boldsymbol{J}^f| \; d\Gamma_{ref} = \boldsymbol{v}\boldsymbol{O}_i \tag{5.5.8}$$

$$\langle \tau\widehat{\phi}^h, v^h \rangle_{\partial\Omega_i \setminus \partial\Omega} = \boldsymbol{v} \int_{\partial\Omega_{ref} \setminus \partial\Omega} \tau \boldsymbol{N}\widehat{\boldsymbol{N}}^T |\boldsymbol{J}^f| \; d\Gamma_{ref} \; \widehat{\boldsymbol{\phi}}_i = \boldsymbol{v}\boldsymbol{F}_i\widehat{\boldsymbol{\phi}}_i \tag{5.5.9}$$

$$\langle \boldsymbol{f}(\phi_i^h) \cdot \boldsymbol{n}, \mu^h \rangle_{\partial\Omega_i \setminus \partial\Omega} = \langle \boldsymbol{u}\phi_i^h \cdot \boldsymbol{n}, \mu^h \rangle_{\partial\Omega_i \setminus \partial\Omega} = \boldsymbol{\mu} \int_{\partial\Omega_{ref} \setminus \partial\Omega} \widehat{\boldsymbol{N}}\boldsymbol{N}^T (\boldsymbol{u}\cdot\boldsymbol{n}) |\boldsymbol{J}^f| \; d\Gamma_{ref} \; \boldsymbol{\phi}_i = \boldsymbol{\mu}\boldsymbol{H}_i\boldsymbol{\phi}_i \tag{5.5.10}$$

$$\langle \tau\phi_i^h, \mu^h \rangle_{\partial\Omega_i \setminus \partial\Omega} = \boldsymbol{\mu} \int_{\partial\Omega_{ref} \setminus \partial\Omega} \tau \widehat{\boldsymbol{N}}\boldsymbol{N}^T |\boldsymbol{J}^f| \; d\Gamma_{ref} \; \boldsymbol{\phi}_i = \boldsymbol{\mu}\boldsymbol{I}_i\boldsymbol{\phi}_i \tag{5.5.11}$$

$$\langle \tau\widehat{\phi}^h, \mu^h \rangle_{\partial\Omega_i \setminus \partial\Omega} = \boldsymbol{\mu} \int_{\partial\Omega_{ref} \setminus \partial\Omega} \tau \widehat{\boldsymbol{N}}\widehat{\boldsymbol{N}}^T |\boldsymbol{J}^f| \; d\Gamma_{ref} \; \widehat{\boldsymbol{\phi}}_i = \boldsymbol{\mu}\boldsymbol{J}_i\widehat{\boldsymbol{\phi}}_i \tag{5.5.12}$$

where $\widehat{\boldsymbol{\phi}}_i = [\widehat{\boldsymbol{\phi}}_{i,1}^T \quad \widehat{\boldsymbol{\phi}}_{i,2}^T \quad ..... \quad \widehat{\boldsymbol{\phi}}_{i,\mathtt{n}_{\mathtt{fc}}^i}^T]^T$, $\mathtt{n}_{\mathtt{fc}}^i$ is the number of faces/edges of element i, $\boldsymbol{J}^e = \partial\boldsymbol{\Phi}^e/\partial\boldsymbol{\xi}^e$ is the Jacobian of the isoparametric mapping $\boldsymbol{\Phi}^e$, and $\boldsymbol{J}^f = \partial\boldsymbol{\Phi}^f/\partial\boldsymbol{\xi}^f$ is the Jacobian of the isoparametric mapping $\boldsymbol{\Phi}^f$.
The reference element Ω_{ref} and the reference face Γ_{ref} are linked to the physical element Ω_i and the physical face Γ_j respectively through isoparametric mappings which are defined as

$$\begin{aligned} \boldsymbol{\Phi}^e : \Omega_{ref} \subset \mathbb{R}^{\mathtt{n}_{\mathtt{sd}}} &\longrightarrow \Omega_i \subset \mathbb{R}^{\mathtt{n}_{\mathtt{sd}}} \\ \boldsymbol{\xi}^e &\longmapsto \boldsymbol{\Phi}^e(\boldsymbol{\xi}^e) := \sum_{j=1}^{\mathtt{n}_{\mathtt{en}}} \boldsymbol{x}_j N_j(\boldsymbol{\xi}^e) \end{aligned} \tag{5.5.13}$$

$$\begin{aligned} \boldsymbol{\Phi}^f : \Gamma_{ref} \subset \mathbb{R}^{\mathtt{n}_{\mathtt{sd}}-1} &\longrightarrow \Gamma_j \subset \mathbb{R}^{\mathtt{n}_{\mathtt{sd}}} \\ \boldsymbol{\xi}^f &\longmapsto \boldsymbol{\Phi}^f(\boldsymbol{\xi}^f) := \sum_{k=1}^{\mathtt{n}_{\mathtt{fn}}} \boldsymbol{x}_k N_k(\boldsymbol{\xi}^f) \end{aligned} \tag{5.5.14}$$

where $\boldsymbol{x}_j$ and $\boldsymbol{x}_k$ are the nodal coordinates of the physical element Ω_i and the physical face Γ_j, respectively.

5.6 Temporal discretization

5.6.1 Explicit discrete forms

Using forward Euler time-integration scheme [65], the semi-discrete form is written as: find $(\phi_i^{h^{n+1}}, \widehat{\phi}^{h^n})$ that satisfies

$$
\begin{aligned}
&(\frac{\phi_i^{h^{n+1}}}{\triangle t}, v^h)_{K_i} - (\frac{\phi_i^{h^n}}{\triangle t}, v^h)_{K_i} - (\boldsymbol{u}\phi_i^{h^n}, \boldsymbol{\nabla} v^h)_{K_i} + \langle \boldsymbol{u}\phi_i^{h^n} \cdot \boldsymbol{n}, v^h \rangle_{\partial K_i} \\
&\quad + \langle \tau\phi_i^{h^n}, v^h \rangle_{\partial K_i} - \langle \tau\phi_D, v^h \rangle_{\partial\Omega_i \cap \Gamma_{in}} - \langle \tau\phi^n_{outflow}, v^h \rangle_{\partial\Omega_i \cap \Gamma_{out}} \\
&\quad - \langle \tau\widehat{\phi}_i^{h^n}, v^h \rangle_{\partial\Omega_i \setminus \partial\Omega} = 0,
\end{aligned} \tag{5.6.1}
$$

$$
\sum_{i=1}^{\mathtt{n_{el}}} \left[\langle \boldsymbol{u}\phi_i^{h^n} \cdot \boldsymbol{n}, \mu^h \rangle_{\partial\Omega_i \setminus \partial\Omega} + \langle \tau\phi_i^{h^n}, \mu^h \rangle_{\partial\Omega_i \setminus \partial\Omega} - \langle \tau\widehat{\phi}_i^{h^n}, \mu^h \rangle_{\partial\Omega_i \setminus \partial\Omega} \right] = 0. \tag{5.6.2}
$$

for all the test functions (v^h, μ^h) and for all $t = n \triangle t$, where $n = 0, 1, 2, 3, ..., n_{steps}$ and $n_{steps} = T/\triangle t$.
Discrete local problems:

$$
\boldsymbol{\phi}_i^{n+1} = \triangle t \boldsymbol{A}_i^{-1} \left[(\boldsymbol{E}_i + \boldsymbol{O}_i) + (\frac{\boldsymbol{A}_i}{\triangle t} + \boldsymbol{B}_i - \boldsymbol{C}_i - \boldsymbol{D}_i)\boldsymbol{\phi}_i^n + \boldsymbol{F}_i \widehat{\boldsymbol{\phi}}_i^n \right] \tag{5.6.3}
$$

Discrete global problem:

$$
\sum_{i=1}^{\mathtt{n_{el}}} \left[(\boldsymbol{H}_i + \boldsymbol{I}_i)\boldsymbol{\phi}_i^n - \boldsymbol{J}_i \widehat{\boldsymbol{\phi}}_i^n \right] = \boldsymbol{0} \tag{5.6.4}
$$

The solution procedure will be as follows

- Step 1: Knowing $\boldsymbol{\phi}^n$, the global problem 5.6.4 is solved for $\widehat{\boldsymbol{\phi}}^n$ explicitly.
- Step 2: Having $\widehat{\boldsymbol{\phi}}^n$ and knowing $\boldsymbol{\phi}^n$, the local problems 5.6.3 are solved element-by-element explicitly to find $\boldsymbol{\phi}_i^{n+1}$.

The disadvantage of explicit method is the limitation on time step, $\triangle t$, by the Courant-Friedrichs-Lewy (CFL) condition, i.e. CFL$= \triangle t \|\boldsymbol{u}\|/h \leq 1$, where h is the minimum length within an element.

5.6.2 Implicit discrete forms

Backward Euler (BDF1)

Using backward Euler time-integration scheme [65], the semi-discrete form is written as: find $(\phi_i^{h^{n+1}}, \widehat{\phi}^{h^{n+1}})$ that satisfies

$$
\begin{aligned}
&(\frac{\phi_i^{h^{n+1}}}{\triangle t}, v^h)_{K_i} - (\frac{\phi_i^{h^n}}{\triangle t}, v^h)_{K_i} - (\boldsymbol{u}\phi_i^{h^{n+1}}, \boldsymbol{\nabla} v^h)_{K_i} + \langle \boldsymbol{u}\phi_i^{h^{n+1}} \cdot \boldsymbol{n}, v^h \rangle_{\partial K_i} \\
&\quad + \langle \tau\phi_i^{h^{n+1}}, v^h \rangle_{\partial K_i} - \langle \tau\phi_D, v^h \rangle_{\partial\Omega_i \cap \Gamma_{in}} - \langle \tau\phi^{n+1}_{outflow}, v^h \rangle_{\partial\Omega_i \cap \Gamma_{out}} \\
&\quad - \langle \tau\widehat{\phi}_i^{h^{n+1}}, v^h \rangle_{\partial\Omega_i \setminus \partial\Omega} = 0
\end{aligned} \tag{5.6.5}
$$

$$
\sum_{i=1}^{\mathtt{n_{el}}} \left[\langle \boldsymbol{u}\phi_i^{h^{n+1}} \cdot \boldsymbol{n}, \mu^h \rangle_{\partial\Omega_i \setminus \partial\Omega} + \langle \tau\phi_i^{h^{n+1}}, \mu^h \rangle_{\partial\Omega_i \setminus \partial\Omega} - \langle \tau\widehat{\phi}_i^{h^{n+1}}, \mu^h \rangle_{\partial\Omega_i \setminus \partial\Omega} \right] = 0 \tag{5.6.6}
$$

for all the test functions (v^h, μ^h) and for all $t = n \triangle t$, where $n = 0, 1, 2, 3, ..., n_{steps}$ and $n_{steps} = T/\triangle t$.

Discrete local problems:

$$\boldsymbol{\phi}_i^{n+1} = (\frac{\boldsymbol{A}_i}{\triangle t} - \boldsymbol{B}_i + \boldsymbol{C}_i + \boldsymbol{D}_i)^{-1}\left[(\boldsymbol{E}_i + \boldsymbol{O}_i) + \frac{\boldsymbol{A}_i}{\triangle t}\boldsymbol{\phi}_i^n + \boldsymbol{F}_i\widehat{\boldsymbol{\phi}}_i^{n+1}\right] \tag{5.6.7}$$

Discrete global problem:

$$\sum_{i=1}^{\mathtt{n_{el}}}\left[(\boldsymbol{H}_i + \boldsymbol{I}_i)\boldsymbol{\phi}_i^{n+1} - \boldsymbol{J}_i\widehat{\boldsymbol{\phi}}_i^{n+1}\right] = \boldsymbol{0} \tag{5.6.8}$$

After substituting 5.6.7 into 5.6.8, to form a global problem which is only function of $\widehat{\boldsymbol{\phi}}^{n+1}$, the solution procedure will be as follows

- Step 1: Solve the global problem for $\widehat{\boldsymbol{\phi}}^{n+1}$ explicitly!
- Step 2: Having $\widehat{\boldsymbol{\phi}}^{n+1}$ and knowing $\boldsymbol{\phi}^n$, the local problems 5.6.7 are solved element-by-element explicitly to find $\boldsymbol{\phi}_i^{n+1}$.

Note: Even though the scheme is implicit, the solution procedure are actually explicit because the equations are linear.

BDF2

Backward Differentiation Formula (BDF) 2 [66] is second order accurate in time and it requires the storage of the solution from the previous two time steps. The discrete forms of the BDF2 are written as follows
Discrete local problems:

$$\boldsymbol{\phi}_i^{n+1} = (\frac{3\boldsymbol{A}_i}{2\triangle t} - \boldsymbol{B}_i + \boldsymbol{C}_i + \boldsymbol{D}_i)^{-1}\left[(\boldsymbol{E}_i + \boldsymbol{O}_i) + \frac{2\boldsymbol{A}_i}{\triangle t}\boldsymbol{\phi}_i^n - \frac{\boldsymbol{A}_i}{2\triangle t}\boldsymbol{\phi}_i^{n-1} + \boldsymbol{F}_i\widehat{\boldsymbol{\phi}}_i^{n+1}\right] \tag{5.6.9}$$

Discrete global problem:

$$\sum_{i=1}^{\mathtt{n_{el}}}\left[(\boldsymbol{H}_i + \boldsymbol{I}_i)\boldsymbol{\phi}_i^{n+1} - \boldsymbol{J}_i\widehat{\boldsymbol{\phi}}_i^{n+1}\right] = \boldsymbol{0} \tag{5.6.10}$$

After substituting 5.6.9 into 5.6.10, to form a global problem which is only function of $\widehat{\boldsymbol{\phi}}^{n+1}$, the solution procedure will be as follows

- Step 1: Solve the global problem for $\widehat{\boldsymbol{\phi}}^{n+1}$ explicitly!
- Step 2: Having $\widehat{\boldsymbol{\phi}}^{n+1}$ and knowing both $\boldsymbol{\phi}^n$ and $\boldsymbol{\phi}^{n-1}$, the local problems 5.6.9 are solved element-by-element explicitly to find $\boldsymbol{\phi}_i^{n+1}$.

Similar to BDF1; even though the scheme is implicit, the solution procedure are actually explicit because the equations are linear.
Note: In the first time step, BDF1 is used due to the absence of $\boldsymbol{\phi}^{n-1}$.

5.7 Numerical examples

5.7.1 Example 1: advection of circle with oblique velocity field

The following problem is solved, with a velocity field $\boldsymbol{u} = [2, 1.2]$ everywhere.

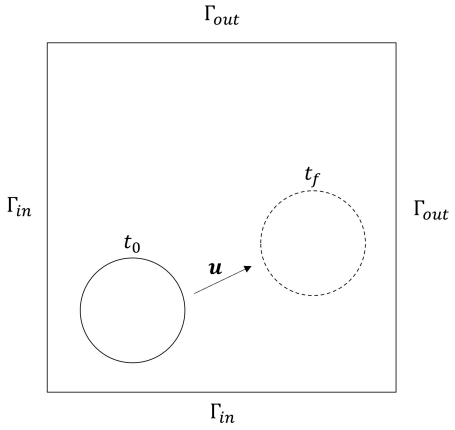

Figure 5.2: Example 1 solved with $\boldsymbol{u} = [2, 1.2]$

Simulation parameters:

- Domain $[-1, 1]^2$, circle with radius $R = 0.3$ initially at $(-0.4, -0.4)$.
- Polynomial approximation $m = 1 : 2$.
- Six levels of mesh refinement $h_{min} = \frac{\sqrt{2}}{2}, \frac{\sqrt{2}}{4}, \frac{\sqrt{2}}{8}, \frac{\sqrt{2}}{16}, \frac{\sqrt{2}}{32}, \frac{\sqrt{2}}{64}$.
- Implicit time integration BDF1 and BDF2 for $t \in [0, 0.4]$.
- For $m = 1$, $CFL = 0.01$ for both BDF1 and BDF2. For $m = 2$, $CFL = 0.001$ for BDF1 and 0.005 for BDF2.
- $\Delta t = \frac{CFL * h_{min}}{\|\boldsymbol{u}\| * m^2}$.
- The distance ϵ around the initial interface is set to 0.25, and the error is computed in the region around the circle at a distance 0.7ϵ.

Optimal convergence rates, $m + 1$ in $\mathcal{L}_2$-norm and m in $\mathcal{H}^1$-norm, are obtained as shown in Figure 5.3 for BDF1 and in Figure 5.4 for BDF2.
The numerical solution at time $t = 0.4$ is shown alongside the initial data in Figure 5.5 for meshes 3:5 and BDF1 temporal discretization.

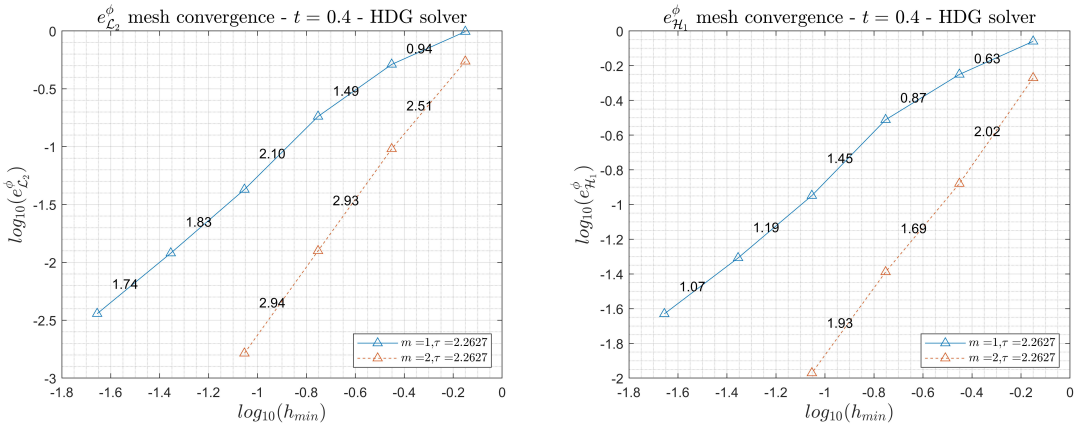

Figure 5.3: Example 1 mesh convergence: Errors in $\mathcal{L}_2$-norm (left) and $\mathcal{H}^1$-norm (right) - Time discretization BDF1.

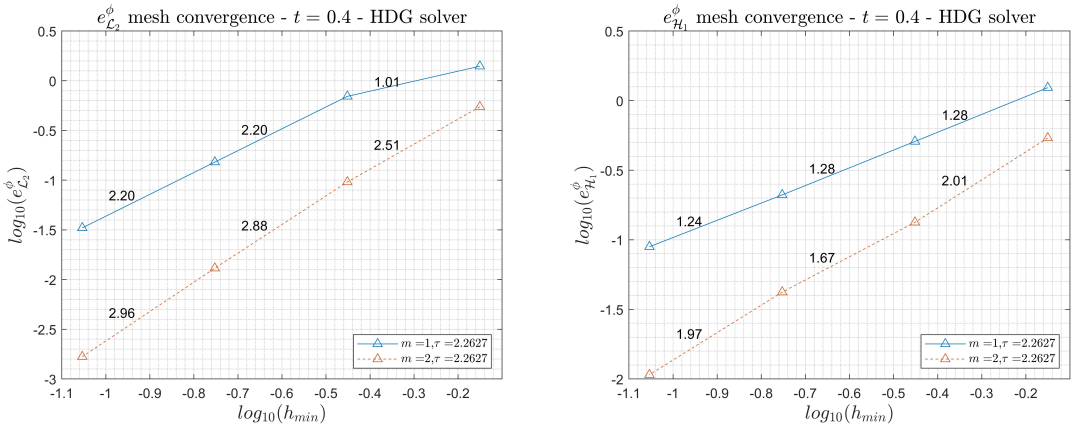

Figure 5.4: Example 1 mesh convergence: Errors in $\mathcal{L}_2$-norm (left) and $\mathcal{H}^1$-norm (right) - Time discretization BDF2.

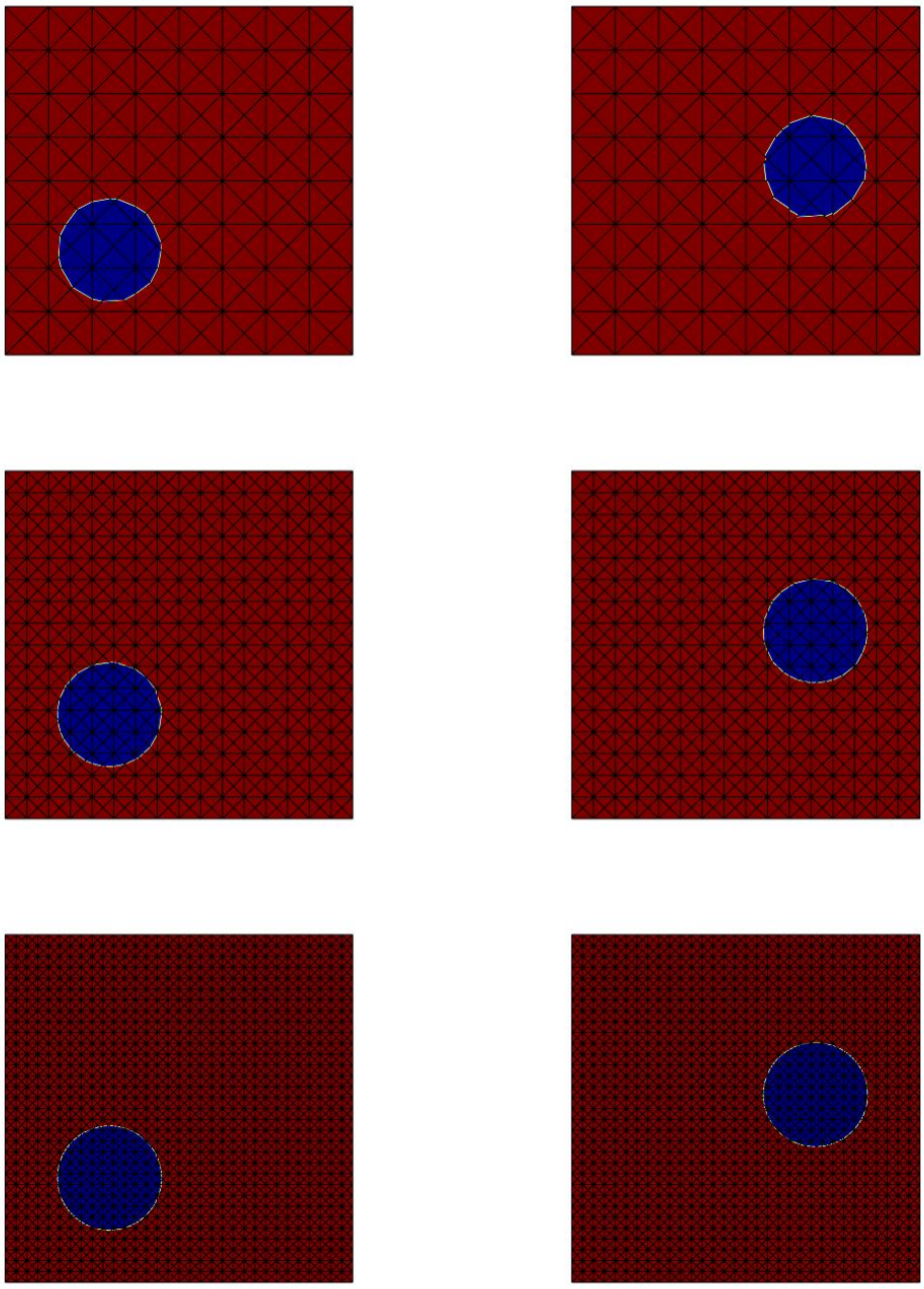

Figure 5.5: Example 1: The location of the interface at $t = 0$ (left) and $t = 0.4$ (right) obtained with $m = 1$ on meshes 3, 4, and 5 using BDF1 temporal discretization.

A test is made to check the convergence in time of the BDF1 and BDF2 temporal discretization schemes. Different values of CFL were tested on a combination of mesh and spatial degree approximation m where spatial discretization error is relatively negligible compared to the temporal discretization error.

- The fifth mesh with $h_{min} = \dfrac{\sqrt{2}}{32}$ is used
- For checking BDF1, the spatial degree approximation is $m = 2$, while for BDF2, $m = 3$.
- Four levels of CFL refinements where $CFL = 0.8, 0.6, 0.4, 0.2$.
- $\Delta t = \dfrac{CFL * h_{min}}{\|\boldsymbol{u}\| * m^2}$.

As shown in Figure 5.6, the temporal discretization schemes perform as expected where first order accuracy is obtained for BDF1 and second order for BDF2.

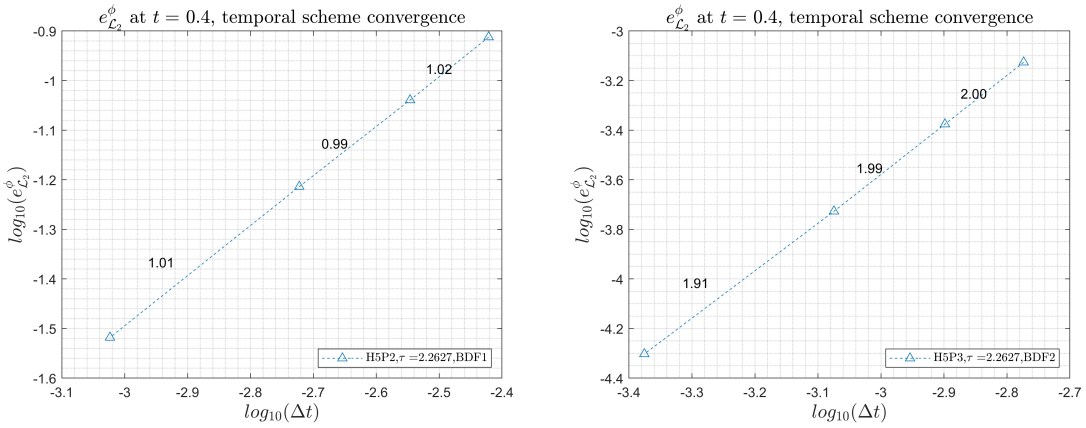

Figure 5.6: Example 1 temporal scheme convergence rate: Spatial errors in $\mathcal{L}_2$-norm computed at $t = 0.4$ when temporal discretization BDF1 is used (left) and when BDF2 is used (right).

5.7.2 Example 2: rotation of a slotted disk

This example was presented for instance in [67, 68, 69]. In a square computational domain $[0, 4]^2$, a slotted disk with radius $R = 0.5$ centered initially at $C(X_C, Y_C) = (2, 2.75)$, with slot parameters $s = 0.126$ and $r = 0.4$, as shown in Figure 5.7, is rotated around the point $O(X_O, Y_O) = (2, 2)$ with an angular velocity $\omega = 0.5$. The rotational velocity field is given by the stream function

$$\psi(x, y) = -\frac{\omega}{2}[(x - X_O)^2 + (y - Y_O)^2] \tag{5.7.1}$$

where the x- and y-velocities are computed as $u = -\dfrac{\partial \psi}{\partial y}$ and $v = \dfrac{\partial \psi}{\partial x}$.

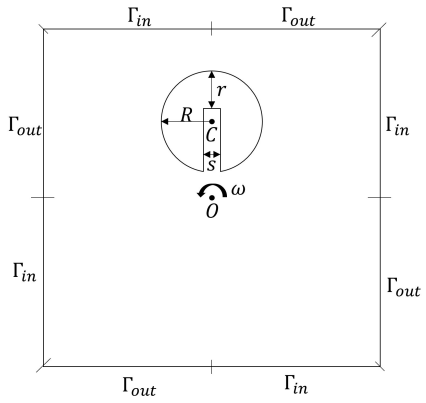

Figure 5.7: Example 2 solved with $\boldsymbol{u} = [-\omega(y - Y_O), \omega(x - X_O)]$

Simulation parameters:

- Polynomial approximation $m = 1$.
- Two levels of mesh refinement $h_{min} = \dfrac{2\sqrt{2}}{64}, \dfrac{2\sqrt{2}}{128}$.
- Implicit time integration BDF1 and BDF2 for $t \in [0, \dfrac{2\pi}{\omega}]$.
- $CFL = 0.25$
- $\Delta t = \dfrac{CFL * h_{min}}{max(\|\boldsymbol{u}\|) * m^2}$, For meshes 1:2, $\Delta t = 0.0078, 0.0039$, respectively.
- The distance ϵ around the initial interface is set to $s/2$.

The numerical solution obtained using BDF1 on the first and second meshes are shown in Figures 5.8 and 5.9, respectively. Furthermore, a comparison between the results of the coarse and fine meshes is shown in Figure 5.10. Furthermore, a comparison between the results obtained using BDF1 and BDF2 on the coarse mesh is shown in Figure 5.11. It can be seen from the comparisons that going for higher-order temporal discretization is more accurate than refining the mesh, in addition to, being less costly in terms of computing time.

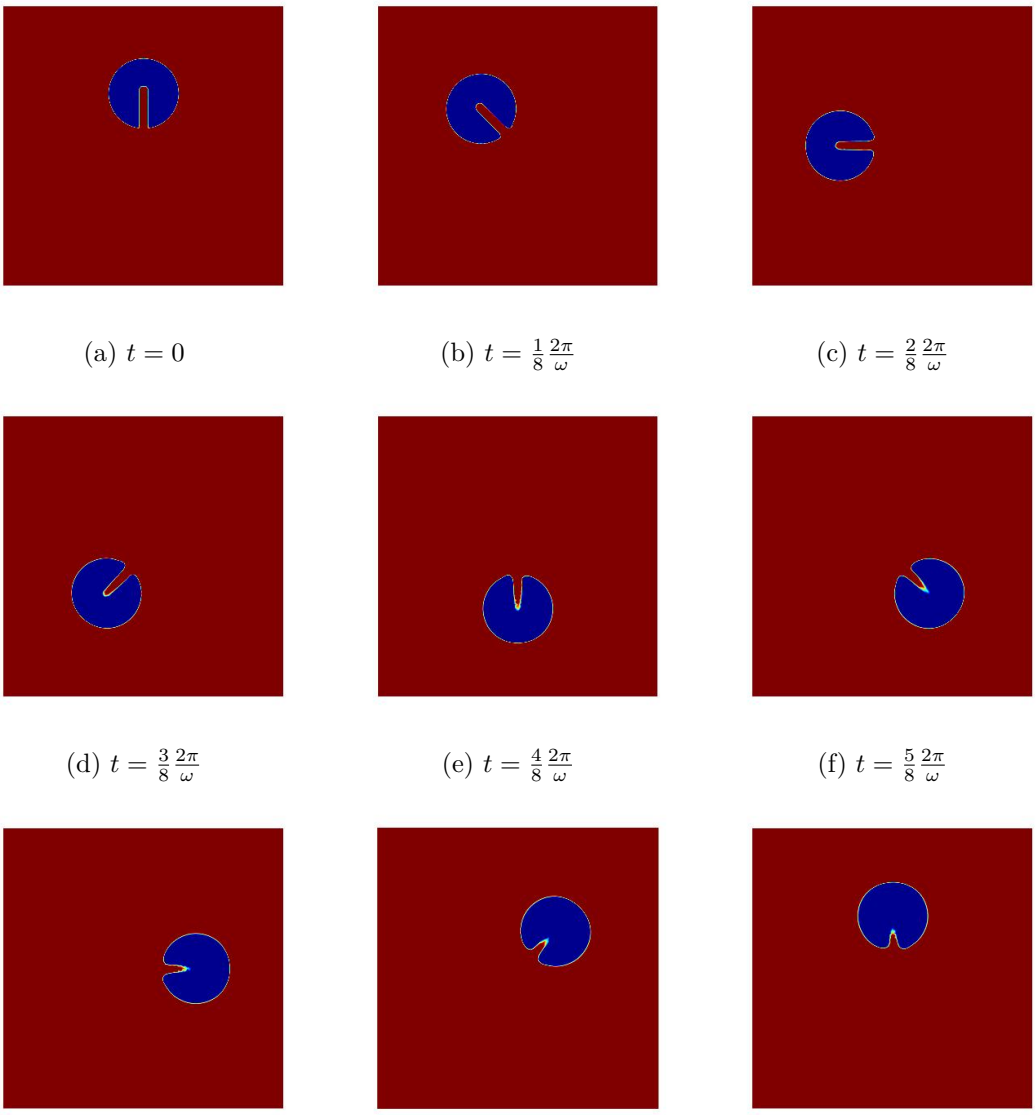

(a) $t = 0$ (b) $t = \frac{1}{8}\frac{2\pi}{\omega}$ (c) $t = \frac{2}{8}\frac{2\pi}{\omega}$

(d) $t = \frac{3}{8}\frac{2\pi}{\omega}$ (e) $t = \frac{4}{8}\frac{2\pi}{\omega}$ (f) $t = \frac{5}{8}\frac{2\pi}{\omega}$

(g) $t = \frac{6}{8}\frac{2\pi}{\omega}$ (h) $t = \frac{7}{8}\frac{2\pi}{\omega}$ (i) $t = \frac{2\pi}{\omega}$

Figure 5.8: Example 2: The location of the interface at various time steps from $t = 0 : 2\pi/\omega$ obtained on mesh 1 - BDF1.

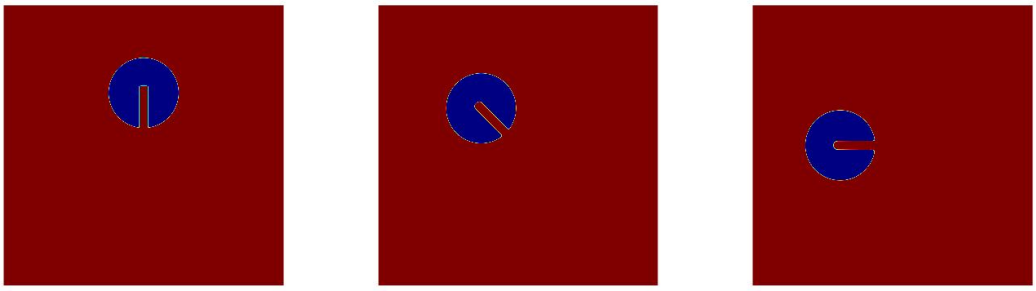

(a) $t = 0$

(b) $t = \frac{1}{8}\frac{2\pi}{\omega}$

(c) $t = \frac{2}{8}\frac{2\pi}{\omega}$

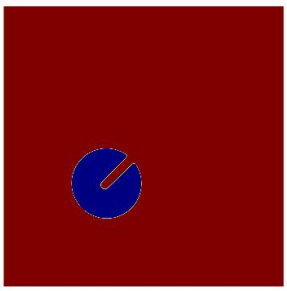

(d) $t = \frac{3}{8}\frac{2\pi}{\omega}$

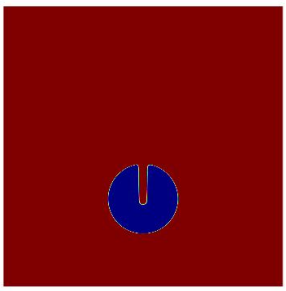

(e) $t = \frac{4}{8}\frac{2\pi}{\omega}$

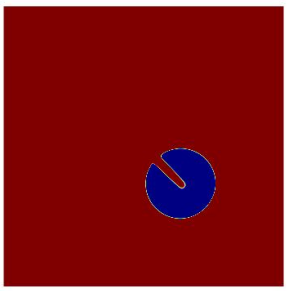

(f) $t = \frac{5}{8}\frac{2\pi}{\omega}$

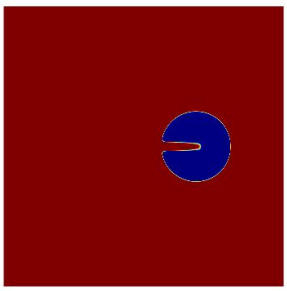

(g) $t = \frac{6}{8}\frac{2\pi}{\omega}$

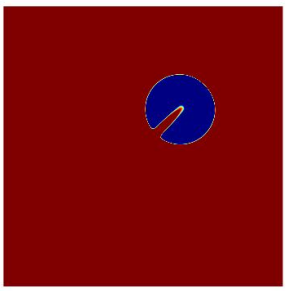

(h) $t = \frac{7}{8}\frac{2\pi}{\omega}$

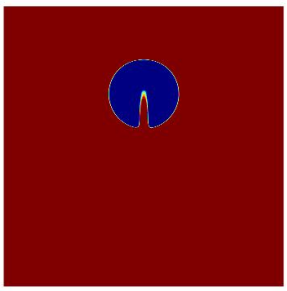

(i) $t = \frac{2\pi}{\omega}$

Figure 5.9: Example 2: The location of the interface at various time steps from $t = 0 : 2\pi/\omega$ obtained on mesh 2 - BDF1.

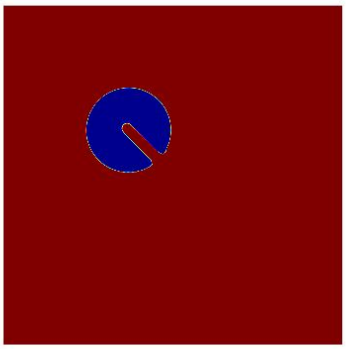

(a) Mesh 1 - $t = \frac{1}{8}\frac{2\pi}{\omega}$

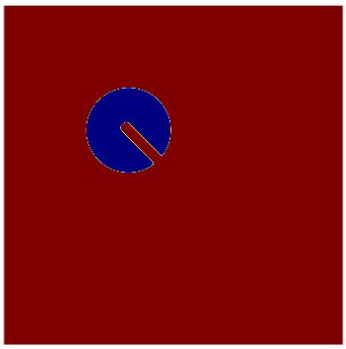

(b) Mesh 2 - $t = \frac{1}{8}\frac{2\pi}{\omega}$

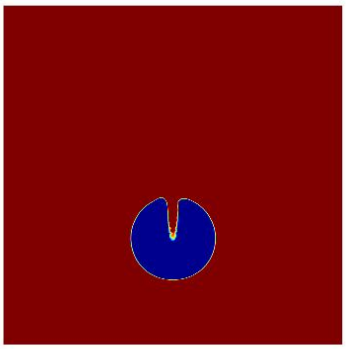

(c) Mesh 1 - $t = \frac{4}{8}\frac{2\pi}{\omega}$

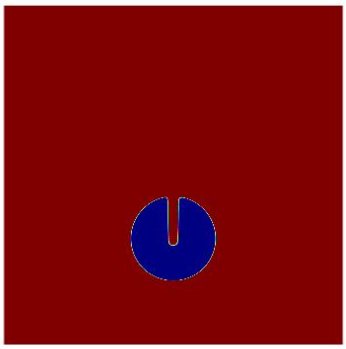

(d) Mesh 2 - $t = \frac{4}{8}\frac{2\pi}{\omega}$

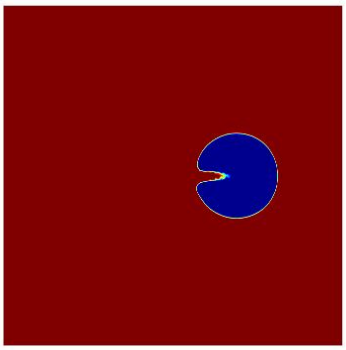

(e) Mesh 1 - $t = \frac{6}{8}\frac{2\pi}{\omega}$

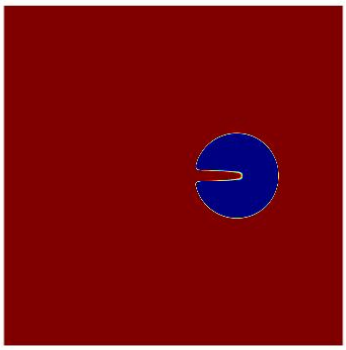

(f) Mesh 2 - $t = \frac{6}{8}\frac{2\pi}{\omega}$

Figure 5.10: Example 2: Comparison between the results obtained on coarse mesh (left) and fine mesh (right) at different time steps - BDF1.

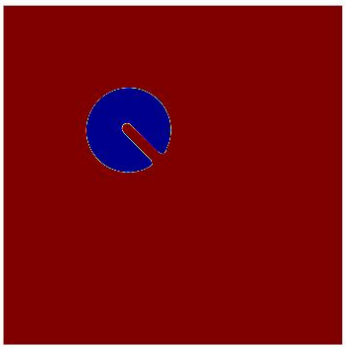

(a) BDF 1 - $t = \frac{1}{8}\frac{2\pi}{\omega}$

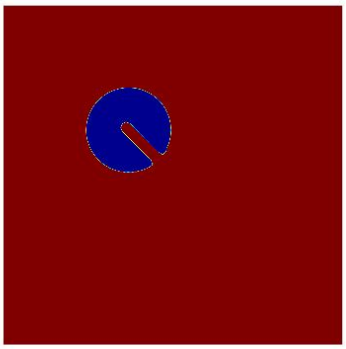

(b) BDF 2 - $t = \frac{1}{8}\frac{2\pi}{\omega}$

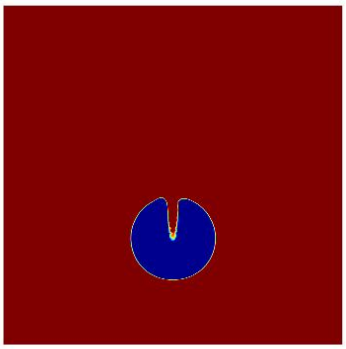

(c) BDF 1 - $t = \frac{4}{8}\frac{2\pi}{\omega}$

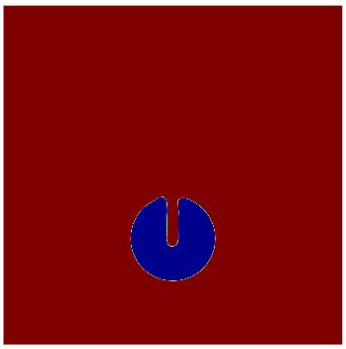

(d) BDF 2 - $t = \frac{4}{8}\frac{2\pi}{\omega}$

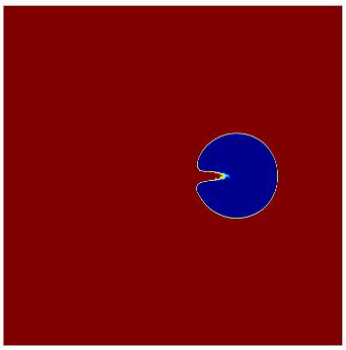

(e) BDF 1 - $t = \frac{6}{8}\frac{2\pi}{\omega}$

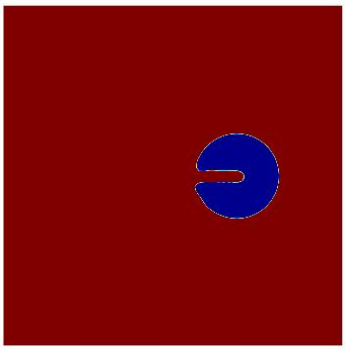

(f) BDF 2 - $t = \frac{6}{8}\frac{2\pi}{\omega}$

Figure 5.11: Example 2: Comparison between the results obtained on coarse mesh using BDF1 (left) and BDF2 (right) at different time steps.

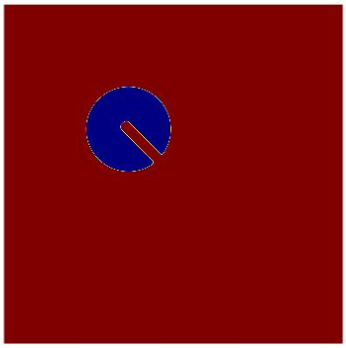

(a) BDF 1 - $t = \frac{1}{8}\frac{2\pi}{\omega}$

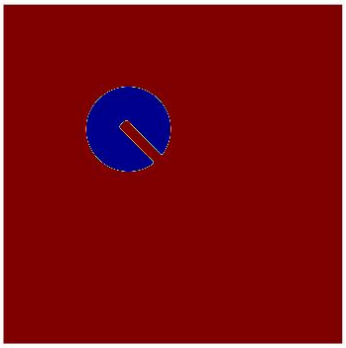

(b) BDF 2 - $t = \frac{1}{8}\frac{2\pi}{\omega}$

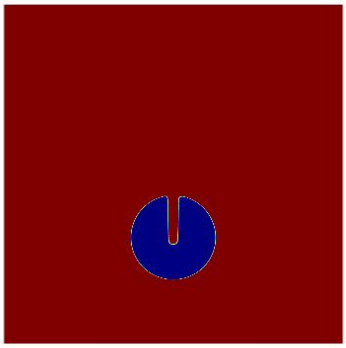

(c) BDF 1 - $t = \frac{4}{8}\frac{2\pi}{\omega}$

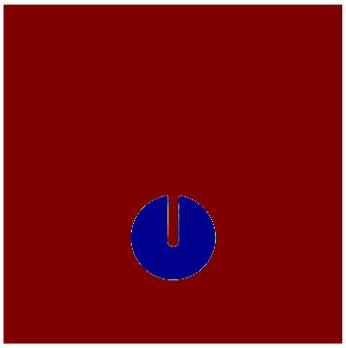

(d) BDF 2 - $t = \frac{4}{8}\frac{2\pi}{\omega}$

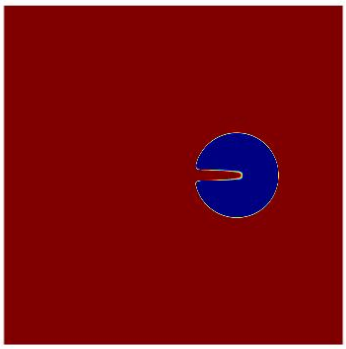

(e) BDF 1 - $t = \frac{6}{8}\frac{2\pi}{\omega}$

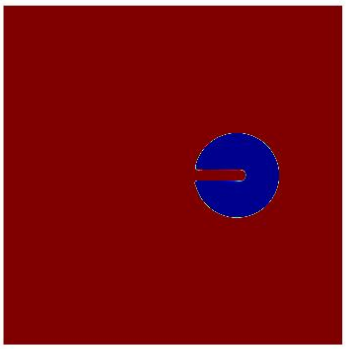

(f) BDF 2 - $t = \frac{6}{8}\frac{2\pi}{\omega}$

Figure 5.12: Example 2: Comparison between the results obtained on fine mesh using BDF1 (left) and BDF2 (right) at different time steps.

5.8 Conclusions and final remarks

In this chapter, the level-set is developed using HDG spatial discretization along with both first and second order implicit BDF temporal discretization. Optimal convergence in space and time is shown in the first example. Furthermore, a more complex problem involving the rotation of a slotted disk is presented, and good results were obtained especially with the second order BDF2 temporal discretization scheme. The level-set solver is now ready to be merged with two-phase Navier-Stokes solver to obtain the position of the moving interface between the two-phases in each time step.

Chapter 6

Divergence-free X-HDG method for two-phase incompressible Navier-Stokes flow problem

6.1 Problem Statement

The incompressible two-phase flow problem is described by the following momentum and mass conservation equations:

$$\begin{cases} \rho(\dfrac{\partial \boldsymbol{u}}{\partial t} + \boldsymbol{u}\cdot\boldsymbol{\nabla}\boldsymbol{u}) - \boldsymbol{\nabla}\cdot\boldsymbol{\sigma} = \rho\boldsymbol{f} & \text{in } \overline{\Omega_1}\cup\overline{\Omega_2}, \text{ for } t\in[0,T_f], \\ \boldsymbol{\nabla}\cdot\boldsymbol{u} = 0 & \text{in } \overline{\Omega_1}\cup\overline{\Omega_2}, \text{ for } t\in[0,T_f]. \end{cases} \tag{6.1.1}$$

with initial conditions for the velocity given as

$$\boldsymbol{u} = \boldsymbol{u}^o \qquad \text{in } \overline{\Omega_1}\cup\overline{\Omega_2}, \text{ for } t = 0 \tag{6.1.2}$$

where t is the time variable, T_f is the final time of interest, ρ is the density that is discontinuous across the interface $\mathcal{I}$ (that is, $\rho = \rho_i$ in Ω_i for $i = 1, 2$), $\boldsymbol{u}(\boldsymbol{x}, t)$ is the velocity field, $\boldsymbol{\sigma}$ is the Cauchy stress tensor, $\boldsymbol{f}$ is the volumetric body forces, $\boldsymbol{u}^o$ is the initial velocity field given at $t = 0$.

Furthermore, the Cauchy stress tensor (for incompressible fluids) is defined as:

$$\boldsymbol{\sigma} = -p\boldsymbol{I} + 2\mu\boldsymbol{\epsilon}(\boldsymbol{u}) \tag{6.1.3}$$

where $p(\boldsymbol{x}, t)$ is the pressure field, μ is the dynamic viscosity that is discontinuous across the interface $\mathcal{I}$ (that is, $\mu = \mu_i$ in Ω_i for $i = 1, 2$), and $\boldsymbol{\epsilon}(\boldsymbol{u})$ is the strain rate tensor which is defined as:

$$\begin{aligned} \boldsymbol{\epsilon} &= \boldsymbol{\nabla}^s\boldsymbol{u} \\ &= \frac{1}{2}(\boldsymbol{\nabla}\boldsymbol{u} + (\boldsymbol{\nabla}\boldsymbol{u})^T) \end{aligned} \tag{6.1.4}$$

where $\boldsymbol{\nabla}^s\boldsymbol{u}$ is the symmetric part of the velocity gradient tensor ($\boldsymbol{\nabla}\boldsymbol{u} := \boldsymbol{\nabla}^s\boldsymbol{u} + \boldsymbol{\nabla}^w\boldsymbol{u}$). For completeness, $\boldsymbol{\nabla}^w\boldsymbol{u} := \dfrac{1}{2}(\boldsymbol{\nabla}\boldsymbol{u} - (\boldsymbol{\nabla}\boldsymbol{u})^T)$ is the skew-symmetric part of the the velocity gradient tensor which is called *vorticity tensor* or *spin tensor*.

Therefore, the first equation in 6.1.1 is written as:

$$\rho(\frac{\partial \boldsymbol{u}}{\partial t} + \boldsymbol{u}\cdot\boldsymbol{\nabla}\boldsymbol{u}) + \boldsymbol{\nabla}p - 2\mu\boldsymbol{\nabla}\cdot\boldsymbol{\nabla}^s\boldsymbol{u} = \rho\boldsymbol{f} \tag{6.1.5}$$

Therefore, an incompressible flow problem is described by:

$$\begin{cases} \rho\dfrac{\partial \boldsymbol{u}}{\partial t} + \boldsymbol{\nabla}\cdot\left(\rho(\boldsymbol{u}\otimes\boldsymbol{u}) + p\boldsymbol{I} - 2\mu\boldsymbol{\nabla}^s\boldsymbol{u}\right) = \rho\boldsymbol{f} & \text{in } \overline{\Omega_1}\cup\overline{\Omega_2},\ \text{for } t\in[0,T_f], \\ \boldsymbol{\nabla}\cdot\boldsymbol{u} = 0 & \text{in } \overline{\Omega_1}\cup\overline{\Omega_2},\ \text{for } t\in[0,T_f]. \end{cases} \tag{6.1.6}$$

Boundary conditions are given as:

- Dirichlet:

$$\boldsymbol{u} = \boldsymbol{u}_D \qquad \text{on } \Gamma_D,\ \text{for } t\in[0,T_f] \tag{6.1.7}$$

- Neumann:

$$\begin{aligned} \left(\rho(\boldsymbol{u}\otimes\boldsymbol{u}) + p\boldsymbol{I} - 2\mu\boldsymbol{\nabla}^s\boldsymbol{u}\right)\boldsymbol{n} &= \boldsymbol{g}_N + \max(\boldsymbol{u}\cdot\boldsymbol{n},0)\boldsymbol{u}\rho \\ &= \boldsymbol{g}_N + \rho(1-\lambda)(\boldsymbol{u}\cdot\boldsymbol{n})\boldsymbol{u} \qquad \text{on } \Gamma_N,\ \text{for } t\in[0,T_f] \end{aligned} \tag{6.1.8}$$

  where $\lambda = 0$ if $\boldsymbol{u}\cdot\boldsymbol{n} > 0, \lambda = 1$ if $\boldsymbol{u}\cdot\boldsymbol{n} < 0$

- If only Dirichlet boundary conditions are considered (i.e. $\Gamma_N = \emptyset$), an additional constraint on the pressure needs to be imposed to avoid its indeterminacy. This is done by imposing the pressure at least at one node on the mesh Skeleton Γ.

where $\boldsymbol{u}_D$ is a prescribed value of the velocity on the Dirichlet boundary Γ_D, $\boldsymbol{g}_N$ is a prescribed normal flux on the Neumann boundary Γ_N.
Furthermore, appropriate **Interface conditions** are considered:

- Surface tension force balancing the jump in normal stress

$$[\![(p\boldsymbol{I} - 2\mu\boldsymbol{\nabla}^s\boldsymbol{u})\,\boldsymbol{n}]\!] = \boldsymbol{g}_s \quad \text{on} \quad \mathcal{I}_i \tag{6.1.9}$$

  where $\boldsymbol{g}_s$ is the surface tension force vector.

- Continuity of the velocity

$$[\![\boldsymbol{u}]\!] = 0 \quad \text{on} \quad \mathcal{I} \tag{6.1.10}$$

  where the jump $[\![\boldsymbol{u}]\!]$ is defined as $[\![\boldsymbol{u}]\!] := \boldsymbol{u}_{\Omega_1\cap\mathcal{I}} - \boldsymbol{u}_{\Omega_2\cap\mathcal{I}} := \boldsymbol{u}_1 - \boldsymbol{u}_2$

6.2 The divergence-free X-HDG method

6.2.1 The mixed strong form

The strong form of incompressible two-phase flow equations presented earlier by (6.1.6) could be written as a system of first order equations by introducing the tensor variable $\boldsymbol{L} = -2\boldsymbol{\nabla}^s\boldsymbol{u}$:

$$\begin{cases} \rho\dfrac{\partial \boldsymbol{u}}{\partial t} + \boldsymbol{\nabla}\cdot\left(\rho(\boldsymbol{u}\otimes\boldsymbol{u}) + p\boldsymbol{I} + \mu\boldsymbol{L}\right) = \rho\boldsymbol{f} & \text{in } \overline{\Omega_1}\cup\overline{\Omega_2},\ \text{for } t\in[0,T_f], \\ \boldsymbol{L} + 2\boldsymbol{\nabla}^s\boldsymbol{u} = \boldsymbol{0} & \text{in } \overline{\Omega_1}\cup\overline{\Omega_2},\ \text{for } t\in[0,T_f], \\ \boldsymbol{\nabla}\cdot\boldsymbol{u} = 0 & \text{in } \overline{\Omega_1}\cup\overline{\Omega_2},\ \text{for } t\in[0,T_f], \\ \boldsymbol{u} = \boldsymbol{u}^o & \text{in } \overline{\Omega_1}\cup\overline{\Omega_2},\ \text{for } t = 0, \\ \boldsymbol{u} = \boldsymbol{u}_D & \text{on } \Gamma_D,\ \text{for } t\in[0,T_f], \\ \left(\rho(\boldsymbol{u}\otimes\boldsymbol{u}) + p\boldsymbol{I} + \mu\boldsymbol{L}\right)\boldsymbol{n} = \boldsymbol{g}_N + \rho(1-\lambda)(\boldsymbol{u}\cdot\boldsymbol{n})\boldsymbol{u} & \text{on } \Gamma_N,\ \text{for } t\in[0,T_f], \\ [\![(p\boldsymbol{I} + \mu\boldsymbol{L})\,\boldsymbol{n}]\!] = \boldsymbol{g}_s & \text{on } \mathcal{I},\ \text{for } t\in[0,T_f], \\ [\![\boldsymbol{u}\cdot\boldsymbol{n}]\!] = 0 & \text{on } \mathcal{I},\ \text{for } t\in[0,T_f]. \end{cases} \tag{6.2.1}$$

This set of equations can be written for a finite element $K_i \in \overline{\Omega}$ as:

(6.2.2)
$$\begin{cases} \rho\dfrac{\partial \boldsymbol{u}}{\partial t} + \boldsymbol{\nabla}\cdot\left(\rho(\boldsymbol{u}\otimes\boldsymbol{u}) + p\boldsymbol{I} + \mu\boldsymbol{L}\right) = \rho\boldsymbol{f} & \text{in } K_i \setminus \mathcal{I},\ \text{for } t\in[0,T_f], \\ \boldsymbol{L} + 2\boldsymbol{\nabla}^s\boldsymbol{u} = \boldsymbol{0} & \text{in } K_i \setminus \mathcal{I},\ \text{for } t\in[0,T_f], \\ \boldsymbol{\nabla}\cdot\boldsymbol{u} = 0 & \text{in } K_i \setminus \mathcal{I},\ \text{for } t\in[0,T_f], \\ \boldsymbol{u} = \boldsymbol{u}^o & \text{in } K_i,\ \text{for } t=0, \\ \boldsymbol{u} = \boldsymbol{u}_D & \text{on } \partial K_i\cap\Gamma_D,\ \text{for } t\in[0,T_f], \\ \left(\rho(\boldsymbol{u}\otimes\boldsymbol{u}) + p\boldsymbol{I} + \mu\boldsymbol{L}\right)\boldsymbol{n} = \boldsymbol{g}_N + \rho(1-\lambda)(\boldsymbol{u}\cdot\boldsymbol{n})\boldsymbol{u} & \text{on } \partial K_i\cap\Gamma_N,\ \text{for } t\in[0,T_f], \\ [\![(p\boldsymbol{I} + \mu\boldsymbol{L})\,\boldsymbol{n}]\!] = \boldsymbol{g}_s & \text{on } \mathcal{I}_i,\ \text{for } t\in[0,T_f], \\ [\![\boldsymbol{u}\cdot\boldsymbol{n}]\!] = 0 & \text{on } \mathcal{I}_i,\ \text{for } t\in[0,T_f]. \end{cases}$$

where $\mathcal{I}_i := K_i \cap \mathcal{I}$ is the part of the interface in element K_i (if K_i is a cut element).

6.2.2 X-HDG strong local and global problems

The *divergence-free X-HDG* method rewrites (6.2.2) as two equivalent problems. First the **local element-by-element problems** with Dirichlet boundary conditions, that is,

(6.2.3a)
$$\left.\begin{array}{rl} \rho\dfrac{\partial \boldsymbol{u}}{\partial t} + \boldsymbol{\nabla}\cdot\left(\rho(\boldsymbol{u}\otimes\boldsymbol{u}) + p\boldsymbol{I} + \mu\boldsymbol{L}\right) = \rho\boldsymbol{f} & \text{in } K_i \setminus \mathcal{I},\ \text{for } t\in[0,T_f], \\ \boldsymbol{L} + 2\boldsymbol{\nabla}^s\boldsymbol{u} = \boldsymbol{0} & \text{in } K_i \setminus \mathcal{I},\ \text{for } t\in[0,T_f], \\ \boldsymbol{\nabla}\cdot\boldsymbol{u} = 0 & \text{in } K_i \setminus \mathcal{I},\ \text{for } t\in[0,T_f], \\ \boldsymbol{u} = \boldsymbol{u}^o & \text{in } K_i,\ \text{for } t=0, \\ \boldsymbol{u} = \boldsymbol{u}_D & \text{on } \partial K_i\cap\Gamma_D,\ \text{for } t\in[0,T_f], \\ \boldsymbol{u} = \widehat{\boldsymbol{u}} & \text{on } \partial K_i\setminus\Gamma_D,\ \text{for } t\in[0,T_f], \\ p = p_N & \text{on } \partial K_i\cap\Gamma_N,\ \text{for } t\in[0,T_f], \\ p = \widehat{p} & \text{on } \partial K_i\setminus\Gamma_N,\ \text{for } t\in[0,T_f], \end{array}\right\} \text{if } K_i\cap\mathcal{I} = \emptyset$$

(6.2.3b)
$$\left.\begin{array}{rl} \rho\dfrac{\partial \boldsymbol{u}}{\partial t} + \boldsymbol{\nabla}\cdot\left(\rho(\boldsymbol{u}\otimes\boldsymbol{u}) + p\boldsymbol{I} + \mu\boldsymbol{L}\right) = \rho\boldsymbol{f} & \text{in } K_i \setminus \mathcal{I},\ \text{for } t\in[0,T_f], \\ \boldsymbol{L} + 2\boldsymbol{\nabla}^s\boldsymbol{u} = \boldsymbol{0} & \text{in } K_i \setminus \mathcal{I},\ \text{for } t\in[0,T_f], \\ \boldsymbol{\nabla}\cdot\boldsymbol{u} = 0 & \text{in } K_i \setminus \mathcal{I},\ \text{for } t\in[0,T_f], \\ \boldsymbol{u} = \boldsymbol{u}^o & \text{in } K_i,\ \text{for } t=0, \\ \boldsymbol{u} = \boldsymbol{u}_D & \text{on } \partial K_i\cap\Gamma_D,\ \text{for } t\in[0,T_f], \\ \boldsymbol{u} = \widehat{\boldsymbol{u}} & \text{on } \partial K_i\setminus\Gamma_D,\ \text{for } t\in[0,T_f], \\ p = p_N & \text{on } \partial K_i\cap\Gamma_N,\ \text{for } t\in[0,T_f], \\ p = \widehat{p} & \text{on } \partial K_i\setminus\Gamma_N,\ \text{for } t\in[0,T_f], \\ [\![(p\boldsymbol{I} + \mu\boldsymbol{L})\,\boldsymbol{n}]\!] = \boldsymbol{g}_s & \text{on } \mathcal{I}_i,\ \text{for } t\in[0,T_f], \\ [\![\boldsymbol{u}\cdot\boldsymbol{n}]\!] = 0 & \text{on } \mathcal{I}_i,\ \text{for } t\in[0,T_f] \end{array}\right\} \text{if } K_i\cap\mathcal{I} \neq \emptyset$$

for $i = 1, ..., \mathtt{n_{el}}$. A new variable $\widehat{\boldsymbol{u}} \in \mathcal{V}_s^h(\Gamma\setminus\Gamma_D)$ is introduced which corresponds to the trace of $\boldsymbol{u}$ at the mesh faces $\Gamma\setminus\Gamma_D$. The trace $\widehat{\boldsymbol{u}}$ is single valued variable on each face, with the same value when seen from both sides of an interior face. It is noted here that an extra equation has been introduced which corresponds to imposing the pressure on the boundary of the element to a newly introduced variable $\widehat{p} \in \mathcal{S}_s^h(\Gamma\setminus\Gamma_N)$ which corresponds to the trace of p at the mesh faces $\Gamma\setminus\Gamma_N$.

For X-HDG, We introduce the velocity trace $\widetilde{\boldsymbol{u}}$ as an extra unknown on the material interface to enforce the transmission or jump condition of the momentum equation across the material interface, i.e. enforce $[\![(p\boldsymbol{I}+\mu\boldsymbol{L})\,\boldsymbol{n}]\!]_{\mathcal{I}}=\boldsymbol{g}_s$.

For divergence-free X-HDG, we also introduces the pressure trace $\widetilde{p}$ as an extra unknown on the material interface to enforce the transmission condition of the continuity equation across the material interface, i.e. enforce $[\![\boldsymbol{u}\cdot\boldsymbol{n}]\!]_{\mathcal{I}}=0$. Note that $\widetilde{\boldsymbol{u}}$ and $\widetilde{p}$ are continuous functions defined on the interface. They act as Shuhr complements that are eliminated after solving for them.

The local problems have been particularized for standard elements 6.2.3a and for cut elements 6.2.3b. Given the traces $(\widehat{\boldsymbol{u}},\widehat{p})$ and the boundary conditions $(\boldsymbol{u}_D,p_N)$, the local problems 6.2.3 can be solved in each element to determine the solution $\boldsymbol{u}\in\mathcal{V}_v^h(\Omega)$, $p\in\mathcal{S}_v^{div\,h}(\Omega)$ and the flux $\boldsymbol{L}\in\mathcal{T}_v^h(\Omega)$. Thus, the problem now reduces to determine the traces $(\widehat{\boldsymbol{u}},\widehat{p})$. This is done by solving a **global problem** that imposes the transmission conditions (of the momentum and continuity equations) across element boundaries plus the Neumann boundary conditions, that is,

(6.2.4)

$$\text{from momentum eqn.:}\quad\begin{cases}[\![\boldsymbol{u}\otimes\boldsymbol{n}]\!]=\boldsymbol{0} & \text{on } \Gamma\setminus\partial\Omega,\\ [\![(\rho(\boldsymbol{u}\otimes\boldsymbol{u})+p\boldsymbol{I}+\mu\boldsymbol{L})\,\boldsymbol{n}]\!]=\boldsymbol{0} & \text{on } \Gamma\setminus\partial\Omega,\\ (\rho(\boldsymbol{u}\otimes\boldsymbol{u})+p\boldsymbol{I}+\mu\boldsymbol{L})\,\boldsymbol{n}=\boldsymbol{g}_N+\rho(1-\lambda)(\boldsymbol{u}\cdot\boldsymbol{n})\boldsymbol{u} & \text{on } \Gamma_N,\end{cases}$$

$$\text{from continuity eqn.:}\quad\begin{cases}[\![\boldsymbol{u}\cdot\boldsymbol{n}]\!]=0 & \text{on } \Gamma\setminus\partial\Omega,\\ \boldsymbol{u}\cdot\boldsymbol{n}=\boldsymbol{u}_D\cdot\boldsymbol{n} & \text{on } \Gamma_D,\\ \boldsymbol{u}\cdot\boldsymbol{n}=\widehat{\boldsymbol{u}}\cdot\boldsymbol{n} & \text{on } \Gamma_N\end{cases}$$

It is important to note that the continuity of the solution $\boldsymbol{u}$ across $\Gamma\setminus\partial\Omega$ is imposed by the Dirichlet boundary condition ($\boldsymbol{u}=\widehat{\boldsymbol{u}}$ on $\partial K_i\setminus\Gamma_D$) in the local problems (6.2.3) and the fact that $\widehat{\boldsymbol{u}}$ is single valued on Γ. Therefore, the first jump condition in equation (6.2.4) could be removed and the global problem is reduced to

(6.2.5)

$$\text{from momentum eqn.:}\quad\begin{cases}[\![(\rho(\boldsymbol{u}\otimes\boldsymbol{u})+p\boldsymbol{I}+\mu\boldsymbol{L})\,\boldsymbol{n}]\!]=\boldsymbol{0} & \text{on } \Gamma\setminus\partial\Omega,\\ (\rho(\boldsymbol{u}\otimes\boldsymbol{u})+p\boldsymbol{I}+\mu\boldsymbol{L})\,\boldsymbol{n}=\boldsymbol{g}_N+\rho(1-\lambda)(\boldsymbol{u}\cdot\boldsymbol{n})\boldsymbol{u} & \text{on } \Gamma_N,\end{cases}$$

$$\text{from continuity eqn.:}\quad\begin{cases}[\![\boldsymbol{u}\cdot\boldsymbol{n}]\!]=0 & \text{on } \Gamma\setminus\partial\Omega,\\ \boldsymbol{u}\cdot\boldsymbol{n}=\boldsymbol{u}_D\cdot\boldsymbol{n} & \text{on } \Gamma_D,\\ \boldsymbol{u}\cdot\boldsymbol{n}=\widehat{\boldsymbol{u}}\cdot\boldsymbol{n} & \text{on } \Gamma_N\end{cases}$$

6.2.3 Temporal discretization

Assume that we discretize in time with a step size Δt that represents the time difference when we move from a time step (n) to a time step $(n+1)$. As a start, we use the implicit BDF1 [65], which is defined for a general equation

$$\frac{\partial u}{\partial t}=f$$

as

$$\frac{u^{n+1}-u^n}{\Delta t}=f^{n+1}$$

which is also written as:

$$u^{n+1} = \Delta t\, f^{n+1} + u^n \tag{6.2.6}$$

In an abuse of notation, all the variables at time step $(n+1)$ will be written without the superscript $(n+1)$ for simplicity. Only variables at time step (n) will have the superscript (n). For example, equation (6.2.6) will be written as:

$$u = \Delta t\, f + u^n \tag{6.2.7}$$

Having this in mind, only the term $\dfrac{\partial \boldsymbol{u}}{\partial t}$ in the momentum equation is changed to $\dfrac{\boldsymbol{u} - \boldsymbol{u}^n}{\Delta t}$. It is important to note that, the enriched approximation space at time n and $n+1$ are not the same due to the fact that the interface location change. Therefore, the Heaviside enrichment function is different. To facilitate the implementation of the discrete system, the solution $\boldsymbol{u}^n$ is interpolated to the approximation space of time t^{n+1}, so the enriched approximation space at time t^{n+1} can be considered for the discretization of all terms in the equations. Since the approximation in each cut element is different at each time step due to the moving interface, special time discretization technique could be needed, see for instance [70] which also discusses the issue of appearance and disappearance of cut elements.

6.2.4 X-HDG weak forms

Briefly, the weak forms are obtained by the following steps:

- First: multiply the governing equations by corresponding test functions and integrate over the two sub-domains (two phases).
- Second: apply integration by parts once to obtain surface integrals. Only in the first equation of 6.2.3a and 6.2.3b, integration by parts is done again for the viscous term.
- Third: replace the physical fluxes by some defined numerical fluxes, this is where stabilization parameters appear.

The detailed derivation of the weak forms is presented in details in Appendix D
Note that in a cut element, the approximations of the functions $(\boldsymbol{u}, \boldsymbol{L}, P)$ are discontinuous.
$\boldsymbol{u} \in [\mathcal{P}^m(K_i)]^d \oplus H[\mathcal{P}^m(K_i)]^d$,
$\boldsymbol{L} \in [\mathcal{P}^m(K_i)]^{d\times d} \oplus H[\mathcal{P}^m(K_i)]^{d\times d}$ and
$P \in \boldsymbol{\nabla}\cdot[\mathcal{P}^m(K_i)]^d \oplus H\boldsymbol{\nabla}\cdot[\mathcal{P}^m(K_i)]^d$.

In the divergence-free X-HDG method, the physical quantities $(\boldsymbol{u}, \boldsymbol{L}, p)$ are replaced by the numerical quantities $(\widehat{\boldsymbol{u}}, \widehat{\boldsymbol{L}}, \widehat{p})$ on $\partial K_i \setminus \Gamma_D$. Further, on the interface $\mathcal{I}_i$, the physical quantities $(\boldsymbol{u}, \boldsymbol{L}_1, \boldsymbol{L}_2, p_1, p_2)$ are replaced by the numerical quantities $(\widetilde{\boldsymbol{u}}^i, \widetilde{\boldsymbol{L}}_1^i + \boldsymbol{\delta}_{\boldsymbol{L}}, \widetilde{\boldsymbol{L}}_2^i, \widetilde{p}^i + \delta_P, \widetilde{p}^i)$. Furthermore, on the intersection with the Dirichlet boundary $\partial K_i \cap \Gamma_D$, the physical quantities $(\boldsymbol{u}, \boldsymbol{L}, p)$ are replaced by $(\boldsymbol{u}_D, \widehat{\boldsymbol{L}}_D, \widehat{p})$. Finally, that pressure trace $\widehat{p}$ is replaced by p_N on the Neumann boundary $\partial K_i \setminus \Gamma_N$.
Note that the discontinuities in the velocity gradient and the pressure across the interface are taken into consideration by introducing the two variables δ_P and $\boldsymbol{\delta}_{\boldsymbol{L}}$. Those two variables are replaced in the weak forms by the surface tension force vector where $\delta_P \widehat{\boldsymbol{n}} + \nu_1 \boldsymbol{\delta}_{\boldsymbol{L}} \widehat{\boldsymbol{n}} = \boldsymbol{g}_s$.

Furthermore, the numerical fluxes used in the weak forms are defined as:

(6.2.8a)

$$\widehat{\boldsymbol{L}} := \boldsymbol{L} + \tau(\boldsymbol{u} - \widehat{\boldsymbol{u}}) \otimes \boldsymbol{n} + \tau \boldsymbol{n} \otimes (\boldsymbol{u} - \widehat{\boldsymbol{u}}),$$

(6.2.8b)

$$\widehat{\boldsymbol{L}}^D := \boldsymbol{L} + \tau(\boldsymbol{u} - \boldsymbol{u}_D) \otimes \boldsymbol{n} + \tau \boldsymbol{n} \otimes (\boldsymbol{u} - \boldsymbol{u}_D),$$

(6.2.8c)

$$\widetilde{\boldsymbol{L}}_1^i := \boldsymbol{L}_1 + \tau^{\mathcal{I}}(\boldsymbol{u}_1 - \widetilde{\boldsymbol{u}}^i) \otimes \widehat{\boldsymbol{n}} + \tau^{\mathcal{I}} \widehat{\boldsymbol{n}} \otimes (\boldsymbol{u}_1 - \widetilde{\boldsymbol{u}}^i),$$

(6.2.8d)

$$\widetilde{\boldsymbol{L}}_2^i := \boldsymbol{L}_2 + \tau^{\mathcal{I}}(\boldsymbol{u}_2 - \widetilde{\boldsymbol{u}}^i) \otimes (-\widehat{\boldsymbol{n}}) + \tau^{\mathcal{I}}(-\widehat{\boldsymbol{n}}) \otimes (\boldsymbol{u}_2 - \widetilde{\boldsymbol{u}}^i),$$

(6.2.8e)

$$\widehat{(\boldsymbol{u} \otimes \boldsymbol{u})} := (\boldsymbol{u} \otimes \boldsymbol{u}) + (\widehat{\boldsymbol{u}} - \boldsymbol{u}) \otimes \lambda \boldsymbol{u}, (\lambda = 0 \text{ if } \boldsymbol{u} \cdot \boldsymbol{n} > 0, \lambda = 1 \text{ if } \boldsymbol{u} \cdot \boldsymbol{n} < 0)$$

(6.2.8f)

$$\widehat{(\boldsymbol{u} \otimes \boldsymbol{u})}_D := (\boldsymbol{u} \otimes \boldsymbol{u}) + (\boldsymbol{u}_D - \boldsymbol{u}) \otimes \lambda \boldsymbol{u}, (\lambda = 0 \text{ if } \boldsymbol{u} \cdot \boldsymbol{n} > 0, \lambda = 1 \text{ if } \boldsymbol{u} \cdot \boldsymbol{n} < 0)$$

(6.2.8g)

$$\widetilde{(\boldsymbol{u}_1 \otimes \boldsymbol{u}_1)}^i := (\boldsymbol{u}_1 \otimes \boldsymbol{u}_1) + (\widetilde{\boldsymbol{u}}^i - \boldsymbol{u}_1) \otimes \lambda \boldsymbol{u}_1, (\lambda = 0 \text{ if } \boldsymbol{u}_1 \cdot \widehat{\boldsymbol{n}} > 0, \lambda = 1 \text{ if } \boldsymbol{u}_1 \cdot \widehat{\boldsymbol{n}} < 0)$$

(6.2.8h)

$$\widetilde{(\boldsymbol{u}_2 \otimes \boldsymbol{u}_2)}^i := (\boldsymbol{u}_2 \otimes \boldsymbol{u}_2) + (\widetilde{\boldsymbol{u}}^i - \boldsymbol{u}_2) \otimes \lambda \boldsymbol{u}_2, (\lambda = 0 \text{ if } \boldsymbol{u}_2 \cdot (-\widehat{\boldsymbol{n}}) > 0, \lambda = 1 \text{ if } \boldsymbol{u}_2 \cdot (-\widehat{\boldsymbol{n}}) < 0)$$

where $\widehat{\boldsymbol{u}} \in \mathcal{V}_s^h(\Gamma_{ij})$ and $\widehat{P} \in \mathcal{S}_s^h(\Gamma_{ij})$ could be continuous (if $\Gamma_{ij} \cap \mathcal{I} = \emptyset$) or discontinuous (if $\Gamma_{ij} \cap \mathcal{I} \neq \emptyset$) functions. Γ_{ij} is face j of element K_i. $\widetilde{\boldsymbol{u}}^i \in [\mathcal{P}^m(\mathcal{I}_i)]^d$ is a continuous vector function defined on the interface $\mathcal{I}$. $\widetilde{P}^i \in \mathcal{P}^m(\mathcal{I}_i)$ is a continuous scalar function defined on the interface $\mathcal{I}$. τ and $\tau^{\mathcal{I}}$ are stabilization parameters for the viscous flux on the element faces ∂K_i and the material interface $\mathcal{I}_i$, respectively. The choice of the stabilization parameter τ is discussed extensively in [35, 59]. Based on several numerical trials, the interface stabilization parameter has to be inversely proportional to the average of μ to ensure optimal convergence, for instance $\tau^{\mathcal{I}} := 1/\{\mu\}$.

Note that the convective flux is approximated using upwinding by introducing the parameter λ that is equal to zero at an inlet and one at an outlet. This would lead to approximating the convective flux using the velocity trace at an inlet and the elemental velocity itself at an outlet.

Weak local problems in cut elements

After the temporal discretization, the weak form of the local problems is: given $\widehat{\boldsymbol{u}} \in \mathcal{V}_s^h(\Gamma_{ij} \setminus \Gamma_D)$, $\boldsymbol{u}_D \in \mathcal{V}_s(\Gamma_{ij} \cap \Gamma_D)$, $\widehat{p} \in \mathcal{S}_s^h(\Gamma_{ij} \setminus \Gamma_N)$ and $p_N \in \mathcal{S}_s^h(\Gamma_{ij} \cap \Gamma_N)$, where Γ_{ij} is the face j (which could be cut or uncut) of element K_i, find $\boldsymbol{u} \in [\mathcal{P}^m(K_i)]^d \oplus H[\mathcal{P}^m(K_i)]^d$, $\boldsymbol{L} \in [\mathcal{P}^m(K_i)]^{d \times d} \oplus H[\mathcal{P}^m(K_i)]^{d \times d}$, $p \in \boldsymbol{\nabla} \cdot [\mathcal{P}^m(K_i)]^d \oplus H\boldsymbol{\nabla} \cdot [\mathcal{P}^m(K_i)]^d$, $\widetilde{\boldsymbol{u}}^i \in [\mathcal{P}^m(\mathcal{I}_i)]^d$,

and $\widetilde{p}^i \in \mathcal{P}^m(\mathcal{I}_i)$ such that

(6.2.9a)

$$
\begin{aligned}
&(\boldsymbol{\psi}, \rho\frac{\partial \boldsymbol{u}}{\partial t})_{K_i} + (\boldsymbol{\psi}, \boldsymbol{\nabla}\cdot(\mu\boldsymbol{L}))_{K_i} - (\boldsymbol{\nabla}\boldsymbol{\psi}, p\boldsymbol{I})_{K_i} - (\boldsymbol{\nabla}\boldsymbol{\psi}, \rho(\boldsymbol{u}\otimes\boldsymbol{u}))_{K_i} + \langle \boldsymbol{\psi}, \rho(\boldsymbol{u}\otimes\boldsymbol{u})\boldsymbol{n}\rangle_{\partial K_i} \\
&\quad - \langle \boldsymbol{\psi}, \lambda\rho(\boldsymbol{u}\otimes\boldsymbol{u})\boldsymbol{n}\rangle_{\partial K_i} + \langle \boldsymbol{\psi}, \mu\tau\boldsymbol{u}\rangle_{\partial K_i} + \langle \boldsymbol{\psi}, \mu\tau(\boldsymbol{u}\cdot\boldsymbol{n})\boldsymbol{n}\rangle_{\partial K_i} \\
&\quad + \langle \boldsymbol{\psi}_1, \rho_1(\boldsymbol{u}_1\otimes\boldsymbol{u}_1)\widehat{\boldsymbol{n}}\rangle_{\mathcal{I}_i} + \langle \boldsymbol{\psi}_1, \widetilde{p}^i\widehat{\boldsymbol{n}}\rangle_{\mathcal{I}_i} + \langle \boldsymbol{\psi}_2, \rho_2(\boldsymbol{u}_2\otimes\boldsymbol{u}_2)(-\widehat{\boldsymbol{n}})\rangle_{\mathcal{I}_i} + \langle \boldsymbol{\psi}_2, \widetilde{p}^i(-\widehat{\boldsymbol{n}})\rangle_{\mathcal{I}_i} \\
&\quad - \langle \boldsymbol{\psi}_1, \lambda\rho_1(\boldsymbol{u}_1\otimes\boldsymbol{u}_1)\widehat{\boldsymbol{n}}\rangle_{\mathcal{I}_i} + \langle \boldsymbol{\psi}_1, \lambda\rho_1(\widetilde{\boldsymbol{u}}^i\otimes\boldsymbol{u}_1)\widehat{\boldsymbol{n}}\rangle_{\mathcal{I}_i} \\
&\quad + \langle \boldsymbol{\psi}_1, \mu_1\tau^{\mathcal{I}}\boldsymbol{u}_1\rangle_{\mathcal{I}_i} - \langle \boldsymbol{\psi}_1, \mu_1\tau^{\mathcal{I}}\widetilde{\boldsymbol{u}}^i\rangle_{\mathcal{I}_i} \\
&\quad + \langle \boldsymbol{\psi}_1, \mu_1\tau^{\mathcal{I}}(\boldsymbol{u}_1\cdot\widehat{\boldsymbol{n}})\widehat{\boldsymbol{n}}\rangle_{\mathcal{I}_i} - \langle \boldsymbol{\psi}_1, \mu_1\tau^{\mathcal{I}}(\widetilde{\boldsymbol{u}}^i\cdot\widehat{\boldsymbol{n}})\widehat{\boldsymbol{n}}\rangle_{\mathcal{I}_i} \\
&\quad - \langle \boldsymbol{\psi}_2, \lambda\rho_2(\boldsymbol{u}_2\otimes\boldsymbol{u}_2)(-\widehat{\boldsymbol{n}})\rangle_{\mathcal{I}_i} + \langle \boldsymbol{\psi}_2, \lambda\rho_2(\widetilde{\boldsymbol{u}}^i\otimes\boldsymbol{u}_2)(-\widehat{\boldsymbol{n}})\rangle_{\mathcal{I}_i} \\
&\quad + \langle \boldsymbol{\psi}_2, \mu_2\tau^{\mathcal{I}}\boldsymbol{u}_2\rangle_{\mathcal{I}_i} - \langle \boldsymbol{\psi}_2, \mu_2\tau^{\mathcal{I}}\widetilde{\boldsymbol{u}}^i\rangle_{\mathcal{I}_i} \\
&\quad + \langle \boldsymbol{\psi}_2, \mu_2\tau^{\mathcal{I}}(\boldsymbol{u}_2\cdot(-\widehat{\boldsymbol{n}}))(-\widehat{\boldsymbol{n}})\rangle_{\mathcal{I}_i} - \langle \boldsymbol{\psi}_2, \mu_2\tau^{\mathcal{I}}(\widetilde{\boldsymbol{u}}^i\cdot(-\widehat{\boldsymbol{n}}))(-\widehat{\boldsymbol{n}})\rangle_{\mathcal{I}_i} \\
&\quad = (\boldsymbol{\psi}, \rho\boldsymbol{f})_{K_i} - \langle \boldsymbol{\psi}, \lambda\rho(\widehat{\boldsymbol{u}}\otimes\boldsymbol{u})\boldsymbol{n}\rangle_{\partial K_i\setminus\Gamma_D} + \langle \boldsymbol{\psi}, \mu\tau\widehat{\boldsymbol{u}}\rangle_{\partial K_i\setminus\Gamma_D} + \langle \boldsymbol{\psi}, \mu\tau(\widehat{\boldsymbol{u}}\cdot\boldsymbol{n})\boldsymbol{n}\rangle_{\partial K_i\setminus\Gamma_D} \\
&\quad - \langle \boldsymbol{\psi}, \lambda\rho(\boldsymbol{u}_D\otimes\boldsymbol{u})\boldsymbol{n}\rangle_{\partial K_i\cap\Gamma_D} + \langle \boldsymbol{\psi}, \mu\tau\boldsymbol{u}_D\rangle_{\partial K_i\cap\Gamma_D} + \langle \boldsymbol{\psi}, \mu\tau(\boldsymbol{u}_D\cdot\boldsymbol{n})\boldsymbol{n}\rangle_{\partial K_i\cap\Gamma_D} \\
&\quad - \langle \boldsymbol{\psi}, \widehat{p}\boldsymbol{n}\rangle_{\partial K_i\setminus\Gamma_N} - \langle \boldsymbol{\psi}, p_N\boldsymbol{n}\rangle_{\partial K_i\cap\Gamma_N} - \langle \boldsymbol{\psi}_1, \boldsymbol{g}_s\rangle_{\mathcal{I}_i}
\end{aligned}
$$

(6.2.9b)

$$
\begin{aligned}
-(\boldsymbol{\Psi}, \boldsymbol{L})_{K_i} + (\boldsymbol{\nabla}^s\cdot\boldsymbol{\Psi}, \boldsymbol{u})_{K_i} &- \langle \boldsymbol{\Psi}_1, \widetilde{\boldsymbol{u}}^i\otimes\widehat{\boldsymbol{n}}\rangle_{\mathcal{I}_i} - \langle \boldsymbol{\Psi}_1, \widehat{\boldsymbol{n}}\otimes\widetilde{\boldsymbol{u}}^i\rangle_{\mathcal{I}_i} \\
&- \langle \boldsymbol{\Psi}_2, \widetilde{\boldsymbol{u}}^i\otimes(-\widehat{\boldsymbol{n}})\rangle_{\mathcal{I}_i} - \langle \boldsymbol{\Psi}_2, (-\widehat{\boldsymbol{n}})\otimes\widetilde{\boldsymbol{u}}^i\rangle_{\mathcal{I}_i} \\
&= \langle \boldsymbol{\Psi}, \widehat{\boldsymbol{u}}\otimes\boldsymbol{n}\rangle_{\partial K_i\setminus\Gamma_D} + \langle \boldsymbol{\Psi}, \boldsymbol{n}\otimes\widehat{\boldsymbol{u}}\rangle_{\partial K_i\setminus\Gamma_D} \\
&+ \langle \boldsymbol{\Psi}, \boldsymbol{u}_D\otimes\boldsymbol{n}\rangle_{\partial K_i\cap\Gamma_D} + \langle \boldsymbol{\Psi}, \boldsymbol{n}\otimes\boldsymbol{u}_D\rangle_{\partial K_i\cap\Gamma_D}
\end{aligned}
$$

(6.2.9c)

$$
-(\phi, \boldsymbol{\nabla}\cdot\boldsymbol{u})_{K_i} = 0
$$

(6.2.9d)

$$
\begin{aligned}
&\langle \widetilde{\boldsymbol{\psi}}, \widetilde{p}^i\widehat{\boldsymbol{n}}\rangle_{\mathcal{I}_i} + \langle \widetilde{\boldsymbol{\psi}}, \mu_1\boldsymbol{L}_1\widehat{\boldsymbol{n}}\rangle_{\mathcal{I}_i} + \langle \widetilde{\boldsymbol{\psi}}, \widetilde{p}^i(-\widehat{\boldsymbol{n}})\rangle_{\mathcal{I}_i} + \langle \widetilde{\boldsymbol{\psi}}, \mu_2\boldsymbol{L}_2(-\widehat{\boldsymbol{n}})\rangle_{\mathcal{I}_i} \\
&+\langle \widetilde{\boldsymbol{\psi}}, \mu_1\tau^{\mathcal{I}}\boldsymbol{u}_1\rangle_{\mathcal{I}_i} - \langle \widetilde{\boldsymbol{\psi}}, \mu_1\tau^{\mathcal{I}}\widetilde{\boldsymbol{u}}^i\rangle_{\mathcal{I}_i} + \langle \widetilde{\boldsymbol{\psi}}, \mu_1\tau^{\mathcal{I}}(\boldsymbol{u}_1\cdot\widehat{\boldsymbol{n}})\widehat{\boldsymbol{n}}\rangle_{\mathcal{I}_i} - \langle \widetilde{\boldsymbol{\psi}}, \mu_1\tau^{\mathcal{I}}(\widetilde{\boldsymbol{u}}^i\cdot\widehat{\boldsymbol{n}})\widehat{\boldsymbol{n}}\rangle_{\mathcal{I}_i} \\
&+\langle \widetilde{\boldsymbol{\psi}}, \mu_2\tau^{\mathcal{I}}\boldsymbol{u}_2\rangle_{\mathcal{I}_i} - \langle \widetilde{\boldsymbol{\psi}}, \mu_2\tau^{\mathcal{I}}\widetilde{\boldsymbol{u}}^i\rangle_{\mathcal{I}_i} + \langle \widetilde{\boldsymbol{\psi}}, \mu_2\tau^{\mathcal{I}}(\boldsymbol{u}_2\cdot(-\widehat{\boldsymbol{n}}))(-\widehat{\boldsymbol{n}})\rangle_{\mathcal{I}_i} - \langle \widetilde{\boldsymbol{\psi}}, \mu_2\tau^{\mathcal{I}}(\widetilde{\boldsymbol{u}}^i\cdot(-\widehat{\boldsymbol{n}}))(-\widehat{\boldsymbol{n}})\rangle_{\mathcal{I}_i} \\
&=0
\end{aligned}
$$

(6.2.9e)

$$
\langle \widetilde{\phi}, \boldsymbol{u}_1\cdot\widehat{\boldsymbol{n}}\rangle_{\mathcal{I}_i} + \langle \widetilde{\phi}, \boldsymbol{u}_2\cdot(-\widehat{\boldsymbol{n}})\rangle_{\mathcal{I}_i} = 0
$$

for all the test functions $\boldsymbol{\psi} \in [\mathcal{P}^m(K_i)]^d \oplus H[\mathcal{P}^m(K_i)]^d$, $\boldsymbol{\Psi} \in [\mathcal{P}^m(K_i)]^{d\times d} \oplus H[\mathcal{P}^m(K_i)]^{d\times d}$, $\phi \in \boldsymbol{\nabla}\cdot[\mathcal{P}^m(K_i)]^d \oplus H\boldsymbol{\nabla}\cdot[\mathcal{P}^m(K_i)]^d$, $\widetilde{\boldsymbol{\psi}} \in [\mathcal{P}^m(\mathcal{I}_i)]^d$, and $\widetilde{\phi} \in \mathcal{P}^m(\mathcal{I}_i)$.

Weak local problems in standard elements

For a standard uncut element K_i, the weak forms of the local problems (6.2.3a) are exactly the same as those for a cut element after removing the interface terms. Note that the approximation spaces for all the functions are continuous. i.e. $(\boldsymbol{\psi}, \boldsymbol{u}) \in [\mathcal{P}^m(K_i)]^d$, $(\boldsymbol{\Psi}, \boldsymbol{L}) \in [\mathcal{P}^m(K_i)]^{d\times d}$, $(\phi, p) \in \boldsymbol{\nabla}\cdot[\mathcal{P}^m(K_i)]^d$, $\widehat{\boldsymbol{u}} \in [\mathcal{P}^m(\Gamma_{ij}\setminus\Gamma_D)]^d$ and $\widehat{p} \in \mathcal{P}^m(\Gamma_{ij})$, where Γ_{ij} is the face j of element K_i.

Therefore, the weak form of the local problems in a standard uncut element is: given $(\widehat{\boldsymbol{u}}, \boldsymbol{u}_D, \widehat{p}, P_N)$, find $(\boldsymbol{u}, \boldsymbol{L}, p)$ such that

(6.2.10a)
$$\begin{aligned}(\boldsymbol{\psi}, \rho\frac{\partial \boldsymbol{u}}{\partial t})_{K_i} + (\boldsymbol{\psi}, \boldsymbol{\nabla}\cdot(\mu\boldsymbol{L}))_{K_i} - (\boldsymbol{\nabla}\boldsymbol{\psi}, p\boldsymbol{I})_{K_i} - (\boldsymbol{\nabla}\boldsymbol{\psi}, \rho(\boldsymbol{u}\otimes\boldsymbol{u}))_{K_i} + \langle \boldsymbol{\psi}, \rho(\boldsymbol{u}\otimes\boldsymbol{u})\boldsymbol{n}\rangle_{\partial K_i} \\ - \langle \boldsymbol{\psi}, \lambda\rho(\boldsymbol{u}\otimes\boldsymbol{u})\boldsymbol{n}\rangle_{\partial K_i} + \langle \boldsymbol{\psi}, \mu\tau\boldsymbol{u}\rangle_{\partial K_i} + \langle \boldsymbol{\psi}, \mu\tau(\boldsymbol{u}\cdot\boldsymbol{n})\boldsymbol{n}\rangle_{\partial K_i} \\ = (\boldsymbol{\psi}, \rho\boldsymbol{f})_{K_i} - \langle \boldsymbol{\psi}, \lambda\rho(\widehat{\boldsymbol{u}}\otimes\boldsymbol{u})\boldsymbol{n}\rangle_{\partial K_i\setminus\Gamma_D} + \langle \boldsymbol{\psi}, \mu\tau\widehat{\boldsymbol{u}}\rangle_{\partial K_i\setminus\Gamma_D} + \langle \boldsymbol{\psi}, \mu\tau(\widehat{\boldsymbol{u}}\cdot\boldsymbol{n})\boldsymbol{n}\rangle_{\partial K_i\setminus\Gamma_D} \\ - \langle \boldsymbol{\psi}, \lambda\rho(\boldsymbol{u}_D\otimes\boldsymbol{u})\boldsymbol{n}\rangle_{\partial K_i\cap\Gamma_D} + \langle \boldsymbol{\psi}, \mu\tau\boldsymbol{u}_D\rangle_{\partial K_i\cap\Gamma_D} + \langle \boldsymbol{\psi}, \mu\tau(\boldsymbol{u}_D\cdot\boldsymbol{n})\boldsymbol{n}\rangle_{\partial K_i\cap\Gamma_D} \\ - \langle \boldsymbol{\psi}, \widehat{p}\boldsymbol{n}\rangle_{\partial K_i\setminus\Gamma_N} - \langle \boldsymbol{\psi}, p_N\boldsymbol{n}\rangle_{\partial K_i\cap\Gamma_N}\end{aligned}$$

(6.2.10b)
$$\begin{aligned}-(\boldsymbol{\Psi}, \boldsymbol{L})_{K_i} + (\boldsymbol{\nabla}^s\cdot\boldsymbol{\Psi}, \boldsymbol{u})_{K_i} &= \langle \boldsymbol{\Psi}, \widehat{\boldsymbol{u}}\otimes\boldsymbol{n}\rangle_{\partial K_i\setminus\Gamma_D} + \langle \boldsymbol{\Psi}, \boldsymbol{n}\otimes\widehat{\boldsymbol{u}}\rangle_{\partial K_i\setminus\Gamma_D} \\ &\quad + \langle \boldsymbol{\Psi}, \boldsymbol{u}_D\otimes\boldsymbol{n}\rangle_{\partial K_i\cap\Gamma_D} + \langle \boldsymbol{\Psi}, \boldsymbol{n}\otimes\boldsymbol{u}_D\rangle_{\partial K_i\cap\Gamma_D}\end{aligned}$$

(6.2.10c)
$$-(\phi, \boldsymbol{\nabla}\cdot\boldsymbol{u})_{K_i} = 0$$

for all the test functions $(\boldsymbol{\psi}, \boldsymbol{\Psi}, \phi)$.

Weak global problem

The weak form of the HDG global problem for Incompressible Navier-Stokes flow is: Find $\widehat{\boldsymbol{u}} \in \mathcal{V}_s^h(\Gamma\setminus\Gamma_D)$ and $\widehat{p} \in \mathcal{S}_s^h(\Gamma\setminus\Gamma_N)$ such that

(6.2.11a)
$$\begin{aligned}\sum_{i=1}^{\mathtt{nel}}\Big\{ &\langle \widehat{\boldsymbol{\psi}}, \rho(\boldsymbol{u}\otimes\boldsymbol{u})\boldsymbol{n}\rangle_{\partial K_i\setminus\Gamma_D} + \langle \widehat{\boldsymbol{\psi}}, \widehat{p}\boldsymbol{n}\rangle_{\partial K_i\setminus\partial\Omega} + \langle \widehat{\boldsymbol{\psi}}, \mu\boldsymbol{L}\boldsymbol{n}\rangle_{\partial K_i\setminus\Gamma_D} \\ &- \langle \widehat{\boldsymbol{\psi}}, \lambda\rho(\boldsymbol{u}\otimes\boldsymbol{u})\boldsymbol{n}\rangle_{\partial K_i\setminus\Gamma_D} + \langle \widehat{\boldsymbol{\psi}}, \lambda\rho(\widehat{\boldsymbol{u}}\otimes\boldsymbol{u})\boldsymbol{n}\rangle_{\partial K_i\setminus\Gamma_D} \\ &+ \langle \widehat{\boldsymbol{\psi}}, \mu\tau\boldsymbol{u}\rangle_{\partial K_i\setminus\Gamma_D} - \langle \widehat{\boldsymbol{\psi}}, \mu\tau\widehat{\boldsymbol{u}}\rangle_{\partial K_i\setminus\Gamma_D} \\ &+ \langle \widehat{\boldsymbol{\psi}}, \mu\tau(\boldsymbol{u}\cdot\boldsymbol{n})\boldsymbol{n}\rangle_{\partial K_i\setminus\Gamma_D} - \langle \widehat{\boldsymbol{\psi}}, \mu\tau(\widehat{\boldsymbol{u}}\cdot\boldsymbol{n})\boldsymbol{n}\rangle_{\partial K_i\setminus\Gamma_D} \\ &- \langle \widehat{\boldsymbol{\psi}}, \rho(1-\lambda)(\boldsymbol{u}\cdot\boldsymbol{n})\widehat{\boldsymbol{u}}\rangle_{\partial K_i\cap\Gamma_N}\Big\} \\ &= \sum_{i=1}^{\mathtt{nel}}\Big\{\langle \widehat{\boldsymbol{\psi}}, \boldsymbol{g}_N\rangle_{\partial K_i\cap\Gamma_N} - \langle \widehat{\boldsymbol{\psi}}, p_N\boldsymbol{n}\rangle_{\partial K_i\cap\Gamma_N}\Big\}\end{aligned}$$

(6.2.11b)
$$\sum_{i=1}^{\mathtt{nel}}\Big\{\langle \widehat{\phi}, \boldsymbol{u}\cdot\boldsymbol{n}\rangle_{\partial K_i} - \langle \widehat{\phi}, \widehat{\boldsymbol{u}}\cdot\boldsymbol{n}\rangle_{\partial K_i\cap\Gamma_N}\Big\} = \sum_{i=1}^{\mathtt{nel}}\langle \widehat{\phi}, \boldsymbol{u}_D\cdot\boldsymbol{n}\rangle_{\partial K_i\cap\Gamma_D}$$

for all the test functions $\widehat{\boldsymbol{\psi}} \in \mathcal{V}_s^h(\Gamma\setminus\Gamma_D)$, and $\widetilde{\phi} \in \mathcal{S}_s^h(\Gamma)$.

6.2.5 X-HDG discrete forms

The local problem 6.2.9 in a cut element K_i is written in a matrix-vector form as:

(6.2.12)

$$\begin{bmatrix} \left[\mathbf{A}_{uu}^{K_i}+\mathbf{A}_{uu}^{\mathcal{I}_i}+\mathbf{C}_{uu}^{K_i}(\mathbf{u}^i)+\mathbf{C}_{uu}^{\mathcal{I}_i}(\mathbf{u}^i)\right] & \mathbf{A}_{uL}^{K_i} & \mathbf{A}_{up}^{K_i} & \left[\mathbf{A}_{u\widetilde{u}^i}^{\mathcal{I}_i}+\mathbf{C}_{u\widetilde{u}^i}^{\mathcal{I}_i}(\mathbf{u}^i)\right] & \mathbf{A}_{up^i}^{\mathcal{I}_i} \\ \mathbf{A}_{Lu}^{K_i} & \mathbf{A}_{LL}^{K_i} & \mathbf{0} & \mathbf{A}_{L\widetilde{u}^i}^{\mathcal{I}_i} & \mathbf{0} \\ \mathbf{A}_{pu}^{K_i} & \mathbf{0} & \mathbf{0} & \mathbf{0} & \mathbf{0} \\ \mathbf{A}_{\widetilde{u}^iu}^{\mathcal{I}_i} & \mathbf{A}_{\widetilde{u}^iL}^{\mathcal{I}_i} & \mathbf{0} & \mathbf{A}_{\widetilde{u}^i\widetilde{u}^i}^{\mathcal{I}_i} & \mathbf{A}_{\widetilde{u}^i\widetilde{p}^i}^{\mathcal{I}_i} \\ \mathbf{A}_{\widetilde{p}^iu}^{\mathcal{I}_i} & \mathbf{0} & \mathbf{0} & \mathbf{0} & \mathbf{0} \end{bmatrix} \begin{Bmatrix} \mathbf{u}^i \\ \mathbf{L}^i \\ \mathbf{p}^i \\ \widetilde{\mathbf{u}}^i \\ \widetilde{\mathbf{p}}^i \end{Bmatrix}$$

$$= \begin{bmatrix} \left[\mathbf{A}_{u\widehat{u}}^{K_i}+\mathbf{C}_{u\widehat{u}}^{K_i}(\mathbf{u}^i)\right] \\ \mathbf{A}_{L\widehat{u}}^{K_i} \\ \mathbf{0} \\ \mathbf{0} \\ \mathbf{0} \end{bmatrix} \widehat{\mathbf{u}}^i + \begin{bmatrix} \mathbf{A}_{u\widehat{p}}^{K_i} \\ \mathbf{0} \\ \mathbf{0} \\ \mathbf{0} \\ \mathbf{0} \end{bmatrix} \widehat{\mathbf{p}}^i + \begin{Bmatrix} \mathbf{f}_u^{K_i}+\mathbf{r}_u^{K_i}(\mathbf{u}^i) \\ \mathbf{f}_L^{K_i} \\ \mathbf{0} \\ \mathbf{0} \\ \mathbf{0} \end{Bmatrix}$$

while in a standard uncut element K_i, the matrix-vector form of the local problem 6.2.10 is written as

(6.2.13)

$$\begin{bmatrix} \left[\mathbf{A}_{uu}^{K_i}+\mathbf{C}_{uu}^{K_i}(\mathbf{u}^i)\right] & \mathbf{A}_{uL}^{K_i} & \mathbf{A}_{up}^{K_i} \\ \mathbf{A}_{Lu}^{K_i} & \mathbf{A}_{LL}^{K_i} & \mathbf{0} \\ \mathbf{A}_{pu}^{K_i} & \mathbf{0} & \mathbf{0} \end{bmatrix} \begin{Bmatrix} \mathbf{u}^i \\ \mathbf{L}^i \\ \mathbf{p}^i \end{Bmatrix} = \begin{bmatrix} \left[\mathbf{A}_{u\widehat{u}}^{K_i}+\mathbf{C}_{u\widehat{u}}^{K_i}(\mathbf{u}^i)\right] \\ \mathbf{A}_{L\widehat{u}}^{K_i} \\ \mathbf{0} \end{bmatrix} \widehat{\mathbf{u}}^i + \begin{bmatrix} \mathbf{A}_{u\widehat{p}}^{K_i} \\ \mathbf{0} \\ \mathbf{0} \end{bmatrix} \widehat{\mathbf{p}}^i + \begin{Bmatrix} \mathbf{f}_u^{K_i}+\mathbf{r}_u^{K_i}(\mathbf{u}^i) \\ \mathbf{f}_L^{K_i} \\ \mathbf{0} \end{Bmatrix}$$

After the hybridization step (inserting the algebraic expressions of $\boldsymbol{u}$ and $\boldsymbol{L}$) from the local problem into the global problem 6.2.11, the full global problem is written in a matrix-vector form as:

(6.2.14)

$$\begin{aligned} &\mathbf{A}_{i=1}^{\mathtt{n_{el}}} \begin{bmatrix} \left[\mathbf{A}_{\widehat{uu}}^{K_i}+\mathbf{C}_{\widehat{uu}}^{K_i}(\mathbf{u}^i)\right]\mathbf{Z}_{u\widehat{u}}^{K_i}(\mathbf{u}^i) & \left[\mathbf{A}_{\widehat{uu}}^{K_i}+\mathbf{C}_{\widehat{uu}}^{K_i}(\mathbf{u}^i)\right]\mathbf{Z}_{u\widehat{p}}^{K_i}(\mathbf{u}^i) \\ +\mathbf{A}_{\widehat{uL}}^{K_i}\mathbf{Z}_{L\widehat{u}}^{K_i}(\mathbf{u}^i) & +\mathbf{A}_{\widehat{uL}}^{K_i}\mathbf{Z}_{L\widehat{p}}^{K_i}(\mathbf{u}^i) \\ +\mathbf{A}_{\widehat{\widehat{uu}}}^{K_i}+\mathbf{C}_{\widehat{\widehat{uu}}}^{K_i}(\mathbf{u}^i) & +\mathbf{A}_{\widehat{up}}^{K_i} \\ \mathbf{A}_{\widehat{pu}}^{K_i}\mathbf{Z}_{u\widehat{u}}^{K_i}(\mathbf{u}^i)+\mathbf{A}_{\widehat{\widehat{pu}}}^{K_i} & \mathbf{A}_{\widehat{pu}}^{K_i}\mathbf{Z}_{u\widehat{p}}^{K_i}(\mathbf{u}^i) \end{bmatrix} \begin{Bmatrix} \widehat{\mathbf{u}}^i \\ \widehat{\mathbf{p}}^i \end{Bmatrix} \\ =&\mathbf{A}_{i=1}^{\mathtt{n_{el}}} \begin{Bmatrix} \mathbf{f}_{\widehat{u}}^{K_i}-\left[\mathbf{A}_{\widehat{uu}}^{K_i}+\mathbf{C}_{\widehat{uu}}^{K_i}(\mathbf{u}^i)\right]\mathbf{z}_u^{K_i}(\mathbf{u}^i)-\mathbf{A}_{\widehat{uL}}^{K_i}\mathbf{z}_L^{K_i}(\mathbf{u}^i) \\ \mathbf{f}_{\widehat{p}}^{K_i}-\mathbf{A}_{\widehat{pu}}^{K_i}\mathbf{z}_u^{K_i}(\mathbf{u}^i) \end{Bmatrix} \end{aligned}$$

The solution procedure is as follows: the discrete trace variables $\widehat{\mathbf{u}}$ and $\widehat{\mathbf{p}}$ are obtained by solving the following discrete global problem

(6.2.15)

$$\widehat{\mathbf{K}}(\mathbf{u}) \begin{Bmatrix} \widehat{\mathbf{u}} \\ \widehat{\mathbf{p}} \end{Bmatrix} = \widehat{\mathbf{f}}(\mathbf{u})$$

then the local problems are solved element-by-element, for $i = 1, ..., \mathtt{n_{el}}$:

$$\begin{Bmatrix} \mathbf{u}^i \\ \mathbf{L}^i \\ \mathbf{p}^i \end{Bmatrix} = \mathbf{Z}^{K_i}_{\widehat{u}}(\mathbf{u}^i)\,\widehat{\mathbf{u}}^i + \mathbf{Z}^{K_i}_{\widehat{p}}(\mathbf{u}^i)\,\widehat{\mathbf{p}}^i + \mathbf{z}^{K_i}(\mathbf{u}^i) \tag{6.2.16}$$

This problem is non-linear due to the convection term. There are basically two standard approaches to deal with the non-linearity: Newton methods and Picard linearization. Newton methods have locally quadratic convergence rates, but require a good initial guess [71]. Picard methods are typically more robust and easier to implement [72]. Here, robustness is chosen as a preference over the faster convergence, therefore, Picard linearization is employed. Picard iterations is shown by the grey box in Figure 6.1.
See Appendix E for more details on spatial discretization and implementation details, where all the presented matrices and vectors are defined.

6.3 Code structure

It is important to mention that the flow field and the interface position has mutual influence on each other. The position of the interface affects the enrichment functions in cut elements as well as the material properties distribution inside the cut elements. On the other hand, the velocity field is responsible for moving the interface.

In this work, a segregated (partitioned) coupling approach is used meaning that the flow field is calculated with respect to a fixed interface and afterwards the interface is advected by the computed velocity field. If this procedure is done once per time step, this would result in a weak coupling. However, if the procedure is repeated (in each time step) until both fields are in equilibrium, a strong coupling is obtained. It can be shown that a weak coupling may lead to completely non-physical results in case of large time steps [73]. Therefore, for higher accuracy and stability, a strong coupling is used.

Figure 6.1 depicts the interaction of the fields. In particular the flowchart shows two loops: (i) The outer loop over time steps (time loop, superscript n) and (ii) the inner loop representing the coupling iterations between the flow and level set field (N-S + level set loop, superscript j). $\boldsymbol{u}$ denotes the complete solution vector of the Navier-Stokes equations consisting of the velocity components, the pressure, and the flux components for all nodes and the extra X-FEM degrees of freedom at enriched nodes. Given initial conditions for the flow field and the level set field, the time loop is started, stepping into the "N-S + level set" loop.

As for the Picard iteration loop (superscript k): Starting from the solution of the previous iteration, $(\boldsymbol{u}^j, \phi^j)$, the Picard iterate $\boldsymbol{u}^{j+1}$ is computed from the linearized weak formulation of the Navier-Stokes equations with respect to the level set solution ϕ^j.

Using the velocity from that solution the level set field from the previous iteration, ϕ^j, is then advected by the level set transport equation, resulting in ϕ^{j+1}. The "N-S + level set" loop is repeated until the convergence condition is fulfilled, that is, until the flow field and the level set field are in equilibrium. As for the Picard iterations, the convergence condition is evaluated as the relative vector norm of the difference between successive iterates. Leaving the "N-S + level set" loop, the final iterates $\boldsymbol{u}^{j+1}$ and ϕ^{j+1} become the solution of the current time step: $\boldsymbol{u}^{n+1}$ and ϕ^{n+1}. If necessary, re-initialization of the level set field takes place at this point. The outer time step loop closes the basic flow of the application

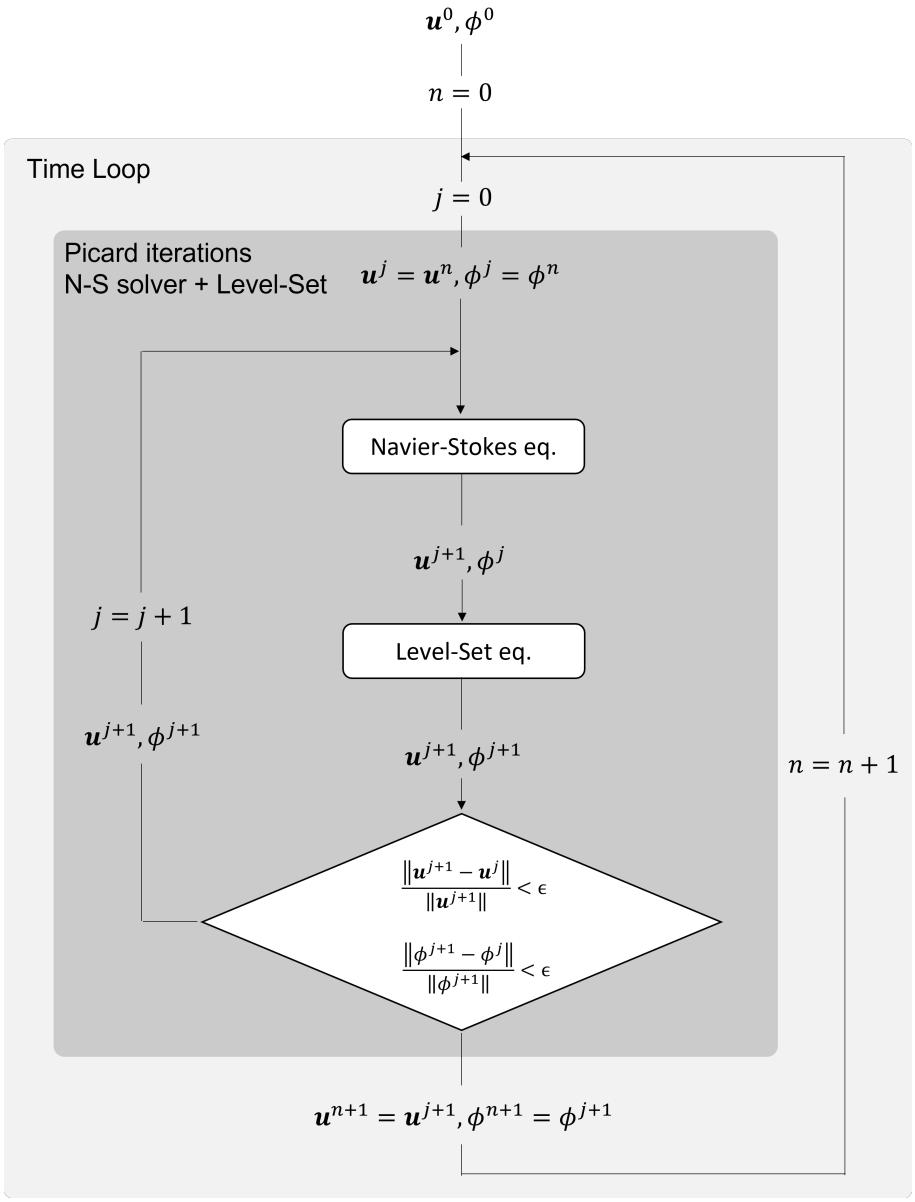

Figure 6.1: Solver flowchart.

6.4 Numerical examples

Two numerical examples are presented in this section. The first example is the steady air bubble in water presented earlier in Section 4.3.3. This examples is used to verify the implementation of the full Navier-Stokes solver after adding the transient term, the convective term, as well as Picard iterations to solve non-linearity due to convection. The second example is the hydrostatic two-phase flow over a slip wall. This example is used to check the robustness of the solver when dealing with the hydrostatic problem. Furthermore, the implementation of slip and outflow boundary conditions is tested. The third example is a two-phase flow in a domain with a bump, that would lead to a wave shape interface. The third example is presented to point out the issue that arises from interpolating the solution $\boldsymbol{u}^n$ to the approximation space of time t^{n+1} when the interface movement is not minimal as mentioned in Section 6.2.3.

6.4.1 Example 1: steady air bubble in water

The example presented earlier in Section 4.3.3 is solved again but this time after accounting for both the transient and convective terms. The initial velocity at time $t = 0$ is set to zero everywhere. Marching in time is done with time-step of value $\Delta t = 1$ until steady state is reached.

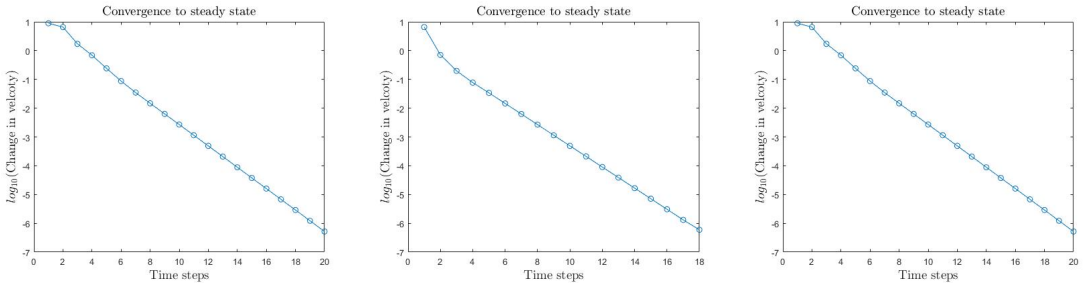

Figure 6.2: Ex 1: Convergence to steady state for velocity order $m = 2$ and mesh 2 (left), mesh 3 (middle), and mesh 4 (right) - Meshes of $(m, m-1)$ triangles.

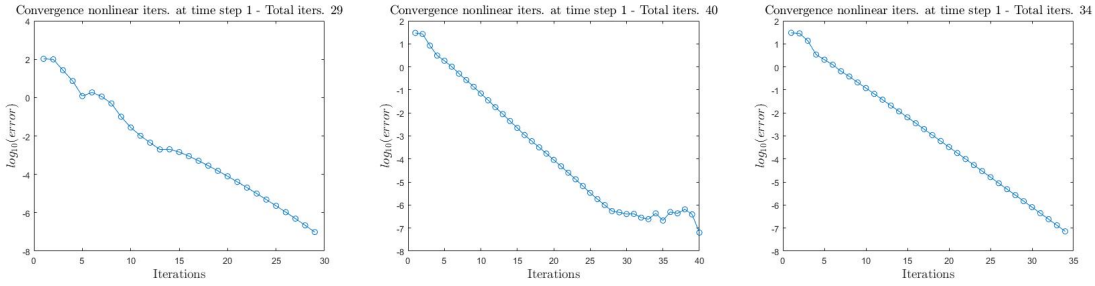

Figure 6.3: Ex 1: Convergence of Picard iterations in the first time step for velocity order $m = 2$ and mesh 2 (left), mesh 3 (middle), and mesh 4 (right) - Meshes of $(m, m-1)$ triangles.

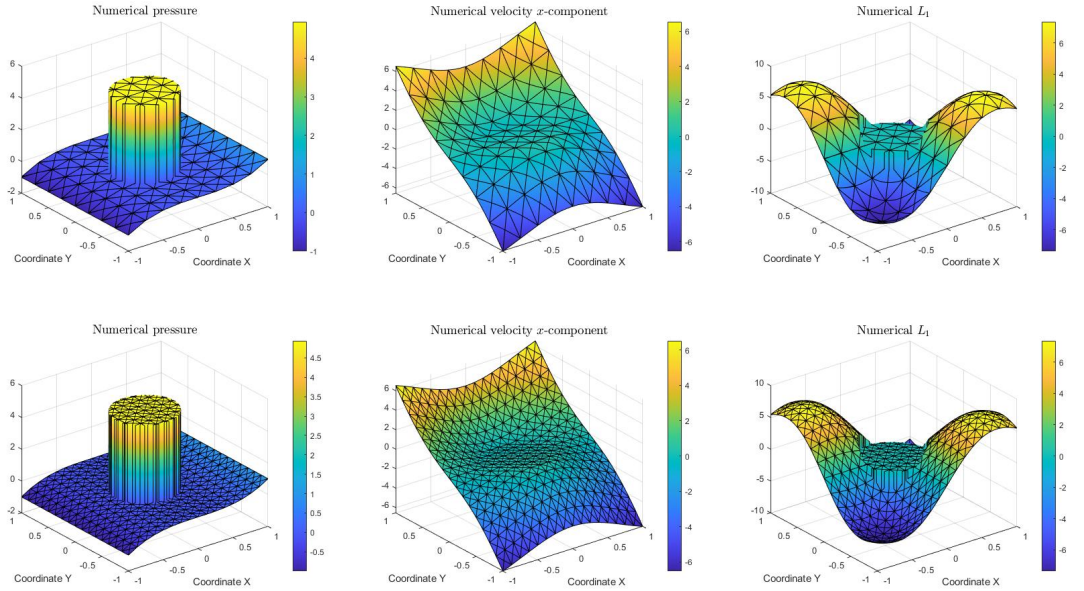

Figure 6.4: Ex 1: Numerical solution obtained using $m = 2$/meshes 3 and 4 of $(m, m-1)$ triangles: Pressure P (left), x-velocity u (middle), and flux component L_1 (right).

Mesh TRIs		$\tau = 1, \tau^{\mathcal{I}} = 0.001$					
		$\|\|u^h - u\|\|_{\mathcal{L}_2}$	rate	$\|\|P^h - P\|\|_{\mathcal{L}_2}$	rate	$\|\|L_1^h - L_1\|\|_{\mathcal{L}_2}$	rate
$m = 2$	mesh 2	2.23E-03	-	1.3E-01	-	1.46E-02	-
	mesh 3	4.08E-04	2.45	2.40E-03	5.8	2.55E-03	2.51
	mesh 4	9.24E-05	2.14	6.18E-04	1.95	5.83E-04	2.13

Table 6.1: Ex 1: Convergence data - Meshes of $(m, m-1)$ triangles.

6.4.2 Example 2: Hydrostatic two-phase flow over a slip wall

The two-phase problem is solved on a domain of size $[-2, 10] \times [-1, 0.2]$, with the air-water interface initially at $y = -0.3$ (unfitted mesh). The initial condition is $\boldsymbol{u} = [1, 0]$ everywhere. For the source term, gravitational force $\rho[0, -9.81]$ is considered in the momentum equation. In addition, Dirichlet boundary condition $\boldsymbol{u} = [1, 0]$ is applied on the left boundary. The bottom boundary is a slip wall. Furthermore, the top boundary is set as a pressure outlet where the pressure p is set to be the hydrostatic pressure. Finally, the right edge is treated as an outflow boundary. The problem is solved using two orders of approximation for the velocity m.

Case 1: the order of approximation of the velocity is $m = 2$, and the size of time step is chosen as $\Delta t = 0.1$. This yields a CFL number $= \triangle t \|\boldsymbol{u}\|/h_{\min} = (0.1 * 1 * 2^2)/0.75 = 0.53$. The solution on mesh 3 after 200 time steps, i.e. $t = 20$s, is shown in Figure 6.5. It can be seen that the maximum error in the x-velocity and y-velocity are of orders 1e-3 and 1e-4, respectively.

Case 2: the order of approximation of the velocity is $m = 3$, and the size of time step is chosen as $\Delta t = 0.045$. This yields a CFL number $= \triangle t \|\boldsymbol{u}\|/h_{\min} = (0.045 * 1 * 3^2)/0.75 = 0.54$. The solution on mesh 3 after 445 time steps, i.e. $t = 20.025$s, is shown in Figure 6.6. It can be seen that the maximum error in the x-velocity and y-velocity are also of orders 1e-3 and 1e-4, respectively.

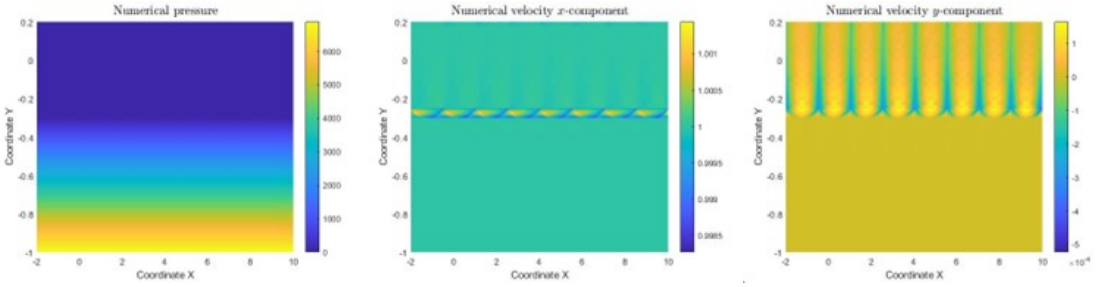

Figure 6.5: Ex 2: The steady state solution obtained after 200 time steps with velocity degree approximation $m = 2$ - Meshes of $(m, m-1)$ triangles.

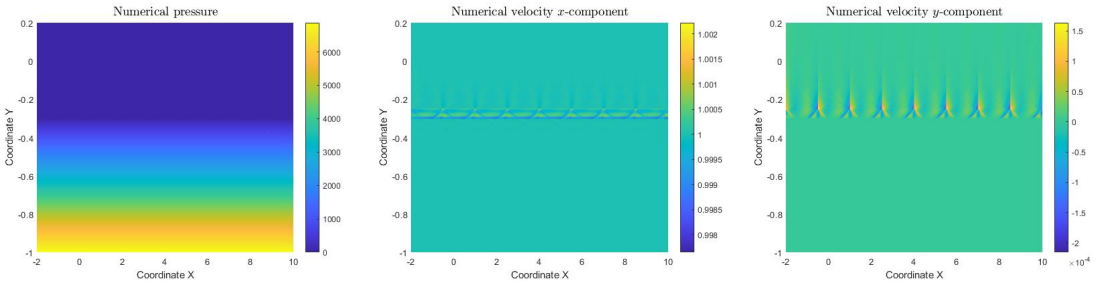

Figure 6.6: Ex 2: The steady state solution obtained after 445 time steps with velocity degree approximation $m = 3$ - Meshes of $(m, m-1)$ triangles.

Furthermore, the mesh convergence plot is shown in Figure 6.7 for the velocity component u_x, where the optimal convergence rate $m+1$ is achieved.

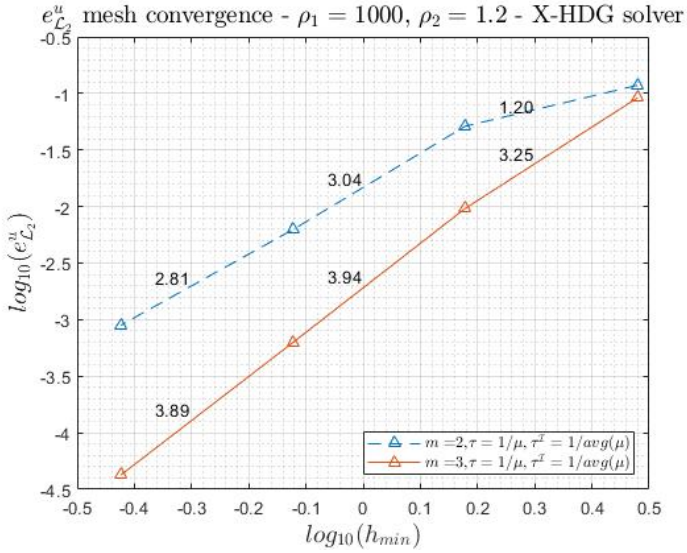

Figure 6.7: Ex 2: Errors in x-velocity u vs. mesh size - $\mathcal{L}_2$-norm - Meshes of $(m, m-1)$ triangles.

This example shows the ability of the developed solver to deal with hydrostatic problems. Here, the level-set equation was solved in each iteration as explained before in the solver flowchart shown in Figure 6.1.

6.4.3 Example 3: two-phase flow over a slip wall with bump

In this example, a two-phase (air and water) flow over a bump is considered. The computational domain has dimensions of $[-2, 10] \times [-1, 0.2]$ with a bump described as follows [74]

$$y(x) = -1 + \frac{27}{4}\frac{H}{L^3}x(x-L)^2, \quad 0 \leq x \leq L. \tag{6.4.1}$$

where here the height and the length of the bump are $H = 0.15$ and $L = 2$.

The computational mesh is shown in Figure 6.8 with the initial position of the material interface at $y = -0.3$, thus dividing the domain into Ω_1 ($y < -0.3$) and Ω_2 ($y > -0.3$).

The material properties are:

$$\rho(\boldsymbol{x}) = \begin{cases} \rho_1 = 1000 \quad \text{kg.m}^{-3} & \text{in } \Omega_1 \\ \rho_2 = 1.2 \quad \text{kg.m}^{-3} & \text{in } \Omega_2 \end{cases}$$

$$\mu(\boldsymbol{x}) = \begin{cases} \mu_1 = 8.96 \times 10^{-4} \quad \text{Pa.s} & \text{in } \Omega_1 \\ \mu_2 = 1.85 \times 10^{-5} \quad \text{Pa.s} & \text{in } \Omega_2 \end{cases}$$

$$\nu(\boldsymbol{x}) = \begin{cases} \nu_1 = 8.97 \times 10^{-7} \quad \text{m}^2.\text{s}^{-1} & \text{in } \Omega_1 \\ \nu_2 = 1.54 \times 10^{-5} \quad \text{m}^2.\text{s}^{-1} & \text{in } \Omega_2 \end{cases}$$

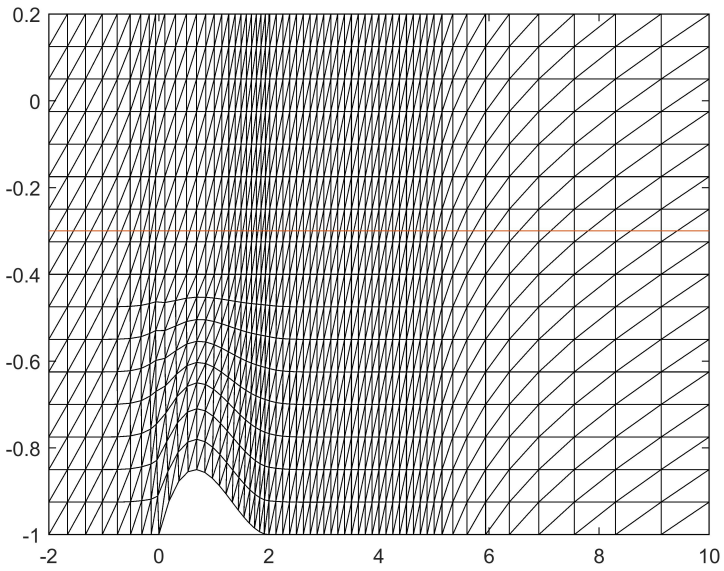

Figure 6.8: The computational mesh for the two-phase flow problem over a bump.

In this simulation, an inlet velocity $U = 1m/s$ in x-direction is applied as Dirichlet boundary condition on the left. The bottom boundary where the bump exist is treated as slip wall. Furthermore, the top boundary is set as a pressure outlet where the pressure p is set to be the hydrostatic pressure. Finally, the right edge is treated as an outflow boundary. For the source term, gravitational force $\rho[0, -9.81]$ is considered in the momentum equation.

Furthermore, $(m, m-1)$ velocity-pressure pair is used where $m = 2$ and $m = 3$ are tested. Stabilization parameters are set to $\tau = 1/\mu$ and $\tau^{\mathcal{I}} = 1/\{\mu\}$.

In this example, since the interface is moving, the transient term in the momentum equation is computed by projecting the velocity $\boldsymbol{u}^n$ and the density ρ^n to the approximation

space at t^{n+1}. This approximation is not accurate and only works (with acceptable error margins) for problems where the interface movement is minimal, i.e. minimal topological changes [39].

In the case of $m = 2$, Figure 6.9 shows the interface location at times $t = 0.01, 0.02, 0.03, 0.04$ and finally $t = 0.05$ just before the solver crashes due to the appearance of new cut cell at t^{n+1} that was uncut at t^n. In case of $m = 3$, the solution is more accurate thus the solver would crash at an earlier time step as shown in Figure 6.10.

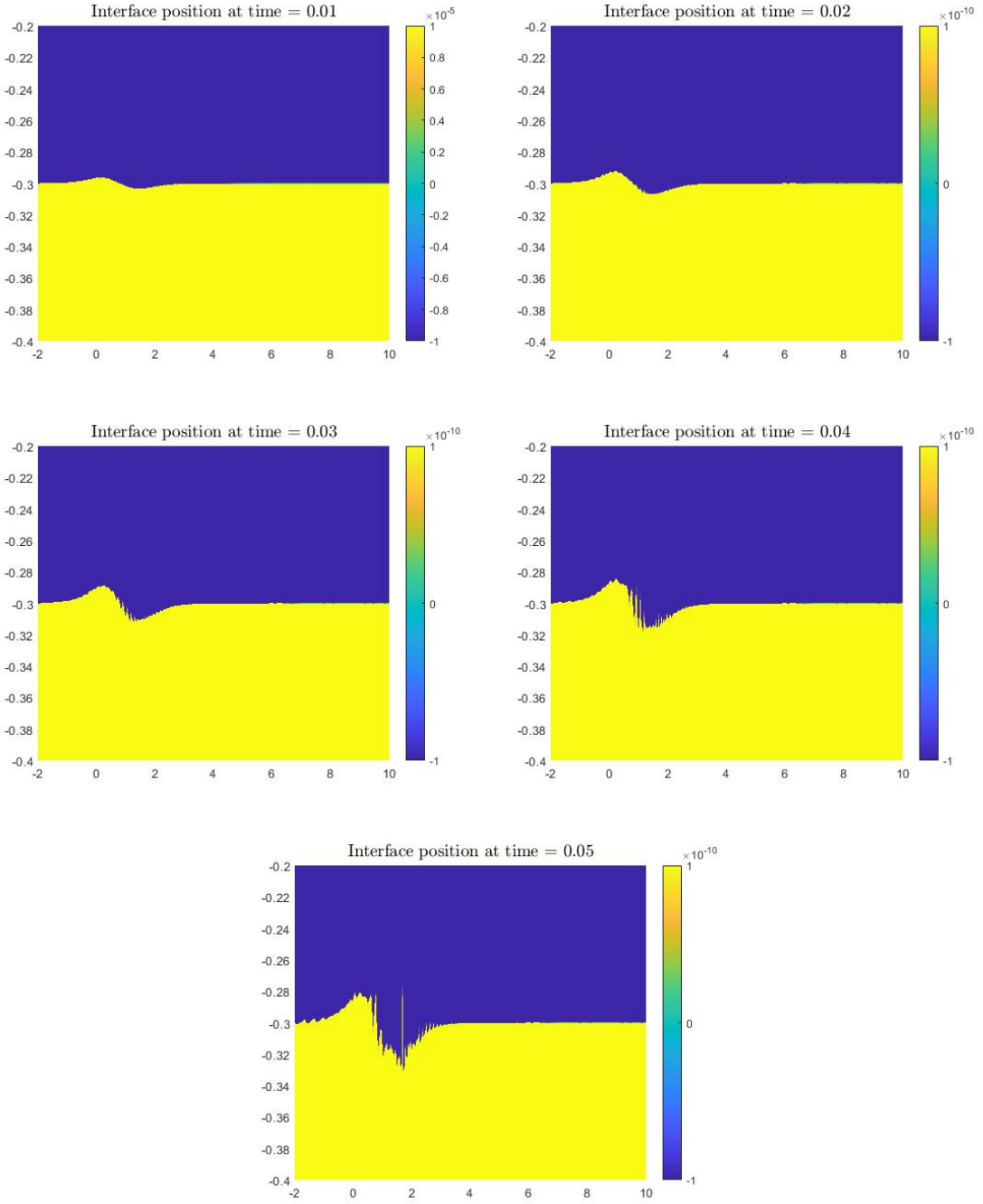

Figure 6.9: Ex 3: The interface location at times $t = 0.01, 0.02, 0.03, 0.04, 0.05$ with velocity degree approximation $m = 2$ - Meshes of $(m, m-1)$ triangles.

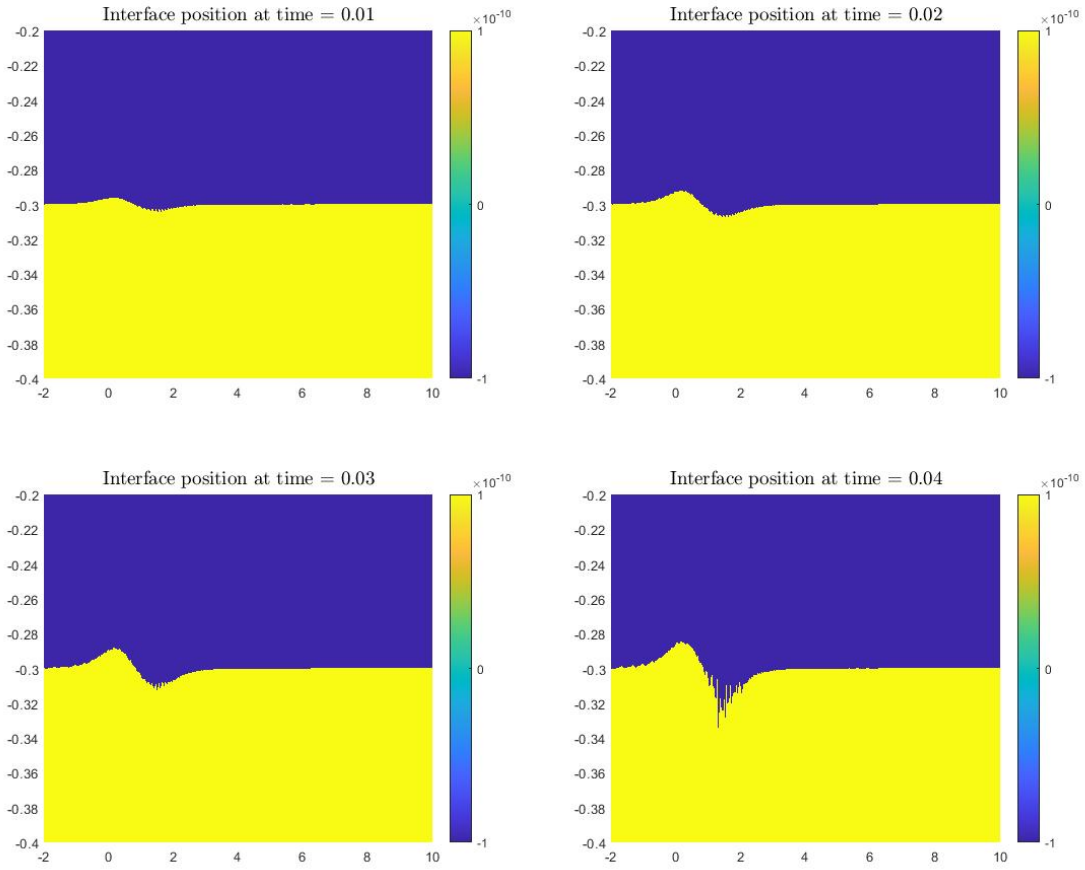

Figure 6.10: Ex 3: The interface location at times $t = 0.01, 0.02, 0.03, 0.04$ with velocity degree approximation $m = 3$ - Meshes of $(m, m-1)$ triangles.

This issue needs further treatment in order to properly integrate in time, see for instance [70] which discusses the issue of appearance and disappearance of cut elements.

A relatively easier proposed solution is to sub-divide the cut element at time t^{n+1} into regions that could be used for integrating both the old and new discontinuities, see for instance Figure 6.11. This development is considered as future work.

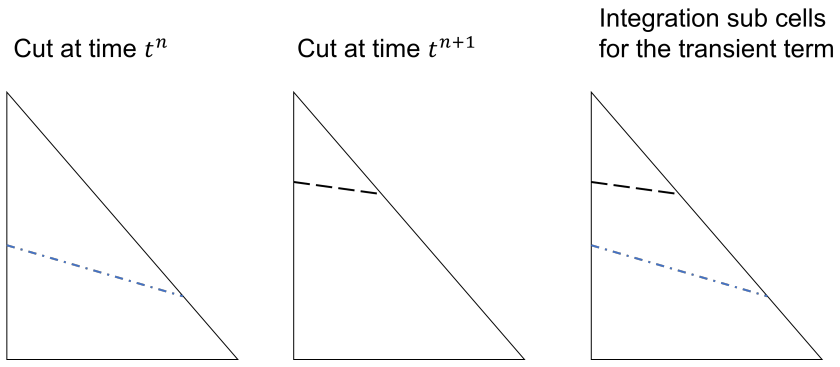

Figure 6.11: The integration sub-cells to be used in integrating the transient term in a cut element with moving interface.

Chapter 7

Conclusions and future work

7.1 Conclusions

The divergence-free X-HDG method for a two-phase flows is introduced in this thesis. The method is energy-stable meaning that the divergence-free condition is satisfied everywhere in the computational domain and the velocity field is $\mathcal{H}(div)$-conforming as demonstrated in the numerical examples. The key point of the proposed method is the usage of pressure elements that uses polynomials in the space of divergence of polynomial basis that are used to approximate the velocity. In addition, traces of velocity and pressure, of the same order m as the velocity, are introduced on the inter-element faces and the interface to enforce the transmission conditions of the conservation equations. What is truly unique in the proposed method is the introduction of the pressure trace variable of degree m on the interface to enforce the continuity of normal velocity, thus enforcing mass conservation across the interface. The results showed the capability of the method to accurately resolve local discontinuities without the need for re-meshing to fit the interface.

For Stokes flow problems, the X-HDG method is validated with the use of manufactured solutions. Higher-order convergence rates were obtained for problems with straight interface that guarantee an exact representation of the interface. On the other hand, for problems with curved interfaces, the observed convergence for degree $m = 1$ is the same as in problems with straight interfaces. However, this is not the case for higher orders of approximation where the convergence rates remain the same as for $m = 1$ but with lower error magnitudes. This is expected because of the linear approximation of the interface, within each cut element, that leads to dominant local errors at the interface. So in order to restore higher-order convergence rates, the interface has to be accurately represented. Such development is not trivial and may be unjustified in engineering applications to complex geometries where robustness is as important as numerical accuracy.

As for the full Navier-Stokes flow problems that encounter moving interfaces, the Level-Set method is used as an interface capturing method that implicitly represents the location of the interface at each time step. A basic implementation of the Level-Set method is done using HDG spatial discretization plus first and second order implicit BDF temporal discretization. The Navier-Stokes solver and the Level-Set solver are coupled using a segregated (partitioned) coupling approach meaning that the flow field is calculated with respect to a fixed interface and afterwards the interface is advected by the computed velocity field. This procedure is repeated (in each time step) until both fields are in equilibrium. The developed algorithm is tested for a problem with steady interface and optimal results are obtained. However, for the problem of two-phase flow over a bump, it is shown that a special treatment is needed to properly integrate in time taking into account the moving nature of the interface that leads to change in the approximation spaces.

As a conclusion of the thesis, a numerical Matlab code is developed to solve the two-phase incompressible Navier-Stokes equations by providing exactly point-wise divergence free velocity fields. However, essential further developments are needed as listed next in the future work section.

7.2 Future work

- Fix the issues in the development of divergence-free cut quadrilaterals: Based on the numerical tests done, the pressure field obtained with divergence-free cut quadrilaterals are not robust and suffer from severe oscillations. The reason behind this is unknown so far and further investigation is needed.
- Develop high-order integration quadrature for cut triangles and tetrahedrals: Since the pair $m, m-1$ triangles worked well in terms of providing divergence-free velocity fields, it is a priority to further develop high-order integration quadrature to accurately integrate inside cut elements with curved cuts.
- Dealing with bad cuts which lead to ill-conditioning problems: This is a common and well known issue related to X-FEM and has been addressed in the literature but it was not the focus of the current study. It is certainly important to address the problems related to bad cuts in order to enhance the robustness of the developed code.
- Further study the interface stabilization parameter: The numerical tests done while solving bi-material Poisson problems using X-HDG showed that the value of the interface stabilization parameter has an effect on the convergence rate. This was a brief study that needs further investigation.
- Further development of the level-set solver, by developing optimized re-initialization strategies and extension velocity strategies: In this thesis, a basic implementation of the Level-Set method is done using HDG. However, for more complex interface movement, re-initialization of the distance function is needed. On the other hand, the developed algorithm for extending the interface velocity to the whole domain needs more optimization to avoid the excessive computational cost as a result of the non-optimal algorithm responsible for searching for the nearest point on the interface.
- Integrating the transient term given that the approximation space changes in time due to the moving material interface. This would lead to different cuts, appearance and disappearance of cut elements. This issue needs special treatment of the transient term to properly integrate in time.
- Extension to 3D problems: It it crucial to extend the developed code to 3D in order to account for real life problems.

Bibliography

[1] Zhijian J Wang et al.
"High-order CFD methods: current status and perspective".
In: *International Journal for Numerical Methods in Fluids* 72.8 (2013), pp. 811–845.

[2] Norbert Kroll.
"ADIGMA: A European project on the development of adaptive higher order variational methods for aerospace applications".
In: *47th AIAA Aerospace Sciences Meeting including The New Horizons Forum and Aerospace Exposition*.
2006,
P. 176.

[3] Jan S Hesthaven and Tim Warburton.
Nodal discontinuous Galerkin methods: algorithms, analysis, and applications.
Springer Science & Business Media, 2007.

[4] Bernardo Cockburn, George E Karniadakis and Chi-Wang Shu.
"The development of discontinuous Galerkin methods".
In: *Discontinuous Galerkin Methods*.
Springer, 2000,
Pp. 3–50.

[5] Douglas N Arnold et al.
"Discontinuous Galerkin methods for elliptic problems".
In: *Discontinuous Galerkin Methods*.
Springer, 2000,
Pp. 89–101.

[6] Douglas N Arnold et al.
"Unified analysis of discontinuous Galerkin methods for elliptic problems".
In: *SIAM journal on numerical analysis* 39.5 (2002), pp. 1749–1779.

[7] Ralf Hartmann.
"Numerical analysis of higher order discontinuous Galerkin finite element methods".
In: (2008).

[8] Bernardo Cockburn, Guido Kanschat and Dominik Schötzau.
"An equal-order DG method for the incompressible Navier-Stokes equations".
In: *Journal of Scientific Computing* 40.1 (2009), pp. 188–210.

[9] Marco Agnese and Robert Nürnberg.
"Fitted finite element discretization of two-phase Stokes flow".
In: *International Journal for Numerical Methods in Fluids* 82.11 (2016), pp. 709–729.

[10] Erik Gros.
"Numerical Modelling of Two-Phase Flow with Moving Boundary Fitted Meshes".
PhD thesis. EPFL, 2018.

[11] Erik Gros, Gustavo R Anjos and John R Thome.
"Interface-fitted moving mesh method for axisymmetric two-phase flow in microchannels".
In: *International Journal for Numerical Methods in Fluids* 86.3 (2018), pp. 201–217.

[12] Maksymilian Dryja.
"On discontinuous Galerkin methods for elliptic problems with discontinuous coefficients".
In: *Computational Methods in Applied Mathematics* 3.1 (2003), pp. 76–85.

[13] LNT Huynh et al.
"A high-order hybridizable discontinuous Galerkin method for elliptic interface problems".
In: *International Journal for Numerical Methods in Engineering* 93.2 (2013), pp. 183–200.

[14] Nicolas Moës, John Dolbow and Ted Belytschko.
"A finite element method for crack growth without remeshing".
In: *International journal for numerical methods in engineering* 46.1 (1999), pp. 131–150.

[15] Henning Sauerland.
An XFEM based sharp interface approach for two-phase and free-surface flows.
Dr. Hut, 2013.

[16] Kwok Wah Cheng.
"h-and p-XFEM with application to two-phase incompressible flow".
PhD thesis. Lehrstuhl für Computergestützte Analyse technischer Systeme, 2011.

[17] Sven Groß.
"Numerical methods for three-dimensional incompressible two-phase flow problems".
PhD thesis. Lehrstuhl für Numerische Mathematik, 2008.

[18] Matthias Kirchhart, Sven Gross and Arnold Reusken.
"Analysis of an XFEM discretization for Stokes interface problems".
In: *SIAM Journal on Scientific Computing* 38.2 (2016), A1019–A1043.

[19] Arnold Reusken.
"Analysis of an extended pressure finite element space for two-phase incompressible flows".
In: *Computing and visualization in science* 11.4 (2008), pp. 293–305.

[20] Henning Sauerland and Thomas-Peter Fries.
"The stable XFEM for two-phase flows".
In: *Computers & Fluids* 87 (2013), pp. 41–49.

[21] Thomas Utz et al.
"An extended discontinuous Galerkin framework for multiphase flows".
In: *Transport Processes at Fluidic Interfaces.*
Springer, 2017,
Pp. 65–91.

[22] Thomas Utz.
"Level set methods for high-order unfitted discontinuous Galerkin schemes".
PhD thesis. Technische Universität, 2018.

[23] Florian Kummer.
"Extended discontinuous Galerkin methods for two-phase flows: the spatial discretization".

In: *International Journal for Numerical Methods in Engineering* 109.2 (2017), pp. 259–289.

[24] Florian Kummer.
"The BoSSS Discontinuous Galerkin solver for incompressible fluid dynamics and an extension to singular equations."
PhD thesis. Technische Universität, 2012.

[25] Ngoc Cuong Nguyen, Jaime Peraire and Bernardo Cockburn.
"An implicit high-order hybridizable discontinuous Galerkin method for linear convection-diffusion equations".
In: *Journal of Computational Physics* 228.9 (2009), pp. 3232–3254.

[26] Ngoc Cuong Nguyen, Jaime Peraire and Bernardo Cockburn.
"An implicit high-order hybridizable discontinuous Galerkin method for nonlinear convection-diffusion equations".
In: *Journal of Computational Physics* 228.23 (2009), pp. 8841–8855.

[27] Ngoc Cuong Nguyen and Jaime Peraire.
"Hybridizable discontinuous Galerkin methods for partial differential equations in continuum mechanics".
In: *Journal of Computational Physics* 231.18 (2012), pp. 5955–5988.

[28] Ngoc Cuong Nguyen, Jaime Peraire and Bernardo Cockburn.
"A hybridizable discontinuous Galerkin method for Stokes flow".
In: *Computer Methods in Applied Mechanics and Engineering* 199.9-12 (2010), pp. 582–597.

[29] Ruben Sevilla and Antonio Huerta.
"Tutorial on Hybridizable Discontinuous Galerkin (HDG) for second-order elliptic problems".
In: *Advanced finite element technologies.*
Springer, 2016,
Pp. 105–129.

[30] Ceren Gürkan, Martin Kronbichler and Sonia Fernández-Méndez.
"eXtended hybridizable discontinuous Galerkin with Heaviside enrichment for heat bimaterial problems".
In: *Journal of scientific computing* 72.2 (2017), pp. 542–567.

[31] Ceren Gürkan et al.
"eXtended hybridizable discontinuous Galerkin (X-HDG) for void and bimaterial problems".
In: *Advances in Discretization Methods.*
Springer, 2016,
Pp. 103–122.

[32] Ceren Gürkan et al.
"eXtended Hybridizable Discontinous Galerkin (X-HDG) for void problems".
In: *Journal of scientific computing* 66.3 (2016), pp. 1313–1333.

[33] Matteo Giacomini, Ruben Sevilla and Antonio Huerta.
"Tutorial on Hybridizable Discontinuous Galerkin (HDG) Formulation for Incompressible Flow Problems".
In: *Modeling in Engineering Using Innovative Numerical Methods for Solids and Fluids.*
Springer, 2020,
Pp. 163–201.

[34] Sander Rhebergen and Garth N Wells.
"A hybridizable discontinuous Galerkin method for the Navier–Stokes equations with pointwise divergence-free velocity field".
In: *Journal of Scientific Computing* 76.3 (2018), pp. 1484–1501.

[35] Hashim Elzaabalawy.
"Towards High-Order Compact Discretization of Unsteady Navier-Stokes Equations for Incompressible Flows on Unstructured Grids".
PhD thesis. École centrale de Nantes; Instituto superior técnico (Lisbonne), 2020.

[36] Hashim Elzaabalawy et al.
"An HDG Method for the Incompressible Navier-Stokes Equations with Pointwise Divergence-Free Velocity Field for Quadrilateral and Hexahedral Elements".
In: *Submitted to Journal of Scientific Computing* (2020).

[37] Hashim Elzaabalawy et al.
"Assessment of solving the RANS equations with two-equation eddy-viscosity models using high-order accurate discretization".
In: *Submitted to Journal of Computational Physics* (2020).

[38] Ceren Gürkan, Martin Kronbichler and Sonia Fernández-Méndez.
"eXtended hybridizable discontinuous Galerkin for incompressible flow problems with unfitted meshes and interfaces".
In: *International Journal for Numerical Methods in Engineering* 117.7 (2019), pp. 756–777.

[39] Ceren Gürkan.
"Extended hybridizable discontinuous Galerkin method".
PhD thesis. 2018.

[40] Ahmed Sherif et al.
"Point-wise divergence-free extended hybridizable discontinuous Galerkin method for two-phase Stokes flow with unfitted meshes and interfaces".
In: *Submitted to Journal of Computational Physics* (2022).

[41] Stanley Osher and Ronald P Fedkiw.
Level set methods and dynamic implicit surfaces.
Vol. 153.
Springer, 2003.

[42] James Albert Sethian.
Level set methods and fast marching methods: evolving interfaces in computational geometry, fluid mechanics, computer vision, and materials science.
Vol. 3.
Cambridge university press, 1999.

[43] David Henneaux et al.
"A High-Order Level-Set Method Coupled with an Extended Discontinuous Galerkin Method for Simulating Moving Interface Problems".
In: *AIAA AVIATION 2021 FORUM.*
2021,
P. 2742.

[44] Sylvie Pommier et al.
Extended finite element method for crack propagation.
Wiley Online Library, 2011.

[45] Esther Sala Lardies, Sonia Fernández Méndez and Antonio Huerta.

"Optimally convergent high-order X-FEM for problems with voids and inclusions".
In: *ECCOMAS 2012: 6th European Congress on Computational Methods in Applied Sciences and Engineering. Programme book of abstracts, September 10-14, 2012, Vienna, Austria.*
2012,
Pp. 1–14.

[46] Sven Groß and Arnold Reusken.
"An extended pressure finite element space for two-phase incompressible flows with surface tension".
In: *Journal of Computational Physics* 224.1 (2007), pp. 40–58.

[47] Natarajan Sukumar et al.
"Modeling holes and inclusions by level sets in the extended finite-element method".
In: *Computer methods in applied mechanics and engineering* 190.46-47 (2001), pp. 6183–6200.

[48] Nicolas Moës et al.
"A computational approach to handle complex microstructure geometries".
In: *Computer methods in applied mechanics and engineering* 192.28-30 (2003), pp. 3163–3177.

[49] Kwok Wah Cheng and Thomas-Peter Fries.
"Higher-order XFEM for curved strong and weak discontinuities".
In: *International Journal for Numerical Methods in Engineering* 82.5 (2010), pp. 564–590.

[50] Kristell Dréau, Nicolas Chevaugeon and Nicolas Moës.
"Studied X-FEM enrichment to handle material interfaces with higher order finite element".
In: *Computer Methods in Applied Mechanics and Engineering* 199.29-32 (2010), pp. 1922–1936.

[51] Thomas-Peter Fries.
"A corrected XFEM approximation without problems in blending elements".
In: *International Journal for Numerical Methods in Engineering* 75.5 (2008), pp. 503–532.

[52] Stanley Osher, Ronald Fedkiw and K Piechor.
"Level set methods and dynamic implicit surfaces".
In: *Appl. Mech. Rev.* 57.3 (2004), B15–B15.

[53] Ruben Sevilla, Sonia Fernández-Méndez and Antonio Huerta.
"Comparison of high-order curved finite elements".
In: *International Journal for Numerical Methods in Engineering* 87.8 (2011), pp. 719–734.

[54] RI Saye.
"High-order quadrature methods for implicitly defined surfaces and volumes in hyper-rectangles".
In: *SIAM Journal on Scientific Computing* 37.2 (2015), A993–A1019.

[55] Björn Müller, Florian Kummer and Martin Oberlack.
"Highly accurate surface and volume integration on implicit domains by means of moment-fitting".
In: *International Journal for Numerical Methods in Engineering* 96.8 (2013), pp. 512–528.

[56] Jean Donea and Antonio Huerta.
Finite element methods for flow problems.
John Wiley & Sons, 2003.

[57] Cx K Batchelor and GK Batchelor.
An introduction to fluid dynamics.
Cambridge university press, 2000.

[58] Zhilin Li and Ming-Chih Lai.
"The immersed interface method for the Navier-Stokes equations with singular forces".
In: *Journal of Computational Physics* 171.2 (2001), pp. 822–842.

[59] Hashim Elzaabalawy et al.
"Analysis of hybridizable discontinuous Galerkin stabilization parameter in convection dominated flows".
In: *Submitted to Journal of Computational Physics* (2020).

[60] Franco Brezzi.
"On the existence, uniqueness and approximation of saddle-point problems arising from Lagrangian multipliers".
In: *Publications mathématiques et informatique de Rennes* S4 (1974), pp. 1–26.

[61] Ravi Malladi, James A Sethian and Baba C Vemuri.
"Shape modeling with front propagation: A level set approach".
In: *IEEE transactions on pattern analysis and machine intelligence* 17.2 (1995), pp. 158–175.

[62] Hashem M Mourad, John Dolbow and Krishna Garikipati.
"An assumed-gradient finite element method for the level set equation".
In: *International Journal for Numerical Methods in Engineering* 64.8 (2005), pp. 1009–1032.

[63] Emilie Marchandise, Jean-François Remacle and Nicolas Chevaugeon.
"A quadrature-free discontinuous Galerkin method for the level set equation".
In: *Journal of Computational Physics* 212.1 (2006), pp. 338–357.

[64] Jaime Peraire, Ngoc Cuong Nguyen and Bernardo Cockburn.
"A Hybridizable Discontinuous Galerkin Method for the Compressible Euler and Navier-Stokes Equations".
In: *48th AIAA Aerospace Sciences Meeting Including the New Horizons Forum and Aerospace Exposition.*
AIAA 2010-363.
Orlando, FL, 2010.

[65] John Charles Butcher.
Numerical methods for ordinary differential equations.
John Wiley & Sons, 2016.

[66] Ernst Hairer, Syvert P. Nørsett and Gerhard Wanner.
Solving ordinary differential equations I: Nonstiff problems.
Springer, 1990.

[67] M Darwish and F Moukalled.
"Convective schemes for capturing interfaces of free-surface flows on unstructured grids".
In: *Numerical heat transfer, part B: Fundamentals* 49.1 (2006), pp. 19–42.

[68] F Moukalled and M Darwish.
"Transient schemes for capturing interfaces of free-surface flows".

In: *Numerical Heat Transfer, Part B: Fundamentals* 61.3 (2012), pp. 171–203.

[69] Qinghai Zhang and Aaron Fogelson.
"Fourth-order interface tracking in two dimensions via an improved polygonal area mapping method".
In: *SIAM Journal on Scientific Computing* 36.5 (2014), A2369–A2400.

[70] Florian Kummer, Björn Müller and Thomas Utz.
"Time integration for extended discontinuous Galerkin methods with moving domains".
In: *International Journal for Numerical Methods in Engineering* 113.5 (2018), pp. 767–788.

[71] Ramon Codina.
"A finite element model for incompressible flow problems".
PhD thesis. 1992.

[72] Bruce M DeBlois.
"Linearizing convection terms in the Navier-Stokes equations".
In: *Computer methods in applied mechanics and engineering* 143.3-4 (1997), pp. 289–297.

[73] Ido Akkerman et al.
"Free-surface flow and fluid-object interaction modeling with emphasis on ship hydrodynamics".
In: *Journal of Applied Mechanics* 79.1 (2012).

[74] EH Van Brummelen, HC Raven and B Koren.
"Efficient numerical solution of steady free-surface Navier–Stokes flow".
In: *Journal of Computational Physics* 174.1 (2001), pp. 120–137.

Appendix A

X-FEM enriched approximation explained

A.1 Heaviside enrichment in a 1D linear element

$$u|_{K_i} \approx u^h|_{K_i} = \underbrace{N_1U_1 + N_2U_2}_{\text{Standard FE}} + \underbrace{HN_1a_1 + HN_2a_2}_{\text{Enrichment}} = \begin{Bmatrix} N_1 & N_2 & HN_1 & HN_2 \end{Bmatrix} \begin{Bmatrix} U_1 \\ U_2 \\ a_1 \\ a_2 \end{Bmatrix}$$

(a) 1D linear reference element cut at $\xi = -0.5$.

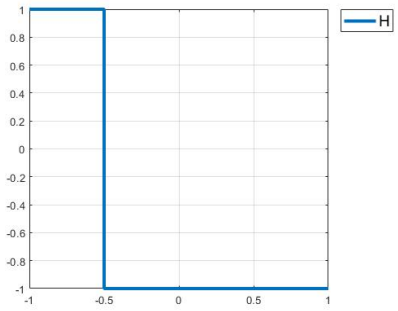

(b) Heaviside function H inside the cut element.

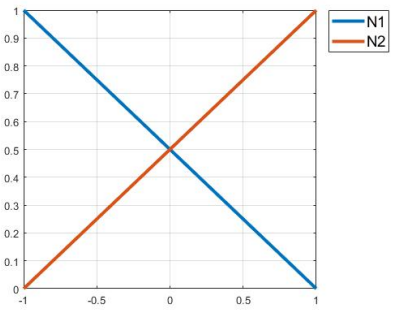

(c) Standard FE linear shape functions.

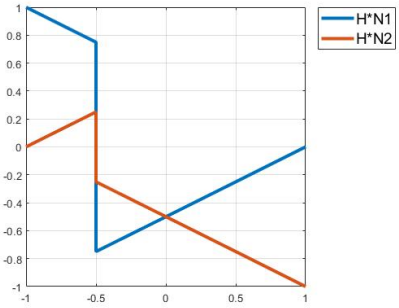

(d) Heaviside enriched linear shape functions.

Figure A.1: Heaviside enrichment in a 1D linear element.

A.2 Heaviside enrichment in a 1D quadratic element

$$u|_{K_i} \approx u^h|_{K_i} = \underbrace{N_1U_1 + N_2U_2 + N_3U_3}_{\text{Standard FE}} + \underbrace{HN_1a_1 + HN_2a_2 + HN_3a_3}_{\text{Enrichment}}$$

$$= \begin{Bmatrix} N_1 & N_2 & N_3 & HN_1 & HN_2 & HN_3 \end{Bmatrix} \begin{Bmatrix} U_1 \\ U_2 \\ U_3 \\ a_1 \\ a_2 \\ a_3 \end{Bmatrix}$$

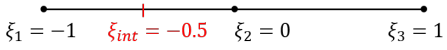

(a) 1D quadratic reference element cut at $\xi = -0.5$.

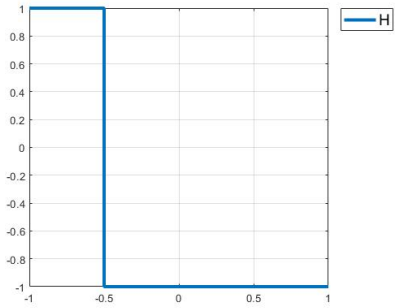

(b) Heaviside function H inside the cut element.

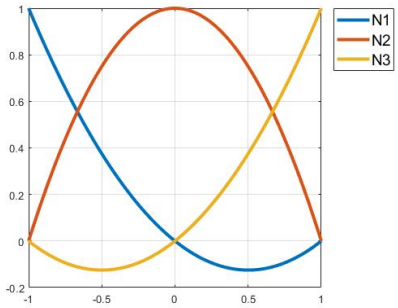

(c) Standard FE quadratic shape functions.

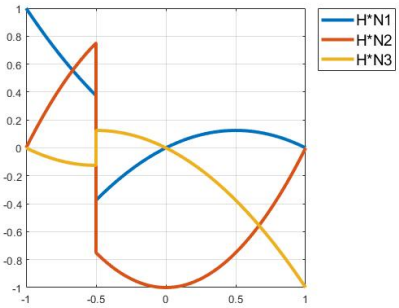

(d) Heaviside enriched quadratic shape functions.

Figure A.2: Heaviside enrichment in a 1D quadratic element.

Appendix B

Divergence-free approximation

To satisfy divergence-free condition point-wise:

- If **velocity** is in polynomial space of degree m

$$\mathcal{V}_v^h = \boldsymbol{\psi} \in [\mathcal{L}_2(\Omega)]^d : \boldsymbol{\psi}_h|_{K_i} \in [\mathcal{P}^m(K_i)]^d$$

- The polynomial space to approximate the **pressure** should be:

$$\mathcal{S}_v^{div\,h} = \phi \in \mathcal{L}_2(\Omega) : \phi_h|_{K_i} \in \boldsymbol{\nabla}\cdot[\mathcal{P}^m(K_i)]^d$$

B.1 Triangular elements

- Velocity $\rightarrow$ FE of order m.
- Pressure $\rightarrow$ FE of order $m-1$.
- $\boldsymbol{\nabla}\cdot[\mathcal{P}^m(K_i)]^d = \mathcal{P}_{m-1}(K_i)$

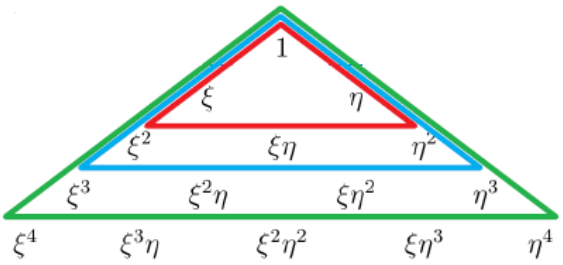

B.2 Quadrilateral elements

- $\boldsymbol{\nabla}\cdot[\mathcal{P}^m(K_i)]^d \neq \mathcal{P}_{m-1}(K_i)$
- $\boldsymbol{\nabla}\cdot[\mathcal{P}^m(K_i)]^d \rightarrow \xi^m\eta^m$ removed
- Pressure element of degree m_{reduced} has one node less

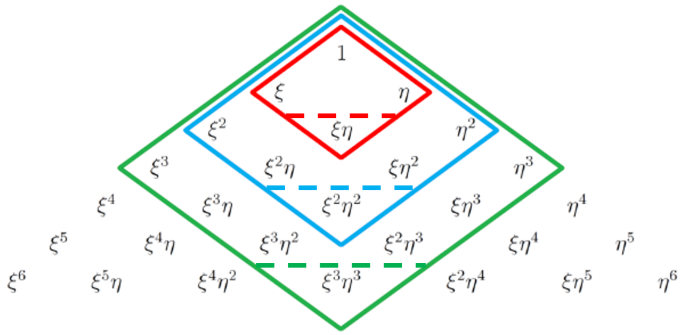
1
ξ
η
ξ²
ξη
η²
ξ³
ξ²η
ξη²
η³
ξ⁴
ξ³η
ξ²η²
ξη³
η⁴
ξ⁵
ξ⁴η
ξ³η²
ξ²η³
ξη⁴
η⁵
ξ⁶
ξ⁵η
ξ⁴η²
ξ³η³
ξ²η⁴
ξη⁵
η⁶

Appendix C

Spatial discretization and implementation details of the X-HDG method for two-phase Stokes problem

C.1 Discrete local problems in cut elements

Terms in equation (4.2.5a) are written as:

$$
\begin{aligned}
\mathbf{A}_{uu}^{K_i}\,\mathbf{u}^i =& \langle \boldsymbol{\psi}, \nu\tau\boldsymbol{u}\rangle_{\partial K_i} + \langle \boldsymbol{\psi}, \nu\tau(\boldsymbol{u}\cdot\boldsymbol{n})\boldsymbol{n}\rangle_{\partial K_i}\\
\mathbf{A}_{uL}^{K_i}\,\mathbf{L}^i =& (\boldsymbol{\psi}, \boldsymbol{\nabla}\cdot(\nu\boldsymbol{L}))_{K_i}\\
\mathbf{A}_{up}^{K_i}\,\mathbf{p}^i =& -(\boldsymbol{\nabla}\boldsymbol{\psi}, P\boldsymbol{I})_{K_i}\\
\mathbf{A}_{u\widetilde{p}^i}^{\mathcal{I}_i}\,\widetilde{\mathbf{p}}^i =& \langle \boldsymbol{\psi}_1 - \boldsymbol{\psi}_2, \widetilde{P}^i\widehat{\boldsymbol{n}}\rangle_{\mathcal{I}_i}\\
\mathbf{A}_{uu}^{\mathcal{I}_i}\,\mathbf{u}^i =& \langle \boldsymbol{\psi}_1, \nu_1\tau^{\mathcal{I}}\boldsymbol{u}_1\rangle_{\mathcal{I}_i} + \langle \boldsymbol{\psi}_2, \nu_2\tau^{\mathcal{I}}\boldsymbol{u}_2\rangle_{\mathcal{I}_i} + \langle \boldsymbol{\psi}_1, \nu_1\tau^{\mathcal{I}}(\boldsymbol{u}_1\cdot\widehat{\boldsymbol{n}})\widehat{\boldsymbol{n}}\rangle_{\mathcal{I}_i} + \langle \boldsymbol{\psi}_2, \nu_2\tau^{\mathcal{I}}(\boldsymbol{u}_2\cdot\widehat{\boldsymbol{n}})\widehat{\boldsymbol{n}}\rangle_{\mathcal{I}_i}\\
\mathbf{A}_{u\widetilde{u}^i}^{\mathcal{I}_i}\,\widetilde{\mathbf{u}}^i =& -\langle \boldsymbol{\psi}_1, \nu_1\tau^{\mathcal{I}}\widetilde{\boldsymbol{u}}^i\rangle_{\mathcal{I}_i} - \langle \boldsymbol{\psi}_2, \nu_2\tau^{\mathcal{I}}\widetilde{\boldsymbol{u}}^i\rangle_{\mathcal{I}_i} - \langle \boldsymbol{\psi}_1, \nu_1\tau^{\mathcal{I}}(\widetilde{\boldsymbol{u}}^i\cdot\widehat{\boldsymbol{n}})\widehat{\boldsymbol{n}}\rangle_{\mathcal{I}_i} - \langle \boldsymbol{\psi}_2, \nu_2\tau^{\mathcal{I}}(\widetilde{\boldsymbol{u}}^i\cdot\widehat{\boldsymbol{n}})\widehat{\boldsymbol{n}}\rangle_{\mathcal{I}_i}\\
\mathbf{f}_u^{K_i} =& (\boldsymbol{\psi}, \boldsymbol{f})_{K_i} + \langle \boldsymbol{\psi}, \nu\tau\boldsymbol{u}_D\rangle_{\partial K_i\cap\Gamma_D} + \langle \boldsymbol{\psi}, \nu\tau(\boldsymbol{u}_D\cdot\boldsymbol{n})\boldsymbol{n}\rangle_{\partial K_i\cap\Gamma_D} - \langle \boldsymbol{\psi}, P_N\boldsymbol{n}\rangle_{\partial K_i\cap\Gamma_N} - \langle \boldsymbol{\psi}_1, \boldsymbol{g}_s\rangle_{\mathcal{I}_i}\\
\mathbf{A}_{u\widehat{u}}^{K_i}\,\widehat{\mathbf{u}}^i =& \langle \boldsymbol{\psi}, \nu\tau\widehat{\boldsymbol{u}}\rangle_{\partial K_i\setminus\Gamma_D} + \langle \boldsymbol{\psi}, \nu\tau(\widehat{\boldsymbol{u}}\cdot\boldsymbol{n})\boldsymbol{n}\rangle_{\partial K_i\setminus\Gamma_D}\\
\mathbf{A}_{u\widehat{p}}^{K_i}\,\widehat{\mathbf{p}}^i =& -\langle \boldsymbol{\psi}, \widehat{P}\boldsymbol{n}\rangle_{\partial K_i\setminus\Gamma_N}
\end{aligned}
$$

Terms in equation (4.2.5b) are written as:

$$
\begin{aligned}
\mathbf{A}_{LL}^{K_i}\,\mathbf{L}^i &= -(\boldsymbol{\Psi}, \boldsymbol{L})_{K_i}\\
\mathbf{A}_{Lu}^{K_i}\,\mathbf{u}^i &= (\boldsymbol{\nabla}^s\cdot\boldsymbol{\Psi}, \boldsymbol{u})_{K_i}\\
\mathbf{A}_{L\widetilde{u}^i}^{\mathcal{I}_i}\,\widetilde{\mathbf{u}}^i &= -\langle \boldsymbol{\Psi}_1, \widetilde{\boldsymbol{u}}^i\otimes\widehat{\boldsymbol{n}}\rangle_{\mathcal{I}_i} - \langle \boldsymbol{\Psi}_1, \widehat{\boldsymbol{n}}\otimes\widetilde{\boldsymbol{u}}^i\rangle_{\mathcal{I}_i} + \langle \boldsymbol{\Psi}_2, \widetilde{\boldsymbol{u}}^i\otimes\widehat{\boldsymbol{n}}\rangle_{\mathcal{I}_i} + \langle \boldsymbol{\Psi}_2, \widehat{\boldsymbol{n}}\otimes\widetilde{\boldsymbol{u}}^i\rangle_{\mathcal{I}_i}\\
\mathbf{A}_{L\widehat{u}}^{K_i}\,\widehat{\mathbf{u}}^i &= \langle \boldsymbol{\Psi}, \widehat{\boldsymbol{u}}\otimes\boldsymbol{n}\rangle_{\partial K_i\setminus\Gamma_D} + \langle \boldsymbol{\Psi}, \boldsymbol{n}\otimes\widehat{\boldsymbol{u}}\rangle_{\partial K_i\setminus\Gamma_D}\\
\mathbf{f}_L^{K_i} &= \langle \boldsymbol{\Psi}, \boldsymbol{u}_D\otimes\boldsymbol{n}\rangle_{\partial K_i\cap\Gamma_D} + \langle \boldsymbol{\Psi}, \boldsymbol{n}\otimes\boldsymbol{u}_D\rangle_{\partial K_i\cap\Gamma_D}
\end{aligned}
$$

Terms in equation (4.2.5c) are written as:

$$
\mathbf{A}_{pu}^{K_i}\,\mathbf{u}^i = -(\phi, \boldsymbol{\nabla}\cdot\boldsymbol{u})_{K_i}
$$

Terms in equation (4.2.5d) are written as:

$$\begin{aligned}
\mathbf{A}^{\mathcal{I}_i}_{\widetilde{u^i}\widetilde{p^i}}\,\widetilde{\mathbf{p}}^i =& \langle\widetilde{\boldsymbol{\psi}}, \widetilde{P}^i\widehat{\boldsymbol{n}}\rangle_{\mathcal{I}_i} + \langle\widetilde{\boldsymbol{\psi}}, \widetilde{P}^i(-\widehat{\boldsymbol{n}})\rangle_{\mathcal{I}_i} = \mathbf{0}\\
\mathbf{A}^{\mathcal{I}_i}_{\widetilde{u^i}L}\,\mathbf{L}^i =& \langle\widetilde{\boldsymbol{\psi}}, \nu_1\boldsymbol{L}_1\widehat{\boldsymbol{n}}\rangle_{\mathcal{I}_i} - \langle\widetilde{\boldsymbol{\psi}}, \nu_2\boldsymbol{L}_2\widehat{\boldsymbol{n}}\rangle_{\mathcal{I}_i}\\
\mathbf{A}^{\mathcal{I}_i}_{\widetilde{u^i}\widetilde{u^i}}\,\widetilde{\mathbf{u}}^i =& -\langle\widetilde{\boldsymbol{\psi}}, \nu_1\tau^{\mathcal{I}}\widetilde{\boldsymbol{u}}^i\rangle_{\mathcal{I}_i} - \langle\widetilde{\boldsymbol{\psi}}, \nu_2\tau^{\mathcal{I}}\widetilde{\boldsymbol{u}}^i\rangle_{\mathcal{I}_i} - \langle\widetilde{\boldsymbol{\psi}}, \nu_1\tau^{\mathcal{I}}(\widetilde{\boldsymbol{u}}^i\cdot\widehat{\boldsymbol{n}})\widehat{\boldsymbol{n}}\rangle_{\mathcal{I}_i} - \langle\widetilde{\boldsymbol{\psi}}, \nu_2\tau^{\mathcal{I}}(\widetilde{\boldsymbol{u}}^i\cdot\widehat{\boldsymbol{n}})\widehat{\boldsymbol{n}}\rangle_{\mathcal{I}_i}\\
\mathbf{A}^{\mathcal{I}_i}_{\widetilde{u^i}u}\,\mathbf{u}^i =& \langle\widetilde{\boldsymbol{\psi}}, \nu_1\tau^{\mathcal{I}}\boldsymbol{u}_1\rangle_{\mathcal{I}_i} + \langle\widetilde{\boldsymbol{\psi}}, \nu_2\tau^{\mathcal{I}}\boldsymbol{u}_2\rangle_{\mathcal{I}_i} + \langle\widetilde{\boldsymbol{\psi}}, \nu_1\tau^{\mathcal{I}}(\boldsymbol{u}_1\cdot\widehat{\boldsymbol{n}})\widehat{\boldsymbol{n}}\rangle_{\mathcal{I}_i} + \langle\widetilde{\boldsymbol{\psi}}, \nu_2\tau^{\mathcal{I}}(\boldsymbol{u}_2\cdot\widehat{\boldsymbol{n}})\widehat{\boldsymbol{n}}\rangle_{\mathcal{I}_i}
\end{aligned}$$

Terms in equation (4.2.5e) are written as:

$$\mathbf{A}^{\mathcal{I}_i}_{\widetilde{p^i}u}\,\mathbf{u}^i = \langle\widetilde{\phi}, \boldsymbol{u}_1\cdot\widehat{\boldsymbol{n}}\rangle_{\mathcal{I}_i} + \langle\widetilde{\phi}, \boldsymbol{u}_2\cdot(-\widehat{\boldsymbol{n}})\rangle_{\mathcal{I}_i}$$

Therefore, the discrete local problem in a cut element is written as:

(C.1.1a)
$$\left[\mathbf{A}^{K_i}_{uu} + \mathbf{A}^{\mathcal{I}_i}_{uu}\right]\,\mathbf{u}^i + \mathbf{A}^{K_i}_{uL}\,\mathbf{L}^i + \mathbf{A}^{K_i}_{up}\,\mathbf{p}^i + \mathbf{A}^{\mathcal{I}_i}_{u\widetilde{p^i}}\,\widetilde{\mathbf{p}}^i + \mathbf{A}^{\mathcal{I}_i}_{u\widetilde{u^i}}\,\widetilde{\mathbf{u}}^i = \mathbf{A}^{K_i}_{u\widehat{u}}\,\widehat{\mathbf{u}}^i + \mathbf{A}^{K_i}_{u\widehat{p}}\,\widehat{\mathbf{p}}^i + \mathbf{f}^{K_i}_u,$$

(C.1.1b)
$$\mathbf{A}^{K_i}_{Lu}\,\mathbf{u}^i + \mathbf{A}^{K_i}_{LL}\,\mathbf{L}^i + \mathbf{A}^{\mathcal{I}_i}_{L\widetilde{u^i}}\,\widetilde{\mathbf{u}}^i = \mathbf{A}^{K_i}_{L\widehat{u}}\,\widehat{\mathbf{u}}^i + \mathbf{f}^{K_i}_L,$$

(C.1.1c)
$$\mathbf{A}^{K_i}_{pu}\,\mathbf{u}^i = \mathbf{0},$$

(C.1.1d)
$$\mathbf{A}^{\mathcal{I}_i}_{\widetilde{u^i}u}\,\mathbf{u}^i + \mathbf{A}^{\mathcal{I}_i}_{\widetilde{u^i}L}\,\mathbf{L}^i + \mathbf{A}^{\mathcal{I}_i}_{\widetilde{u^i}\widetilde{p^i}}\,\widetilde{\mathbf{p}}^i + \mathbf{A}^{\mathcal{I}_i}_{\widetilde{u^i}\widetilde{u^i}}\,\widetilde{\mathbf{u}}^i = \mathbf{f}^{\mathcal{I}_i}_{\widetilde{u^i}},$$

(C.1.1e)
$$\mathbf{A}^{\mathcal{I}_i}_{\widetilde{p^i}u}\,\mathbf{u}^i = \mathbf{0}.$$

Which could be written in a matrix-vector form as:

(C.1.2)
$$\begin{bmatrix}
\left[\mathbf{A}^{K_i}_{uu} + \mathbf{A}^{\mathcal{I}_i}_{uu}\right] & \mathbf{A}^{K_i}_{uL} & \mathbf{A}^{K_i}_{up} & \mathbf{A}^{\mathcal{I}_i}_{u\widetilde{u^i}} & \mathbf{A}^{\mathcal{I}_i}_{u\widetilde{p^i}}\\
\mathbf{A}^{K_i}_{Lu} & \mathbf{A}^{K_i}_{LL} & \mathbf{0} & \mathbf{A}^{\mathcal{I}_i}_{L\widetilde{u^i}} & \mathbf{0}\\
\mathbf{A}^{K_i}_{pu} & \mathbf{0} & \mathbf{0} & \mathbf{0} & \mathbf{0}\\
\mathbf{A}^{\mathcal{I}_i}_{\widetilde{u^i}u} & \mathbf{A}^{\mathcal{I}_i}_{\widetilde{u^i}L} & \mathbf{0} & \mathbf{A}^{\mathcal{I}_i}_{\widetilde{u^i}\widetilde{u^i}} & \mathbf{0}\\
\mathbf{A}^{\mathcal{I}_i}_{\widetilde{p^i}u} & \mathbf{0} & \mathbf{0} & \mathbf{0} & \mathbf{0}
\end{bmatrix}
\begin{Bmatrix}\mathbf{u}^i\\ \mathbf{L}^i\\ \mathbf{p}^i\\ \widetilde{\mathbf{u}}^i\\ \widetilde{\mathbf{p}}^i\end{Bmatrix} =
\begin{bmatrix}\mathbf{A}^{K_i}_{u\widehat{u}}\\ \mathbf{A}^{K_i}_{L\widehat{u}}\\ \mathbf{0}\\ \mathbf{0}\\ \mathbf{0}\end{bmatrix}\widehat{\mathbf{u}}^i +
\begin{bmatrix}\mathbf{A}^{K_i}_{u\widehat{p}}\\ \mathbf{0}\\ \mathbf{0}\\ \mathbf{0}\\ \mathbf{0}\end{bmatrix}\widehat{\mathbf{p}}^i +
\begin{Bmatrix}\mathbf{f}^{K_i}_u\\ \mathbf{f}^{K_i}_L\\ \mathbf{0}\\ \mathbf{0}\\ \mathbf{0}\end{Bmatrix}$$

where the elemental variables are obtained by inverting the matrix to the left hand side (which is referred-to as $\mathbb{A}_i$)

(C.1.3)
$$\begin{Bmatrix}\mathbf{u}^i\\ \mathbf{L}^i\\ \mathbf{p}^i\\ \widetilde{\mathbf{u}}^i\\ \widetilde{\mathbf{p}}^i\end{Bmatrix} = \mathbb{A}_i^{-1}\begin{bmatrix}\mathbf{A}^{K_i}_{u\widehat{u}}\\ \mathbf{A}^{K_i}_{L\widehat{u}}\\ \mathbf{0}\\ \mathbf{0}\\ \mathbf{0}\end{bmatrix}\widehat{\mathbf{u}}^i + \mathbb{A}_i^{-1}\begin{bmatrix}\mathbf{A}^{K_i}_{u\widehat{p}}\\ \mathbf{0}\\ \mathbf{0}\\ \mathbf{0}\\ \mathbf{0}\end{bmatrix}\widehat{\mathbf{p}}^i + \mathbb{A}_i^{-1}\begin{Bmatrix}\mathbf{f}^{K_i}_u\\ \mathbf{f}^{K_i}_L\\ \mathbf{0}\\ \mathbf{0}\\ \mathbf{0}\end{Bmatrix}$$

Assume that the inverse of matrix $\mathbb{A}_i$ is written as:

$$\mathbb{A}_i^{-1} = \begin{bmatrix} [\mathrm{A}_{uu}^{K_i}]^{-1} & [\mathrm{A}_{uL}^{K_i}]^{-1} & [\mathrm{A}_{up}^{K_i}]^{-1} & [\mathrm{A}_{u\widetilde{u}^i}^{K_i}]^{-1} & [\mathrm{A}_{u\widetilde{p}^i}^{K_i}]^{-1} \\ [\mathrm{A}_{Lu}^{K_i}]^{-1} & [\mathrm{A}_{LL}^{K_i}]^{-1} & [\mathrm{A}_{Lp}^{K_i}]^{-1} & [\mathrm{A}_{L\widetilde{u}^i}^{K_i}]^{-1} & [\mathrm{A}_{L\widetilde{p}^i}^{K_i}]^{-1} \\ [\mathrm{A}_{pu}^{K_i}]^{-1} & [\mathrm{A}_{pL}^{K_i}]^{-1} & [\mathrm{A}_{pp}^{K_i}]^{-1} & [\mathrm{A}_{p\widetilde{u}^i}^{K_i}]^{-1} & [\mathrm{A}_{p\widetilde{p}^i}^{K_i}]^{-1} \\ [\mathrm{A}_{\widetilde{u}^iu}^{K_i}]^{-1} & [\mathrm{A}_{\widetilde{u}^iL}^{K_i}]^{-1} & [\mathrm{A}_{\widetilde{u}^ip}^{K_i}]^{-1} & [\mathrm{A}_{\widetilde{u}^i\widetilde{u}^i}^{K_i}]^{-1} & [\mathrm{A}_{\widetilde{u}^i\widetilde{p}^i}^{K_i}]^{-1} \\ [\mathrm{A}_{\widetilde{p}^iu}^{K_i}]^{-1} & [\mathrm{A}_{\widetilde{p}^iL}^{K_i}]^{-1} & [\mathrm{A}_{\widetilde{p}^ip}^{K_i}]^{-1} & [\mathrm{A}_{\widetilde{p}^i\widetilde{u}^i}^{K_i}]^{-1} & [\mathrm{A}_{\widetilde{p}^i\widetilde{p}^i}^{K_i}]^{-1} \end{bmatrix} \tag{C.1.4}$$

where all the matrix blocks in $\mathbb{A}_i$ are extracted from the computed inverse and not derived analytically. i.e. extracted from the output of the coded inverse.
The variables $(\mathbf{u}^i, \mathbf{L}^i, \mathbf{p}^i)$ are then extracted as:

(C.1.5)

$$\begin{Bmatrix} \mathbf{u}^i \\ \mathbf{L}^i \\ \mathbf{p}^i \end{Bmatrix} = \begin{bmatrix} [\mathrm{A}_{uu}^{K_i}]^{-1}\mathbf{A}_{u\widehat{u}}^{K_i} + [\mathrm{A}_{uL}^{K_i}]^{-1}\mathbf{A}_{L\widehat{u}}^{K_i} \\ [\mathrm{A}_{Lu}^{K_i}]^{-1}\mathbf{A}_{u\widehat{u}}^{K_i} + [\mathrm{A}_{LL}^{K_i}]^{-1}\mathbf{A}_{L\widehat{u}}^{K_i} \\ [\mathrm{A}_{pu}^{K_i}]^{-1}\mathbf{A}_{u\widehat{u}}^{K_i} + [\mathrm{A}_{pL}^{K_i}]^{-1}\mathbf{A}_{L\widehat{u}}^{K_i} \end{bmatrix} \widehat{\mathbf{u}}^i + \begin{bmatrix} [\mathrm{A}_{uu}^{K_i}]^{-1}\mathbf{A}_{up}^{K_i} \\ [\mathrm{A}_{Lu}^{K_i}]^{-1}\mathbf{A}_{up}^{K_i} \\ [\mathrm{A}_{pu}^{K_i}]^{-1}\mathbf{A}_{up}^{K_i} \end{bmatrix} \widehat{\mathbf{p}}^i + \begin{Bmatrix} [\mathrm{A}_{uu}^{K_i}]^{-1}\mathbf{f}_u^{K_i} + [\mathrm{A}_{uL}^{K_i}]^{-1}\mathbf{f}_L^{K_i} \\ [\mathrm{A}_{Lu}^{K_i}]^{-1}\mathbf{f}_u^{K_i} + [\mathrm{A}_{LL}^{K_i}]^{-1}\mathbf{f}_L^{K_i} \\ [\mathrm{A}_{pu}^{K_i}]^{-1}\mathbf{f}_u^{K_i} + [\mathrm{A}_{pL}^{K_i}]^{-1}\mathbf{f}_L^{K_i} \end{Bmatrix}$$

which is also written as:

$$\begin{Bmatrix} \mathbf{u}^i \\ \mathbf{L}^i \\ \mathbf{p}^i \end{Bmatrix} = \begin{bmatrix} \mathbf{Z}_{u\widehat{u}}^{K_i} \\ \mathbf{Z}_{L\widehat{u}}^{K_i} \\ \mathbf{Z}_{p\widehat{u}}^{K_i} \end{bmatrix} \widehat{\mathbf{u}}^i + \begin{bmatrix} \mathbf{Z}_{up}^{K_i} \\ \mathbf{Z}_{Lp}^{K_i} \\ \mathbf{Z}_{pp}^{K_i} \end{bmatrix} \widehat{\mathbf{p}}^i + \begin{Bmatrix} \mathbf{z}_u^{K_i} \\ \mathbf{z}_L^{K_i} \\ \mathbf{z}_p^{K_i} \end{Bmatrix} \tag{C.1.6}$$

which is further simplified to:

$$\begin{Bmatrix} \mathbf{u}^i \\ \mathbf{L}^i \\ \mathbf{p}^i \end{Bmatrix} = \mathbf{Z}_{\widehat{u}}^{K_i}\,\widehat{\mathbf{u}}^i + \mathbf{Z}_{\widehat{p}}^{K_i}\,\widehat{\mathbf{p}}^i + \mathbf{z}^{K_i} \tag{C.1.7}$$

C.2 Discrete local problems in standard elements

Terms in equation (4.2.6a) are written as:

$$\begin{aligned}
\mathbf{A}_{uu}^{K_i}\,\mathbf{u}^i &= \langle \boldsymbol{\psi}, \nu\tau\boldsymbol{u}\rangle_{\partial K_i} + \langle \boldsymbol{\psi}, \nu\tau(\boldsymbol{u}\cdot\boldsymbol{n})\boldsymbol{n}\rangle_{\partial K_i} \\
\mathbf{A}_{uL}^{K_i}\,\mathbf{L}^i &= (\boldsymbol{\psi}, \boldsymbol{\nabla}\cdot(\nu\boldsymbol{L}))_{K_i} \\
\mathbf{A}_{up}^{K_i}\,\mathbf{p}^i &= -\,(\boldsymbol{\nabla}\boldsymbol{\psi}, P\boldsymbol{I})_{K_i} \\
\mathbf{f}_u^{K_i} &= (\boldsymbol{\psi}, \boldsymbol{f})_{K_i} + \langle \boldsymbol{\psi}, \nu\tau\boldsymbol{u}_D\rangle_{\partial K_i\cap\Gamma_D} + \langle \boldsymbol{\psi}, \nu\tau(\boldsymbol{u}_D\cdot\boldsymbol{n})\boldsymbol{n}\rangle_{\partial K_i\cap\Gamma_D} - \langle \boldsymbol{\psi}, P_N\boldsymbol{n}\rangle_{\partial K_i\cap\Gamma_N} \\
\mathbf{A}_{u\widehat{u}}^{K_i}\,\widehat{\mathbf{u}}^i &= \langle \boldsymbol{\psi}, \nu\tau\widehat{\boldsymbol{u}}\rangle_{\partial K_i\setminus\Gamma_D} + \langle \boldsymbol{\psi}, \nu\tau(\widehat{\boldsymbol{u}}\cdot\boldsymbol{n})\boldsymbol{n}\rangle_{\partial K_i\setminus\Gamma_D} \\
\mathbf{A}_{up}^{K_i}\,\widehat{\mathbf{p}}^i &= -\,\langle \boldsymbol{\psi}, \widehat{P}\boldsymbol{n}\rangle_{\partial K_i\setminus\Gamma_N}
\end{aligned}$$

Terms in equation (4.2.6b) are written as:

$$\begin{aligned}
\mathbf{A}_{LL}^{K_i}\,\mathbf{L}^i &= -(\boldsymbol{\Psi},\boldsymbol{L})_{K_i}\\
\mathbf{A}_{Lu}^{K_i}\,\mathbf{u}^i &= (\boldsymbol{\nabla}^s\cdot\boldsymbol{\Psi},\boldsymbol{u})_{K_i}\\
\mathbf{A}_{L\widehat{u}}^{K_i}\,\widehat{\mathbf{u}}^i &= \langle\boldsymbol{\Psi},\widehat{\boldsymbol{u}}\otimes\boldsymbol{n}\rangle_{\partial K_i\setminus\Gamma_D} + \langle\boldsymbol{\Psi},\boldsymbol{n}\otimes\widehat{\boldsymbol{u}}\rangle_{\partial K_i\setminus\Gamma_D}\\
\mathbf{f}_L^{K_i} &= \langle\boldsymbol{\Psi},\boldsymbol{u}_D\otimes\boldsymbol{n}\rangle_{\partial K_i\cap\Gamma_D} + \langle\boldsymbol{\Psi},\boldsymbol{n}\otimes\boldsymbol{u}_D\rangle_{\partial K_i\cap\Gamma_D}
\end{aligned}$$

Terms in equation (4.2.6c) are written as:

$$\mathbf{A}_{pu}^{K_i}\,\mathbf{u}^i = -(\phi,\boldsymbol{\nabla}\cdot\boldsymbol{u})_{K_i}$$

Therefore, the discrete local problem in a standard element is written as:

$$\mathbf{A}_{uu}^{K_i}\,\mathbf{u}^i + \mathbf{A}_{uL}^{K_i}\,\mathbf{L}^i + \mathbf{A}_{up}^{K_i}\,\mathbf{p}^i = \mathbf{A}_{u\widehat{u}}^{K_i}\,\widehat{\mathbf{u}}^i + \mathbf{A}_{u\widehat{p}}^{K_i}\,\widehat{\mathbf{p}}^i + \mathbf{f}_u^{K_i} + \mathbf{r}_u^{K_i}(\mathbf{u}^i), \tag{C.2.1a}$$

$$\mathbf{A}_{Lu}^{K_i}\,\mathbf{u}^i + \mathbf{A}_{LL}^{K_i}\,\mathbf{L}^i = \mathbf{A}_{L\widehat{u}}^{K_i}\,\widehat{\mathbf{u}}^i + \mathbf{f}_L^{K_i}, \tag{C.2.1b}$$

$$\mathbf{A}_{pu}^{K_i}\,\mathbf{u}^i = \mathbf{0} \tag{C.2.1c}$$

which is then written in matrix-vector form as

$$\begin{bmatrix}\mathbf{A}_{uu}^{K_i} & \mathbf{A}_{uL}^{K_i} & \mathbf{A}_{up}^{K_i}\\ \mathbf{A}_{Lu}^{K_i} & \mathbf{A}_{LL}^{K_i} & \mathbf{0}\\ \mathbf{A}_{pu}^{K_i} & \mathbf{0} & \mathbf{0}\end{bmatrix}\begin{Bmatrix}\mathbf{u}^i\\ \mathbf{L}^i\\ \mathbf{p}^i\end{Bmatrix} = \begin{bmatrix}\mathbf{A}_{u\widehat{u}}^{K_i}\\ \mathbf{A}_{L\widehat{u}}^{K_i}\\ \mathbf{0}\end{bmatrix}\widehat{\mathbf{u}}^i + \begin{bmatrix}\mathbf{A}_{u\widehat{p}}^{K_i}\\ \mathbf{0}\\ \mathbf{0}\end{bmatrix}\widehat{\mathbf{p}}^i + \begin{Bmatrix}\mathbf{f}_u^{K_i}\\ \mathbf{f}_L^{K_i}\\ \mathbf{0}\end{Bmatrix} \tag{C.2.2}$$

where the elemental variables are obtained by inverting the matrix to the left hand side (which is referred-to as $\mathbb{A}_i$)

$$\begin{Bmatrix}\mathbf{u}^i\\ \mathbf{L}^i\\ \mathbf{p}^i\end{Bmatrix} = \mathbb{A}_i^{-1}\begin{bmatrix}\mathbf{A}_{u\widehat{u}}^{K_i}\\ \mathbf{A}_{L\widehat{u}}^{K_i}\\ \mathbf{0}\end{bmatrix}\widehat{\mathbf{u}}^i + \mathbb{A}_i^{-1}\begin{bmatrix}\mathbf{A}_{u\widehat{p}}^{K_i}\\ \mathbf{0}\\ \mathbf{0}\end{bmatrix}\widehat{\mathbf{p}}^i + \mathbb{A}_i^{-1}\begin{Bmatrix}\mathbf{f}_u^{K_i}\\ \mathbf{f}_L^{K_i}\\ \mathbf{0}\end{Bmatrix} \tag{C.2.3}$$

Assume that the inverse of matrix $\mathbb{A}_i$ is written as:

$$\mathbb{A}_i^{-1} = \begin{bmatrix}[\mathrm{A}_{uu}^{K_i}]^{-1} & [\mathrm{A}_{uL}^{K_i}]^{-1} & [\mathrm{A}_{up}^{K_i}]^{-1}\\ [\mathrm{A}_{Lu}^{K_i}]^{-1} & [\mathrm{A}_{LL}^{K_i}]^{-1} & [\mathrm{A}_{Lp}^{K_i}]^{-1}\\ [\mathrm{A}_{pu}^{K_i}]^{-1} & [\mathrm{A}_{pL}^{K_i}]^{-1} & [\mathrm{A}_{pp}^{K_i}]^{-1}\end{bmatrix} \tag{C.2.4}$$

The variables $(\mathbf{u}^i,\mathbf{L}^i,\mathbf{p}^i)$ are written as:

(C.2.5)

$$\begin{Bmatrix}\mathbf{u}^i\\ \mathbf{L}^i\\ \mathbf{p}^i\end{Bmatrix} = \begin{bmatrix}[\mathrm{A}_{uu}^{K_i}]^{-1}\mathbf{A}_{u\widehat{u}}^{K_i} + [\mathrm{A}_{uL}^{K_i}]^{-1}\mathbf{A}_{L\widehat{u}}^{K_i}\\ [\mathrm{A}_{Lu}^{K_i}]^{-1}\mathbf{A}_{u\widehat{u}}^{K_i} + [\mathrm{A}_{LL}^{K_i}]^{-1}\mathbf{A}_{L\widehat{u}}^{K_i}\\ [\mathrm{A}_{pu}^{K_i}]^{-1}\mathbf{A}_{u\widehat{u}}^{K_i} + [\mathrm{A}_{pL}^{K_i}]^{-1}\mathbf{A}_{L\widehat{u}}^{K_i}\end{bmatrix}\widehat{\mathbf{u}}^i + \begin{bmatrix}[\mathrm{A}_{uu}^{K_i}]^{-1}\mathbf{A}_{u\widehat{p}}^{K_i}\\ [\mathrm{A}_{Lu}^{K_i}]^{-1}\mathbf{A}_{u\widehat{p}}^{K_i}\\ [\mathrm{A}_{pu}^{K_i}]^{-1}\mathbf{A}_{u\widehat{p}}^{K_i}\end{bmatrix}\widehat{\mathbf{p}}^i + \begin{Bmatrix}[\mathrm{A}_{uu}^{K_i}]^{-1}\mathbf{f}_u^{K_i} + [\mathrm{A}_{uL}^{K_i}]^{-1}\mathbf{f}_L^{K_i}\\ [\mathrm{A}_{Lu}^{K_i}]^{-1}\mathbf{f}_u^{K_i} + [\mathrm{A}_{LL}^{K_i}]^{-1}\mathbf{f}_L^{K_i}\\ [\mathrm{A}_{pu}^{K_i}]^{-1}\mathbf{f}_u^{K_i} + [\mathrm{A}_{pL}^{K_i}]^{-1}\mathbf{f}_L^{K_i}\end{Bmatrix}$$

which is also written as:

$$\begin{Bmatrix} \mathbf{u}^i \\ \mathbf{L}^i \\ \mathbf{p}^i \end{Bmatrix} = \begin{bmatrix} \mathbf{Z}_{u\widehat{u}}^{K_i} \\ \mathbf{Z}_{L\widehat{u}}^{K_i} \\ \mathbf{Z}_{p\widehat{u}}^{K_i} \end{bmatrix} \widehat{\mathbf{u}}^i + \begin{bmatrix} \mathbf{Z}_{u\widehat{p}}^{K_i} \\ \mathbf{Z}_{L\widehat{p}}^{K_i} \\ \mathbf{Z}_{p\widehat{p}}^{K_i} \end{bmatrix} \widehat{\mathbf{p}}^i + \begin{Bmatrix} \mathbf{z}_u^{K_i} \\ \mathbf{z}_L^{K_i} \\ \mathbf{z}_p^{K_i} \end{Bmatrix} \tag{C.2.6}$$

which is further simplified to:

$$\begin{Bmatrix} \mathbf{u}^i \\ \mathbf{L}^i \\ \mathbf{p}^i \end{Bmatrix} = \mathbf{Z}_{\widehat{u}}^{K_i}\, \widehat{\mathbf{u}}^i + \mathbf{Z}_{\widehat{p}}^{K_i}\, \widehat{\mathbf{p}}^i + \mathbf{z}^{K_i} \tag{C.2.7}$$

C.3 Discrete global problem

Terms in equation (4.2.7a) are written as:

$$\begin{aligned}
\mathbf{A}_{\widehat{up}}^{K_i}\, \widehat{\mathbf{p}}^i &= \langle \widehat{\boldsymbol{\psi}}, \widehat{P}\boldsymbol{n} \rangle_{\partial K_i \setminus \partial\Omega} \\
\mathbf{A}_{\widehat{uL}}^{K_i}\, \mathbf{L}^i &= \langle \widehat{\boldsymbol{\psi}}, \nu \boldsymbol{L}\boldsymbol{n} \rangle_{\partial K_i \setminus \Gamma_D} \\
\mathbf{A}_{\widehat{uu}}^{K_i}\, \mathbf{u}^i &= \langle \widehat{\boldsymbol{\psi}}, \nu\tau \boldsymbol{u} \rangle_{\partial K_i \setminus \Gamma_D} + \langle \widehat{\boldsymbol{\psi}}, \nu\tau(\boldsymbol{u}\cdot\boldsymbol{n})\boldsymbol{n} \rangle_{\partial K_i \setminus \Gamma_D} \\
\mathbf{A}_{\widehat{uu}}^{K_i}\, \widehat{\mathbf{u}}^i &= -\langle \widehat{\boldsymbol{\psi}}, \nu\tau \widehat{\boldsymbol{u}} \rangle_{\partial K_i \setminus \Gamma_D} - \langle \widehat{\boldsymbol{\psi}}, \nu\tau(\widehat{\boldsymbol{u}}\cdot\boldsymbol{n})\boldsymbol{n} \rangle_{\partial K_i \setminus \Gamma_D} \\
\mathbf{f}_{\widehat{u}}^{K_i} &= \langle \widehat{\boldsymbol{\psi}}, \boldsymbol{g}_N \rangle_{\partial K_i \cap \Gamma_N} - \langle \widehat{\boldsymbol{\psi}}, P_N \boldsymbol{n} \rangle_{\partial K_i \cap \Gamma_N}
\end{aligned}$$

Terms in equation (4.2.7b) are written as:

$$\begin{aligned}
\mathbf{A}_{\widehat{pu}}^{K_i}\, \mathbf{u}^i &= \langle \widehat{\phi}, \boldsymbol{u}\cdot\boldsymbol{n} \rangle_{\partial K_i} \\
\mathbf{A}_{\widehat{pu}}^{K_i}\, \widehat{\mathbf{u}}^i &= -\langle \widehat{\phi}, \widehat{\boldsymbol{u}}\cdot\boldsymbol{n} \rangle_{\partial K_i \cap \Gamma_N} \\
\mathbf{f}_{\widehat{p}}^{K_i} &= \langle \widehat{\phi}, \boldsymbol{u}_D\cdot\boldsymbol{n} \rangle_{\partial K_i \cap \Gamma_D}
\end{aligned}$$

Therefore, the discrete global problem is written as:

$$\sum_{i=1}^{\mathtt{n_{el}}} \Big\{ \mathbf{A}_{\widehat{uu}}^{K_i}\, \mathbf{u}^i + \mathbf{A}_{\widehat{uL}}^{K_i}\, \mathbf{L}^i + \mathbf{A}_{\widehat{uu}}^{K_i}\, \widehat{\mathbf{u}}^i + \mathbf{A}_{\widehat{up}}^{K_i}\, \widehat{\mathbf{p}}^i \Big\} = \sum_{i=1}^{\mathtt{n_{el}}} \mathbf{f}_{\widehat{u}}^{K_i} \tag{C.3.1a}$$

$$\sum_{i=1}^{\mathtt{n_{el}}} \{ \mathbf{A}_{\widehat{pu}}^{K_i}\, \mathbf{u}^i + \mathbf{A}_{\widehat{pu}}^{K_i}\, \widehat{\mathbf{u}}^i \} = \sum_{i=1}^{\mathtt{n_{el}}} \mathbf{f}_{\widehat{p}}^{K_i} \tag{C.3.1b}$$

By inserting the solutions $(\mathbf{u}^i, \mathbf{L}^i)$ from the local problem, (C.1.7) or (C.2.7), into (C.3.1a), and the solution $(\mathbf{u}^i)$ into (C.3.1b), we get

$$\begin{aligned}
\sum_{i=1}^{\mathtt{n_{el}}} \Big\{ & \mathbf{A}_{\widehat{uu}}^{K_i}\, \mathbf{Z}_{u\widehat{u}}^{K_i}\, \widehat{\mathbf{u}}^i + \mathbf{A}_{\widehat{uu}}^{K_i}\, \mathbf{Z}_{u\widehat{p}}^{K_i}\, \widehat{\mathbf{p}}^i + \mathbf{A}_{\widehat{uu}}^{K_i}\, \mathbf{z}_u^{K_i} + \mathbf{A}_{\widehat{uL}}^{K_i}\, \mathbf{Z}_{L\widehat{u}}^{K_i}\, \widehat{\mathbf{u}}^i + \mathbf{A}_{\widehat{uL}}^{K_i}\, \mathbf{Z}_{L\widehat{p}}^{K_i}\, \widehat{\mathbf{p}}^i \\
& + \mathbf{A}_{\widehat{uL}}^{K_i}\, \mathbf{z}_L^{K_i} + \mathbf{A}_{\widehat{uu}}^{K_i}\, \widehat{\mathbf{u}}^i + \mathbf{A}_{\widehat{up}}^{K_i}\, \widehat{\mathbf{p}}^i \Big\} = \sum_{i=1}^{\mathtt{n_{el}}} \mathbf{f}_{\widehat{u}}^{K_i}
\end{aligned} \tag{C.3.2a}$$

$$\sum_{i=1}^{\mathtt{n_{el}}}\{\mathbf{A}_{\widehat{pu}}^{K_i}\,\mathbf{Z}_{u\widehat{u}}^{K_i}\,\widehat{\mathbf{u}}^i+\mathbf{A}_{\widehat{pu}}^{K_i}\,\mathbf{Z}_{u\widehat{p}}^{K_i}\,\widehat{\mathbf{p}}^i+\mathbf{A}_{\widehat{pu}}^{K_i}\,\mathbf{z}_u^{K_i}+\mathbf{A}_{\widetilde{pu}}^{K_i}\,\widehat{\mathbf{u}}^i\}=\sum_{i=1}^{\mathtt{n_{el}}}\mathbf{f}_{\widehat{p}}^{K_i} \tag{C.3.2b}$$

Finally, the full global problem is written in a matrix-vector form as:

$$\begin{aligned}\mathbf{A}_{i=1}^{\mathtt{n_{el}}}&\begin{bmatrix}\left[\mathbf{A}_{\widehat{uu}}^{K_i}\,\mathbf{Z}_{u\widehat{u}}^{K_i}+\mathbf{A}_{\widehat{uL}}^{K_i}\,\mathbf{Z}_{L\widehat{u}}^{K_i}+\mathbf{A}_{\widetilde{uu}}^{K_i}\right] & \left[\mathbf{A}_{\widehat{uu}}^{K_i}\,\mathbf{Z}_{u\widehat{p}}^{K_i}+\mathbf{A}_{\widehat{uL}}^{K_i}\,\mathbf{Z}_{L\widehat{p}}^{K_i}+\mathbf{A}_{\widetilde{up}}^{K_i}\right]\\ \left[\mathbf{A}_{\widehat{pu}}^{K_i}\,\mathbf{Z}_{u\widehat{u}}^{K_i}+\mathbf{A}_{\widetilde{pu}}^{K_i}\right] & \left[\mathbf{A}_{\widehat{pu}}^{K_i}\,\mathbf{Z}_{u\widehat{p}}^{K_i}\right]\end{bmatrix}\begin{Bmatrix}\widehat{\mathbf{u}}^i\\ \widehat{\mathbf{p}}^i\end{Bmatrix}\\ &=\mathbf{A}_{i=1}^{\mathtt{n_{el}}}\begin{Bmatrix}\mathbf{f}_{\widehat{u}}^{K_i}-\mathbf{A}_{\widehat{uu}}^{K_i}\,\mathbf{z}_u^{K_i}-\mathbf{A}_{\widehat{uL}}^{K_i}\,\mathbf{z}_L^{K_i}\\ \mathbf{f}_{\widehat{p}}^{K_i}-\mathbf{A}_{\widehat{pu}}^{K_i}\,\mathbf{z}_u^{K_i}\end{Bmatrix}\end{aligned} \tag{C.3.3}$$

which is written in simplified notation as

$$\mathbf{A}_{i=1}^{\mathtt{n_{el}}}\widehat{\mathbf{K}}^i\begin{Bmatrix}\widehat{\mathbf{u}}^i\\ \widehat{\mathbf{p}}^i\end{Bmatrix}=\mathbf{A}_{i=1}^{\mathtt{n_{el}}}\widehat{\mathbf{f}}^i \tag{C.3.4}$$

where $\mathbf{A}_{i=1}^{\mathtt{n_{el}}}$ denotes the assembly of all the finite element matrices/vectors into a global matrix/vector. Simplifying furthermore yields the global system of equations which is written as

$$\widehat{\mathbf{K}}\begin{Bmatrix}\widehat{\mathbf{u}}\\ \widehat{\mathbf{p}}\end{Bmatrix}=\widehat{\mathbf{f}} \tag{C.3.5}$$

Appendix D

Derivation of X-HDG weak forms for two-phase incompressible Navier-Stokes problem

D.1 Weak local problems in cut elements

In the derivation of the weak forms for a cut element, a generic element K_i which is cut by the interface $\mathcal{I}$ is considered. This element is divided into two sub-volumes; $K_i \cap \Omega_1$ and $K_i \cap \Omega_2$ as shown in Figure D.1. Recall also remark 1.

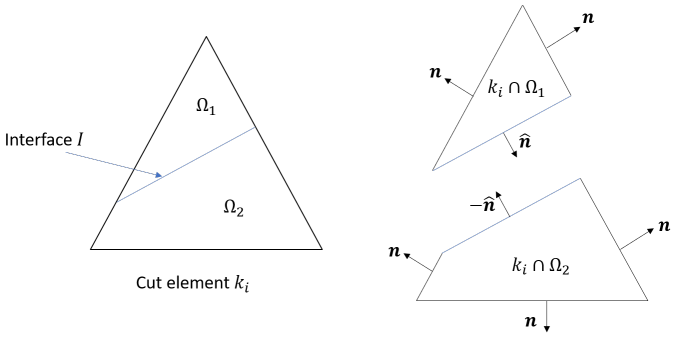

Figure D.1: A schematic of a generic cut element.

Note that in a cut element, the approximations of the functions $(\boldsymbol{u}, \boldsymbol{L}, p)$ are discontinuous. i.e. $\boldsymbol{u} \in [\mathcal{P}^m(K_i)]^d \oplus H[\mathcal{P}^m(K_i)]^d$, $\boldsymbol{L} \in [\mathcal{P}^m(K_i)]^{d\times d} \oplus H[\mathcal{P}^m(K_i)]^{d\times d}$ and $p \in \boldsymbol{\nabla}\cdot[\mathcal{P}^m(K_i)]^d \oplus H\boldsymbol{\nabla}\cdot[\mathcal{P}^m(K_i)]^d$.

In an abuse of notations, all the approximated functions that should have a subscript (h) will be denoted without the subscript for simplicity.

To obtain the weak form of the *first* equation (equation of $\boldsymbol{u}$) in the local problems (6.2.3b), we go through the following steps:

Step 1: the governing equation is multiplied by a discontinuous vector test function $\boldsymbol{\psi} \in [\mathcal{P}^m(K_i)]^d \oplus H[\mathcal{P}^m(K_i)]^d$, and integrated over the two subdomains of the element K_i

$$
\begin{aligned}
(\boldsymbol{\psi}, \rho\frac{\partial \boldsymbol{u}}{\partial t})_{K_i} + (\boldsymbol{\psi}_1, \boldsymbol{\nabla}\cdot(\rho_1(\boldsymbol{u}_1\otimes\boldsymbol{u}_1) + p_1\boldsymbol{I} + \mu_1\boldsymbol{L}_1))_{K_i\cap\Omega_1} \\
+ (\boldsymbol{\psi}_2, \boldsymbol{\nabla}\cdot(\rho_2(\boldsymbol{u}_2\otimes\boldsymbol{u}_2) + p_2\boldsymbol{I} + \mu_2\boldsymbol{L}_2))_{K_i\cap\Omega_2} = (\boldsymbol{\psi}, \rho\boldsymbol{f})_{K_i}
\end{aligned}
\tag{D.1.1}
$$

Step 2: Green's theorem (integration by parts) is applied to incorporate surface integrals

(D.1.2)

$$
\begin{aligned}
&\left(\boldsymbol{\psi}, \rho\frac{\partial \boldsymbol{u}}{\partial t}\right)_{K_i} \\
&-\left(\boldsymbol{\nabla}\boldsymbol{\psi}_1, \rho_1(\boldsymbol{u}_1\otimes\boldsymbol{u}_1) + p_1\boldsymbol{I} + \mu_1\boldsymbol{L}_1\right)_{K_i\cap\Omega_1} + \left\langle \boldsymbol{\psi}_1, \left(\rho_1(\boldsymbol{u}_1\otimes\boldsymbol{u}_1) + p_1\boldsymbol{I} + \mu_1\boldsymbol{L}_1\right)\boldsymbol{n}\right\rangle_{(\partial K_i\cap\Omega_1)\setminus\Gamma_D} \\
&+\left\langle \boldsymbol{\psi}_1, \left(\rho_1(\boldsymbol{u}_1\otimes\boldsymbol{u}_1) + p_1\boldsymbol{I} + \mu_1\boldsymbol{L}_1\right)\boldsymbol{n}\right\rangle_{(\partial K_i\cap\Omega_1)\cap\Gamma_D} + \left\langle \boldsymbol{\psi}_1, \left(\rho_1(\boldsymbol{u}_1\otimes\boldsymbol{u}_1) + p_1\boldsymbol{I} + \mu_1\boldsymbol{L}_1\right)\widehat{\boldsymbol{n}}\right\rangle_{\mathcal{I}_i} \\
&-\left(\boldsymbol{\nabla}\boldsymbol{\psi}_2, \rho_2(\boldsymbol{u}_2\otimes\boldsymbol{u}_2) + p_2\boldsymbol{I} + \mu_2\boldsymbol{L}_2\right)_{K_i\cap\Omega_2} + \left\langle \boldsymbol{\psi}_2, \left(\rho_2(\boldsymbol{u}_2\otimes\boldsymbol{u}_2) + p_2\boldsymbol{I} + \mu_2\boldsymbol{L}_2\right)\boldsymbol{n}\right\rangle_{(\partial K_i\cap\Omega_2)\setminus\Gamma_D} \\
&+\left\langle \boldsymbol{\psi}_2, \left(\rho_2(\boldsymbol{u}_2\otimes\boldsymbol{u}_2) + p_2\boldsymbol{I} + \mu_2\boldsymbol{L}_2\right)\boldsymbol{n}\right\rangle_{(\partial K_i\cap\Omega_2)\cap\Gamma_D} + \left\langle \boldsymbol{\psi}_2, \left(\rho_2(\boldsymbol{u}_2\otimes\boldsymbol{u}_2) + p_2\boldsymbol{I} + \mu_2\boldsymbol{L}_2\right)(-\widehat{\boldsymbol{n}})\right\rangle_{\mathcal{I}_i} \\
&=\left(\boldsymbol{\psi}, \rho\boldsymbol{f}\right)_{K_i}
\end{aligned}
$$

where we get surface integrals over the element boundary ∂K_i and the interface $\mathcal{I}_i$. Note that some terms could be combined and the equation could be written as

(D.1.3)

$$
\begin{aligned}
\left(\boldsymbol{\psi}, \rho\frac{\partial \boldsymbol{u}}{\partial t}\right)_{K_i} &- \left(\boldsymbol{\nabla}\boldsymbol{\psi}, \rho(\boldsymbol{u}\otimes\boldsymbol{u}) + p\boldsymbol{I} + \mu\boldsymbol{L}\right)_{K_i} + \left\langle \boldsymbol{\psi}, \left(\rho(\boldsymbol{u}\otimes\boldsymbol{u}) + p\boldsymbol{I} + \mu\boldsymbol{L}\right)\boldsymbol{n}\right\rangle_{\partial K_i\setminus\Gamma_D} \\
&+ \left\langle \boldsymbol{\psi}, \left(\rho(\boldsymbol{u}\otimes\boldsymbol{u}) + p\boldsymbol{I} + \mu\boldsymbol{L}\right)\boldsymbol{n}\right\rangle_{\partial K_i\cap\Gamma_D} \\
&+ \left\langle \boldsymbol{\psi}_1, \left(\rho_1(\boldsymbol{u}_1\otimes\boldsymbol{u}_1) + p_1\boldsymbol{I} + \mu_1\boldsymbol{L}_1\right)\widehat{\boldsymbol{n}}\right\rangle_{\mathcal{I}_i} + \left\langle \boldsymbol{\psi}_2, \left(\rho_2(\boldsymbol{u}_2\otimes\boldsymbol{u}_2) + p_2\boldsymbol{I} + \mu_2\boldsymbol{L}_2\right)(-\widehat{\boldsymbol{n}})\right\rangle_{\mathcal{I}_i} \\
&= \left(\boldsymbol{\psi}, \rho\boldsymbol{f}\right)_{K_i}
\end{aligned}
$$

Step 3: In the HDG method, the physical quantities $((\boldsymbol{u}\otimes\boldsymbol{u}), \boldsymbol{L}, p)$ are replaced by the numerical quantities $(\widehat{(\boldsymbol{u}\otimes\boldsymbol{u})}, \widehat{\boldsymbol{L}}, \widehat{p})$. Further, on the interface $\mathcal{I}_i$, the physical quantities $((\boldsymbol{u}\otimes\boldsymbol{u}), \boldsymbol{L}_1, \boldsymbol{L}_2, p_1, p_2)$ are replaced by the numerical quantities $(\widetilde{(\boldsymbol{u}\otimes\boldsymbol{u})}^{\,i}, \widetilde{\boldsymbol{L}}_1^i + \boldsymbol{\delta}_{\boldsymbol{L}}, \widetilde{\boldsymbol{L}}_2^i, \widetilde{p}^i + \delta_p, \widetilde{p}^i)$. Furthermore, on the intersection with the Dirichlet boundary $\partial K_i\cap\Gamma_D$, the physical quantities $((\boldsymbol{u}\otimes\boldsymbol{u}), \boldsymbol{L}, p)$ are replaced by $(\widehat{(\boldsymbol{u}\otimes\boldsymbol{u})}_D, \widehat{\boldsymbol{L}}_D, \widehat{p})$. Finally, that pressure trace $\widehat{p}$ is replaced by p_N on the Neumann boundary $\partial K_i\setminus\Gamma_N$:

(D.1.4)

$$
\begin{aligned}
\left(\boldsymbol{\psi}, \rho\frac{\partial \boldsymbol{u}}{\partial t}\right)_{K_i} &- \left(\boldsymbol{\nabla}\boldsymbol{\psi}, \rho(\boldsymbol{u}\otimes\boldsymbol{u}) + p\boldsymbol{I} + \mu\boldsymbol{L}\right)_{K_i} + \left\langle \boldsymbol{\psi}, \left(\rho\widehat{(\boldsymbol{u}\otimes\boldsymbol{u})} + \widehat{p}\boldsymbol{I} + \mu\widehat{\boldsymbol{L}}\right)\boldsymbol{n}\right\rangle_{\partial K_i\setminus\Gamma_D} \\
&+ \left\langle \boldsymbol{\psi}, \left(\rho\widehat{(\boldsymbol{u}\otimes\boldsymbol{u})}_D + \widehat{p}\boldsymbol{I} + \mu\widehat{\boldsymbol{L}}_D\right)\boldsymbol{n}\right\rangle_{\partial K_i\cap\Gamma_D} \\
&+ \left\langle \boldsymbol{\psi}_1, \left(\rho_1\widetilde{(\boldsymbol{u}_1\otimes\boldsymbol{u}_1)}^{\,i} + (\widetilde{p}^i + \delta_P)\boldsymbol{I} + \mu_1(\widetilde{\boldsymbol{L}}_1^i + \boldsymbol{\delta}_{\boldsymbol{L}})\right)\widehat{\boldsymbol{n}}\right\rangle_{\mathcal{I}_i} \\
&+ \left\langle \boldsymbol{\psi}_2, \left(\rho_2\widetilde{(\boldsymbol{u}_2\otimes\boldsymbol{u}_2)}^{\,i} + \widetilde{p}^i\boldsymbol{I} + \mu_2\widetilde{\boldsymbol{L}}_2^i\right)(-\widehat{\boldsymbol{n}})\right\rangle_{\mathcal{I}_i} \\
&= \left(\boldsymbol{\psi}, \rho\boldsymbol{f}\right)_{K_i}
\end{aligned}
$$

where the numerical quantities are defined as

(D.1.5a)
$$\widehat{\boldsymbol{L}} := \boldsymbol{L} + \tau(\boldsymbol{u} - \widehat{\boldsymbol{u}}) \otimes \boldsymbol{n} + \tau \boldsymbol{n} \otimes (\boldsymbol{u} - \widehat{\boldsymbol{u}}),$$
(D.1.5b)
$$\widehat{\boldsymbol{L}}^D := \boldsymbol{L} + \tau(\boldsymbol{u} - \boldsymbol{u}_D) \otimes \boldsymbol{n} + \tau \boldsymbol{n} \otimes (\boldsymbol{u} - \boldsymbol{u}_D),$$
(D.1.5c)
$$\widetilde{\boldsymbol{L}}_1^i := \boldsymbol{L}_1 + \tau^{\mathcal{I}}(\boldsymbol{u}_1 - \widetilde{\boldsymbol{u}}^i) \otimes \widehat{\boldsymbol{n}} + \tau^{\mathcal{I}} \widehat{\boldsymbol{n}} \otimes (\boldsymbol{u}_1 - \widetilde{\boldsymbol{u}}^i),$$
(D.1.5d)
$$\widetilde{\boldsymbol{L}}_2^i := \boldsymbol{L}_2 + \tau^{\mathcal{I}}(\boldsymbol{u}_2 - \widetilde{\boldsymbol{u}}^i) \otimes (-\widehat{\boldsymbol{n}}) + \tau^{\mathcal{I}}(-\widehat{\boldsymbol{n}}) \otimes (\boldsymbol{u}_2 - \widetilde{\boldsymbol{u}}^i),$$
(D.1.5e)
$$\widehat{(\boldsymbol{u} \otimes \boldsymbol{u})} := (\boldsymbol{u} \otimes \boldsymbol{u}) + (\widehat{\boldsymbol{u}} - \boldsymbol{u}) \otimes \lambda \boldsymbol{u}, (\lambda = 0 \text{ if } \boldsymbol{u} \cdot \boldsymbol{n} > 0, \lambda = 1 \text{ if } \boldsymbol{u} \cdot \boldsymbol{n} < 0)$$
(D.1.5f)
$$\widehat{(\boldsymbol{u} \otimes \boldsymbol{u})}_D := (\boldsymbol{u} \otimes \boldsymbol{u}) + (\boldsymbol{u}_D - \boldsymbol{u}) \otimes \lambda \boldsymbol{u}, (\lambda = 0 \text{ if } \boldsymbol{u} \cdot \boldsymbol{n} > 0, \lambda = 1 \text{ if } \boldsymbol{u} \cdot \boldsymbol{n} < 0)$$
(D.1.5g)
$$\widetilde{(\boldsymbol{u}_1 \otimes \boldsymbol{u}_1)}^i := (\boldsymbol{u}_1 \otimes \boldsymbol{u}_1) + (\widetilde{\boldsymbol{u}}^i - \boldsymbol{u}_1) \otimes \lambda \boldsymbol{u}_1, (\lambda = 0 \text{ if } \boldsymbol{u}_1 \cdot \widehat{\boldsymbol{n}} > 0, \lambda = 1 \text{ if } \boldsymbol{u}_1 \cdot \widehat{\boldsymbol{n}} < 0)$$
(D.1.5h)
$$\widetilde{(\boldsymbol{u}_2 \otimes \boldsymbol{u}_2)}^i := (\boldsymbol{u}_2 \otimes \boldsymbol{u}_2) + (\widetilde{\boldsymbol{u}}^i - \boldsymbol{u}_2) \otimes \lambda \boldsymbol{u}_2, (\lambda = 0 \text{ if } \boldsymbol{u}_2 \cdot (-\widehat{\boldsymbol{n}}) > 0, \lambda = 1 \text{ if } \boldsymbol{u}_2 \cdot (-\widehat{\boldsymbol{n}}) < 0)$$

where $\widehat{\boldsymbol{u}} \in \mathcal{V}_s^h(\Gamma_{ij})$ and $\widehat{p} \in \mathcal{S}_s^h(\Gamma_{ij})$ could be continuous (if $\Gamma_{ij} \cap \mathcal{I} = \emptyset$) or discontinuous (if $\Gamma_{ij} \cap \mathcal{I} \neq \emptyset$) functions. Γ_{ij} is face j of element K_i. $\widetilde{\boldsymbol{u}}^i \in [\mathcal{P}^m(\mathcal{I}_i)]^d$ is a continuous vector function defined on the interface $\mathcal{I}$. $\widetilde{p}^i \in \mathcal{P}^m(\mathcal{I}_i)$ is a continuous scalar function defined on the interface $\mathcal{I}$. τ and $\tau^{\mathcal{I}}$ are stabilization parameters for the viscous flux on the element faces ∂K_i and the material interface $\mathcal{I}_i$, respectively. The choice of the stabilization parameter τ is discussed extensively in [59]. The interface stabilization parameter has to be inversely proportional to the average of μ to ensure optimal convergence, for instance $\tau^{\mathcal{I}} := 1/\{\mu\}$.

Note that the jump conditions in p and L were introduced by the variables δ_p and $\boldsymbol{\delta}_{\boldsymbol{L}}$.

By introducing the definitions of the numerical fluxes into D.1.4, we get:
(D.1.6)
$$\begin{aligned}
&(\boldsymbol{\psi}, \rho \frac{\partial \boldsymbol{u}}{\partial t})_{K_i} - (\boldsymbol{\nabla}\boldsymbol{\psi}, \rho(\boldsymbol{u} \otimes \boldsymbol{u}) + p\boldsymbol{I} + \mu \boldsymbol{L})_{K_i} \\
&+ \langle \boldsymbol{\psi}, (\rho(\boldsymbol{u} \otimes \boldsymbol{u}) + \rho(\widehat{\boldsymbol{u}} - \boldsymbol{u}) \otimes \lambda \boldsymbol{u} + \widehat{p}\boldsymbol{I} + \mu \boldsymbol{L} + \mu\tau(\boldsymbol{u} - \widehat{\boldsymbol{u}}) \otimes \boldsymbol{n} + \mu\tau \boldsymbol{n} \otimes (\boldsymbol{u} - \widehat{\boldsymbol{u}}))\, \boldsymbol{n} \rangle_{\partial K_i \setminus \Gamma_D} \\
&+ \langle \boldsymbol{\psi}, (\rho(\boldsymbol{u} \otimes \boldsymbol{u}) + \rho(\boldsymbol{u}_D - \boldsymbol{u}) \otimes \lambda \boldsymbol{u} + \widehat{p}\boldsymbol{I} + \mu \boldsymbol{L} + \mu\tau(\boldsymbol{u} - \boldsymbol{u}_D) \otimes \boldsymbol{n} + \mu\tau \boldsymbol{n} \otimes (\boldsymbol{u} - \boldsymbol{u}_D))\, \boldsymbol{n} \rangle_{\partial K_i \cap \Gamma_D} \\
&+ \langle \boldsymbol{\psi}_1, \left(\rho_1(\boldsymbol{u}_1 \otimes \boldsymbol{u}_1) + \rho_1(\widetilde{\boldsymbol{u}}^i - \boldsymbol{u}_1) \otimes \lambda \boldsymbol{u}_1\right) \widehat{\boldsymbol{n}} \rangle_{\mathcal{I}_i} \\
&+ \langle \boldsymbol{\psi}_1, \left((\widetilde{p}^i + \delta_P)\boldsymbol{I} + \mu_1 \boldsymbol{L}_1 + \mu_1 \tau^{\mathcal{I}}(\boldsymbol{u}_1 - \widetilde{\boldsymbol{u}}^i) \otimes \widehat{\boldsymbol{n}} + \mu_1 \tau^{\mathcal{I}} \widehat{\boldsymbol{n}} \otimes (\boldsymbol{u}_1 - \widetilde{\boldsymbol{u}}^i) + \mu_1 \boldsymbol{\delta}_{\boldsymbol{L}}\right) \widehat{\boldsymbol{n}} \rangle_{\mathcal{I}_i} \\
&+ \langle \boldsymbol{\psi}_2, \left(\rho_2(\boldsymbol{u}_2 \otimes \boldsymbol{u}_2) + \rho_2(\widetilde{\boldsymbol{u}}^i - \boldsymbol{u}_2) \otimes \lambda \boldsymbol{u}_2\right) (-\widehat{\boldsymbol{n}}) \rangle_{\mathcal{I}_i} \\
&+ \langle \boldsymbol{\psi}_2, \left(\widetilde{p}^i \boldsymbol{I} + \mu_2 \boldsymbol{L}_2 + \mu_2 \tau^{\mathcal{I}}(\boldsymbol{u}_2 - \widetilde{\boldsymbol{u}}^i) \otimes (-\widehat{\boldsymbol{n}}) + \mu_2 \tau^{\mathcal{I}}(-\widehat{\boldsymbol{n}}) \otimes (\boldsymbol{u}_2 - \widetilde{\boldsymbol{u}}^i)\right) (-\widehat{\boldsymbol{n}}) \rangle_{\mathcal{I}_i} \\
&= (\boldsymbol{\psi}, \rho \boldsymbol{f})_{K_i}
\end{aligned}$$

note that some terms could be added so we get

(D.1.7)

$$
\begin{aligned}
(\boldsymbol{\psi}, \rho\frac{\partial \boldsymbol{u}}{\partial t})_{K_i} &- (\boldsymbol{\nabla}\boldsymbol{\psi}, \rho(\boldsymbol{u}\otimes\boldsymbol{u}) + p\boldsymbol{I} + \mu\boldsymbol{L})_{K_i} \\
&+ \langle \boldsymbol{\psi}, (\rho(\boldsymbol{u}\otimes\boldsymbol{u}) + \widehat{p}\boldsymbol{I} + \mu\boldsymbol{L})\,\boldsymbol{n}\rangle_{\partial K_i} \\
&+ \langle \boldsymbol{\psi}, (\rho(\widehat{\boldsymbol{u}} - \boldsymbol{u})\otimes\lambda\boldsymbol{u} + \mu\tau(\boldsymbol{u}-\widehat{\boldsymbol{u}})\otimes\boldsymbol{n} + \mu\tau\boldsymbol{n}\otimes(\boldsymbol{u}-\widehat{\boldsymbol{u}}))\,\boldsymbol{n}\rangle_{\partial K_i\setminus\Gamma_D} \\
&+ \langle \boldsymbol{\psi}, (\rho(\boldsymbol{u}_D - \boldsymbol{u})\otimes\lambda\boldsymbol{u} + \mu\tau(\boldsymbol{u}-\boldsymbol{u}_D)\otimes\boldsymbol{n} + \mu\tau\boldsymbol{n}\otimes(\boldsymbol{u}-\boldsymbol{u}_D))\,\boldsymbol{n}\rangle_{\partial K_i\cap\Gamma_D} \\
&+ \langle \boldsymbol{\psi}_1, \Big(\rho_1(\boldsymbol{u}_1\otimes\boldsymbol{u}_1) + (\widetilde{p}^i + \delta_P)\boldsymbol{I} + \mu_1\boldsymbol{L}_1 + \mu_1\boldsymbol{\delta}_{\boldsymbol{L}}\Big)\,\widehat{\boldsymbol{n}}\rangle_{\mathcal{I}_i} \\
&+ \langle \boldsymbol{\psi}_2, \Big(\rho_2(\boldsymbol{u}_2\otimes\boldsymbol{u}_2) + \widetilde{p}^i\boldsymbol{I} + \mu_2\boldsymbol{L}_2\Big)\,(-\widehat{\boldsymbol{n}})\rangle_{\mathcal{I}_i} \\
&+ \langle \boldsymbol{\psi}_1, \Big(\rho_1(\widetilde{\boldsymbol{u}}^i - \boldsymbol{u}_1)\otimes\lambda\boldsymbol{u}_1\Big)\,\widehat{\boldsymbol{n}}\rangle_{\mathcal{I}_i} \\
&+ \langle \boldsymbol{\psi}_1, \Big(\mu_1\tau^{\mathcal{I}}(\boldsymbol{u}_1 - \widetilde{\boldsymbol{u}}^i)\otimes\widehat{\boldsymbol{n}} + \mu_1\tau^{\mathcal{I}}\widehat{\boldsymbol{n}}\otimes(\boldsymbol{u}_1 - \widetilde{\boldsymbol{u}}^i)\Big)\,\widehat{\boldsymbol{n}}\rangle_{\mathcal{I}_i} \\
&+ \langle \boldsymbol{\psi}_2, \Big(\rho_2(\widetilde{\boldsymbol{u}}^i - \boldsymbol{u}_2)\otimes\lambda\boldsymbol{u}_2\Big)\,(-\widehat{\boldsymbol{n}})\rangle_{\mathcal{I}_i} \\
&+ \langle \boldsymbol{\psi}_2, \Big(\mu_2\tau^{\mathcal{I}}(\boldsymbol{u}_2 - \widetilde{\boldsymbol{u}}^i)\otimes(-\widehat{\boldsymbol{n}}) + \mu_2\tau^{\mathcal{I}}(-\widehat{\boldsymbol{n}})\otimes(\boldsymbol{u}_2 - \widetilde{\boldsymbol{u}}^i)\Big)\,(-\widehat{\boldsymbol{n}})\rangle_{\mathcal{I}_i} \\
&= (\boldsymbol{\psi}, \rho\boldsymbol{f})_{K_i}
\end{aligned}
$$

using the tensor identity $(\boldsymbol{a}\otimes\boldsymbol{u})\boldsymbol{n} = (\boldsymbol{u}\cdot\boldsymbol{n})\boldsymbol{a}$, the previous equation is simplified to

(D.1.8)

$$
\begin{aligned}
(\boldsymbol{\psi}, \rho\frac{\partial \boldsymbol{u}}{\partial t})_{K_i} &- (\boldsymbol{\nabla}\boldsymbol{\psi}, \rho(\boldsymbol{u}\otimes\boldsymbol{u}) + p\boldsymbol{I} + \mu\boldsymbol{L})_{K_i} \\
&+ \langle \boldsymbol{\psi}, (\rho(\boldsymbol{u}\otimes\boldsymbol{u}) + \widehat{p}\boldsymbol{I} + \mu\boldsymbol{L})\,\boldsymbol{n}\rangle_{\partial K_i} \\
&+ \langle \boldsymbol{\psi}, (\rho(\widehat{\boldsymbol{u}} - \boldsymbol{u})\otimes\lambda\boldsymbol{u})\boldsymbol{n} + \mu\tau(\boldsymbol{u}-\widehat{\boldsymbol{u}}) + \mu\tau(\boldsymbol{u}\cdot\boldsymbol{n} - \widehat{\boldsymbol{u}}\cdot\boldsymbol{n})\boldsymbol{n}\rangle_{\partial K_i\setminus\Gamma_D} \\
&+ \langle \boldsymbol{\psi}, (\rho(\boldsymbol{u}_D - \boldsymbol{u})\otimes\lambda\boldsymbol{u})\boldsymbol{n} + \mu\tau(\boldsymbol{u}-\boldsymbol{u}_D) + \mu\tau(\boldsymbol{u}\cdot\boldsymbol{n} - \boldsymbol{u}_D\cdot\boldsymbol{n})\boldsymbol{n}\rangle_{\partial K_i\cap\Gamma_D} \\
&+ \langle \boldsymbol{\psi}_1, \Big(\rho_1(\boldsymbol{u}_1\otimes\boldsymbol{u}_1) + (\widetilde{p}^i + \delta_P)\boldsymbol{I} + \mu_1\boldsymbol{L}_1 + \mu_1\boldsymbol{\delta}_{\boldsymbol{L}}\Big)\,\widehat{\boldsymbol{n}}\rangle_{\mathcal{I}_i} \\
&+ \langle \boldsymbol{\psi}_2, \Big(\rho_2(\boldsymbol{u}_2\otimes\boldsymbol{u}_2) + \widetilde{p}^i\boldsymbol{I} + \mu_2\boldsymbol{L}_2\Big)\,(-\widehat{\boldsymbol{n}})\rangle_{\mathcal{I}_i} \\
&+ \langle \boldsymbol{\psi}_1, \Big(\rho_1(\widetilde{\boldsymbol{u}}^i - \boldsymbol{u}_1)\otimes\lambda\boldsymbol{u}_1\Big)\,\widehat{\boldsymbol{n}}\rangle_{\mathcal{I}_i} \\
&+ \langle \boldsymbol{\psi}_1, \Big(\mu_1\tau^{\mathcal{I}}(\boldsymbol{u}_1 - \widetilde{\boldsymbol{u}}^i)\otimes\widehat{\boldsymbol{n}} + \mu_1\tau^{\mathcal{I}}\widehat{\boldsymbol{n}}\otimes(\boldsymbol{u}_1 - \widetilde{\boldsymbol{u}}^i)\Big)\,\widehat{\boldsymbol{n}}\rangle_{\mathcal{I}_i} \\
&+ \langle \boldsymbol{\psi}_2, \Big(\rho_2(\widetilde{\boldsymbol{u}}^i - \boldsymbol{u}_2)\otimes\lambda\boldsymbol{u}_2\Big)\,(-\widehat{\boldsymbol{n}})\rangle_{\mathcal{I}_i} \\
&+ \langle \boldsymbol{\psi}_2, \Big(\mu_2\tau^{\mathcal{I}}(\boldsymbol{u}_2 - \widetilde{\boldsymbol{u}}^i)\otimes(-\widehat{\boldsymbol{n}}) + \mu_2\tau^{\mathcal{I}}(-\widehat{\boldsymbol{n}})\otimes(\boldsymbol{u}_2 - \widetilde{\boldsymbol{u}}^i)\Big)\,(-\widehat{\boldsymbol{n}})\rangle_{\mathcal{I}_i} \\
&= (\boldsymbol{\psi}, \rho\boldsymbol{f})_{K_i}
\end{aligned}
$$

Step 4: Doing integration by parts again but only for the diffusive term, considering that $K_i = (K_i \cap \Omega_1) \cup (K_i \cap \Omega_2)$ yields

(D.1.9)

$$
\begin{aligned}
(\boldsymbol{\psi}, \rho\frac{\partial \boldsymbol{u}}{\partial t})_{K_i} &+ (\boldsymbol{\psi}, \boldsymbol{\nabla}\cdot(\mu\boldsymbol{L}))_{K_i} - (\boldsymbol{\nabla}\boldsymbol{\psi}, p\boldsymbol{I})_{K_i} - (\boldsymbol{\nabla}\boldsymbol{\psi}, \rho(\boldsymbol{u}\otimes\boldsymbol{u}))_{K_i} \\
&+ \langle \boldsymbol{\psi}, (\rho(\boldsymbol{u}\otimes\boldsymbol{u}) + \widehat{p}\boldsymbol{I})\,\boldsymbol{n}\rangle_{\partial K_i} \\
&+ \langle \boldsymbol{\psi}, (\rho(\widehat{\boldsymbol{u}}-\boldsymbol{u})\otimes\lambda\boldsymbol{u})\boldsymbol{n} + \mu\tau(\boldsymbol{u}-\widehat{\boldsymbol{u}}) + \mu\tau(\boldsymbol{u}\cdot\boldsymbol{n} - \widehat{\boldsymbol{u}}\cdot\boldsymbol{n})\boldsymbol{n}\rangle_{\partial K_i\setminus\Gamma_D} \\
&+ \langle \boldsymbol{\psi}, (\rho(\boldsymbol{u}_D-\boldsymbol{u})\otimes\lambda\boldsymbol{u})\boldsymbol{n} + \mu\tau(\boldsymbol{u}-\boldsymbol{u}_D) + \mu\tau(\boldsymbol{u}\cdot\boldsymbol{n} - \boldsymbol{u}_D\cdot\boldsymbol{n})\boldsymbol{n}\rangle_{\partial K_i\cap\Gamma_D} \\
&+ \langle \boldsymbol{\psi}_1, \left(\rho_1(\boldsymbol{u}_1\otimes\boldsymbol{u}_1) + (\widetilde{p}^i + \delta_P)\boldsymbol{I} + \mu_1\boldsymbol{\delta}_{\boldsymbol{L}}\right)\widehat{\boldsymbol{n}}\rangle_{\mathcal{I}_i} \\
&+ \langle \boldsymbol{\psi}_2, \left(\rho_2(\boldsymbol{u}_2\otimes\boldsymbol{u}_2) + \widetilde{p}^i\boldsymbol{I}\right)(-\widehat{\boldsymbol{n}})\rangle_{\mathcal{I}_i} \\
&+ \langle \boldsymbol{\psi}_1, \left(\rho_1(\widetilde{\boldsymbol{u}}^i-\boldsymbol{u}_1)\otimes\lambda\boldsymbol{u}_1\right)\widehat{\boldsymbol{n}}\rangle_{\mathcal{I}_i} \\
&+ \langle \boldsymbol{\psi}_1, \left(\mu_1\tau^{\mathcal{I}}(\boldsymbol{u}_1-\widetilde{\boldsymbol{u}}^i)\otimes\widehat{\boldsymbol{n}} + \mu_1\tau^{\mathcal{I}}\widehat{\boldsymbol{n}}\otimes(\boldsymbol{u}_1-\widetilde{\boldsymbol{u}}^i)\right)\widehat{\boldsymbol{n}}\rangle_{\mathcal{I}_i} \\
&+ \langle \boldsymbol{\psi}_2, \left(\rho_2(\widetilde{\boldsymbol{u}}^i-\boldsymbol{u}_2)\otimes\lambda\boldsymbol{u}_2\right)(-\widehat{\boldsymbol{n}})\rangle_{\mathcal{I}_i} \\
&+ \langle \boldsymbol{\psi}_2, \left(\mu_2\tau^{\mathcal{I}}(\boldsymbol{u}_2-\widetilde{\boldsymbol{u}}^i)\otimes(-\widehat{\boldsymbol{n}}) + \mu_2\tau^{\mathcal{I}}(-\widehat{\boldsymbol{n}})\otimes(\boldsymbol{u}_2-\widetilde{\boldsymbol{u}}^i)\right)(-\widehat{\boldsymbol{n}})\rangle_{\mathcal{I}_i} \\
&= (\boldsymbol{\psi}, \rho\boldsymbol{f})_{K_i}
\end{aligned}
$$

and by taking the known terms to the right hand side we get (assuming $\widehat{\boldsymbol{u}}$ and $\widehat{p}$ are known)

(D.1.10)

$$
\begin{aligned}
(\boldsymbol{\psi}, \rho\frac{\partial \boldsymbol{u}}{\partial t})_{K_i} &+ (\boldsymbol{\psi}, \boldsymbol{\nabla}\cdot(\mu\boldsymbol{L}))_{K_i} - (\boldsymbol{\nabla}\boldsymbol{\psi}, p\boldsymbol{I})_{K_i} - (\boldsymbol{\nabla}\boldsymbol{\psi}, \rho(\boldsymbol{u}\otimes\boldsymbol{u}))_{K_i} \\
&+ \langle \boldsymbol{\psi}, \rho(\boldsymbol{u}\otimes\boldsymbol{u})\boldsymbol{n}\rangle_{\partial K_i} \\
&+ \langle \boldsymbol{\psi}, -\lambda\rho(\boldsymbol{u}\otimes\boldsymbol{u})\boldsymbol{n} + \mu\tau\boldsymbol{u} + \mu\tau(\boldsymbol{u}\cdot\boldsymbol{n})\boldsymbol{n}\rangle_{\partial K_i\setminus\Gamma_D} \\
&+ \langle \boldsymbol{\psi}, -\lambda\rho(\boldsymbol{u}\otimes\boldsymbol{u})\boldsymbol{n} + \mu\tau\boldsymbol{u} + \mu\tau(\boldsymbol{u}\cdot\boldsymbol{n})\boldsymbol{n}\rangle_{\partial K_i\cap\Gamma_D} \\
&+ \langle \boldsymbol{\psi}_1, \left(\rho_1(\boldsymbol{u}_1\otimes\boldsymbol{u}_1) + \widetilde{p}^i\boldsymbol{I}\right)\widehat{\boldsymbol{n}}\rangle_{\mathcal{I}_i} + \langle \boldsymbol{\psi}_2, \left(\rho_2(\boldsymbol{u}_2\otimes\boldsymbol{u}_2) + \widetilde{p}^i\boldsymbol{I}\right)(-\widehat{\boldsymbol{n}})\rangle_{\mathcal{I}_i} \\
&+ \langle \boldsymbol{\psi}_1, \left(\rho_1(\widetilde{\boldsymbol{u}}^i-\boldsymbol{u}_1)\otimes\lambda\boldsymbol{u}_1\right)\widehat{\boldsymbol{n}}\rangle_{\mathcal{I}_i} \\
&+ \langle \boldsymbol{\psi}_1, \left(\mu_1\tau^{\mathcal{I}}(\boldsymbol{u}_1-\widetilde{\boldsymbol{u}}^i)\otimes\widehat{\boldsymbol{n}} + \mu_1\tau^{\mathcal{I}}\widehat{\boldsymbol{n}}\otimes(\boldsymbol{u}_1-\widetilde{\boldsymbol{u}}^i)\right)\widehat{\boldsymbol{n}}\rangle_{\mathcal{I}_i} \\
&+ \langle \boldsymbol{\psi}_2, \left(\rho_2(\widetilde{\boldsymbol{u}}^i-\boldsymbol{u}_2)\otimes\lambda\boldsymbol{u}_2\right)(-\widehat{\boldsymbol{n}})\rangle_{\mathcal{I}_i} \\
&+ \langle \boldsymbol{\psi}_2, \left(\mu_2\tau^{\mathcal{I}}(\boldsymbol{u}_2-\widetilde{\boldsymbol{u}}^i)\otimes(-\widehat{\boldsymbol{n}}) + \mu_2\tau^{\mathcal{I}}(-\widehat{\boldsymbol{n}})\otimes(\boldsymbol{u}_2-\widetilde{\boldsymbol{u}}^i)\right)(-\widehat{\boldsymbol{n}})\rangle_{\mathcal{I}_i} \\
&= (\boldsymbol{\psi}, \rho\boldsymbol{f})_{K_i} + \langle \boldsymbol{\psi}, -\lambda\rho(\widehat{\boldsymbol{u}}\otimes\boldsymbol{u})\boldsymbol{n} + \mu\tau\widehat{\boldsymbol{u}} + \mu\tau(\widehat{\boldsymbol{u}}\cdot\boldsymbol{n})\boldsymbol{n}\rangle_{\partial K_i\setminus\Gamma_D} \\
&+ \langle \boldsymbol{\psi}, -\lambda\rho(\boldsymbol{u}_D\otimes\boldsymbol{u})\boldsymbol{n} + \mu\tau\boldsymbol{u}_D + \mu\tau(\boldsymbol{u}_D\cdot\boldsymbol{n})\boldsymbol{n}\rangle_{\partial K_i\cap\Gamma_D} \\
&- \langle \boldsymbol{\psi}, \widehat{p}\boldsymbol{I}\boldsymbol{n}\rangle_{\partial K_i} - \langle \boldsymbol{\psi}_1, (\delta_P\boldsymbol{I} + \mu_1\boldsymbol{\delta}_{\boldsymbol{L}})\,\widehat{\boldsymbol{n}}\rangle_{\mathcal{I}_i}
\end{aligned}
$$

by combining and rearranging some terms, and using the identity $\boldsymbol{I}\boldsymbol{n} = \boldsymbol{n}$, we get

(D.1.11)
$$
\begin{aligned}
&(\boldsymbol{\psi}, \rho\frac{\partial \boldsymbol{u}}{\partial t})_{K_i} + (\boldsymbol{\psi}, \boldsymbol{\nabla}\cdot(\mu\boldsymbol{L}))_{K_i} - (\boldsymbol{\nabla}\boldsymbol{\psi}, p\boldsymbol{I})_{K_i} - (\boldsymbol{\nabla}\boldsymbol{\psi}, \rho(\boldsymbol{u}\otimes\boldsymbol{u}))_{K_i} + \langle \boldsymbol{\psi}, \rho(\boldsymbol{u}\otimes\boldsymbol{u})\boldsymbol{n}\rangle_{\partial K_i} \\
&\quad - \langle \boldsymbol{\psi}, \lambda\rho(\boldsymbol{u}\otimes\boldsymbol{u})\boldsymbol{n}\rangle_{\partial K_i} + \langle \boldsymbol{\psi}, \mu\tau\boldsymbol{u}\rangle_{\partial K_i} + \langle \boldsymbol{\psi}, \mu\tau(\boldsymbol{u}\cdot\boldsymbol{n})\boldsymbol{n}\rangle_{\partial K_i} \\
&\quad + \langle \boldsymbol{\psi}_1, \rho_1(\boldsymbol{u}_1\otimes\boldsymbol{u}_1)\widehat{\boldsymbol{n}}\rangle_{\mathcal{I}_i} + \langle \boldsymbol{\psi}_1, (\widetilde{p}^i + \delta_P)\widehat{\boldsymbol{n}}\rangle_{\mathcal{I}_i} + \langle \boldsymbol{\psi}_2, \rho_2(\boldsymbol{u}_2\otimes\boldsymbol{u}_2)(-\widehat{\boldsymbol{n}})\rangle_{\mathcal{I}_i} + \langle \boldsymbol{\psi}_2, \widetilde{p}^i(-\widehat{\boldsymbol{n}})\rangle_{\mathcal{I}_i} \\
&\quad - \langle \boldsymbol{\psi}_1, \lambda\rho_1(\boldsymbol{u}_1\otimes\boldsymbol{u}_1)\widehat{\boldsymbol{n}}\rangle_{\mathcal{I}_i} + \langle \boldsymbol{\psi}_1, \lambda\rho_1(\widetilde{\boldsymbol{u}}^i\otimes\boldsymbol{u}_1)\widehat{\boldsymbol{n}}\rangle_{\mathcal{I}_i} \\
&\quad + \langle \boldsymbol{\psi}_1, \mu_1\tau^{\mathcal{I}}\boldsymbol{u}_1\rangle_{\mathcal{I}_i} - \langle \boldsymbol{\psi}_1, \mu_1\tau^{\mathcal{I}}\widetilde{\boldsymbol{u}}^i\rangle_{\mathcal{I}_i} \\
&\quad + \langle \boldsymbol{\psi}_1, \mu_1\tau^{\mathcal{I}}(\boldsymbol{u}_1\cdot\widehat{\boldsymbol{n}})\widehat{\boldsymbol{n}}\rangle_{\mathcal{I}_i} - \langle \boldsymbol{\psi}_1, \mu_1\tau^{\mathcal{I}}(\widetilde{\boldsymbol{u}}^i\cdot\widehat{\boldsymbol{n}})\widehat{\boldsymbol{n}}\rangle_{\mathcal{I}_i} \\
&\quad - \langle \boldsymbol{\psi}_2, \lambda\rho_2(\boldsymbol{u}_2\otimes\boldsymbol{u}_2)(-\widehat{\boldsymbol{n}})\rangle_{\mathcal{I}_i} + \langle \boldsymbol{\psi}_2, \lambda\rho_2(\widetilde{\boldsymbol{u}}^i\otimes\boldsymbol{u}_2)(-\widehat{\boldsymbol{n}})\rangle_{\mathcal{I}_i} \\
&\quad + \langle \boldsymbol{\psi}_2, \mu_2\tau^{\mathcal{I}}\boldsymbol{u}_2\rangle_{\mathcal{I}_i} - \langle \boldsymbol{\psi}_2, \mu_2\tau^{\mathcal{I}}\widetilde{\boldsymbol{u}}^i\rangle_{\mathcal{I}_i} \\
&\quad + \langle \boldsymbol{\psi}_2, \mu_2\tau^{\mathcal{I}}(\boldsymbol{u}_2\cdot(-\widehat{\boldsymbol{n}}))(-\widehat{\boldsymbol{n}})\rangle_{\mathcal{I}_i} - \langle \boldsymbol{\psi}_2, \mu_2\tau^{\mathcal{I}}(\widetilde{\boldsymbol{u}}^i\cdot(-\widehat{\boldsymbol{n}}))(-\widehat{\boldsymbol{n}})\rangle_{\mathcal{I}_i} \\
&\quad = (\boldsymbol{\psi}, \rho\boldsymbol{f})_{K_i} - \langle \boldsymbol{\psi}, \lambda\rho(\widehat{\boldsymbol{u}}\otimes\boldsymbol{u})\boldsymbol{n}\rangle_{\partial K_i\setminus\Gamma_D} + \langle \boldsymbol{\psi}, \mu\tau\widehat{\boldsymbol{u}}\rangle_{\partial K_i\setminus\Gamma_D} + \langle \boldsymbol{\psi}, \mu\tau(\widehat{\boldsymbol{u}}\cdot\boldsymbol{n})\boldsymbol{n}\rangle_{\partial K_i\setminus\Gamma_D} \\
&\quad - \langle \boldsymbol{\psi}, \lambda\rho(\boldsymbol{u}_D\otimes\boldsymbol{u})\boldsymbol{n}\rangle_{\partial K_i\cap\Gamma_D} + \langle \boldsymbol{\psi}, \mu\tau\boldsymbol{u}_D\rangle_{\partial K_i\cap\Gamma_D} + \langle \boldsymbol{\psi}, \mu\tau(\boldsymbol{u}_D\cdot\boldsymbol{n})\boldsymbol{n}\rangle_{\partial K_i\cap\Gamma_D} \\
&\quad - \langle \boldsymbol{\psi}, \widehat{p}\boldsymbol{n}\rangle_{\partial K_i\setminus\Gamma_N} - \langle \boldsymbol{\psi}, p_N\boldsymbol{n}\rangle_{\partial K_i\cap\Gamma_N} - \langle \boldsymbol{\psi}_1, \boldsymbol{g}_s\rangle_{\mathcal{I}_i}
\end{aligned}
$$

note that in the last line of the previous equation, $\widehat{p}$ is replaced by p_N on the Neumann boundary.$(\delta_P\boldsymbol{I} + \mu_1\boldsymbol{\delta_L})\widehat{\boldsymbol{n}}$ is replaced by $\boldsymbol{g}_s$.

To obtain the weak form of the *second* equation (equation of $\boldsymbol{L}$) in the local problems (6.2.3b), we go through the following steps:

Step 1: the governing equation is multiplied by a discontinuous tensor test function $\boldsymbol{\Psi} \in [\mathcal{P}^m(K_i)]^{d\times d} \oplus H[\mathcal{P}^m(K_i)]^{d\times d}$, and integrated over the two subdomains of the element K_i

$$
(\boldsymbol{\Psi}, \boldsymbol{L})_{K_i} + (\boldsymbol{\Psi}_1, 2\boldsymbol{\nabla}^s\boldsymbol{u}_1)_{K_i\cap\Omega_1} + (\boldsymbol{\Psi}_2, 2\boldsymbol{\nabla}^s\boldsymbol{u}_2)_{K_i\cap\Omega_2} = 0 \tag{D.1.12}
$$

and by using the definition of the symmetric gradient given by (6.1.4) we get

$$
\begin{aligned}
&(\boldsymbol{\Psi}, \boldsymbol{L})_{K_i} + (\boldsymbol{\Psi}_1, \boldsymbol{\nabla}\boldsymbol{u}_1)_{K_i\cap\Omega_1} + (\boldsymbol{\Psi}_1, (\boldsymbol{\nabla}\boldsymbol{u}_1)^T)_{K_i\cap\Omega_1} \\
&\qquad + (\boldsymbol{\Psi}_1, \boldsymbol{\nabla}\boldsymbol{u}_2)_{K_i\cap\Omega_1} + (\boldsymbol{\Psi}_1, (\boldsymbol{\nabla}\boldsymbol{u}_2)^T)_{K_i\cap\Omega_1} = 0
\end{aligned} \tag{D.1.13}
$$

Step 2: Green's theorem (integration by parts) is applied to incorporate surface integrals

(D.1.14)
$$
\begin{aligned}
&(\boldsymbol{\Psi}, \boldsymbol{L})_{K_i} - (\boldsymbol{\nabla}\cdot\boldsymbol{\Psi}_1, \boldsymbol{u}_1)_{K_i\cap\Omega_1} + \langle \boldsymbol{\Psi}_1, \boldsymbol{u}_1\otimes\boldsymbol{n}\rangle_{(\partial K_i\cap\Omega_1)\setminus\Gamma_D} + \langle \boldsymbol{\Psi}_1, \boldsymbol{u}_1\otimes\boldsymbol{n}\rangle_{(\partial K_i\cap\Omega_1)\cap\Gamma_D} \\
&\quad + \langle \boldsymbol{\Psi}_1, \boldsymbol{u}_1\otimes\widehat{\boldsymbol{n}}\rangle_{\mathcal{I}_i} \\
&\quad - (\boldsymbol{\nabla}\cdot\boldsymbol{\Psi}_1^T, \boldsymbol{u}_1)_{K_i\cap\Omega_1} + \langle \boldsymbol{\Psi}_1, (\boldsymbol{u}_1\otimes\boldsymbol{n})^T\rangle_{(\partial K_i\cap\Omega_1)\setminus\Gamma_D} + \langle \boldsymbol{\Psi}_1, (\boldsymbol{u}_1\otimes\boldsymbol{n})^T\rangle_{(\partial K_i\cap\Omega_1)\cap\Gamma_D} \\
&\quad + \langle \boldsymbol{\Psi}_1, (\boldsymbol{u}_1\otimes\widehat{\boldsymbol{n}})^T\rangle_{\mathcal{I}_i} \\
&\quad - (\boldsymbol{\nabla}\cdot\boldsymbol{\Psi}_2, \boldsymbol{u}_2)_{K_i\cap\Omega_2} + \langle \boldsymbol{\Psi}_2, \boldsymbol{u}_2\otimes\boldsymbol{n}\rangle_{(\partial K_i\cap\Omega_2)\setminus\Gamma_D} + \langle \boldsymbol{\Psi}_2, \boldsymbol{u}_2\otimes\boldsymbol{n}\rangle_{(\partial K_i\cap\Omega_2)\cap\Gamma_D} \\
&\quad + \langle \boldsymbol{\Psi}_2, \boldsymbol{u}_2\otimes(-\widehat{\boldsymbol{n}})\rangle_{\mathcal{I}_i} \\
&\quad - (\boldsymbol{\nabla}\cdot\boldsymbol{\Psi}_2^T, \boldsymbol{u}_2)_{K_i\cap\Omega_2} + \langle \boldsymbol{\Psi}_2, (\boldsymbol{u}_2\otimes\boldsymbol{n})^T\rangle_{(\partial K_i\cap\Omega_2)\setminus\Gamma_D} + \langle \boldsymbol{\Psi}_2, (\boldsymbol{u}_2\otimes\boldsymbol{n})^T\rangle_{(\partial K_i\cap\Omega_2)\cap\Gamma_D} \\
&\quad + \langle \boldsymbol{\Psi}_2, (\boldsymbol{u}_2\otimes(-\widehat{\boldsymbol{n}}))^T\rangle_{\mathcal{I}_i} = 0
\end{aligned}
$$

where we get surface integrals over the element boundary ∂K_i and the interface $\mathcal{I}_i$. Note that some terms could be combined and the equation could be written as

$$\begin{aligned}(\boldsymbol{\Psi},\boldsymbol{L})_{K_i} - (\boldsymbol{\nabla}\cdot\boldsymbol{\Psi},\boldsymbol{u})_{K_i} - (\boldsymbol{\nabla}\cdot\boldsymbol{\Psi}^T,\boldsymbol{u})_{K_i} \\ + \langle\boldsymbol{\Psi},\boldsymbol{u}\otimes\boldsymbol{n}\rangle_{\partial K_i\setminus\Gamma_D} + \langle\boldsymbol{\Psi},\boldsymbol{n}\otimes\boldsymbol{u}\rangle_{\partial K_i\setminus\Gamma_D} \\ + \langle\boldsymbol{\Psi},\boldsymbol{u}\otimes\boldsymbol{n}\rangle_{\partial K_i\cap\Gamma_D} + \langle\boldsymbol{\Psi},\boldsymbol{n}\otimes\boldsymbol{u}\rangle_{\partial K_i\cap\Gamma_D} \\ + \langle\boldsymbol{\Psi}_1,\boldsymbol{u}_1\otimes\widehat{\boldsymbol{n}}\rangle_{\mathcal{I}_i} + \langle\boldsymbol{\Psi}_1,\widehat{\boldsymbol{n}}\otimes\boldsymbol{u}_1\rangle_{\mathcal{I}_i} \\ + \langle\boldsymbol{\Psi}_2,\boldsymbol{u}_2\otimes(-\widehat{\boldsymbol{n}})\rangle_{\mathcal{I}_i} + \langle\boldsymbol{\Psi}_2,(-\widehat{\boldsymbol{n}})\otimes\boldsymbol{u}_2\rangle_{\mathcal{I}_i} = 0\end{aligned} \tag{D.1.15}$$

Step 3: In the HDG method, the physical quantity $\boldsymbol{u}$ is replaced by the numerical quantity $\widehat{\boldsymbol{u}}$ and $\widetilde{\boldsymbol{u}}^i$ on $\partial K_i\setminus\Gamma_D$ and the interface $\mathcal{I}_i$, respectively. While on the intersection with the Dirichlet boundary, $\boldsymbol{u}=\boldsymbol{u}_D$,

$$\begin{aligned}(\boldsymbol{\Psi},\boldsymbol{L})_{K_i} - (\boldsymbol{\nabla}^s\cdot\boldsymbol{\Psi},\boldsymbol{u})_{K_i} + \langle\boldsymbol{\Psi},\widehat{\boldsymbol{u}}\otimes\boldsymbol{n}\rangle_{\partial K_i\setminus\Gamma_D} + \langle\boldsymbol{\Psi},\boldsymbol{n}\otimes\widehat{\boldsymbol{u}}\rangle_{\partial K_i\setminus\Gamma_D} \\ + \langle\boldsymbol{\Psi},\boldsymbol{u}_D\otimes\boldsymbol{n}\rangle_{\partial K_i\cap\Gamma_D} + \langle\boldsymbol{\Psi},\boldsymbol{n}\otimes\boldsymbol{u}_D\rangle_{\partial K_i\cap\Gamma_D} \\ + \langle\boldsymbol{\Psi}_1,\widetilde{\boldsymbol{u}}^i\otimes\widehat{\boldsymbol{n}}\rangle_{\mathcal{I}_i} + \langle\boldsymbol{\Psi}_1,\widehat{\boldsymbol{n}}\otimes\widetilde{\boldsymbol{u}}^i\rangle_{\mathcal{I}_i} \\ + \langle\boldsymbol{\Psi}_2,\widetilde{\boldsymbol{u}}^i\otimes(-\widehat{\boldsymbol{n}})\rangle_{\mathcal{I}_i} + \langle\boldsymbol{\Psi}_2,(-\widehat{\boldsymbol{n}})\otimes\widetilde{\boldsymbol{u}}^i\rangle_{\mathcal{I}_i} = 0\end{aligned} \tag{D.1.16}$$

and by taking the known terms to the right hand side we get (assuming $\widehat{\boldsymbol{u}}$ is known)

$$\begin{aligned}-(\boldsymbol{\Psi},\boldsymbol{L})_{K_i} + (\boldsymbol{\nabla}^s\cdot\boldsymbol{\Psi},\boldsymbol{u})_{K_i} - \langle\boldsymbol{\Psi}_1,\widetilde{\boldsymbol{u}}^i\otimes\widehat{\boldsymbol{n}}\rangle_{\mathcal{I}_i} - \langle\boldsymbol{\Psi}_1,\widehat{\boldsymbol{n}}\otimes\widetilde{\boldsymbol{u}}^i\rangle_{\mathcal{I}_i} \\ - \langle\boldsymbol{\Psi}_2,\widetilde{\boldsymbol{u}}^i\otimes(-\widehat{\boldsymbol{n}})\rangle_{\mathcal{I}_i} - \langle\boldsymbol{\Psi}_2,(-\widehat{\boldsymbol{n}})\otimes\widetilde{\boldsymbol{u}}^i\rangle_{\mathcal{I}_i} \\ = \langle\boldsymbol{\Psi},\widehat{\boldsymbol{u}}\otimes\boldsymbol{n}\rangle_{\partial K_i\setminus\Gamma_D} + \langle\boldsymbol{\Psi},\boldsymbol{n}\otimes\widehat{\boldsymbol{u}}\rangle_{\partial K_i\setminus\Gamma_D} \\ + \langle\boldsymbol{\Psi},\boldsymbol{u}_D\otimes\boldsymbol{n}\rangle_{\partial K_i\cap\Gamma_D} + \langle\boldsymbol{\Psi},\boldsymbol{n}\otimes\boldsymbol{u}_D\rangle_{\partial K_i\cap\Gamma_D}\end{aligned} \tag{D.1.17}$$

note that the sign of the equation is changed in order to have a symmetric operator for the local problems (will be more obvious in the matrix forms shown later).

To obtain the weak form of the *third* equation (equation of p) in the local problems (6.2.3b), we go through the following steps:
The governing equation is multiplied by a discontinuous scalar test function $\phi\in\boldsymbol{\nabla}\cdot[\mathcal{P}^m(K_i)]^d\oplus H\boldsymbol{\nabla}\cdot[\mathcal{P}^m(K_i)]^d$, and integrated over the element K_i

$$-(\phi,\boldsymbol{\nabla}\cdot\boldsymbol{u})_{K_i} = 0 \tag{D.1.18}$$

note that the sign of the equation is changed in order to have a symmetric operator for the local problems (will be more obvious in the matrix forms shown later).

Regarding the *fourth* equation, $\boldsymbol{u}=\boldsymbol{u}^o$ in K_i at $t=0$, in the local problems (6.2.3b), it is an initial condition that will be used when time integration is considered later.

Regarding the *fifth* and *sixth* equations, $\boldsymbol{u}=\boldsymbol{u}_D$ on $\partial K_i\cap\Gamma_D$ and $\boldsymbol{u}=\widehat{\boldsymbol{u}}$ on $\partial K_i\setminus\Gamma_D$, in the local problems (6.2.3b), they have already been used in the step of going from equation (D.1.15) to equation (D.1.17) when $\boldsymbol{u}$ is replaced by $\widehat{\boldsymbol{u}}$ and $\boldsymbol{u}_D$ in the third and fourth terms on the left hand side, respectively.

Regarding the *seventh* and *eighth* equations, $p=\widehat{p}$ on $\Gamma\setminus\Gamma_N$ and $p=p_N$ on Γ_N, in the local problems (6.2.3b), it has already been used in the step of going from equation (D.1.3)

to equation (D.1.4) when p is replaced by $\widehat{p}$ in the third and fourth terms on the left hand side, respectively. Then when $\widehat{p}$ is replaced by p_N on Γ_N in equation (D.1.11).

To obtain the weak form of the *ninth* equation (equation of $\widetilde{\boldsymbol{u}}^i$) in the local problems 6.2.3b, we go through the following steps:

Step 1: the governing equation is multiplied by a continuous vector test function $\widetilde{\boldsymbol{\psi}} \in [\mathcal{P}^m(\mathcal{I}_i)]^d$, and integrated over the interface $\mathcal{I}_i$. In this step the expression of the jump is written in an extended form where the components from the left and the right appear

$$\langle\widetilde{\boldsymbol{\psi}}, (p_1\boldsymbol{I} + \mu_1\boldsymbol{L}_1)\,\widehat{\boldsymbol{n}}\rangle_{\mathcal{I}_i} + \langle\widetilde{\boldsymbol{\psi}}, (p_2\boldsymbol{I} + \mu_2\boldsymbol{L}_2)\,(-\widehat{\boldsymbol{n}})\rangle_{\mathcal{I}_i} = \langle\widetilde{\boldsymbol{\psi}}, \boldsymbol{g}_s\rangle_{\mathcal{I}_i} \tag{D.1.19}$$

Step 2: In the HDG method, the physical quantities $(\boldsymbol{u}, \boldsymbol{L}_1, \boldsymbol{L}_2, p_1, p_2)$ are replaced by the numerical quantities $(\widetilde{\boldsymbol{u}}^i, \widetilde{\boldsymbol{L}}_1^i + \boldsymbol{\delta}_{\boldsymbol{L}}, \widetilde{\boldsymbol{L}}_2^i, \widetilde{p}^i + \delta_p, \widetilde{p}^i)$ on the interface $\mathcal{I}_i$

$$\langle\widetilde{\boldsymbol{\psi}}, \left((\widetilde{p}^i + \delta_P)\boldsymbol{I} + \mu_1\widetilde{\boldsymbol{L}}_1^i + \mu_1\boldsymbol{\delta}_{\boldsymbol{L}}\right)\widehat{\boldsymbol{n}}\rangle_{\mathcal{I}_i} + \langle\widetilde{\boldsymbol{\psi}}, \left(\widetilde{p}^i\boldsymbol{I} + \mu_2\widetilde{\boldsymbol{L}}_2^i\right)(-\widehat{\boldsymbol{n}})\rangle_{\mathcal{I}_i} = \langle\widetilde{\boldsymbol{\psi}}, \boldsymbol{g}_s\rangle_{\mathcal{I}_i} \tag{D.1.20}$$

After introducing the numerical fluxes, that were defined earlier, into equation D.1.20, we get

$$\begin{aligned}
&\langle\widetilde{\boldsymbol{\psi}}, \left((\widetilde{p}^i + \delta_P)\boldsymbol{I} + \mu_1\boldsymbol{L}_1 + \mu_1\tau^{\mathcal{I}}(\boldsymbol{u}_1 - \widetilde{\boldsymbol{u}}^i)\otimes\widehat{\boldsymbol{n}} + \mu_1\tau^{\mathcal{I}}\widehat{\boldsymbol{n}}\otimes(\boldsymbol{u}_1 - \widetilde{\boldsymbol{u}}^i) + \mu_1\boldsymbol{\delta}_{\boldsymbol{L}}\right)\widehat{\boldsymbol{n}}\rangle_{\mathcal{I}_i} \\
&+\langle\widetilde{\boldsymbol{\psi}}, \left(\widetilde{p}^i\boldsymbol{I} + \mu_2\boldsymbol{L}_2 + \mu_2\tau^{\mathcal{I}}(\boldsymbol{u}_2 - \widetilde{\boldsymbol{u}}^i)\otimes(-\widehat{\boldsymbol{n}}) + \mu_2\tau^{\mathcal{I}}(-\widehat{\boldsymbol{n}})\otimes(\boldsymbol{u}_2 - \widetilde{\boldsymbol{u}}^i)\right)(-\widehat{\boldsymbol{n}})\rangle_{\mathcal{I}_i} \\
&=\langle\widetilde{\boldsymbol{\psi}}, \boldsymbol{g}_s\rangle_{\mathcal{I}_i}
\end{aligned} \tag{D.1.21}$$

by splitting the terms we get

$$\begin{aligned}
&\langle\widetilde{\boldsymbol{\psi}}, \left((\widetilde{p}^i + \delta_P)\boldsymbol{I} + \mu_1\boldsymbol{L}_1 + \mu_1\boldsymbol{\delta}_{\boldsymbol{L}}\right)\widehat{\boldsymbol{n}}\rangle_{\mathcal{I}_i} + \langle\widetilde{\boldsymbol{\psi}}, \left(\widetilde{p}^i\boldsymbol{I} + \mu_2\boldsymbol{L}_2\right)(-\widehat{\boldsymbol{n}})\rangle_{\mathcal{I}_i} \\
&+\langle\widetilde{\boldsymbol{\psi}}, \left(\mu_1\tau^{\mathcal{I}}(\boldsymbol{u}_1 - \widetilde{\boldsymbol{u}}^i)\otimes\widehat{\boldsymbol{n}}\right)\widehat{\boldsymbol{n}}\rangle_{\mathcal{I}_i} + \langle\widetilde{\boldsymbol{\psi}}, \left(\mu_1\tau^{\mathcal{I}}\widehat{\boldsymbol{n}}\otimes(\boldsymbol{u}_1 - \widetilde{\boldsymbol{u}}^i)\right)\widehat{\boldsymbol{n}}\rangle_{\mathcal{I}_i} \\
&+\langle\widetilde{\boldsymbol{\psi}}, \left(\mu_2\tau^{\mathcal{I}}(\boldsymbol{u}_2 - \widetilde{\boldsymbol{u}}^i)\otimes(-\widehat{\boldsymbol{n}})\right)(-\widehat{\boldsymbol{n}})\rangle_{\mathcal{I}_i} + \langle\widetilde{\boldsymbol{\psi}}, \left(\mu_2\tau^{\mathcal{I}}(-\widehat{\boldsymbol{n}})\otimes(\boldsymbol{u}_2 - \widetilde{\boldsymbol{u}}^i)\right)(-\widehat{\boldsymbol{n}})\rangle_{\mathcal{I}_i} \\
&=\langle\widetilde{\boldsymbol{\psi}}, \boldsymbol{g}_s\rangle_{\mathcal{I}_i}
\end{aligned} \tag{D.1.22}$$

using the tensor identity $(\boldsymbol{a}\otimes\boldsymbol{u})\boldsymbol{n} = (\boldsymbol{u}\cdot\boldsymbol{n})\boldsymbol{a}$, the previous equation is simplified to

$$\begin{aligned}
&\langle\widetilde{\boldsymbol{\psi}}, \left((\widetilde{p}^i + \delta_P)\boldsymbol{I} + \mu_1\boldsymbol{L}_1 + \mu_1\boldsymbol{\delta}_{\boldsymbol{L}}\right)\widehat{\boldsymbol{n}}\rangle_{\mathcal{I}_i} + \langle\widetilde{\boldsymbol{\psi}}, \left(\widetilde{p}^i\boldsymbol{I} + \mu_2\boldsymbol{L}_2\right)(-\widehat{\boldsymbol{n}})\rangle_{\mathcal{I}_i} \\
&+\langle\widetilde{\boldsymbol{\psi}}, \mu_1\tau^{\mathcal{I}}(\boldsymbol{u}_1 - \widetilde{\boldsymbol{u}}^i)\rangle_{\mathcal{I}_i} + \langle\widetilde{\boldsymbol{\psi}}, \mu_1\tau^{\mathcal{I}}(\boldsymbol{u}_1\cdot\widehat{\boldsymbol{n}} - \widetilde{\boldsymbol{u}}^i\cdot\widehat{\boldsymbol{n}})\widehat{\boldsymbol{n}}\rangle_{\mathcal{I}_i} \\
&+\langle\widetilde{\boldsymbol{\psi}}, \mu_2\tau^{\mathcal{I}}(\boldsymbol{u}_2 - \widetilde{\boldsymbol{u}}^i)\rangle_{\mathcal{I}_i} + \langle\widetilde{\boldsymbol{\psi}}, \mu_2\tau^{\mathcal{I}}(\boldsymbol{u}_2\cdot(-\widehat{\boldsymbol{n}}) - \widetilde{\boldsymbol{u}}^i\cdot(-\widehat{\boldsymbol{n}}))(-\widehat{\boldsymbol{n}})\rangle_{\mathcal{I}_i} \\
&=\langle\widetilde{\boldsymbol{\psi}}, \boldsymbol{g}_s\rangle_{\mathcal{I}_i}
\end{aligned} \tag{D.1.23}$$

by combining and rearranging some terms, and using the identity $\boldsymbol{I}\boldsymbol{n} = \boldsymbol{n}$, we get

$$\begin{aligned}
&\langle\widetilde{\boldsymbol{\psi}}, \widetilde{p}^i\widehat{\boldsymbol{n}}\rangle_{\mathcal{I}_i} + \langle\widetilde{\boldsymbol{\psi}}, \mu_1\boldsymbol{L}_1\widehat{\boldsymbol{n}}\rangle_{\mathcal{I}_i} + \langle\widetilde{\boldsymbol{\psi}}, \widetilde{p}^i(-\widehat{\boldsymbol{n}})\rangle_{\mathcal{I}_i} + \langle\widetilde{\boldsymbol{\psi}}, \mu_2\boldsymbol{L}_2(-\widehat{\boldsymbol{n}})\rangle_{\mathcal{I}_i} \\
&+\langle\widetilde{\boldsymbol{\psi}}, \mu_1\tau^{\mathcal{I}}\boldsymbol{u}_1\rangle_{\mathcal{I}_i} - \langle\widetilde{\boldsymbol{\psi}}, \mu_1\tau^{\mathcal{I}}\widetilde{\boldsymbol{u}}^i\rangle_{\mathcal{I}_i} + \langle\widetilde{\boldsymbol{\psi}}, \mu_1\tau^{\mathcal{I}}(\boldsymbol{u}_1\cdot\widehat{\boldsymbol{n}})\widehat{\boldsymbol{n}}\rangle_{\mathcal{I}_i} - \langle\widetilde{\boldsymbol{\psi}}, \mu_1\tau^{\mathcal{I}}(\widetilde{\boldsymbol{u}}^i\cdot\widehat{\boldsymbol{n}})\widehat{\boldsymbol{n}}\rangle_{\mathcal{I}_i} \\
&+\langle\widetilde{\boldsymbol{\psi}}, \mu_2\tau^{\mathcal{I}}\boldsymbol{u}_2\rangle_{\mathcal{I}_i} - \langle\widetilde{\boldsymbol{\psi}}, \mu_2\tau^{\mathcal{I}}\widetilde{\boldsymbol{u}}^i\rangle_{\mathcal{I}_i} + \langle\widetilde{\boldsymbol{\psi}}, \mu_2\tau^{\mathcal{I}}(\boldsymbol{u}_2\cdot(-\widehat{\boldsymbol{n}}))(-\widehat{\boldsymbol{n}})\rangle_{\mathcal{I}_i} - \langle\widetilde{\boldsymbol{\psi}}, \mu_2\tau^{\mathcal{I}}(\widetilde{\boldsymbol{u}}^i\cdot(-\widehat{\boldsymbol{n}}))(-\widehat{\boldsymbol{n}})\rangle_{\mathcal{I}_i} \\
&=\langle\widetilde{\boldsymbol{\psi}}, \boldsymbol{g}_s\rangle_{\mathcal{I}_i} - \langle\widetilde{\boldsymbol{\psi}}, (\delta_P\boldsymbol{I} + \mu_1\boldsymbol{\delta}_{\boldsymbol{L}})\,\widehat{\boldsymbol{n}}\rangle_{\mathcal{I}_i} = 0
\end{aligned} \tag{D.1.24}$$

where in the last line $(\delta_P\boldsymbol{I} + \mu_1\boldsymbol{\delta}_{\boldsymbol{L}})$ is replaced by $\boldsymbol{g}_s$.

To obtain the weak form of the *tenth* equation (equation of $\widetilde{p}^i$) in the local problems (6.2.3b), we go through the following steps:

Step 1: the governing equation is multiplied by a scalar test function $\widetilde{\phi} \in \mathcal{S}_s^h(\mathcal{I}_i)$, and integrated over the interface $\mathcal{I}_i$

$$\langle \widetilde{\phi}, [\![\boldsymbol{u} \cdot \boldsymbol{n}]\!] \rangle_{\mathcal{I}_i} = 0 \tag{D.1.25}$$

by using the definition of the jump operator, the equation can be written in an extended form as

$$\langle \widetilde{\phi}, \boldsymbol{u}_1 \cdot \widehat{\boldsymbol{n}} \rangle_{\mathcal{I}_i} + \langle \widetilde{\phi}, \boldsymbol{u}_2 \cdot (-\widehat{\boldsymbol{n}}) \rangle_{\mathcal{I}_i} = 0 \tag{D.1.26}$$

The complete set of equations in a weak form for the local problem in a cut element

Recalling equations (D.1.11), (D.1.17), (D.1.18) and (D.1.24), the weak form of the local problems in a cut element is: given $\widehat{\boldsymbol{u}} \in \mathcal{V}_s^h(\Gamma_{ij} \setminus \Gamma_D)$, $\boldsymbol{u}_D \in \mathcal{V}_s(\Gamma_{ij} \cap \Gamma_D)$, $\widehat{p} \in \mathcal{S}_s^h(\Gamma_{ij})$ and $p_N \in \mathcal{S}_s^h(\Gamma_{ij} \cap \Gamma_N)$, where Γ_{ij} is the face j (which could be cut or uncut) of element K_i, find $\boldsymbol{u} \in [\mathcal{P}^m(K_i)]^d \oplus H[\mathcal{P}^m(K_i)]^d$, $\boldsymbol{L} \in [\mathcal{P}^m(K_i)]^{d\times d} \oplus H[\mathcal{P}^m(K_i)]^{d\times d}$, $p \in \boldsymbol{\nabla}\cdot[\mathcal{P}^m(K_i)]^d \oplus H\boldsymbol{\nabla}\cdot[\mathcal{P}^m(K_i)]^d$, $\widetilde{\boldsymbol{u}}^i \in [\mathcal{P}^m(\mathcal{I}_i)]^d$, and $\widetilde{p}^i \in \mathcal{P}^m(\mathcal{I}_i)$ such that

(D.1.27a)

$$
\begin{aligned}
&(\boldsymbol{\psi}, \rho\frac{\partial \boldsymbol{u}}{\partial t})_{K_i} + (\boldsymbol{\psi}, \boldsymbol{\nabla}\cdot(\mu\boldsymbol{L}))_{K_i} - (\boldsymbol{\nabla}\boldsymbol{\psi}, p\boldsymbol{I})_{K_i} - (\boldsymbol{\nabla}\boldsymbol{\psi}, \rho(\boldsymbol{u}\otimes\boldsymbol{u}))_{K_i} + \langle \boldsymbol{\psi}, \rho(\boldsymbol{u}\otimes\boldsymbol{u})\boldsymbol{n}\rangle_{\partial K_i} \\
&\quad - \langle \boldsymbol{\psi}, \lambda\rho(\boldsymbol{u}\otimes\boldsymbol{u})\boldsymbol{n}\rangle_{\partial K_i} + \langle \boldsymbol{\psi}, \mu\tau\boldsymbol{u}\rangle_{\partial K_i} + \langle \boldsymbol{\psi}, \mu\tau(\boldsymbol{u}\cdot\boldsymbol{n})\boldsymbol{n}\rangle_{\partial K_i} \\
&\quad + \langle \boldsymbol{\psi}_1, \rho_1(\boldsymbol{u}_1\otimes\boldsymbol{u}_1)\widehat{\boldsymbol{n}}\rangle_{\mathcal{I}_i} + \langle \boldsymbol{\psi}_1, \widetilde{p}^i\widehat{\boldsymbol{n}}\rangle_{\mathcal{I}_i} + \langle \boldsymbol{\psi}_2, \rho_2(\boldsymbol{u}_2\otimes\boldsymbol{u}_2)(-\widehat{\boldsymbol{n}})\rangle_{\mathcal{I}_i} + \langle \boldsymbol{\psi}_2, \widetilde{p}^i(-\widehat{\boldsymbol{n}})\rangle_{\mathcal{I}_i} \\
&\quad - \langle \boldsymbol{\psi}_1, \lambda\rho_1(\boldsymbol{u}_1\otimes\boldsymbol{u}_1)\widehat{\boldsymbol{n}}\rangle_{\mathcal{I}_i} + \langle \boldsymbol{\psi}_1, \lambda\rho_1(\widetilde{\boldsymbol{u}}^i\otimes\boldsymbol{u}_1)\widehat{\boldsymbol{n}}\rangle_{\mathcal{I}_i} \\
&\quad + \langle \boldsymbol{\psi}_1, \mu_1\tau^{\mathcal{I}}\boldsymbol{u}_1\rangle_{\mathcal{I}_i} - \langle \boldsymbol{\psi}_1, \mu_1\tau^{\mathcal{I}}\widetilde{\boldsymbol{u}}^i\rangle_{\mathcal{I}_i} \\
&\quad + \langle \boldsymbol{\psi}_1, \mu_1\tau^{\mathcal{I}}(\boldsymbol{u}_1\cdot\widehat{\boldsymbol{n}})\widehat{\boldsymbol{n}}\rangle_{\mathcal{I}_i} - \langle \boldsymbol{\psi}_1, \mu_1\tau^{\mathcal{I}}(\widetilde{\boldsymbol{u}}^i\cdot\widehat{\boldsymbol{n}})\widehat{\boldsymbol{n}}\rangle_{\mathcal{I}_i} \\
&\quad - \langle \boldsymbol{\psi}_2, \lambda\rho_2(\boldsymbol{u}_2\otimes\boldsymbol{u}_2)(-\widehat{\boldsymbol{n}})\rangle_{\mathcal{I}_i} + \langle \boldsymbol{\psi}_2, \lambda\rho_2(\widetilde{\boldsymbol{u}}^i\otimes\boldsymbol{u}_2)(-\widehat{\boldsymbol{n}})\rangle_{\mathcal{I}_i} \\
&\quad + \langle \boldsymbol{\psi}_2, \mu_2\tau^{\mathcal{I}}\boldsymbol{u}_2\rangle_{\mathcal{I}_i} - \langle \boldsymbol{\psi}_2, \mu_2\tau^{\mathcal{I}}\widetilde{\boldsymbol{u}}^i\rangle_{\mathcal{I}_i} \\
&\quad + \langle \boldsymbol{\psi}_2, \mu_2\tau^{\mathcal{I}}(\boldsymbol{u}_2\cdot(-\widehat{\boldsymbol{n}}))(-\widehat{\boldsymbol{n}})\rangle_{\mathcal{I}_i} - \langle \boldsymbol{\psi}_2, \mu_2\tau^{\mathcal{I}}(\widetilde{\boldsymbol{u}}^i\cdot(-\widehat{\boldsymbol{n}}))(-\widehat{\boldsymbol{n}})\rangle_{\mathcal{I}_i} \\
&\quad = (\boldsymbol{\psi}, \rho\boldsymbol{f})_{K_i} - \langle \boldsymbol{\psi}, \lambda\rho(\widehat{\boldsymbol{u}}\otimes\boldsymbol{u})\boldsymbol{n}\rangle_{\partial K_i\setminus\Gamma_D} + \langle \boldsymbol{\psi}, \mu\tau\widehat{\boldsymbol{u}}\rangle_{\partial K_i\setminus\Gamma_D} + \langle \boldsymbol{\psi}, \mu\tau(\widehat{\boldsymbol{u}}\cdot\boldsymbol{n})\boldsymbol{n}\rangle_{\partial K_i\setminus\Gamma_D} \\
&\quad - \langle \boldsymbol{\psi}, \lambda\rho(\boldsymbol{u}_D\otimes\boldsymbol{u})\boldsymbol{n}\rangle_{\partial K_i\cap\Gamma_D} + \langle \boldsymbol{\psi}, \mu\tau\boldsymbol{u}_D\rangle_{\partial K_i\cap\Gamma_D} + \langle \boldsymbol{\psi}, \mu\tau(\boldsymbol{u}_D\cdot\boldsymbol{n})\boldsymbol{n}\rangle_{\partial K_i\cap\Gamma_D} \\
&\quad - \langle \boldsymbol{\psi}, \widehat{p}\boldsymbol{n}\rangle_{\partial K_i\setminus\Gamma_N} - \langle \boldsymbol{\psi}, p_N\boldsymbol{n}\rangle_{\partial K_i\cap\Gamma_N} - \langle \boldsymbol{\psi}_1, \boldsymbol{g}_s\rangle_{\mathcal{I}_i}
\end{aligned}
$$

(D.1.27b)

$$
\begin{aligned}
-(\boldsymbol{\Psi}, \boldsymbol{L})_{K_i} + (\boldsymbol{\nabla}^s\cdot\boldsymbol{\Psi}, \boldsymbol{u})_{K_i} &- \langle \boldsymbol{\Psi}_1, \widetilde{\boldsymbol{u}}^i\otimes\widehat{\boldsymbol{n}}\rangle_{\mathcal{I}_i} - \langle \boldsymbol{\Psi}_1, \widehat{\boldsymbol{n}}\otimes\widetilde{\boldsymbol{u}}^i\rangle_{\mathcal{I}_i} \\
&- \langle \boldsymbol{\Psi}_2, \widetilde{\boldsymbol{u}}^i\otimes(-\widehat{\boldsymbol{n}})\rangle_{\mathcal{I}_i} - \langle \boldsymbol{\Psi}_2, (-\widehat{\boldsymbol{n}})\otimes\widetilde{\boldsymbol{u}}^i\rangle_{\mathcal{I}_i} \\
&= \langle \boldsymbol{\Psi}, \widehat{\boldsymbol{u}}\otimes\boldsymbol{n}\rangle_{\partial K_i\setminus\Gamma_D} + \langle \boldsymbol{\Psi}, \boldsymbol{n}\otimes\widehat{\boldsymbol{u}}\rangle_{\partial K_i\setminus\Gamma_D} \\
&+ \langle \boldsymbol{\Psi}, \boldsymbol{u}_D\otimes\boldsymbol{n}\rangle_{\partial K_i\cap\Gamma_D} + \langle \boldsymbol{\Psi}, \boldsymbol{n}\otimes\boldsymbol{u}_D\rangle_{\partial K_i\cap\Gamma_D}
\end{aligned}
$$

(D.1.27c)

$$
-(\phi, \boldsymbol{\nabla}\cdot\boldsymbol{u})_{K_i} = 0
$$

(D.1.27d)

$$
\begin{aligned}
&\langle \widetilde{\boldsymbol{\psi}}, \widetilde{p}^i\widehat{\boldsymbol{n}}\rangle_{\mathcal{I}_i} + \langle \widetilde{\boldsymbol{\psi}}, \mu_1\boldsymbol{L}_1\widehat{\boldsymbol{n}}\rangle_{\mathcal{I}_i} + \langle \widetilde{\boldsymbol{\psi}}, \widetilde{p}^i(-\widehat{\boldsymbol{n}})\rangle_{\mathcal{I}_i} + \langle \widetilde{\boldsymbol{\psi}}, \mu_2\boldsymbol{L}_2(-\widehat{\boldsymbol{n}})\rangle_{\mathcal{I}_i} \\
&+\langle \widetilde{\boldsymbol{\psi}}, \mu_1\tau^{\mathcal{I}}\boldsymbol{u}_1\rangle_{\mathcal{I}_i} - \langle \widetilde{\boldsymbol{\psi}}, \mu_1\tau^{\mathcal{I}}\widetilde{\boldsymbol{u}}^i\rangle_{\mathcal{I}_i} + \langle \widetilde{\boldsymbol{\psi}}, \mu_1\tau^{\mathcal{I}}(\boldsymbol{u}_1\cdot\widehat{\boldsymbol{n}})\widehat{\boldsymbol{n}}\rangle_{\mathcal{I}_i} - \langle \widetilde{\boldsymbol{\psi}}, \mu_1\tau^{\mathcal{I}}(\widetilde{\boldsymbol{u}}^i\cdot\widehat{\boldsymbol{n}})\widehat{\boldsymbol{n}}\rangle_{\mathcal{I}_i} \\
&+\langle \widetilde{\boldsymbol{\psi}}, \mu_2\tau^{\mathcal{I}}\boldsymbol{u}_2\rangle_{\mathcal{I}_i} - \langle \widetilde{\boldsymbol{\psi}}, \mu_2\tau^{\mathcal{I}}\widetilde{\boldsymbol{u}}^i\rangle_{\mathcal{I}_i} + \langle \widetilde{\boldsymbol{\psi}}, \mu_2\tau^{\mathcal{I}}(\boldsymbol{u}_2\cdot(-\widehat{\boldsymbol{n}}))(-\widehat{\boldsymbol{n}})\rangle_{\mathcal{I}_i} - \langle \widetilde{\boldsymbol{\psi}}, \mu_2\tau^{\mathcal{I}}(\widetilde{\boldsymbol{u}}^i\cdot(-\widehat{\boldsymbol{n}}))(-\widehat{\boldsymbol{n}})\rangle_{\mathcal{I}_i} = 0
\end{aligned}
$$

(D.1.27e)

$$
\langle \widetilde{\phi}, \boldsymbol{u}_1\cdot\widehat{\boldsymbol{n}}\rangle_{\mathcal{I}_i} + \langle \widetilde{\phi}, \boldsymbol{u}_2\cdot(-\widehat{\boldsymbol{n}})\rangle_{\mathcal{I}_i} = 0
$$

for all the test functions $\boldsymbol{\psi} \in [\mathcal{P}^m(K_i)]^d \oplus H[\mathcal{P}^m(K_i)]^d$, $\boldsymbol{\Psi} \in [\mathcal{P}^m(K_i)]^{d\times d} \oplus H[\mathcal{P}^m(K_i)]^{d\times d}$, $\phi \in \boldsymbol{\nabla}\cdot[\mathcal{P}^m(K_i)]^d \oplus H\boldsymbol{\nabla}\cdot[\mathcal{P}^m(K_i)]^d$, $\widetilde{\boldsymbol{\psi}} \in [\mathcal{P}^m(\mathcal{I}_i)]^d$, and $\widetilde{\phi} \in \mathcal{P}^m(\mathcal{I}_i)$.

D.2 Weak local problems in standard elements

For a standard uncut element K_i, the weak forms of the local problems (6.2.3a) are exactly the same as those for a cut element after removing the interface terms. Note that the approximation spaces for all the functions will be continuous. i.e. $(\boldsymbol{\psi}, \boldsymbol{u}) \in [\mathcal{P}^m(K_i)]^d$, $(\boldsymbol{\Psi}, \boldsymbol{L}) \in [\mathcal{P}^m(K_i)]^{d\times d}$, $(\phi, p) \in \boldsymbol{\nabla}\cdot[\mathcal{P}^m(K_i)]^d$, $\widehat{\boldsymbol{u}} \in [\mathcal{P}^m(\Gamma_{ij} \setminus \Gamma_D)]^d$ and $\widehat{p} \in \mathcal{P}^m(\Gamma_{ij})$, where Γ_{ij} is the face j of element K_i.
Therefore, the weak form of the local problems in a standard uncut element is: given $(\widehat{\boldsymbol{u}}, \boldsymbol{u}_D, \widehat{p}, p_N)$, find $(\boldsymbol{u}, \boldsymbol{L}, p)$ such that

(D.2.1a)

$$
\begin{aligned}
(\boldsymbol{\psi}, \rho\frac{\partial \boldsymbol{u}}{\partial t})_{K_i} + (\boldsymbol{\psi}, \boldsymbol{\nabla}\cdot(\mu\boldsymbol{L}))_{K_i} - (\boldsymbol{\nabla}\boldsymbol{\psi}, p\boldsymbol{I})_{K_i} - (\boldsymbol{\nabla}\boldsymbol{\psi}, \rho(\boldsymbol{u}\otimes\boldsymbol{u}))_{K_i} + \langle \boldsymbol{\psi}, \rho(\boldsymbol{u}\otimes\boldsymbol{u})\boldsymbol{n}\rangle_{\partial K_i} \\
- \langle \boldsymbol{\psi}, \lambda\rho(\boldsymbol{u}\otimes\boldsymbol{u})\boldsymbol{n}\rangle_{\partial K_i} + \langle \boldsymbol{\psi}, \mu\tau\boldsymbol{u}\rangle_{\partial K_i} + \langle \boldsymbol{\psi}, \mu\tau(\boldsymbol{u}\cdot\boldsymbol{n})\boldsymbol{n}\rangle_{\partial K_i} \\
= (\boldsymbol{\psi}, \rho\boldsymbol{f})_{K_i} - \langle \boldsymbol{\psi}, \lambda\rho(\widehat{\boldsymbol{u}}\otimes\boldsymbol{u})\boldsymbol{n}\rangle_{\partial K_i\setminus\Gamma_D} + \langle \boldsymbol{\psi}, \mu\tau\widehat{\boldsymbol{u}}\rangle_{\partial K_i\setminus\Gamma_D} + \langle \boldsymbol{\psi}, \mu\tau(\widehat{\boldsymbol{u}}\cdot\boldsymbol{n})\boldsymbol{n}\rangle_{\partial K_i\setminus\Gamma_D} \\
- \langle \boldsymbol{\psi}, \lambda\rho(\boldsymbol{u}_D\otimes\boldsymbol{u})\boldsymbol{n}\rangle_{\partial K_i\cap\Gamma_D} + \langle \boldsymbol{\psi}, \mu\tau\boldsymbol{u}_D\rangle_{\partial K_i\cap\Gamma_D} + \langle \boldsymbol{\psi}, \mu\tau(\boldsymbol{u}_D\cdot\boldsymbol{n})\boldsymbol{n}\rangle_{\partial K_i\cap\Gamma_D} \\
- \langle \boldsymbol{\psi}, \widehat{p}\boldsymbol{n}\rangle_{\partial K_i\setminus\Gamma_N} - \langle \boldsymbol{\psi}, p_N\boldsymbol{n}\rangle_{\partial K_i\cap\Gamma_N}
\end{aligned}
$$

(D.2.1b)

$$
\begin{aligned}
-(\boldsymbol{\Psi}, \boldsymbol{L})_{K_i} + (\boldsymbol{\nabla}^s\cdot\boldsymbol{\Psi}, \boldsymbol{u})_{K_i} = \langle \boldsymbol{\Psi}, \widehat{\boldsymbol{u}}\otimes\boldsymbol{n}\rangle_{\partial K_i\setminus\Gamma_D} + \langle \boldsymbol{\Psi}, \boldsymbol{n}\otimes\widehat{\boldsymbol{u}}\rangle_{\partial K_i\setminus\Gamma_D} \\
+ \langle \boldsymbol{\Psi}, \boldsymbol{u}_D\otimes\boldsymbol{n}\rangle_{\partial K_i\cap\Gamma_D} + \langle \boldsymbol{\Psi}, \boldsymbol{n}\otimes\boldsymbol{u}_D\rangle_{\partial K_i\cap\Gamma_D}
\end{aligned}
$$

(D.2.1c)

$$
-(\phi, \boldsymbol{\nabla}\cdot\boldsymbol{u})_{K_i} = 0
$$

for all the test functions $(\boldsymbol{\psi}, \boldsymbol{\Psi}, \phi)$.

D.3 Weak global problem

We recall that the trace variables $\widehat{\boldsymbol{u}} \in \mathcal{V}_s^h(\Gamma \setminus \Gamma_D)$ and $\widehat{p} \in \mathcal{S}_s^h(\Gamma \setminus \Gamma_N)$ are required to solve the element-by-element local problems. These variable are obtained by solving the global problem (6.2.5).

To obtain the weak form of the *first* and *second* equations in the global problem (6.2.5), we go through the following steps:

Step 1: the first governing equation is multiplied by a vector test function $\widehat{\boldsymbol{\psi}} \in \mathcal{V}_s^h(\Gamma \setminus \Gamma_D)$, and integrated over the edges $\Gamma \setminus \partial\Omega$. In this step the expression of the jump is written in an extended form. The second governing equation (the Neumann boundary condition) is also multiplied by the same test function $\widehat{\boldsymbol{\psi}}$, and integrated over the Neumann boundary Γ_N.

(D.3.1)
$$\langle\widehat{\boldsymbol{\psi}}, \left(\rho(\boldsymbol{u}^+ \otimes \boldsymbol{u}^+) + p^+\boldsymbol{I} + \mu^+\boldsymbol{L}^+\right)\boldsymbol{n}^+\rangle_{\Gamma\setminus\partial\Omega} + \langle\widehat{\boldsymbol{\psi}}, \left(\rho(\boldsymbol{u}^- \otimes \boldsymbol{u}^-) + p^-\boldsymbol{I} + \mu^-\boldsymbol{L}^-\right)\boldsymbol{n}^-\rangle_{\Gamma\setminus\partial\Omega} = 0,$$

(D.3.2)
$$\langle\widehat{\boldsymbol{\psi}}, \left(\rho(\boldsymbol{u} \otimes \boldsymbol{u}) + p\boldsymbol{I} + \mu\boldsymbol{L}\right)\boldsymbol{n} - \boldsymbol{g}_N - \rho(1-\lambda)(\boldsymbol{u}\cdot\boldsymbol{n})\boldsymbol{u}\rangle_{\Gamma_N} = 0,$$

by summing the previous equations we get

(D.3.3)
$$\begin{aligned}&\langle\widehat{\boldsymbol{\psi}}, \left(\rho(\boldsymbol{u}^+ \otimes \boldsymbol{u}^+) + p^+\boldsymbol{I} + \mu^+\boldsymbol{L}^+\right)\boldsymbol{n}^+\rangle_{\Gamma\setminus\partial\Omega} + \langle\widehat{\boldsymbol{\psi}}, \left(\rho(\boldsymbol{u}^- \otimes \boldsymbol{u}^-) + p^-\boldsymbol{I} + \mu^-\boldsymbol{L}^-\right)\boldsymbol{n}^-\rangle_{\Gamma\setminus\partial\Omega}\\ &+\langle\widehat{\boldsymbol{\psi}}, \left(\rho(\boldsymbol{u} \otimes \boldsymbol{u}) + p\boldsymbol{I} + \mu\boldsymbol{L}\right)\boldsymbol{n} - \boldsymbol{g}_N - \rho(1-\lambda)(\boldsymbol{u}\cdot\boldsymbol{n})\boldsymbol{u}\rangle_{\Gamma_N} = 0\end{aligned}$$

Step 2: In the HDG method, the physical quantities $((\boldsymbol{u}\otimes\boldsymbol{u}), \boldsymbol{L}, p)$ are replaced by the numerical quantities $((\widehat{\boldsymbol{u}\otimes\boldsymbol{u}}), \widehat{\boldsymbol{L}}, \widehat{p})$ on the edges $\Gamma \setminus \Gamma_D$

(D.3.4)
$$\begin{aligned}&\langle\widehat{\boldsymbol{\psi}}, \left(\rho(\widehat{\boldsymbol{u}^+\otimes\boldsymbol{u}^+}) + \widehat{p}\boldsymbol{I} + \mu^+\widehat{\boldsymbol{L}}^+\right)\boldsymbol{n}^+\rangle_{\Gamma\setminus\partial\Omega} + \langle\widehat{\boldsymbol{\psi}}, \left(\rho(\widehat{\boldsymbol{u}^-\otimes\boldsymbol{u}^-}) + \widehat{p}\boldsymbol{I} + \mu^-\widehat{\boldsymbol{L}}^-\right)\boldsymbol{n}^-\rangle_{\Gamma\setminus\partial\Omega}\\ &+\langle\widehat{\boldsymbol{\psi}}, \left(\rho(\widehat{\boldsymbol{u}\otimes\boldsymbol{u}}) + \widehat{p}\boldsymbol{I} + \mu\widehat{\boldsymbol{L}}\right)\boldsymbol{n} - \boldsymbol{g}_N - \rho(1-\lambda)(\boldsymbol{u}\cdot\boldsymbol{n})\widehat{\boldsymbol{u}}\rangle_{\Gamma_N} = 0\end{aligned}$$

After introducing the numerical fluxes, that were defined earlier, into equation (D.3.4), we get

(D.3.5)
$$\begin{aligned}&\langle\widehat{\boldsymbol{\psi}}, \left(\rho(\boldsymbol{u}^+ \otimes \boldsymbol{u}^+) + \rho(\widehat{\boldsymbol{u}} - \boldsymbol{u}^+)\otimes\lambda\boldsymbol{u}^+ + \widehat{p}\boldsymbol{I} + \mu^+\boldsymbol{L}^+ + \mu^+\tau(\boldsymbol{u}^+ - \widehat{\boldsymbol{u}})\otimes\boldsymbol{n}^+\right)\boldsymbol{n}^+\rangle_{\Gamma\setminus\partial\Omega}\\ &+\langle\widehat{\boldsymbol{\psi}}, \left(\mu^+\tau\boldsymbol{n}^+ \otimes (\boldsymbol{u}^+ - \widehat{\boldsymbol{u}})\right)\boldsymbol{n}^+\rangle_{\Gamma\setminus\partial\Omega}\\ &+\langle\widehat{\boldsymbol{\psi}}, \left(\rho(\boldsymbol{u}^- \otimes \boldsymbol{u}^-) + \rho(\widehat{\boldsymbol{u}} - \boldsymbol{u}^-)\otimes\lambda\boldsymbol{u}^- + \widehat{p}\boldsymbol{I} + \mu^-\boldsymbol{L}^- + \mu^-\tau(\boldsymbol{u}^- - \widehat{\boldsymbol{u}})\otimes\boldsymbol{n}^-\right)\boldsymbol{n}^-\rangle_{\Gamma\setminus\partial\Omega}\\ &+\langle\widehat{\boldsymbol{\psi}}, \left(\mu^-\tau\boldsymbol{n}^- \otimes (\boldsymbol{u}^- - \widehat{\boldsymbol{u}})\right)\boldsymbol{n}^-\rangle_{\Gamma\setminus\partial\Omega}\\ &+\langle\widehat{\boldsymbol{\psi}}, \left(\rho(\boldsymbol{u} \otimes \boldsymbol{u}) + \rho(\widehat{\boldsymbol{u}} - \boldsymbol{u})\otimes\lambda\boldsymbol{u} + \widehat{p}\boldsymbol{I} + \mu\boldsymbol{L} + \mu\tau(\boldsymbol{u} - \widehat{\boldsymbol{u}})\otimes\boldsymbol{n}\right)\boldsymbol{n}\rangle_{\Gamma_N}\\ &+\langle\widehat{\boldsymbol{\psi}}, \left(\mu\tau\boldsymbol{n} \otimes (\boldsymbol{u} - \widehat{\boldsymbol{u}})\right)\boldsymbol{n}\rangle_{\Gamma_N}\\ &-\langle\widehat{\boldsymbol{\psi}}, \rho(1-\lambda)(\boldsymbol{u}\cdot\boldsymbol{n})\widehat{\boldsymbol{u}}\rangle_{\Gamma_N}\\ &=\langle\widehat{\boldsymbol{\psi}}, \boldsymbol{g}_N\rangle_{\Gamma_N}\end{aligned}$$

by splitting the terms we get

$$
\begin{aligned}
&\langle\widehat{\boldsymbol{\psi}}, \left(\rho(\boldsymbol{u}^+\otimes\boldsymbol{u}^+)+\widehat{p}\boldsymbol{I}+\mu^+\boldsymbol{L}^+\right)\boldsymbol{n}^+\rangle_{\Gamma\setminus\partial\Omega}\\
+&\langle\widehat{\boldsymbol{\psi}}, \left(\rho(\boldsymbol{u}^-\otimes\boldsymbol{u}^-)+\widehat{p}\boldsymbol{I}+\mu^-\boldsymbol{L}^-\right)\boldsymbol{n}^-\rangle_{\Gamma\setminus\partial\Omega}\\
+&\langle\widehat{\boldsymbol{\psi}}, \left(\rho(\boldsymbol{u}\otimes\boldsymbol{u})+\widehat{p}\boldsymbol{I}+\mu\boldsymbol{L}\right)\boldsymbol{n}\rangle_{\Gamma_N}\\
+&\langle\widehat{\boldsymbol{\psi}}, \left(\rho(\widehat{\boldsymbol{u}}-\boldsymbol{u}^+)\otimes\lambda\boldsymbol{u}^+ + \mu^+\tau(\boldsymbol{u}^+-\widehat{\boldsymbol{u}})\otimes\boldsymbol{n}^+\right)\boldsymbol{n}^+\rangle_{\Gamma\setminus\partial\Omega}\\
+&\langle\widehat{\boldsymbol{\psi}}, \left(\mu^+\tau\boldsymbol{n}^+\otimes(\boldsymbol{u}^+-\widehat{\boldsymbol{u}})\right)\boldsymbol{n}^+\rangle_{\Gamma\setminus\partial\Omega}\\
+&\langle\widehat{\boldsymbol{\psi}}, \left(\rho(\widehat{\boldsymbol{u}}-\boldsymbol{u}^-)\otimes\lambda\boldsymbol{u}^- + \mu^-\tau(\boldsymbol{u}^--\widehat{\boldsymbol{u}})\otimes\boldsymbol{n}^-\right)\boldsymbol{n}^-\rangle_{\Gamma\setminus\partial\Omega}\\
+&\langle\widehat{\boldsymbol{\psi}}, \left(\mu^-\tau\boldsymbol{n}^-\otimes(\boldsymbol{u}^--\widehat{\boldsymbol{u}})\right)\boldsymbol{n}^-\rangle_{\Gamma\setminus\partial\Omega}\\
+&\langle\widehat{\boldsymbol{\psi}}, \left(\rho(\widehat{\boldsymbol{u}}-\boldsymbol{u})\otimes\lambda\boldsymbol{u} + \mu\tau(\boldsymbol{u}-\widehat{\boldsymbol{u}})\otimes\boldsymbol{n}\right)\boldsymbol{n}\rangle_{\Gamma_N}\\
+&\langle\widehat{\boldsymbol{\psi}}, \left(\mu\tau\boldsymbol{n}\otimes(\boldsymbol{u}-\widehat{\boldsymbol{u}})\right)\boldsymbol{n}\rangle_{\Gamma_N}\\
-&\langle\widehat{\boldsymbol{\psi}}, \rho(1-\lambda)(\boldsymbol{u}\cdot\boldsymbol{n})\widehat{\boldsymbol{u}}\rangle_{\Gamma_N}\\
=&\langle\widehat{\boldsymbol{\psi}}, \boldsymbol{g}_N\rangle_{\Gamma_N}
\end{aligned}
\tag{D.3.6}
$$

using the tensor identity $(\boldsymbol{a}\otimes\boldsymbol{u})\boldsymbol{n} = (\boldsymbol{u}\cdot\boldsymbol{n})\boldsymbol{a}$, the previous equation is simplified to

$$
\begin{aligned}
&\langle\widehat{\boldsymbol{\psi}}, \left(\rho(\boldsymbol{u}^+\otimes\boldsymbol{u}^+)+\widehat{p}\boldsymbol{I}+\mu^+\boldsymbol{L}^+\right)\boldsymbol{n}^+\rangle_{\Gamma\setminus\partial\Omega}\\
+&\langle\widehat{\boldsymbol{\psi}}, \left(\rho(\boldsymbol{u}^-\otimes\boldsymbol{u}^-)+\widehat{p}\boldsymbol{I}+\mu^-\boldsymbol{L}^-\right)\boldsymbol{n}^-\rangle_{\Gamma\setminus\partial\Omega}\\
+&\langle\widehat{\boldsymbol{\psi}}, \left(\rho(\boldsymbol{u}\otimes\boldsymbol{u})+\widehat{p}\boldsymbol{I}+\mu\boldsymbol{L}\right)\boldsymbol{n}\rangle_{\Gamma_N}\\
+&\langle\widehat{\boldsymbol{\psi}}, (\rho(\widehat{\boldsymbol{u}}-\boldsymbol{u}^+)\otimes\lambda\boldsymbol{u}^+)\boldsymbol{n}^+\rangle_{\Gamma\setminus\partial\Omega} + \langle\widehat{\boldsymbol{\psi}}, \mu^+\tau(\boldsymbol{u}^+-\widehat{\boldsymbol{u}})\rangle_{\Gamma\setminus\partial\Omega}\\
+&\langle\widehat{\boldsymbol{\psi}}, \mu^+\tau(\boldsymbol{u}^+\cdot\boldsymbol{n}^+-\widehat{\boldsymbol{u}}\cdot\boldsymbol{n}^+)\boldsymbol{n}^+\rangle_{\Gamma\setminus\partial\Omega}\\
+&\langle\widehat{\boldsymbol{\psi}}, (\rho(\widehat{\boldsymbol{u}}-\boldsymbol{u}^-)\otimes\lambda\boldsymbol{u}^-)\boldsymbol{n}^-\rangle_{\Gamma\setminus\partial\Omega} + \langle\widehat{\boldsymbol{\psi}}, \mu^-\tau(\boldsymbol{u}^--\widehat{\boldsymbol{u}})\rangle_{\Gamma\setminus\partial\Omega}\\
+&\langle\widehat{\boldsymbol{\psi}}, \mu^-\tau(\boldsymbol{u}^-\cdot\boldsymbol{n}^--\widehat{\boldsymbol{u}}\cdot\boldsymbol{n}^-)\boldsymbol{n}^-\rangle_{\Gamma\setminus\partial\Omega}\\
+&\langle\widehat{\boldsymbol{\psi}}, (\rho(\widehat{\boldsymbol{u}}-\boldsymbol{u})\otimes\lambda\boldsymbol{u})\boldsymbol{n}\rangle_{\Gamma_N} + \langle\widehat{\boldsymbol{\psi}}, \mu\tau(\boldsymbol{u}-\widehat{\boldsymbol{u}})\rangle_{\Gamma_N}\\
+&\langle\widehat{\boldsymbol{\psi}}, \mu\tau(\boldsymbol{u}\cdot\boldsymbol{n}-\widehat{\boldsymbol{u}}\cdot\boldsymbol{n})\boldsymbol{n}\rangle_{\Gamma_N}\\
-&\langle\widehat{\boldsymbol{\psi}}, \rho(1-\lambda)(\boldsymbol{u}\cdot\boldsymbol{n})\widehat{\boldsymbol{u}}\rangle_{\Gamma_N}\\
=&\langle\widehat{\boldsymbol{\psi}}, \boldsymbol{g}_N\rangle_{\Gamma_N}
\end{aligned}
\tag{D.3.7}
$$

by combining and rearranging some terms, and using the identity $\boldsymbol{I}\boldsymbol{n} = \boldsymbol{n}$, we get

(D.3.8)
$$
\begin{aligned}
&\langle\widehat{\boldsymbol{\psi}}, \rho(\boldsymbol{u}^+\otimes\boldsymbol{u}^+)\boldsymbol{n}^+\rangle_{\Gamma\setminus\partial\Omega} + \langle\widehat{\boldsymbol{\psi}}, \widehat{p}\boldsymbol{n}^+\rangle_{\Gamma\setminus\partial\Omega} + \langle\widehat{\boldsymbol{\psi}}, \mu^+\boldsymbol{L}^+\boldsymbol{n}^+\rangle_{\Gamma\setminus\partial\Omega}\\
&+\langle\widehat{\boldsymbol{\psi}}, \rho(\boldsymbol{u}^-\otimes\boldsymbol{u}^-)\boldsymbol{n}^-\rangle_{\Gamma\setminus\partial\Omega} + \langle\widehat{\boldsymbol{\psi}}, \widehat{p}\boldsymbol{n}^-\rangle_{\Gamma\setminus\partial\Omega} + \langle\widehat{\boldsymbol{\psi}}, \mu^-\boldsymbol{L}^-\boldsymbol{n}^-\rangle_{\Gamma\setminus\partial\Omega}\\
&+\langle\widehat{\boldsymbol{\psi}}, \rho(\boldsymbol{u}\otimes\boldsymbol{u})\boldsymbol{n}\rangle_{\Gamma_N} + \langle\widehat{\boldsymbol{\psi}}, \widehat{p}\boldsymbol{n}\rangle_{\Gamma_N} + \langle\widehat{\boldsymbol{\psi}}, \mu\boldsymbol{L}\boldsymbol{n}\rangle_{\Gamma_N}\\
&-\langle\widehat{\boldsymbol{\psi}}, \lambda\rho(\boldsymbol{u}^+\otimes\boldsymbol{u}^+)\boldsymbol{n}^+\rangle_{\Gamma\setminus\partial\Omega} + \langle\widehat{\boldsymbol{\psi}}, \lambda\rho(\widehat{\boldsymbol{u}}\otimes\boldsymbol{u}^+)\boldsymbol{n}^+\rangle_{\Gamma\setminus\partial\Omega} + \langle\widehat{\boldsymbol{\psi}}, \mu^+\tau\boldsymbol{u}^+\rangle_{\Gamma\setminus\partial\Omega} - \langle\widehat{\boldsymbol{\psi}}, \mu^+\tau\widehat{\boldsymbol{u}}\rangle_{\Gamma\setminus\partial\Omega}\\
&+\langle\widehat{\boldsymbol{\psi}}, \mu^+\tau(\boldsymbol{u}^+\cdot\boldsymbol{n}^+)\boldsymbol{n}^+\rangle_{\Gamma\setminus\partial\Omega} - \langle\widehat{\boldsymbol{\psi}}, \mu^+\tau(\widehat{\boldsymbol{u}}\cdot\boldsymbol{n}^+)\boldsymbol{n}^+\rangle_{\Gamma\setminus\partial\Omega}\\
&-\langle\widehat{\boldsymbol{\psi}}, \lambda\rho(\boldsymbol{u}^-\otimes\boldsymbol{u}^-)\boldsymbol{n}^-\rangle_{\Gamma\setminus\partial\Omega} + \langle\widehat{\boldsymbol{\psi}}, \lambda\rho(\widehat{\boldsymbol{u}}\otimes\boldsymbol{u}^-)\boldsymbol{n}^-\rangle_{\Gamma\setminus\partial\Omega} + \langle\widehat{\boldsymbol{\psi}}, \mu^-\tau\boldsymbol{u}^-\rangle_{\Gamma\setminus\partial\Omega} - \langle\widehat{\boldsymbol{\psi}}, \mu^-\tau\widehat{\boldsymbol{u}}\rangle_{\Gamma\setminus\partial\Omega}\\
&+\langle\widehat{\boldsymbol{\psi}}, \mu^-\tau(\boldsymbol{u}^-\cdot\boldsymbol{n}^-)\boldsymbol{n}^-\rangle_{\Gamma\setminus\partial\Omega} - \langle\widehat{\boldsymbol{\psi}}, \mu^-\tau(\widehat{\boldsymbol{u}}\cdot\boldsymbol{n}^-)\boldsymbol{n}^-\rangle_{\Gamma\setminus\partial\Omega}\\
&-\langle\widehat{\boldsymbol{\psi}}, \lambda\rho(\boldsymbol{u}\otimes\boldsymbol{u})\boldsymbol{n}\rangle_{\Gamma_N} + \langle\widehat{\boldsymbol{\psi}}, \lambda\rho(\widehat{\boldsymbol{u}}\otimes\boldsymbol{u})\boldsymbol{n}\rangle_{\Gamma_N} + \langle\widehat{\boldsymbol{\psi}}, \mu\tau\boldsymbol{u}\rangle_{\Gamma_N} - \langle\widehat{\boldsymbol{\psi}}, \mu\tau\widehat{\boldsymbol{u}}\rangle_{\Gamma_N}\\
&+\langle\widehat{\boldsymbol{\psi}}, \mu\tau(\boldsymbol{u}\cdot\boldsymbol{n})\boldsymbol{n}\rangle_{\Gamma_N} - \langle\widehat{\boldsymbol{\psi}}, \mu\tau(\widehat{\boldsymbol{u}}\cdot\boldsymbol{n})\boldsymbol{n}\rangle_{\Gamma_N}\\
&-\langle\widehat{\boldsymbol{\psi}}, \rho(1-\lambda)(\boldsymbol{u}\cdot\boldsymbol{n})\widehat{\boldsymbol{u}}\rangle_{\Gamma_N}\\
&=\langle\widehat{\boldsymbol{\psi}}, \boldsymbol{g}_N\rangle_{\Gamma_N}
\end{aligned}
$$

For ease of implementation, the weak form of the global problem could be written as a summation of surface integrals from all the elements in the computational domain

(D.3.9)
$$
\begin{aligned}
\sum_{i=1}^{\mathtt{n_{el}}}\Big\{&\langle\widehat{\boldsymbol{\psi}}, \rho(\boldsymbol{u}\otimes\boldsymbol{u})\boldsymbol{n}\rangle_{\partial K_i\setminus\Gamma_D} + \langle\widehat{\boldsymbol{\psi}}, \widehat{p}\boldsymbol{n}\rangle_{\partial K_i\setminus\Gamma_D} + \langle\widehat{\boldsymbol{\psi}}, \mu\boldsymbol{L}\boldsymbol{n}\rangle_{\partial K_i\setminus\Gamma_D}\\
&-\langle\widehat{\boldsymbol{\psi}}, \lambda\rho(\boldsymbol{u}\otimes\boldsymbol{u})\boldsymbol{n}\rangle_{\partial K_i\setminus\Gamma_D} + \langle\widehat{\boldsymbol{\psi}}, \lambda\rho(\widehat{\boldsymbol{u}}\otimes\boldsymbol{u})\boldsymbol{n}\rangle_{\partial K_i\setminus\Gamma_D}\\
&+\langle\widehat{\boldsymbol{\psi}}, \mu\tau\boldsymbol{u}\rangle_{\partial K_i\setminus\Gamma_D} - \langle\widehat{\boldsymbol{\psi}}, \mu\tau\widehat{\boldsymbol{u}}\rangle_{\partial K_i\setminus\Gamma_D}\\
&+\langle\widehat{\boldsymbol{\psi}}, \mu\tau(\boldsymbol{u}\cdot\boldsymbol{n})\boldsymbol{n}\rangle_{\partial K_i\setminus\Gamma_D} - \langle\widehat{\boldsymbol{\psi}}, \mu\tau(\widehat{\boldsymbol{u}}\cdot\boldsymbol{n})\boldsymbol{n}\rangle_{\partial K_i\setminus\Gamma_D}\\
&-\langle\widehat{\boldsymbol{\psi}}, \rho(1-\lambda)(\boldsymbol{u}\cdot\boldsymbol{n})\widehat{\boldsymbol{u}}\rangle_{\partial K_i\cap\Gamma_N}\Big\} = \sum_{i=1}^{\mathtt{n_{el}}}\langle\widehat{\boldsymbol{\psi}}, \boldsymbol{g}_N\rangle_{\partial K_i\cap\Gamma_N}
\end{aligned}
$$

Finally, $\widehat{p}$ is replaced by p_N on Γ_N, so we get

(D.3.10)
$$
\begin{aligned}
\sum_{i=1}^{\mathtt{n_{el}}}\Big\{&\langle\widehat{\boldsymbol{\psi}}, \rho(\boldsymbol{u}\otimes\boldsymbol{u})\boldsymbol{n}\rangle_{\partial K_i\setminus\Gamma_D} + \langle\widehat{\boldsymbol{\psi}}, \widehat{p}\boldsymbol{n}\rangle_{\partial K_i\setminus\partial\Omega} + \langle\widehat{\boldsymbol{\psi}}, \mu\boldsymbol{L}\boldsymbol{n}\rangle_{\partial K_i\setminus\Gamma_D}\\
&-\langle\widehat{\boldsymbol{\psi}}, \lambda\rho(\boldsymbol{u}\otimes\boldsymbol{u})\boldsymbol{n}\rangle_{\partial K_i\setminus\Gamma_D} + \langle\widehat{\boldsymbol{\psi}}, \lambda\rho(\widehat{\boldsymbol{u}}\otimes\boldsymbol{u})\boldsymbol{n}\rangle_{\partial K_i\setminus\Gamma_D}\\
&+\langle\widehat{\boldsymbol{\psi}}, \mu\tau\boldsymbol{u}\rangle_{\partial K_i\setminus\Gamma_D} - \langle\widehat{\boldsymbol{\psi}}, \mu\tau\widehat{\boldsymbol{u}}\rangle_{\partial K_i\setminus\Gamma_D}\\
&+\langle\widehat{\boldsymbol{\psi}}, \mu\tau(\boldsymbol{u}\cdot\boldsymbol{n})\boldsymbol{n}\rangle_{\partial K_i\setminus\Gamma_D} - \langle\widehat{\boldsymbol{\psi}}, \mu\tau(\widehat{\boldsymbol{u}}\cdot\boldsymbol{n})\boldsymbol{n}\rangle_{\partial K_i\setminus\Gamma_D}\\
&-\langle\widehat{\boldsymbol{\psi}}, \rho(1-\lambda)(\boldsymbol{u}\cdot\boldsymbol{n})\widehat{\boldsymbol{u}}\rangle_{\partial K_i\cap\Gamma_N}\Big\}\\
&= \sum_{i=1}^{\mathtt{n_{el}}}\Big\{\langle\widehat{\boldsymbol{\psi}}, \boldsymbol{g}_N\rangle_{\partial K_i\cap\Gamma_N} - \langle\widehat{\boldsymbol{\psi}}, p_N\boldsymbol{n}\rangle_{\partial K_i\cap\Gamma_N}\Big\}
\end{aligned}
$$

To obtain the weak form of the *third* equation in the global problem (6.2.5), we go through the following steps:

Step 1: The governing equations are:

$$[\![\boldsymbol{u}\cdot\boldsymbol{n}]\!] = 0, \qquad \text{on } \Gamma\setminus\partial\Omega \tag{D.3.11}$$

$$\boldsymbol{u}\cdot\boldsymbol{n} = \boldsymbol{u}_D\cdot\boldsymbol{n}, \qquad \text{on } \Gamma_D \tag{D.3.12}$$

$$\boldsymbol{u}\cdot\boldsymbol{n} = \widehat{\boldsymbol{u}}\cdot\boldsymbol{n}, \qquad \text{on } \Gamma_N \tag{D.3.13}$$

.

Step 2: The governing equations are multiplied by a scalar test function $\widehat{\phi}\in\mathcal{S}_s^h(\Gamma)$, and integrated over the respective faces:

$$\langle\widehat{\phi},[\![\boldsymbol{u}\cdot\boldsymbol{n}]\!]\rangle_{\Gamma\setminus\partial\Omega}+\langle\widehat{\phi},\boldsymbol{u}\cdot\boldsymbol{n}-\boldsymbol{u}_D\cdot\boldsymbol{n}\rangle_{\Gamma_D}+\langle\widehat{\phi},\boldsymbol{u}\cdot\boldsymbol{n}-\widehat{\boldsymbol{u}}\cdot\boldsymbol{n}\rangle_{\Gamma_N}=0 \tag{D.3.14}$$

by splitting the terms we get

$$\langle\widehat{\phi},[\![\boldsymbol{u}\cdot\boldsymbol{n}]\!]\rangle_{\Gamma\setminus\partial\Omega}+\langle\widehat{\phi},\boldsymbol{u}\cdot\boldsymbol{n}\rangle_{\Gamma_D}+\langle\widehat{\phi},\boldsymbol{u}\cdot\boldsymbol{n}\rangle_{\Gamma_N}-\langle\widehat{\phi},\boldsymbol{u}_D\cdot\boldsymbol{n}\rangle_{\Gamma_D}-\langle\widehat{\phi},\widehat{\boldsymbol{u}}\cdot\boldsymbol{n}\rangle_{\Gamma_N}=0 \tag{D.3.15}$$

and by moving the known terms to the right hand side we get

$$\langle\widehat{\phi},[\![\boldsymbol{u}\cdot\boldsymbol{n}]\!]\rangle_{\Gamma\setminus\partial\Omega}+\langle\widehat{\phi},\boldsymbol{u}\cdot\boldsymbol{n}\rangle_{\Gamma_D}+\langle\widehat{\phi},\boldsymbol{u}\cdot\boldsymbol{n}\rangle_{\Gamma_N}-\langle\widehat{\phi},\widehat{\boldsymbol{u}}\cdot\boldsymbol{n}\rangle_{\Gamma_N}=\langle\widehat{\phi},\boldsymbol{u}_D\cdot\boldsymbol{n}\rangle_{\Gamma_D} \tag{D.3.16}$$

For ease of implementation, this weak form could be written as a summation of surface integrals from all the elements in the computational domain

$$\sum_{i=1}^{\mathtt{n_{el}}}\Big\{\langle\widehat{\phi},\boldsymbol{u}\cdot\boldsymbol{n}\rangle_{\partial K_i}-\langle\widehat{\phi},\widehat{\boldsymbol{u}}\cdot\boldsymbol{n}\rangle_{\partial K_i\cap\Gamma_N}\Big\}=\sum_{i=1}^{\mathtt{n_{el}}}\langle\widehat{\phi},\boldsymbol{u}_D\cdot\boldsymbol{n}\rangle_{\partial K_i\cap\Gamma_D} \tag{D.3.17}$$

The complete set of equations in a weak form for the global problem
Find $\widehat{\boldsymbol{u}}\in\mathcal{V}_s^h(\Gamma\setminus\Gamma_D)$ and $\widehat{p}\in\mathcal{S}_s^h(\Gamma\setminus\Gamma_N)$ such that

$$\begin{aligned}\sum_{i=1}^{\mathtt{n_{el}}}\Big\{&\langle\widehat{\boldsymbol{\psi}},\rho(\boldsymbol{u}\otimes\boldsymbol{u})\boldsymbol{n}\rangle_{\partial K_i\setminus\Gamma_D}+\langle\widehat{\boldsymbol{\psi}},\widehat{p}\boldsymbol{n}\rangle_{\partial K_i\setminus\partial\Omega}+\langle\widehat{\boldsymbol{\psi}},\mu\boldsymbol{L}\boldsymbol{n}\rangle_{\partial K_i\setminus\Gamma_D}\\
&-\langle\widehat{\boldsymbol{\psi}},\lambda\rho(\boldsymbol{u}\otimes\boldsymbol{u})\boldsymbol{n}\rangle_{\partial K_i\setminus\Gamma_D}+\langle\widehat{\boldsymbol{\psi}},\lambda\rho(\widehat{\boldsymbol{u}}\otimes\boldsymbol{u})\boldsymbol{n}\rangle_{\partial K_i\setminus\Gamma_D}\\
&+\langle\widehat{\boldsymbol{\psi}},\mu\tau\boldsymbol{u}\rangle_{\partial K_i\setminus\Gamma_D}-\langle\widehat{\boldsymbol{\psi}},\mu\tau\widehat{\boldsymbol{u}}\rangle_{\partial K_i\setminus\Gamma_D}\\
&+\langle\widehat{\boldsymbol{\psi}},\mu\tau(\boldsymbol{u}\cdot\boldsymbol{n})\boldsymbol{n}\rangle_{\partial K_i\setminus\Gamma_D}-\langle\widehat{\boldsymbol{\psi}},\mu\tau(\widehat{\boldsymbol{u}}\cdot\boldsymbol{n})\boldsymbol{n}\rangle_{\partial K_i\setminus\Gamma_D}\\
&-\langle\widehat{\boldsymbol{\psi}},\rho(1-\lambda)(\boldsymbol{u}\cdot\boldsymbol{n})\widehat{\boldsymbol{u}}\rangle_{\partial K_i\cap\Gamma_N}\Big\}\\
&=\sum_{i=1}^{\mathtt{n_{el}}}\Big\{\langle\widehat{\boldsymbol{\psi}},\boldsymbol{g}_N\rangle_{\partial K_i\cap\Gamma_N}-\langle\widehat{\boldsymbol{\psi}},p_N\boldsymbol{n}\rangle_{\partial K_i\cap\Gamma_N}\Big\}\end{aligned} \tag{D.3.18a}$$

$$\sum_{i=1}^{\mathtt{n_{el}}}\Big\{\langle\widehat{\phi},\boldsymbol{u}\cdot\boldsymbol{n}\rangle_{\partial K_i}-\langle\widehat{\phi},\widehat{\boldsymbol{u}}\cdot\boldsymbol{n}\rangle_{\partial K_i\cap\Gamma_N}\Big\}=\sum_{i=1}^{\mathtt{n_{el}}}\langle\widehat{\phi},\boldsymbol{u}_D\cdot\boldsymbol{n}\rangle_{\partial K_i\cap\Gamma_D} \tag{D.3.18b}$$

for all the test functions $\widehat{\boldsymbol{\psi}}\in\mathcal{V}_s^h(\Gamma\setminus\Gamma_D)$, and $\widetilde{\phi}\in\mathcal{S}_s^h(\Gamma)$.

Appendix E

Spatial discretization and implementation details of X-HDG method for two-phase Incompressible Navier-Stokes problem

E.1 Discrete local problems in cut elements

Terms in equation 6.2.9a are written as:

$$
\begin{aligned}
\mathbf{A}_{uu}^{K_i}\,\mathbf{u}^i =& (\boldsymbol{\psi}, \rho\frac{\boldsymbol{u}}{\Delta t})_{K_i} + \langle \boldsymbol{\psi}, \mu\tau\boldsymbol{u}\rangle_{\partial K_i} + \langle \boldsymbol{\psi}, \mu\tau(\boldsymbol{u}\cdot\boldsymbol{n})\boldsymbol{n}\rangle_{\partial K_i}\\
\mathbf{A}_{uL}^{K_i}\,\mathbf{L}^i =& (\boldsymbol{\psi}, \boldsymbol{\nabla}\cdot(\mu\boldsymbol{L}))_{K_i}\\
\mathbf{A}_{up}^{K_i}\,\mathbf{p}^i =& -(\boldsymbol{\nabla}\boldsymbol{\psi}, p\boldsymbol{I})_{K_i}\\
\mathbf{A}_{u\widetilde{p}^i}^{\mathcal{I}_i}\,\widetilde{\mathbf{p}}^i =& \langle \psi_1, \widetilde{p}^i\widehat{\boldsymbol{n}}\rangle_{\mathcal{I}_i} + \langle \boldsymbol{\psi}_2, \widetilde{p}^i(-\widehat{\boldsymbol{n}})\rangle_{\mathcal{I}_i}\\
\mathbf{A}_{uu}^{\mathcal{I}_i}\,\mathbf{u}^i =& \langle \psi_1, \mu_1\tau^{\mathcal{I}}\boldsymbol{u}_1\rangle_{\mathcal{I}_i} + \langle \boldsymbol{\psi}_2, \mu_2\tau^{\mathcal{I}}\boldsymbol{u}_2\rangle_{\mathcal{I}_i}\\
&+ \langle \boldsymbol{\psi}_1, \mu_1\tau^{\mathcal{I}}(\boldsymbol{u}_1\cdot\widehat{\boldsymbol{n}})\widehat{\boldsymbol{n}}\rangle_{\mathcal{I}_i} + \langle \boldsymbol{\psi}_2, \mu_2\tau^{\mathcal{I}}(\boldsymbol{u}_2\cdot(-\widehat{\boldsymbol{n}}))(-\widehat{\boldsymbol{n}})\rangle_{\mathcal{I}_i}\\
\mathbf{A}_{u\widetilde{u}^i}^{\mathcal{I}_i}\,\widetilde{\mathbf{u}}^i =& -\langle \boldsymbol{\psi}_1, \mu_1\tau^{\mathcal{I}}\widetilde{\boldsymbol{u}}^i\rangle_{\mathcal{I}_i} - \langle \boldsymbol{\psi}_2, \mu_2\tau^{\mathcal{I}}\widetilde{\boldsymbol{u}}^i\rangle_{\mathcal{I}_i}\\
&- \langle \boldsymbol{\psi}_1, \mu_1\tau^{\mathcal{I}}(\widetilde{\boldsymbol{u}}^i\cdot\widehat{\boldsymbol{n}})\widehat{\boldsymbol{n}}\rangle_{\mathcal{I}_i} - \langle \boldsymbol{\psi}_2, \mu_2\tau^{\mathcal{I}}(\widetilde{\boldsymbol{u}}^i\cdot(-\widehat{\boldsymbol{n}}))(-\widehat{\boldsymbol{n}})\rangle_{\mathcal{I}_i}\\
\mathbf{f}_u^{K_i} =& (\boldsymbol{\psi}, \rho\boldsymbol{f})_{K_i} + \langle \boldsymbol{\psi}, \mu\tau\boldsymbol{u}_D\rangle_{\partial K_i\cap\Gamma_D} + (\boldsymbol{\psi}, \rho\frac{\boldsymbol{u}^n}{\Delta t})_{K_i} + \langle \boldsymbol{\psi}, \mu\tau(\boldsymbol{u}_D\cdot\boldsymbol{n})\boldsymbol{n}\rangle_{\partial K_i\cap\Gamma_D}\\
&- \langle \boldsymbol{\psi}, p_N\boldsymbol{n}\rangle_{\partial K_i\cap\Gamma_N} - \langle \boldsymbol{\psi}_1, \boldsymbol{g}_s\rangle_{\mathcal{I}_i}\\
\mathbf{A}_{u\widehat{u}}^{K_i}\,\widehat{\mathbf{u}}^i =& \langle \boldsymbol{\psi}, \mu\tau\widehat{\boldsymbol{u}}\rangle_{\partial K_i\setminus\Gamma_D} + \langle \boldsymbol{\psi}, \mu\tau(\widehat{\boldsymbol{u}}\cdot\boldsymbol{n})\boldsymbol{n}\rangle_{\partial K_i\setminus\Gamma_D}\\
\mathbf{A}_{u\widehat{p}}^{K_i}\,\widehat{\mathbf{p}}^i =& -\langle \boldsymbol{\psi}, \widehat{p}\boldsymbol{n}\rangle_{\partial K_i\setminus\Gamma_N}\\
\mathbf{C}_{uu}^{K_i}(\mathbf{u}^i)\,\mathbf{u}^i =& -(\boldsymbol{\nabla}\boldsymbol{\psi}, \rho(\boldsymbol{u}\otimes\boldsymbol{u}))_{K_i} + \langle \boldsymbol{\psi}, \rho(\boldsymbol{u}\otimes\boldsymbol{u})\boldsymbol{n}\rangle_{\partial K_i} - \langle \boldsymbol{\psi}, \lambda\rho(\boldsymbol{u}\otimes\boldsymbol{u})\boldsymbol{n}\rangle_{\partial K_i}\\
\mathbf{C}_{uu}^{\mathcal{I}_i}(\mathbf{u}^i)\,\mathbf{u}^i =& \langle \psi_1, \rho_1(\boldsymbol{u}_1\otimes\boldsymbol{u}_1)\widehat{\boldsymbol{n}}\rangle_{\mathcal{I}_i} + \langle \boldsymbol{\psi}_2, \rho_2(\boldsymbol{u}_2\otimes\boldsymbol{u}_2)(-\widehat{\boldsymbol{n}})\rangle_{\mathcal{I}_i}\\
&- \langle \boldsymbol{\psi}_1, \lambda\rho_1(\boldsymbol{u}_1\otimes\boldsymbol{u}_1)\widehat{\boldsymbol{n}}\rangle_{\mathcal{I}_i} - \langle \boldsymbol{\psi}_2, \lambda\rho_2(\boldsymbol{u}_2\otimes\boldsymbol{u}_2)(-\widehat{\boldsymbol{n}})\rangle_{\mathcal{I}_i}\\
\mathbf{C}_{u\widetilde{u}^i}^{\mathcal{I}_i}(\mathbf{u}^i)\,\widetilde{\mathbf{u}}^i =& \langle \psi_1, \lambda\rho_1(\widetilde{\boldsymbol{u}}^i\otimes\boldsymbol{u}_1)\widehat{\boldsymbol{n}}\rangle_{\mathcal{I}_i} + \langle \boldsymbol{\psi}_2, \lambda\rho_2(\widetilde{\boldsymbol{u}}^i\otimes\boldsymbol{u}_2)(-\widehat{\boldsymbol{n}})\rangle_{\mathcal{I}_i}\\
\mathbf{C}_{u\widehat{u}}^{K_i}(\mathbf{u}^i)\,\widehat{\mathbf{u}}^i =& -\langle \boldsymbol{\psi}, \lambda\rho(\widehat{\boldsymbol{u}}\otimes\boldsymbol{u})\boldsymbol{n}\rangle_{\partial K_i\setminus\Gamma_D}\\
\mathbf{r}_u^{K_i}(\mathbf{u}^i) =& -\langle \boldsymbol{\psi}, \lambda\rho(\boldsymbol{u}_D\otimes\boldsymbol{u})\boldsymbol{n}\rangle_{\partial K_i\cap\Gamma_D}
\end{aligned}
$$

Terms in equation 6.2.9b are written as:

$$
\begin{aligned}
\mathbf{A}_{LL}^{K_i}\,\mathbf{L}^i &= -(\boldsymbol{\Psi},\boldsymbol{L})_{K_i}\\
\mathbf{A}_{Lu}^{K_i}\,\mathbf{u}^i &= (\boldsymbol{\nabla}^s\cdot\boldsymbol{\Psi},\boldsymbol{u})_{K_i}\\
\mathbf{A}_{L\widetilde{u}^i}^{\mathcal{I}_i}\,\widetilde{\mathbf{u}}^i &= -\langle\boldsymbol{\Psi}_1,\widetilde{\boldsymbol{u}}^i\otimes\widehat{\boldsymbol{n}}\rangle_{\mathcal{I}_i}-\langle\boldsymbol{\Psi}_1,\widehat{\boldsymbol{n}}\otimes\widetilde{\boldsymbol{u}}^i\rangle_{\mathcal{I}_i}-\langle\boldsymbol{\Psi}_2,\widetilde{\boldsymbol{u}}^i\otimes(-\widehat{\boldsymbol{n}})\rangle_{\mathcal{I}_i}-\langle\boldsymbol{\Psi}_2,(-\widehat{\boldsymbol{n}})\otimes\widetilde{\boldsymbol{u}}^i\rangle_{\mathcal{I}_i}\\
\mathbf{A}_{L\widehat{u}}^{K_i}\,\widehat{\mathbf{u}}^i &= \langle\boldsymbol{\Psi},\widehat{\boldsymbol{u}}\otimes\boldsymbol{n}\rangle_{\partial K_i\setminus\Gamma_D}+\langle\boldsymbol{\Psi},\boldsymbol{n}\otimes\widehat{\boldsymbol{u}}\rangle_{\partial K_i\setminus\Gamma_D}\\
\mathbf{f}_L^{K_i} &= \langle\boldsymbol{\Psi},\boldsymbol{u}_D\otimes\boldsymbol{n}\rangle_{\partial K_i\cap\Gamma_D}+\langle\boldsymbol{\Psi},\boldsymbol{n}\otimes\boldsymbol{u}_D\rangle_{\partial K_i\cap\Gamma_D}
\end{aligned}
$$

Terms in equation 6.2.9c are written as:

$$
\mathbf{A}_{pu}^{K_i}\,\mathbf{u}^i = -(\phi,\boldsymbol{\nabla}\cdot\boldsymbol{u})_{K_i}
$$

Terms in equation 6.2.9d are written as:

$$
\begin{aligned}
\mathbf{A}_{\widetilde{u}^i\widetilde{p}^i}^{\mathcal{I}_i}\,\widetilde{\mathbf{p}}^i =&\langle\widetilde{\boldsymbol{\psi}},\widetilde{p}^i\widehat{\boldsymbol{n}}\rangle_{\mathcal{I}_i}+\langle\widetilde{\boldsymbol{\psi}},\widetilde{p}^i(-\widehat{\boldsymbol{n}})\rangle_{\mathcal{I}_i}=\mathbf{0}\\
\mathbf{A}_{\widetilde{u}^iL}^{\mathcal{I}_i}\,\mathbf{L}^i =&\langle\widetilde{\boldsymbol{\psi}},\mu_1\boldsymbol{L}_1\widehat{\boldsymbol{n}}\rangle_{\mathcal{I}_i}+\langle\widetilde{\boldsymbol{\psi}},\mu_2\boldsymbol{L}_2(-\widehat{\boldsymbol{n}})\rangle_{\mathcal{I}_i}\\
\mathbf{A}_{\widetilde{u}^i\widetilde{u}^i}^{\mathcal{I}_i}\,\widetilde{\mathbf{u}}^i =&-\langle\widetilde{\boldsymbol{\psi}},\mu_1\tau^{\mathcal{I}}\widetilde{\boldsymbol{u}}^i\rangle_{\mathcal{I}_i}-\langle\widetilde{\boldsymbol{\psi}},\mu_2\tau^{\mathcal{I}}\widetilde{\boldsymbol{u}}^i\rangle_{\mathcal{I}_i}\\
&-\langle\widetilde{\boldsymbol{\psi}},\mu_1\tau^{\mathcal{I}}(\widetilde{\boldsymbol{u}}^i\cdot\widehat{\boldsymbol{n}})\widehat{\boldsymbol{n}}\rangle_{\mathcal{I}_i}-\langle\widetilde{\boldsymbol{\psi}},\mu_2\tau^{\mathcal{I}}(\widetilde{\boldsymbol{u}}^i\cdot(-\widehat{\boldsymbol{n}}))(-\widehat{\boldsymbol{n}})\rangle_{\mathcal{I}_i}\\
\mathbf{A}_{\widetilde{u}^iu}^{\mathcal{I}_i}\,\mathbf{u}^i =&\langle\widetilde{\boldsymbol{\psi}},\mu_1\tau^{\mathcal{I}}\boldsymbol{u}_1\rangle_{\mathcal{I}_i}+\langle\widetilde{\boldsymbol{\psi}},\mu_2\tau^{\mathcal{I}}\boldsymbol{u}_2\rangle_{\mathcal{I}_i}\\
&+\langle\widetilde{\boldsymbol{\psi}},\mu_1\tau^{\mathcal{I}}(\boldsymbol{u}_1\cdot\widehat{\boldsymbol{n}})\widehat{\boldsymbol{n}}\rangle_{\mathcal{I}_i}+\langle\widetilde{\boldsymbol{\psi}},\mu_2\tau^{\mathcal{I}}(\boldsymbol{u}_2\cdot(-\widehat{\boldsymbol{n}}))(-\widehat{\boldsymbol{n}})\rangle_{\mathcal{I}_i}
\end{aligned}
$$

Terms in equation 6.2.9e are written as:

$$
\mathbf{A}_{\widetilde{p}^iu}^{\mathcal{I}_i}\,\mathbf{u}^i = \langle\widetilde{\phi},\boldsymbol{u}_1\cdot\widehat{\boldsymbol{n}}\rangle_{\mathcal{I}_i}+\langle\widetilde{\phi},\boldsymbol{u}_2\cdot(-\widehat{\boldsymbol{n}})\rangle_{\mathcal{I}_i}
$$

Therefore, the discrete local problem in a cut element is written as:

(E.1.1a)

$$
\begin{aligned}
\left[\mathbf{A}_{uu}^{K_i}+\mathbf{A}_{uu}^{\mathcal{I}_i}+\mathbf{C}_{uu}^{K_i}(\mathbf{u}^i)+\mathbf{C}_{uu}^{\mathcal{I}_i}(\mathbf{u}^i)\right]\,\mathbf{u}^i+\mathbf{A}_{uL}^{K_i}\,\mathbf{L}^i+\mathbf{A}_{up}^{K_i}\,\mathbf{p}^i+\mathbf{A}_{u\widetilde{p}^i}^{\mathcal{I}_i}\,\widetilde{\mathbf{p}}^i+\left[\mathbf{A}_{u\widetilde{u}^i}^{\mathcal{I}_i}+\mathbf{C}_{u\widetilde{u}^i}^{\mathcal{I}_i}(\mathbf{u}^i)\right]\,\widetilde{\mathbf{u}}^i\\
=\left[\mathbf{A}_{u\widehat{u}}^{K_i}+\mathbf{C}_{u\widehat{u}}^{K_i}(\mathbf{u}^i)\right]\,\widehat{\mathbf{u}}^i+\mathbf{A}_{u\widehat{p}}^{K_i}\,\widehat{\mathbf{p}}^i+\mathbf{f}_u^{K_i}+\mathbf{r}_u^{K_i}(\mathbf{u}^i),
\end{aligned}
$$

(E.1.1b)

$$
\mathbf{A}_{Lu}^{K_i}\,\mathbf{u}^i+\mathbf{A}_{LL}^{K_i}\,\mathbf{L}^i+\mathbf{A}_{L\widetilde{u}^i}^{\mathcal{I}_i}\,\widetilde{\mathbf{u}}^i=\mathbf{A}_{L\widehat{u}}^{K_i}\,\widehat{\mathbf{u}}^i+\mathbf{f}_L^{K_i},
$$

(E.1.1c)

$$
\mathbf{A}_{pu}^{K_i}\,\mathbf{u}^i=\mathbf{0},
$$

(E.1.1d)

$$
\mathbf{A}_{\widetilde{u}^iu}^{\mathcal{I}_i}\,\mathbf{u}^i+\mathbf{A}_{\widetilde{u}^iL}^{\mathcal{I}_i}\,\mathbf{L}^i+\mathbf{A}_{\widetilde{u}^i\widetilde{p}^i}^{\mathcal{I}_i}\,\widetilde{\mathbf{p}}^i+\mathbf{A}_{\widetilde{u}^i\widetilde{u}^i}^{\mathcal{I}_i}\,\widetilde{\mathbf{u}}^i=\mathbf{0},
$$

(E.1.1e)

$$
\mathbf{A}_{\widetilde{p}^iu}^{\mathcal{I}_i}\,\mathbf{u}^i=\mathbf{0}.
$$

Which could be written in a matrix-vector form as:

(E.1.2)

$$\begin{bmatrix} \left[\mathbf{A}_{uu}^{K_i}+\mathbf{A}_{uu}^{\mathcal{I}_i}+\mathbf{C}_{uu}^{K_i}(\mathbf{u}^i)+\mathbf{C}_{uu}^{\mathcal{I}_i}(\mathbf{u}^i)\right] & \mathbf{A}_{uL}^{K_i} & \mathbf{A}_{up}^{K_i} & \left[\mathbf{A}_{u\widetilde{u}^i}^{\mathcal{I}_i}+\mathbf{C}_{u\widetilde{u}^i}^{\mathcal{I}_i}(\mathbf{u}^i)\right] & \mathbf{A}_{u\widetilde{p}^i}^{\mathcal{I}_i} \\ \mathbf{A}_{Lu}^{K_i} & \mathbf{A}_{LL}^{K_i} & \mathbf{0} & \mathbf{A}_{L\widetilde{u}^i}^{\mathcal{I}_i} & \mathbf{0} \\ \mathbf{A}_{pu}^{K_i} & \mathbf{0} & \mathbf{0} & \mathbf{0} & \mathbf{0} \\ \mathbf{A}_{\widetilde{u}^iu}^{\mathcal{I}_i} & \mathbf{A}_{\widetilde{u}^iL}^{\mathcal{I}_i} & \mathbf{0} & \mathbf{A}_{\widetilde{u}^i\widetilde{u}^i}^{\mathcal{I}_i} & \mathbf{A}_{\widetilde{u}^i\widetilde{p}^i}^{\mathcal{I}_i} \\ \mathbf{A}_{\widetilde{p}^iu}^{\mathcal{I}_i} & \mathbf{0} & \mathbf{0} & \mathbf{0} & \mathbf{0} \end{bmatrix} \begin{Bmatrix} \mathbf{u}^i \\ \mathbf{L}^i \\ \mathbf{p}^i \\ \widetilde{\mathbf{u}}^i \\ \widetilde{\mathbf{p}}^i \end{Bmatrix}$$

$$= \begin{bmatrix} \left[\mathbf{A}_{u\widehat{u}}^{K_i}+\mathbf{C}_{u\widehat{u}}^{K_i}(\mathbf{u}^i)\right] \\ \mathbf{A}_{L\widehat{u}}^{K_i} \\ \mathbf{0} \\ \mathbf{0} \\ \mathbf{0} \end{bmatrix} \widehat{\mathbf{u}}^i + \begin{bmatrix} \mathbf{A}_{up}^{K_i} \\ \mathbf{0} \\ \mathbf{0} \\ \mathbf{0} \\ \mathbf{0} \end{bmatrix} \widehat{\mathbf{p}}^i + \begin{Bmatrix} \mathbf{f}_u^{K_i}+\mathbf{r}_u^{K_i}(\mathbf{u}^i) \\ \mathbf{f}_L^{K_i} \\ \mathbf{0} \\ \mathbf{0} \\ \mathbf{0} \end{Bmatrix}$$

where the elemental variables are obtained by inverting the matrix to the left hand side (which is referred-to as $\mathbb{A}_i$)

(E.1.3)

$$\begin{Bmatrix} \mathbf{u}^i \\ \mathbf{L}^i \\ \mathbf{p}^i \\ \widetilde{\mathbf{u}}^i \\ \widetilde{\mathbf{p}}^i \end{Bmatrix} = \mathbb{A}_i^{-1} \begin{bmatrix} \left[\mathbf{A}_{u\widehat{u}}^{K_i}+\mathbf{C}_{u\widehat{u}}^{K_i}(\mathbf{u}^i)\right] \\ \mathbf{A}_{L\widehat{u}}^{K_i} \\ \mathbf{0} \\ \mathbf{0} \\ \mathbf{0} \end{bmatrix} \widehat{\mathbf{u}}^i + \mathbb{A}_i^{-1} \begin{bmatrix} \mathbf{A}_{up}^{K_i} \\ \mathbf{0} \\ \mathbf{0} \\ \mathbf{0} \\ \mathbf{0} \end{bmatrix} \widehat{\mathbf{p}}^i + \mathbb{A}_i^{-1} \begin{Bmatrix} \mathbf{f}_u^{K_i}+\mathbf{r}_u^{K_i}(\mathbf{u}^i) \\ \mathbf{f}_L^{K_i} \\ \mathbf{0} \\ \mathbf{0} \\ \mathbf{0} \end{Bmatrix}$$

Assume that the inverse of matrix $\mathbb{A}_i$ is written as:

(E.1.4)

$$\mathbb{A}_i^{-1} = \begin{bmatrix} [\mathrm{A}_{uu}^{K_i}]^{-1} & [\mathrm{A}_{uL}^{K_i}]^{-1} & [\mathrm{A}_{up}^{K_i}]^{-1} & [\mathrm{A}_{u\widetilde{u}^i}^{K_i}]^{-1} & [\mathrm{A}_{up^i}^{K_i}]^{-1} \\ [\mathrm{A}_{Lu}^{K_i}]^{-1} & [\mathrm{A}_{LL}^{K_i}]^{-1} & [\mathrm{A}_{Lp}^{K_i}]^{-1} & [\mathrm{A}_{L\widetilde{u}^i}^{K_i}]^{-1} & [\mathrm{A}_{L\widetilde{p}^i}^{K_i}]^{-1} \\ [\mathrm{A}_{pu}^{K_i}]^{-1} & [\mathrm{A}_{pL}^{K_i}]^{-1} & [\mathrm{A}_{pp}^{K_i}]^{-1} & [\mathrm{A}_{p\widetilde{u}^i}^{K_i}]^{-1} & [\mathrm{A}_{pp^i}^{K_i}]^{-1} \\ [\mathrm{A}_{\widetilde{u}^iu}^{K_i}]^{-1} & [\mathrm{A}_{\widetilde{u}^iL}^{K_i}]^{-1} & [\mathrm{A}_{\widetilde{u}^ip}^{K_i}]^{-1} & [\mathrm{A}_{\widetilde{u}^i\widetilde{u}^i}^{K_i}]^{-1} & [\mathrm{A}_{\widetilde{u}^ip^i}^{K_i}]^{-1} \\ [\mathrm{A}_{\widetilde{p}^iu}^{K_i}]^{-1} & [\mathrm{A}_{\widetilde{p}^iL}^{K_i}]^{-1} & [\mathrm{A}_{\widetilde{p}^ip}^{K_i}]^{-1} & [\mathrm{A}_{\widetilde{p}^i\widetilde{u}^i}^{K_i}]^{-1} & [\mathrm{A}_{\widetilde{p}^ip^i}^{K_i}]^{-1} \end{bmatrix}$$

where all the matrix blocks in $\mathbb{A}_i$ are extracted from the computed inverse and not derived analytically. i.e. extracted from the output of the coded inverse!

The variables $(\mathbf{u}^i, \mathbf{L}^i, \mathbf{p}^i)$ are then extracted as:

$$\begin{Bmatrix} \mathbf{u}^i \\ \mathbf{L}^i \\ \mathbf{p}^i \end{Bmatrix} = \begin{bmatrix} [\mathrm{A}_{uu}^{K_i}]^{-1}\left[\mathbf{A}_{u\widehat{u}}^{K_i} + \mathbf{C}_{u\widehat{u}}^{K_i}(\mathbf{u}^i)\right] + [\mathrm{A}_{uL}^{K_i}]^{-1}\mathbf{A}_{L\widehat{u}}^{K_i} \\ [\mathrm{A}_{Lu}^{K_i}]^{-1}\left[\mathbf{A}_{u\widehat{u}}^{K_i} + \mathbf{C}_{u\widehat{u}}^{K_i}(\mathbf{u}^i)\right] + [\mathrm{A}_{LL}^{K_i}]^{-1}\mathbf{A}_{L\widehat{u}}^{K_i} \\ [\mathrm{A}_{pu}^{K_i}]^{-1}\left[\mathbf{A}_{u\widehat{u}}^{K_i} + \mathbf{C}_{u\widehat{u}}^{K_i}(\mathbf{u}^i)\right] + [\mathrm{A}_{pL}^{K_i}]^{-1}\mathbf{A}_{L\widehat{u}}^{K_i} \end{bmatrix} \widehat{\mathbf{u}}^i + \begin{bmatrix} [\mathrm{A}_{uu}^{K_i}]^{-1}\mathbf{A}_{u\widehat{p}}^{K_i} \\ [\mathrm{A}_{Lu}^{K_i}]^{-1}\mathbf{A}_{u\widehat{p}}^{K_i} \\ [\mathrm{A}_{pu}^{K_i}]^{-1}\mathbf{A}_{u\widehat{p}}^{K_i} \end{bmatrix} \widehat{\mathbf{p}}^i + \begin{Bmatrix} [\mathrm{A}_{uu}^{K_i}]^{-1}\{\mathbf{f}_u^{K_i} + \mathbf{r}_u^{K_i}(\mathbf{u}^i)\} + [\mathrm{A}_{uL}^{K_i}]^{-1}\mathbf{f}_L^{K_i} \\ [\mathrm{A}_{Lu}^{K_i}]^{-1}\{\mathbf{f}_u^{K_i} + \mathbf{r}_u^{K_i}(\mathbf{u}^i)\} + [\mathrm{A}_{LL}^{K_i}]^{-1}\mathbf{f}_L^{K_i} \\ [\mathrm{A}_{pu}^{K_i}]^{-1}\{\mathbf{f}_u^{K_i} + \mathbf{r}_u^{K_i}(\mathbf{u}^i)\} + [\mathrm{A}_{pL}^{K_i}]^{-1}\mathbf{f}_L^{K_i} \end{Bmatrix} \tag{E.1.5}$$

which is also written as:

$$\begin{Bmatrix} \mathbf{u}^i \\ \mathbf{L}^i \\ \mathbf{p}^i \end{Bmatrix} = \begin{bmatrix} \mathbf{Z}_{u\widehat{u}}^{K_i}(\mathbf{u}^i) \\ \mathbf{Z}_{L\widehat{u}}^{K_i}(\mathbf{u}^i) \\ \mathbf{Z}_{p\widehat{u}}^{K_i}(\mathbf{u}^i) \end{bmatrix} \widehat{\mathbf{u}}^i + \begin{bmatrix} \mathbf{Z}_{u\widehat{p}}^{K_i}(\mathbf{u}^i) \\ \mathbf{Z}_{L\widehat{p}}^{K_i}(\mathbf{u}^i) \\ \mathbf{Z}_{p\widehat{p}}^{K_i}(\mathbf{u}^i) \end{bmatrix} \widehat{\mathbf{p}}^i + \begin{Bmatrix} \mathbf{z}_u^{K_i}(\mathbf{u}^i) \\ \mathbf{z}_L^{K_i}(\mathbf{u}^i) \\ \mathbf{z}_p^{K_i}(\mathbf{u}^i) \end{Bmatrix} \tag{E.1.6}$$

which is further simplified to:

$$\begin{Bmatrix} \mathbf{u}^i \\ \mathbf{L}^i \\ \mathbf{p}^i \end{Bmatrix} = \mathbf{Z}_{\widehat{u}}^{K_i}(\mathbf{u}^i)\,\widehat{\mathbf{u}}^i + \mathbf{Z}_{\widehat{p}}^{K_i}(\mathbf{u}^i)\,\widehat{\mathbf{p}}^i + \mathbf{z}^{K_i}(\mathbf{u}^i) \tag{E.1.7}$$

E.2 Discrete local problems in standard elements

Terms in equation 6.2.10a are written as:

$$\begin{aligned}
\mathbf{A}_{uu}^{K_i}\,\mathbf{u}^i &= (\boldsymbol{\psi}, \rho\frac{\boldsymbol{u}}{\Delta t})_{K_i} + \langle \boldsymbol{\psi}, \mu\tau\boldsymbol{u}\rangle_{\partial K_i} + \langle \boldsymbol{\psi}, \mu\tau(\boldsymbol{u}\cdot\boldsymbol{n})\boldsymbol{n}\rangle_{\partial K_i} \\
\mathbf{A}_{uL}^{K_i}\,\mathbf{L}^i &= (\boldsymbol{\psi}, \boldsymbol{\nabla}\cdot(\mu\boldsymbol{L}))_{K_i} \\
\mathbf{A}_{up}^{K_i}\,\mathbf{p}^i &= -(\boldsymbol{\nabla}\boldsymbol{\psi}, p\boldsymbol{I})_{K_i} \\
\mathbf{f}_u^{K_i} &= (\boldsymbol{\psi}, \rho\boldsymbol{f})_{K_i} + \langle \boldsymbol{\psi}, \mu\tau\boldsymbol{u}_D\rangle_{\partial K_i\cap\Gamma_D} + (\boldsymbol{\psi}, \rho\frac{\boldsymbol{u}^n}{\Delta t})_{K_i} + \langle \boldsymbol{\psi}, \mu\tau(\boldsymbol{u}_D\cdot\boldsymbol{n})\boldsymbol{n}\rangle_{\partial K_i\cap\Gamma_D} - \langle \boldsymbol{\psi}, p_N\boldsymbol{n}\rangle_{\partial K_i\cap\Gamma_N} \\
\mathbf{A}_{u\widehat{u}}^{K_i}\,\widehat{\mathbf{u}}^i &= \langle \boldsymbol{\psi}, \mu\tau\widehat{\boldsymbol{u}}\rangle_{\partial K_i\setminus\Gamma_D} + \langle \boldsymbol{\psi}, \mu\tau(\widehat{\boldsymbol{u}}\cdot\boldsymbol{n})\boldsymbol{n}\rangle_{\partial K_i\setminus\Gamma_D} \\
\mathbf{A}_{u\widehat{p}}^{K_i}\,\widehat{\mathbf{p}}^i &= -\langle \boldsymbol{\psi}, \widehat{p}\boldsymbol{n}\rangle_{\partial K_i\setminus\Gamma_N} \\
\mathbf{C}_{uu}^{K_i}(\mathbf{u}^i)\,\mathbf{u}^i &= -(\boldsymbol{\nabla}\boldsymbol{\psi}, \rho(\boldsymbol{u}\otimes\boldsymbol{u}))_{K_i} + \langle \boldsymbol{\psi}, \rho(\boldsymbol{u}\otimes\boldsymbol{u})\boldsymbol{n}\rangle_{\partial K_i} - \langle \boldsymbol{\psi}, \lambda\rho(\boldsymbol{u}\otimes\boldsymbol{u})\boldsymbol{n}\rangle_{\partial K_i} \\
\mathbf{C}_{u\widehat{u}}^{K_i}(\mathbf{u}^i)\,\widehat{\mathbf{u}}^i &= -\langle \boldsymbol{\psi}, \lambda\rho(\widehat{\boldsymbol{u}}\otimes\boldsymbol{u})\boldsymbol{n}\rangle_{\partial K_i\setminus\Gamma_D} \\
\mathbf{r}_u^{K_i}(\mathbf{u}^i) &= -\langle \boldsymbol{\psi}, \lambda\rho(\boldsymbol{u}_D\otimes\boldsymbol{u})\boldsymbol{n}\rangle_{\partial K_i\cap\Gamma_D}
\end{aligned}$$

Terms in equation 6.2.10b are written as:

$$\begin{aligned}
\mathbf{A}_{LL}^{K_i}\,\mathbf{L}^i &= -(\boldsymbol{\Psi},\boldsymbol{L})_{K_i}\\
\mathbf{A}_{Lu}^{K_i}\,\mathbf{u}^i &= (\boldsymbol{\nabla}^s\cdot\boldsymbol{\Psi},\boldsymbol{u})_{K_i}\\
\mathbf{A}_{L\widehat{u}}^{K_i}\,\widehat{\mathbf{u}}^i &= \langle\boldsymbol{\Psi},\widehat{\boldsymbol{u}}\otimes\boldsymbol{n}\rangle_{\partial K_i\setminus\Gamma_D} + \langle\boldsymbol{\Psi},\boldsymbol{n}\otimes\widehat{\boldsymbol{u}}\rangle_{\partial K_i\setminus\Gamma_D}\\
\mathbf{f}_L^{K_i} &= \langle\boldsymbol{\Psi},\boldsymbol{u}_D\otimes\boldsymbol{n}\rangle_{\partial K_i\cap\Gamma_D} + \langle\boldsymbol{\Psi},\boldsymbol{n}\otimes\boldsymbol{u}_D\rangle_{\partial K_i\cap\Gamma_D}
\end{aligned}$$

Terms in equation 6.2.10c are written as:

$$\mathbf{A}_{pu}^{K_i}\,\mathbf{u}^i = -(\phi,\boldsymbol{\nabla}\cdot\boldsymbol{u})_{K_i}$$

Therefore, the discrete local problem in a standard element is written as:

(E.2.1a)
$$\left[\mathbf{A}_{uu}^{K_i}+\mathbf{C}_{uu}^{K_i}(\mathbf{u}^i)\right]\,\mathbf{u}^i+\mathbf{A}_{uL}^{K_i}\,\mathbf{L}^i+\mathbf{A}_{up}^{K_i}\,\mathbf{p}^i=\left[\mathbf{A}_{u\widehat{u}}^{K_i}+\mathbf{C}_{u\widehat{u}}^{K_i}(\mathbf{u}^i)\right]\,\widehat{\mathbf{u}}^i+\mathbf{A}_{u\widehat{p}}^{K_i}\,\widehat{\mathbf{p}}^i+\mathbf{f}_u^{K_i}+\mathbf{r}_u^{K_i}(\mathbf{u}^i),$$

(E.2.1b)
$$\mathbf{A}_{Lu}^{K_i}\,\mathbf{u}^i+\mathbf{A}_{LL}^{K_i}\,\mathbf{L}^i=\mathbf{A}_{L\widehat{u}}^{K_i}\,\widehat{\mathbf{u}}^i+\mathbf{f}_L^{K_i},$$

(E.2.1c)
$$\mathbf{A}_{pu}^{K_i}\,\mathbf{u}^i=\mathbf{0}$$

which is then written in matrix-vector form as

(E.2.2)
$$\begin{bmatrix}\left[\mathbf{A}_{uu}^{K_i}+\mathbf{C}_{uu}^{K_i}(\mathbf{u}^i)\right] & \mathbf{A}_{uL}^{K_i} & \mathbf{A}_{up}^{K_i}\\ \mathbf{A}_{Lu}^{K_i} & \mathbf{A}_{LL}^{K_i} & \mathbf{0}\\ \mathbf{A}_{pu}^{K_i} & \mathbf{0} & \mathbf{0}\end{bmatrix}\begin{Bmatrix}\mathbf{u}^i\\ \mathbf{L}^i\\ \mathbf{p}^i\end{Bmatrix}=\begin{bmatrix}\left[\mathbf{A}_{u\widehat{u}}^{K_i}+\mathbf{C}_{u\widehat{u}}^{K_i}(\mathbf{u}^i)\right]\\ \mathbf{A}_{L\widehat{u}}^{K_i}\\ \mathbf{0}\end{bmatrix}\widehat{\mathbf{u}}^i+\begin{bmatrix}\mathbf{A}_{u\widehat{p}}^{K_i}\\ \mathbf{0}\\ \mathbf{0}\end{bmatrix}\widehat{\mathbf{p}}^i+\begin{Bmatrix}\mathbf{f}_u^{K_i}+\mathbf{r}_u^{K_i}(\mathbf{u}^i)\\ \mathbf{f}_L^{K_i}\\ \mathbf{0}\end{Bmatrix}$$

where the elemental variables are obtained by inverting the matrix to the left hand side (which is referred-to as $\mathbb{A}_i$)

(E.2.3)
$$\begin{Bmatrix}\mathbf{u}^i\\ \mathbf{L}^i\\ \mathbf{p}^i\end{Bmatrix}=\mathbb{A}_i^{-1}\begin{bmatrix}\left[\mathbf{A}_{u\widehat{u}}^{K_i}+\mathbf{C}_{u\widehat{u}}^{K_i}(\mathbf{u}^i)\right]\\ \mathbf{A}_{L\widehat{u}}^{K_i}\\ \mathbf{0}\end{bmatrix}\widehat{\mathbf{u}}^i+\mathbb{A}_i^{-1}\begin{bmatrix}\mathbf{A}_{u\widehat{p}}^{K_i}\\ \mathbf{0}\\ \mathbf{0}\end{bmatrix}\widehat{\mathbf{p}}^i+\mathbb{A}_i^{-1}\begin{Bmatrix}\mathbf{f}_u^{K_i}+\mathbf{r}_u^{K_i}(\mathbf{u}^i)\\ \mathbf{f}_L^{K_i}\\ \mathbf{0}\end{Bmatrix}$$

Assume that the inverse of matrix $\mathbb{A}_i$ is written as:

(E.2.4)
$$\mathbb{A}_i^{-1}=\begin{bmatrix}[\mathrm{A}_{uu}^{K_i}]^{-1} & [\mathrm{A}_{uL}^{K_i}]^{-1} & [\mathrm{A}_{up}^{K_i}]^{-1}\\ [\mathrm{A}_{Lu}^{K_i}]^{-1} & [\mathrm{A}_{LL}^{K_i}]^{-1} & [\mathrm{A}_{Lp}^{K_i}]^{-1}\\ [\mathrm{A}_{pu}^{K_i}]^{-1} & [\mathrm{A}_{pL}^{K_i}]^{-1} & [\mathrm{A}_{pp}^{K_i}]^{-1}\end{bmatrix}$$

The variables $(\mathbf{u}^i, \mathbf{L}^i, \mathbf{p}^i)$ are written as:

$$\begin{Bmatrix} \mathbf{u}^i \\ \mathbf{L}^i \\ \mathbf{p}^i \end{Bmatrix} = \begin{bmatrix} [\mathrm{A}_{uu}^{K_i}]^{-1}\left[\mathbf{A}_{u\widehat{u}}^{K_i} + \mathbf{C}_{u\widehat{u}}^{K_i}(\mathbf{u}^i)\right] + [\mathrm{A}_{uL}^{K_i}]^{-1}\mathbf{A}_{L\widehat{u}}^{K_i} \\ [\mathrm{A}_{Lu}^{K_i}]^{-1}\left[\mathbf{A}_{u\widehat{u}}^{K_i} + \mathbf{C}_{u\widehat{u}}^{K_i}(\mathbf{u}^i)\right] + [\mathrm{A}_{LL}^{K_i}]^{-1}\mathbf{A}_{L\widehat{u}}^{K_i} \\ [\mathrm{A}_{pu}^{K_i}]^{-1}\left[\mathbf{A}_{u\widehat{u}}^{K_i} + \mathbf{C}_{u\widehat{u}}^{K_i}(\mathbf{u}^i)\right] + [\mathrm{A}_{pL}^{K_i}]^{-1}\mathbf{A}_{L\widehat{u}}^{K_i} \end{bmatrix} \widehat{\mathbf{u}}^i + \begin{bmatrix} [\mathrm{A}_{uu}^{K_i}]^{-1}\mathbf{A}_{u\widehat{p}}^{K_i} \\ [\mathrm{A}_{Lu}^{K_i}]^{-1}\mathbf{A}_{u\widehat{p}}^{K_i} \\ [\mathrm{A}_{pu}^{K_i}]^{-1}\mathbf{A}_{u\widehat{p}}^{K_i} \end{bmatrix} \widehat{\mathbf{p}}^i + \begin{Bmatrix} [\mathrm{A}_{uu}^{K_i}]^{-1}\{\mathbf{f}_u^{K_i} + \mathbf{r}_u^{K_i}(\mathbf{u}^i)\} + [\mathrm{A}_{uL}^{K_i}]^{-1}\mathbf{f}_L^{K_i} \\ [\mathrm{A}_{Lu}^{K_i}]^{-1}\{\mathbf{f}_u^{K_i} + \mathbf{r}_u^{K_i}(\mathbf{u}^i)\} + [\mathrm{A}_{LL}^{K_i}]^{-1}\mathbf{f}_L^{K_i} \\ [\mathrm{A}_{pu}^{K_i}]^{-1}\{\mathbf{f}_u^{K_i} + \mathbf{r}_u^{K_i}(\mathbf{u}^i)\} + [\mathrm{A}_{pL}^{K_i}]^{-1}\mathbf{f}_L^{K_i} \end{Bmatrix} \tag{E.2.5}$$

which is also written as:

$$\begin{Bmatrix} \mathbf{u}^i \\ \mathbf{L}^i \\ \mathbf{p}^i \end{Bmatrix} = \begin{bmatrix} \mathbf{Z}_{u\widehat{u}}^{K_i}(\mathbf{u}^i) \\ \mathbf{Z}_{L\widehat{u}}^{K_i}(\mathbf{u}^i) \\ \mathbf{Z}_{p\widehat{u}}^{K_i}(\mathbf{u}^i) \end{bmatrix} \widehat{\mathbf{u}}^i + \begin{bmatrix} \mathbf{Z}_{up}^{K_i}(\mathbf{u}^i) \\ \mathbf{Z}_{L\widehat{p}}^{K_i}(\mathbf{u}^i) \\ \mathbf{Z}_{p\widehat{p}}^{K_i}(\mathbf{u}^i) \end{bmatrix} \widehat{\mathbf{p}}^i + \begin{Bmatrix} \mathbf{z}_u^{K_i}(\mathbf{u}^i) \\ \mathbf{z}_L^{K_i}(\mathbf{u}^i) \\ \mathbf{z}_p^{K_i}(\mathbf{u}^i) \end{Bmatrix} \tag{E.2.6}$$

which is further simplified to:

$$\begin{Bmatrix} \mathbf{u}^i \\ \mathbf{L}^i \\ \mathbf{p}^i \end{Bmatrix} = \mathbf{Z}_{\widehat{u}}^{K_i}(\mathbf{u}^i)\,\widehat{\mathbf{u}}^i + \mathbf{Z}_{\widehat{p}}^{K_i}(\mathbf{u}^i)\,\widehat{\mathbf{p}}^i + \mathbf{z}^{K_i}(\mathbf{u}^i) \tag{E.2.7}$$

E.3 Discrete global problem

Terms in equation 6.2.11a are written as:

$$\begin{aligned}
\mathbf{A}_{\widehat{up}}^{K_i}\,\widehat{\mathbf{p}}^i &= \langle \widehat{\boldsymbol{\psi}}, \widehat{p}\boldsymbol{n}\rangle_{\partial K_i \setminus \partial\Omega} \\
\mathbf{A}_{\widehat{uL}}^{K_i}\,\mathbf{L}^i &= \langle \widehat{\boldsymbol{\psi}}, \mu \boldsymbol{L}\boldsymbol{n}\rangle_{\partial K_i \setminus \Gamma_D} \\
\mathbf{A}_{\widehat{uu}}^{K_i}\,\mathbf{u}^i &= \langle \widehat{\boldsymbol{\psi}}, \mu\tau\boldsymbol{u}\rangle_{\partial K_i \setminus \Gamma_D} + \langle \widehat{\boldsymbol{\psi}}, \mu\tau(\boldsymbol{u}\cdot\boldsymbol{n})\boldsymbol{n}\rangle_{\partial K_i \setminus \Gamma_D} \\
\mathbf{A}_{\widehat{uu}}^{K_i}\,\widehat{\mathbf{u}}^i &= -\langle \widehat{\boldsymbol{\psi}}, \mu\tau\widehat{\boldsymbol{u}}\rangle_{\partial K_i \setminus \Gamma_D} - \langle \widehat{\boldsymbol{\psi}}, \mu\tau(\widehat{\boldsymbol{u}}\cdot\boldsymbol{n})\boldsymbol{n}\rangle_{\partial K_i \setminus \Gamma_D} \\
\mathbf{f}_{\widehat{u}}^{K_i} &= \langle \widehat{\boldsymbol{\psi}}, \boldsymbol{g}_N\rangle_{\partial K_i \cap \Gamma_N} - \langle \widehat{\boldsymbol{\psi}}, p_N\boldsymbol{n}\rangle_{\partial K_i \cap \Gamma_N} \\
\mathbf{C}_{\widehat{uu}}^{K_i}(\mathbf{u}^i)\,\mathbf{u}^i &= \langle \widehat{\boldsymbol{\psi}}, \rho(\boldsymbol{u}\otimes\boldsymbol{u})\boldsymbol{n}\rangle_{\partial K_i \setminus \Gamma_D} - \langle \widehat{\boldsymbol{\psi}}, \lambda\rho(\boldsymbol{u}\otimes\boldsymbol{u})\boldsymbol{n}\rangle_{\partial K_i \setminus \Gamma_D} \\
\mathbf{C}_{\widehat{uu}}^{K_i}(\mathbf{u}^i)\,\widehat{\mathbf{u}}^i &= \langle \widehat{\boldsymbol{\psi}}, \lambda\rho(\widehat{\boldsymbol{u}}\otimes\boldsymbol{u})\boldsymbol{n}\rangle_{\partial K_i \setminus \Gamma_D} - \langle \widehat{\boldsymbol{\psi}}, \rho(1-\lambda)(\boldsymbol{u}\cdot\boldsymbol{n})\widehat{\boldsymbol{u}}\rangle_{\partial K_i \cap \Gamma_N}
\end{aligned}$$

Terms in equation 6.2.11b are written as:

$$\begin{aligned}
\mathbf{A}_{\widehat{pu}}^{K_i}\,\mathbf{u}^i &= \langle \widehat{\phi}, \boldsymbol{u}\cdot\boldsymbol{n}\rangle_{\partial K_i} \\
\mathbf{A}_{\widehat{pu}}^{K_i}\,\widehat{\mathbf{u}}^i &= -\langle \widehat{\phi}, \widehat{\boldsymbol{u}}\cdot\boldsymbol{n}\rangle_{\partial K_i \cap \Gamma_N} \\
\mathbf{f}_{\widehat{p}}^{K_i} &= \langle \widehat{\phi}, \boldsymbol{u}_D\cdot\boldsymbol{n}\rangle_{\partial K_i \cap \Gamma_D}
\end{aligned}$$

Therefore, the discrete global problem is written as:

$$\sum_{i=1}^{\mathtt{n_{el}}}\Big\{[\mathbf{A}_{\widehat{uu}}^{K_i}+\mathbf{C}_{\widehat{uu}}^{K_i}(\mathbf{u}^i)]\,\mathbf{u}^i+\mathbf{A}_{\widehat{uL}}^{K_i}\,\mathbf{L}^i+[\mathbf{A}_{\widetilde{uu}}^{K_i}+\mathbf{C}_{\widetilde{uu}}^{K_i}(\mathbf{u}^i)]\,\widehat{\mathbf{u}}^i+\mathbf{A}_{\widetilde{up}}^{K_i}\,\widehat{\mathbf{p}}^i\Big\}=\sum_{i=1}^{\mathtt{n_{el}}}\mathbf{f}_{\widehat{u}}^{K_i} \tag{E.3.1a}$$

$$\sum_{i=1}^{\mathtt{n_{el}}}\{\mathbf{A}_{\widehat{pu}}^{K_i}\,\mathbf{u}^i+\mathbf{A}_{\widetilde{pu}}^{K_i}\,\widehat{\mathbf{u}}^i\}=\sum_{i=1}^{\mathtt{n_{el}}}\mathbf{f}_{\widehat{p}}^{K_i} \tag{E.3.1b}$$

By inserting the solutions $(\mathbf{u}^i,\mathbf{L}^i)$ from the local problem, E.1.7 or E.2.7, into E.3.1a, and the solution $(\mathbf{u}^i)$ into E.3.1b, we get

(E.3.2a)

$$\begin{aligned}\sum_{i=1}^{\mathtt{n_{el}}}\Big\{&[\mathbf{A}_{\widehat{uu}}^{K_i}+\mathbf{C}_{\widehat{uu}}^{K_i}(\mathbf{u}^i)]\,\mathbf{Z}_{u\widehat{u}}^{K_i}(\mathbf{u}^i)\,\widehat{\mathbf{u}}^i+[\mathbf{A}_{\widehat{uu}}^{K_i}+\mathbf{C}_{\widehat{uu}}^{K_i}(\mathbf{u}^i)]\,\mathbf{Z}_{u\widehat{p}}^{K_i}(\mathbf{u}^i)\,\widehat{\mathbf{p}}^i+[\mathbf{A}_{\widehat{uu}}^{K_i}+\mathbf{C}_{\widehat{uu}}^{K_i}(\mathbf{u}^i)]\,\mathbf{z}_u^{K_i}(\mathbf{u}^i)\\&+\mathbf{A}_{\widehat{uL}}^{K_i}\,\mathbf{Z}_{L\widehat{u}}^{K_i}(\mathbf{u}^i)\,\widehat{\mathbf{u}}^i+\mathbf{A}_{\widehat{uL}}^{K_i}\,\mathbf{Z}_{L\widehat{p}}^{K_i}(\mathbf{u}^i)\,\widehat{\mathbf{p}}^i+\mathbf{A}_{\widehat{uL}}^{K_i}\,\mathbf{z}_L^{K_i}(\mathbf{u}^i)\\&+[\mathbf{A}_{\widetilde{uu}}^{K_i}+\mathbf{C}_{\widetilde{uu}}^{K_i}(\mathbf{u}^i)]\,\widehat{\mathbf{u}}^i+\mathbf{A}_{\widetilde{up}}^{K_i}\,\widehat{\mathbf{p}}^i\Big\}=\sum_{i=1}^{\mathtt{n_{el}}}\mathbf{f}_{\widehat{u}}^{K_i}\end{aligned}$$

$$\sum_{i=1}^{\mathtt{n_{el}}}\{\mathbf{A}_{\widehat{pu}}^{K_i}\,\mathbf{Z}_{u\widehat{u}}^{K_i}(\mathbf{u}^i)\,\widehat{\mathbf{u}}^i+\mathbf{A}_{\widehat{pu}}^{K_i}\,\mathbf{Z}_{u\widehat{p}}^{K_i}(\mathbf{u}^i)\,\widehat{\mathbf{p}}^i+\mathbf{A}_{\widehat{pu}}^{K_i}\,\mathbf{z}_u^{K_i}(\mathbf{u}^i)+\mathbf{A}_{\widetilde{pu}}^{K_i}\,\widehat{\mathbf{u}}^i\}=\sum_{i=1}^{\mathtt{n_{el}}}\mathbf{f}_{\widehat{p}}^{K_i} \tag{E.3.2b}$$

Finally, the full global problem is written in a matrix-vector form as:

$$\begin{aligned}&\mathbf{A}_{i=1}^{\mathtt{n_{el}}}\begin{bmatrix}[\mathbf{A}_{\widehat{uu}}^{K_i}+\mathbf{C}_{\widehat{uu}}^{K_i}(\mathbf{u}^i)]\,\mathbf{Z}_{u\widehat{u}}^{K_i}(\mathbf{u}^i)&[\mathbf{A}_{\widehat{uu}}^{K_i}+\mathbf{C}_{\widehat{uu}}^{K_i}(\mathbf{u}^i)]\,\mathbf{Z}_{u\widehat{p}}^{K_i}(\mathbf{u}^i)\\+\mathbf{A}_{\widehat{uL}}^{K_i}\,\mathbf{Z}_{L\widehat{u}}^{K_i}(\mathbf{u}^i)&+\mathbf{A}_{\widehat{uL}}^{K_i}\,\mathbf{Z}_{L\widehat{p}}^{K_i}(\mathbf{u}^i)\\+\mathbf{A}_{\widetilde{uu}}^{K_i}+\mathbf{C}_{\widetilde{uu}}^{K_i}(\mathbf{u}^i)&+\mathbf{A}_{\widetilde{up}}^{K_i}\\\mathbf{A}_{\widehat{pu}}^{K_i}\,\mathbf{Z}_{u\widehat{u}}^{K_i}(\mathbf{u}^i)+\mathbf{A}_{\widetilde{pu}}^{K_i}&\mathbf{A}_{\widehat{pu}}^{K_i}\,\mathbf{Z}_{u\widehat{p}}^{K_i}(\mathbf{u}^i)\end{bmatrix}\begin{Bmatrix}\widehat{\mathbf{u}}^i\\\widehat{\mathbf{p}}^i\end{Bmatrix}\\=&\mathbf{A}_{i=1}^{\mathtt{n_{el}}}\begin{Bmatrix}\mathbf{f}_{\widehat{u}}^{K_i}-[\mathbf{A}_{\widehat{uu}}^{K_i}+\mathbf{C}_{\widehat{uu}}^{K_i}(\mathbf{u}^i)]\,\mathbf{z}_u^{K_i}(\mathbf{u}^i)-\mathbf{A}_{\widehat{uL}}^{K_i}\,\mathbf{z}_L^{K_i}(\mathbf{u}^i)\\\mathbf{f}_{\widehat{p}}^{K_i}-\mathbf{A}_{\widehat{pu}}^{K_i}\,\mathbf{z}_u^{K_i}(\mathbf{u}^i)\end{Bmatrix}\end{aligned} \tag{E.3.3}$$

which is written in simplified notation as

$$\mathbf{A}_{i=1}^{\mathtt{n_{el}}}\widehat{\mathbf{K}}^i(\mathbf{u}^i)\begin{Bmatrix}\widehat{\mathbf{u}}^i\\\widehat{\mathbf{p}}^i\end{Bmatrix}=\mathbf{A}_{i=1}^{\mathtt{n_{el}}}\widehat{\mathbf{f}}^i(\mathbf{u}^i) \tag{E.3.4}$$

where $\mathbf{A}_{i=1}^{\mathtt{n_{el}}}$ denotes the assembly of all the finite element matrices/vectors into a global matrix/vector. Simplifying furthermore yields the global system of equations which is written as

$$\widehat{\mathbf{K}}(\mathbf{u})\begin{Bmatrix}\widehat{\mathbf{u}}\\\widehat{\mathbf{p}}\end{Bmatrix}=\widehat{\mathbf{f}}(\mathbf{u}) \tag{E.3.5}$$

Titre : Schéma précis compact élevé pour les flux de deux phases incompressibles laminaires

Mots clés : Galerkine Discontinue Hybridisable (HDG); Méthode étendue des éléments finis (X-FEM); Écoulements incompressibles diphasiques ; Méthode sans divergence.

Résumé : L'objectif de cette thèse est de développer une méthode précise d'ordre élevé pour résoudre le problème d'écoulement laminaire incompressible à deux phases. Trois tâches principales sont à accomplir. Premièrement, la méthode doit être stable en énergie, ce qui signifie que la condition sans divergence de l'équation de Navier-Stokes incompressible est satisfaite partout dans le domaine de calcul. Deuxièmement, les discontinuités locales apparaissant dans le champ d'écoulement diphasique doivent être capturées avec précision. Troisièmement, l'interface matérielle entre les deux fluides doit être représentée avec précision à chaque pas de temps.

Dans ce travail, une nouvelle méthode Hybridizable Discontinuous Galerkin (HDG) est utilisée pour la discrétisation spatiale. Cette méthode hybride qui appartient à la famille des méthodes DG-FEM satisfait la condition sans divergence en introduisant des variables de trace de vitesse et de pression du même ordre plus une approximation de vitesse et de pression adaptée à l'intérieur des éléments. De plus, les concepts de FEM eXtended (X-FEM) sont utilisés pour approximer les discontinuités dans le champ d'écoulement en enrichissant l'approximation FEM standard dans les éléments où deux fluides existent. Enfin, l'interface du matériau en mouvement entre les deux fluides est capturée à l'aide de la méthode Level-Set.

Title : Compact High-Order Accurate Scheme for Laminar Incompressible Two-Phase Flows

Keywords : Hybridizable Discontinuous Galerkin (HDG); Extended Finite Element Method (X-FEM); Two-Phase Incompressible Flows; Divergence-Free Method

Abstract : The objective of this thesis is to develop a high-order accurate method to solve the two-phase incompressible laminar flow problem. Three main tasks are to be achieved. First, the method has to be energy-stable meaning that the divergence-free condition of the incompressible Navier-Stokes equation is satisfied everywhere in the computational domain. Second, the local discontinuities arising in the two-phase flow field have to be captured accurately. Third, the material interface between the two fluids has to be represented accurately in each time step.

In this work, a novel Hybridizable Discontinuous Galerkin (HDG) method is used for the spatial discretization. This hybrid method that belongs to the family of DG-FEM methods satisfies the divergence-free condition by introducing velocity and pressure trace variables of the same order plus a tailored velocity and pressure approximation inside the elements. Furthermore, the concepts of eXtended FEM (X-FEM) are used to approximate discontinuities in the flow field by enriching the standard FEM approximation in elements where two fluids exist. Finally, the moving material interface between the two fluids is captured using the Level-Set method.